Splitting Techniques in Vertical Pneumatic Conveying

By Jacob Thomas Roberts MENG

Thesis submitted to the University of Nottingham
for the degree of Doctor of Philosophy.

PAGE NUMBERING AS ORIGINAL

For Emma

Dedication

"Yesterday, we only probed your positions. When we attack today, our arrows will blot out the sun!" - Haydranes

"Good; then we will fight in the shade." – Dienekes

Conversation between Haydranes commander of the Immortals of Persia and Dienekes of Sparta, Soldier following King Leonaidas.
Thermopylae Pass in 480 BC
Important note: Sparta lost.

King Leonaidas showed that despite the conditions, sometimes you have to act. He lead 300 Spartan warriors and a few thousand volunteers against the greatest army of the age, that of Persia. The Spartans weren't the goodies and the Persians the baddies, not to mention the fact that the Spartans lost. All that should be remembered is that a few stood against many despite the overwhelming odds. In the same way this thesis is the result of a few standing against many. To the many, in the words of Frankie Howard (with hand action): Saluté.

This work is dedicated to every one who has been my friend; the space is not permitted to mention them all yet they know who they are.

This work is dedicated to my family who have always been supportive; it is for them that is work is written.

This work is dedicated to all the technical staff at Nottingham University; for it take a dozen toiling men on the ground to keep one man with his head in the skies.

This work is dedicated to my fellow academics; for research is nothing without debate and argument.

This work is dedicated to the people in the student registry and their infinite patience.

This work is dedicated to those I love with all my heart: for strength is the son of courage; courage is drawn from faith, faith is derived from hope and without love there is no hope. Ergo Strength = Love. You are my strength.

This work is dedicated to those who I have lost; for loss is like love, it serves as a reminder of what life may hold. It is a rousing call for battle and a sobering cry for peace.

Finally this work is dedicated to David Allen of Skegby, Nottinghamshire, for without David Allen, there is no Jake Roberts. Rest in peace my friend.

"No man is truly dead till the events he sets in motion finally stop"

Abstract

The following work details an investigation into improving efficiency in pulverised-fuel-fired power stations. The particular area of focus is the splitter box; this is located in the pneumatic conveying pipeline within the power station. The conveying pipelines take the pulverised fuel from the mill to the burner face, at some point the air/fuel mixture has to be split to feed the individual burners. It is at these points that the splitter boxes occur, dividing the pipe into multiple legs.

It is common for some of these splits to produce poor fuel balance between legs, leading to excess air being required for their combustion at the burner wall. The increased supply of air increases the chance of the formation of NO_X gases as well as reducing the overall efficiency of the plant. The poor fuel balance is caused by a particle rope, a dense area of particle stratification that creates an area of high fuel density that is not easily divided by the splitter boxes.

The objective of this work is to develop devices to improve the fuel balance at splitter boxes. The work involves an investigation into existing devices and station geometries to see why existing devices have not become commonplace in coal-fired power stations. It also involves conceptual design of devices and then their testing, both computationally and experimentally. Finally, the devices are assessed for their suitability for full-scale power station implementation.

This thesis used both experimental and computational techniques to develop devices to overcome the problems at splitter boxes and successfully produced several devices that could be developed and deployed in full scale testing.

Contents

Appendix B - **Settings for CFD simulation**
Appendix C – **Moving Plate Paper**
Appendix D - **Tables of results for experimentation**

Contents of Figures

Contents of Tables

Nomenclature

τ_p	Response time of the particle
τ_f	Response time of the fluid
ρ_p	Particle density (kg/m^3)
d	particle diameter (m),
u	conveying velocity (m/s)
μ	dynamic viscosity of the conveying medium (kg/ms)
D	pipe diameter (m)
g	Acceleration due to gravity (m/s^2)
Re_d	Reynolds Number based on pipe diameter.
ρ_f	Density of the Fluid (kg/m^3)
D	Pipe diameter (m)
St	Stokes Number
Fr	Froude Number
BTU	British Thermal Units
AFR	Air to Fuel Ratio

Chapter 1

Introduction to the Project

1.1 Preface

This thesis describes the process undertaken to solve the problem of poor pulverised fuel splitting at pipe junctions in coal-fired power stations. The work is motivated on a range of real cases presented by various coal-fired power stations in the United Kingdom.

Pneumatic conveying is a common means of efficiently transporting granular materials and powders during industrial process. In coal-fired power plants, pneumatic conveying is employed to transport pulverised coal from a number of mills to several burners at the furnace wall.

For reduced pressure loss, a single conveying pipe is used before subsequent bifurcation or trifurcation (or in some cases quadrafurcation) to distribute fuel to individual burners. Typically pipe diameters are 660mm, made of steel and lined with ceramic tiles.

The air velocity in the pipes tends to vary from approximately 16m/s to as high as 26m/s in some power stations. However, certain requirements for running means that the velocity rarely drops below 20m/s. It is known that at lower air velocities explosions can occur. The air to fuel ratio tends to vary between 1: 1 and 3: 1 depending on the individual power station and other internal factors such as: fuel type, power demands and localised splitting data.

The conveying air constitutes around 20% of the total air required for combustion; the remaining air is supplied at the furnace, all burners receive the same quantity of air. However, due to phase mal-distribution and stratification at the splitting points, fuel ratios can be uneven across the furnace. This results in the production of harmful carbon monoxide and NO_X emissions through inefficient combustion, higher levels of carbon in the ash and increased fuel costs.

The mal-distribution in the pneumatic conveying pipeline is normally caused by poor splits. This poor splitting is caused by stratification in the pipe network, which is caused by the momentum effects of bends in the pipe network. A common stratification phenomenon observed in much of the work undertaken for this thesis is that of particle roping. A particle rope is essentially a dense

area of particles that act as a third phase in the pneumatic conveying pipelines. The particle rope will tend to comprise a significant proportion of the particulate material in the pipe.

The thesis attempts to introduce concepts and devices that tackle the problems of stratification, with particular attention to "rope flow" before a pipeline split and hopefully deliver a 50/50 split by mass.

1.2 Introducing Pulverised Fuel fired power plants

It may seem to the laymen that pulverised fuel (PF) research was resolved centuries ago in the time of James Watt and Robert Stevenson. It is instead a constantly changing industry based heavily on advanced retrofitting of western stations to improve efficiency and research into developing more efficient and cleaner systems for new stations. This can be seen by looking in the references section of this thesis to see how recent research has been carried out on the subject. This makes the study of PF an exciting and cutting edge area of research.

Whilst PF maybe seen as a dirty fuel and more at home in the industrial revolution than in the 21st century, it is being touted by the Government's own white paper on emissions (HM Government, 2003) and a DTI report (DTI, 2006) into the future of energy production in this country as still a major contributor to the energy requirements of this country as far in the future as 2030.

Pulverised Fuel is the term given to any fuel source that is ground or otherwise reduced to a powder for combustion. Whilst the most common example is coal in coal-fired power stations, paper, biomass and wood chips are amongst the various fuels that are pulverised for use in combustion.

The use of other fuels is important as using renewable sources of PF (such as biomass) is one of the many ways of slowly moving away from our dependency on fossil fuels as a fuel source. The percentage of other fuels added to pulverised coal is considered, including the increased likelihood localised mill combustion (mill pops) due to the increased percentage of volatiles in the pulverised fuel. The use of biomass as PF is important as carbon cycle-wise no new carbon is being released into the atmosphere, as new biomass will need to be grown to replace that which is being used in combustion. (European Commission, 2004)

The decline in the use of PF is not linked to the lack of fuel, but from self imposed emissions targets put in place by the Kyoto Agreement and the cost in comparison to constructing Gas-fired power stations of similar sizes. If current power stations can be cost effectively retro-fitted to increase efficiency and reduce CO_2 emissions then PF-fired power stations are likely to remain in place.

The work undertaken for this thesis focuses on this goal, increasing the efficiency of PF-fired power stations with a view to not only wasting less fuel, but in reaching emissions and efficiency targets imposed by legislation and government policy. The specific area of efficiency tackled is that of powder balance at splitting faces.

1.3 The use of Computational Fluid Dynamics in pipe flow.

The use of Computational Fluid Dynamics (CFD) is widely used in modelling pipe flows (Miller et al, 2000). Whilst it has not yet become mainstream in the industry it is used heavily in research. The CFD methodology chapter will explain the theory and use of CFD systems and the Literature review will also detail previous CFD carried out on pneumatic conveying.

CFD work had been carried out previously at the University of Nottingham on both pneumatic conveying and the combustion of coal. The techniques employed in these previous studies verify that CFD is a viable tool in researching pneumatic conveying and modelling coal. (Giddings et al, 2004)

The work undertaken for the thesis took this work and developed it and employed new techniques and methods of solving cases that had only been touched upon in previous studies. The CFD used for this project used far more detailed models than previously used by this research group.

The use of CFD was invaluable in the study as it allowed cases and situations to be modelled that couldn't otherwise be tested in the test facilities available at the University of Nottingham. CFD also allows quick and effective parametric studies to be undertaken on a certain device allowing zero cost optimisation of a design.

1.4 The use of experimental rigs at the University of Nottingham.

The University of Nottingham has several rigs designed to test the various aspects of coal combustion. The experimental used in this project was the 1/4 scale metal rig. The rig has been used in the past for other projects related to the subject matter of this thesis. Familiarity and improvement to the rigs were a major part of the work undertaken in for this thesis.

The 1/4 scale test rig was constructed by Greenbank Terotech Ltd. It is purpose built to simulate the transport of coal-laden air in a power station. The rig is described in detail by Giddings et al 2001. The rig is modular and can be arranged into a variety of different arrangements.

The main focus of the rig is the ability to measure the amount of particulates that go down each leg of the split. The rig is designed to be able to fit both a bifurcator and a trifurcator splitting device. The rig utilizes load cells and a Labview programme to calculate the splits.

1.5 Aims

In any piece of work a set of aims or objectives should be set out at the outset. These aims will change as the work develops and they should not be seen as rigid pillars of the work. However, it is good to have a starting point and a direction in which to head when embarking upon a piece of work such as this.

The first aim of this work was to create a validated CFD model a pneumatic conveying pipeline. This validated model could then be applied, with adaptation, to industrial scale scenarios and used in industrial case studies.

The second aim of this work was to develop several devices to attempt to solve the problem of powder imbalance at splitter boxes in pneumatic conveying networks. These devices must be viable for industrial situations and take into account industrial conditions.

The final aim of this work was to design devices that can be manufactured and turned into successful products for industrial scenarios. The industrial scenarios are detailed in the industrial application section of this work.

1.6 Approach

The approach to successfully completing the aims of this project is multi-facetted. The work will contain a combination of computational and experimental modelling of devices. The devices will be developed based on industrial knowledge and previous studies. In addition to modelling real industrial cases will be used to both get a feel and to debut the devices created in this work. Finally the devices will be investigated and ways of optimising the devices will be attempted.

Chapter 2

Literature Review

2.1 Preface

The field of pneumatic conveying is broad; it requires the detailed examination of various techniques and procedures. A wide range of sources have been investigated in an attempt to gain a full understanding of the problem. Information was required, not only on previous attempts to solve the problem, but also on the various techniques required to measure, observe and predict the flow of the pneumatically conveyed particulate.

The literature review is divided into sections. First a historical background of pneumatic conveying will be considered. The next section will discuss the nature of coal and its various properties and different types of coal. The next section deals with pneumatic conveying systems and phenomena. Following this are sections on experimentation, computational and numerical techniques. The chapter is then finished off with a conclusion to the literature review.

2.2 Historical Context of Coal

The industrial development of Europe in the 19th century led to the birth of pneumatic conveying processes. The first recorded use of pneumatic conveying was in 1847 in the Peugeot plant of Valentigney, France. It was used for dust extraction from grindstones in the plant. (Molerus, 1996) The British Patent for "Improvements in grinding, preparing and burning coal" in 1868, the so named Crampton patent (Molerus, 1996) was another reported case. The Crampton patent can be considered to be the first coal conveying pneumatic system. This case shows how coal fired processes and pneumatic conveying have been interlinked since coal started becoming an industrial power source. Further, the problems of early pneumatic conveying are the same problems that are faced at present.

These problems include high power consumption, high erosion rates and particulate stratification. The Crampton patent was not exploited because gas was an easier fuel to manipulate at the time and because of the gasification of coal into town gas. This delayed for some time the first pneumatic conveying systems in energy producing coal-fired power stations. The only major

difference between Crampton designs and modern plants is that Crampton designed individual pipes from the mill to each burner; whilst most modern plants have a single pipe that splits before the burners to reduce loses due to friction.

The pneumatic conveying continued to be used in a variety of different industrial applications. In the early twentieth century pneumatic conveying pipelines were used as a mail delivery system by some companies (Liu, 2004). They transported mail, parcels, and messages within buildings in the same way as an internal phone system or email system transfer messages.

Modem pneumatic conveying began in the United States and was utilised to move grain quickly between silos and mills. Following World War 2 European countries started to rebuild their infrastructure employing many pneumatic conveying in many industries (Pacific Pneumatics 2002).

In the United Kingdom Power generation began in privately owned stations which were warehouses containing all the electricity generating equipment (British Science Museum, 2005). These were used almost entirely for lighting of perhaps a few dozen homes. The first electricity generators, designed by Thomas Edison, came into use in 1882 in both London and New York providing a DC supply to perhaps a mile radius.

DC supplies, due to transmission losses, were not acceptable and in the early 20th century Charles Parsons resolved the problem by inventing the AC generator driven by a steam turbine. The steam turbine in its various forms is the cornerstone of electricity generation. The steam was produced by taking a fuel (usually gas or coal) and using it to heat a boiler. In 1904 the First coal fed power station "Carville A" was commissioned for Tyneside.

The major coal fired power stations in the UK and the rest of the world use pneumatic conveying to transport the coal from the mills to the burner- face. Most modern coal fired power stations were designed and constructed in the 1960-1970s (Drax Power, 1989). The huge capital investment required to build new power stations means that the current power stations are constantly being refitted in attempts to meet with the increasing demand for power output.

2.3 The Nature of Coal.

Coal is the altered remains of prehistoric vegetation, which originally accumulated in swamps and peat bogs millions of years ago. After settling, the material is compacted by movements in the Earth and it is then subjected to great pressures and elevated temperatures over a period of millions of years to become coal.

Coal can be divided into 4 groups, these grouping relate to how much metamorphosis or coalification has taken place on the decaying vegetable matter (Smoot, 1993). The process of coalification' is the changing of peat to graphite through application of pressure and time. The different types of coal represent stages in the progressive coalification process:

- The first type is called Lignate or "brown coal" (Figure 2.1). It is similar to peat and tends to have high moisture content as well as a low heating value when compared to other coals, between 1.91 MJ/kg and 19.26 MJ/kg. The carbon content is low in comparison to other coals, typically between 25-35%.

- Sub bituminous coal (Figure 2.2) is the second type and has a carbon content typically between 35-45%. It has a lower moisture content than Lignate but still have a relatively low heating value, 19.26 MJ/kg and 30.17 MJ/kg.

- Bituminous coal is dense and brittle (Figure 2.3). Its moisture content is low and its volatile content varies from type to type. The carbon content is typically between 45-86%. There are several recognisable types of bituminous coal. Bituminous coal tends to have a high heating value, 24.37 MJ/kg to 35.98 MJ/kg.

- Anthracite coal is the highly metamorphosed coal (Figure 2.4). It is Jet black and both hard and brittle. Its moisture content is minimum and its carbon content is high, typically 86-98%. It has a high heating value, 35.98 MJ/kg.

The coal is usually ground (pulverised) to a fine powder, so that less than 2% is >300μm and 70-75% is below 75μm, for a bituminous coal. This is done so that it can be conveyed pneumatically by air to the burners. The pulverised coal is blown with part of the combustion air into the boiler plant through a series of burner nozzles. Secondary and tertiary air may also be added.

Combustion takes place at temperatures from 1300-1700°C, depending largely on coal rank. Steam is generated, driving a steam turbine. Particle residence time in the boiler is typically 2-5 seconds, and the particles must be small enough for complete burnout to have taken place during this time.

The technology is well developed, and there are thousands of units around the world, accounting for well over 90% of coal-fired capacity. Pulverised coal combustion can be used to fire a wide variety of coals, although it is not always appropriate for those with high ash content (World Coal Council, 2000).

Figure 2.1- Lignite

Figure 2.2 - Sub-Bituminous Coal

Figure 2.3 - Bituminous Coal

Figure 2.4 - Anthracitic Coal

Two broadly different boiler designs are used. One is the traditional two-pass layout where there is a furnace chamber, topped by some heat transfer tubing to reduce the furnace exit gas temperature. The flue gases then turn through 180°, and pass downwards through the main heat transfer and economiser sections. The other design is to use a tower boiler, where virtually all the heat transfer sections are mounted vertically above each other, over the combustion chamber.

The relative advantages and disadvantages almost balance each other out. Tower designs have been favoured recently in Europe. They result in taller structures, and this is one reason why they are not used in Japan, which is in an earthquake zone. It is thought to be preferable to reduce the height of structures there wherever possible (World Coal Council, 2000).

There are variations in the positioning of the burners in the combustion chamber, and designs are offered which use:

- Wall-mounted burners on one side
- Opposed-fired wall mounted burners, or
- Tangential burners in the corners or on the walls

When the particles enter the furnace, radiated heat releases the volatiles from the coal. The volatiles are mainly methane, although other volatiles can be held in coal (Smoot,1993). These gases serve as the primary fuel for the combustion; the char (the remaining coal) burns at a lower rate serving as a secondary fuel.

The efficiency of the combustion is governed by the degree of mixing of the volatiles and the oxygen (contained in air) into the furnace. Excess air however can cause the formation of NOx gases. Nitrogenous species, other than molecular nitrogen, are usually harmful to the environment (Smoot, 1993). NOx gases are formed in the flames of the burner banks by three main mechanisms (Giddings, 2000):

- Fixation of molecular nitrogen by oxygen produced at high temperatures (in excess of 1400°C). This is called Thermal NOx
- The oxidation of nitrogen contained in the fuel during the combustion process. This is called Fuel NOx.
- The attack of hydrocarbon free radicals on molecular nitrogen producing a NOx precursor. This is formed in the flame zone and is known as Prompt NOx

The source of the nitrogen varies; with 80-90% of the NOx gas produced is Fuel NOx (Fokeer, 2003). The remaining 10-20% is thermal NOx and prompt NOx. Controlling the amount of excess air supplied to the burners can reduce the thermal NOx. Part of being able to control this is providing an equal amount of pulverized fuel to each burner.

Although coal at present contributes about 36% of fuel for electricity generation, other burnable fuels such as biomass, waste paper and tyre chips have recently been forming an increasing share of the market. In 1987 this formed about 1 % of the total fuel supplied for electricity production, now rising to over 5%. The use of renewable fuels in tandem with coal is one way that coal fired power stations are contributing to the reduction of hazardous emissions. (Carbon Trust, 2006) This is because Carbon neutral materials do not add carbon into the Carbon Cycle, shown in figure 2.5.

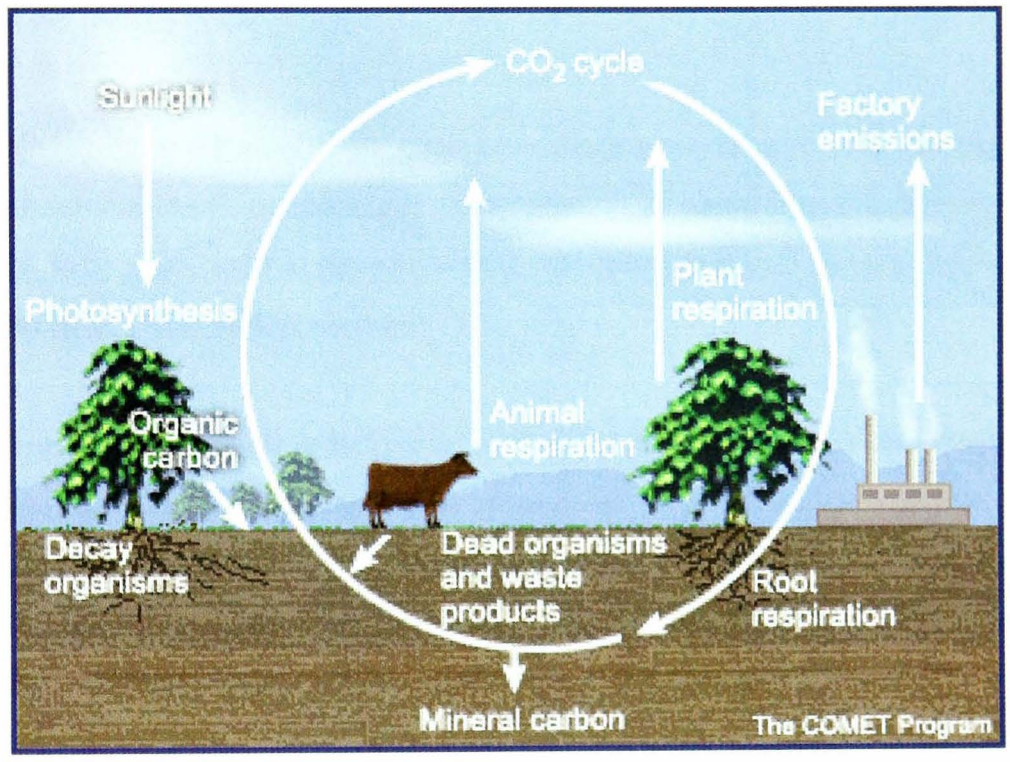

Figure 2.5 - Carbon cycle.

The Carbon Cycle is the cycle through which elemental carbon is moved through the biosphere. Carbon is only removed from the cycle through mineral carbon and it is only added by its combustion. When resources like wood, grown specifically for combustion, are used as fuels the Carbon released in combustion becomes trapped in new trees and then burn again, hence no Carbon is added to the Carbon cycle. At present the use of alternative fuels is low, it is likely to increase so that coal-fired power stations can attempt to improve their efficiency.

2.4 Pneumatic Conveying systems and phenomena

2.4.1 Pneumatic conveying regimes

Due to the importance of pneumatic conveying in industrial processes, many authors have attempted to define and codify what is essentially a complex system. One way of codifying pneumatic conveying is to break down the large field into smaller regimes, which exhibit different behaviour and structures. A simple way of dividing pneumatic conveying regimes is done by breaking into two broad categories: lean phase and dense phase conveying (Fokeer et al, 2003).

Lean phase conveying is frequently the most cost-effective method of transporting granular and pelletised products such as flour and sugar. In the lean phase conditions the solid particles behave as individually, fully suspended in the gas, whilst aerodynamic forces govern their motion. These regimes tend to have a low Stokes number.

Dense phase conveying is found in industries such as coal fire power stations (the subject of this thesis); cement factories and drug and food processing. It is particularly suitable for high rate transport as particle mixing and segregation is not important in the flow. In dense phase transport the particles are not fully suspended in the gas. The motion of the particles is dominated by particle-particle collisions. These regimes tend to have a high Stokes number.

A different method of categorising pneumatic conveying is considered by Pan et al (Pan et al, 1999). This method divides all pneumatic conveying into three regimes:

- Smooth transition from dilute to fluidised dense-phase,
- Dilute-phase, unstable zone and
- Slug flow and dilute phase only.

Pulverised coal flow is in the smooth transition from dilute to fluidised dense-phase but often in the dense phase regime. It tends to have air to fuel (AFR) ratios higher than 3:1. It has a high stokes number and is dominated by particle-particle interactions. In dense phase pneumatic conveying three different regimes can be identified in describing the dispersion of the solid phase. These are Homogenous, Stratified and Roped. The dense area is known as a particle rope. The three regimes are shown in figure 2.6.

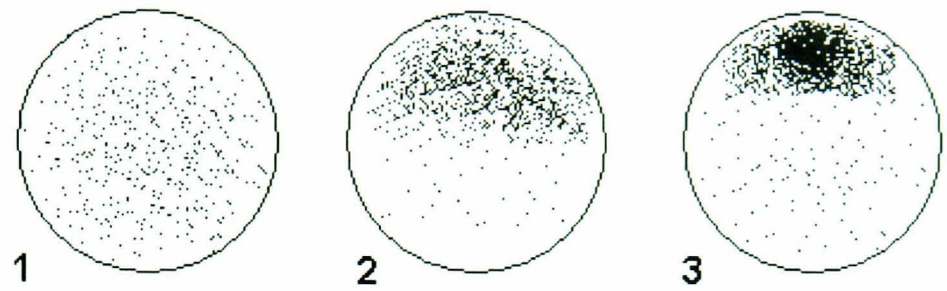

Figure 2.6 - The three pneumatic conveying regimes in dense phase; 1) homogenous, 2) stratified and 3) roped flow.

Homogenous means the particles are dispersed equally around the cross section of the pipe. A Stratified regime means that there is a bias with one area of the pipe cross section being more densely occupied by particles than the other, Roped flow means that the particles are concentrated in a small area of the cross section. The rest of the cross section is sparsely populated by particles,

2.4.2 The Effects of Bends on Pneumatic Conveying

Bends are necessary for pipe networks but cause problems for pneumatic conveying systems. When a fluid passes through a curved path it is subjected to force acting radially inwards on the fluid to provide the inwards acceleration. There is therefore an increase in pressure near the outer wall of the bend, this corresponds to a reduction in pressure near the inner wall. This creates an adverse pressure gradient. It is this adverse pressure gradient that leads to the secondary flows witnessed after a bend. The adverse pressure gradient is also responsible for the energy loses that arise from pipe bends (Massey, 1998).

The secondary motions in pipe bends are said to arise due to the response of a viscous element to an imbalance between the centripetal acceleration and cross-stream pressure gradient induced by lateral curvature of the main flow (Levy et al, 2001). This results in the axial velocity profile being distorted and the point of the velocity peak being shifted towards the outer wall of the pipe, this is shown in figure 2.7.

In pipe networks in power stations single 90° bends are common. More common are several bends close together. These double bends can create some interesting secondary flows. Further more bends spanning other angles are common as the pipe network is often constructed to fit

through existing structures.

The effect of two double bends perpendicular to each other has been reported by (Schallart et al, 2000). U-bends and S-bends, which occasionally appear in power station geometries, have been investigated heavily in heat exchangers where they commonly appear. The present author investigated the known phenomena arising from double bends. (Roberts et al, 2004).

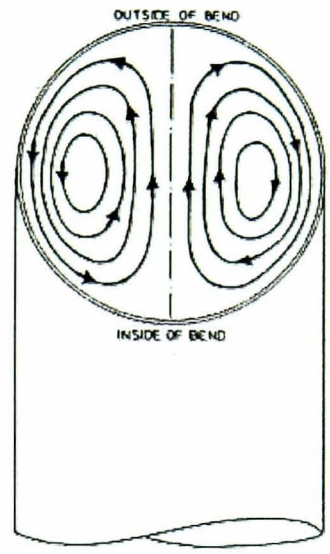

Figure 2.7- Secondary flow pattern

Particulate ropes are formed at pipe bends, with the larger particles having greater inertia and concentrating towards the outside of bend radii creating stratified mixtures and severely affecting splitting ratios at subsequent junctions (Akilli et al, 2001). The particle rope is described as an area of relatively high particle concentration formed by either inertial or gravitation forces. From vertical to horizontal bends it has been shown that the velocity of the particles in the rope tends to have a velocity of approximately one third of that of the airflow in the bend (McCluskey et al, 1989).

The rope acts as a third phase in the pipeline travelling at reduced velocities and increasing erosion, often taking up to 100 pipe diameters to completely disperse (Akilli et al, 2001). It tends to be affected less by secondary flows and changes in flow direction than its constituent particles. Particle roping has been identified as a major problem by the power generation industry and it is one of the primary concerns fuel balancing at splits (Cook and Harworth, 1980), figure 2.8 shows a particle rope. Poor splitting means excess air need to be implemented into the boiler with can lead to increased production of NO_X gases. In addition to the problems with splitting, rope flow at

burner tips creates unstable flames and leads to poor reaction of solids.

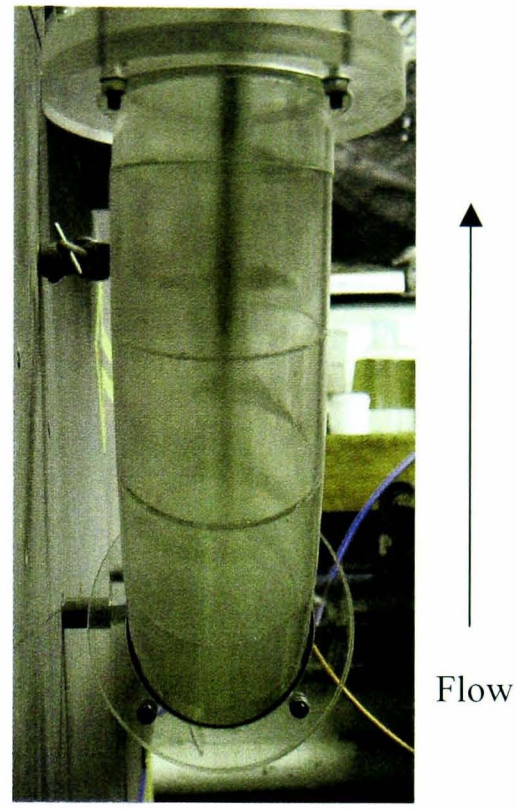

Figure 2.8 - The formation of a particle rope.

2.4.3 Interaction between particles and fluid

The particles in a two-phase gas/solid flow interact in a variety of ways. The process of pneumatic conveying gives the air particles momentum, which they then impart to the solid phase, conveying them. Pick-up velocity of the conveying gas is a measure of the amount of momentum that needs to be imparted to the conveying gas to move the solid phase.

The pick-up velocity is the minimum velocity required for the fluid medium to pick up and convey the particulates from rest. The pick up velocity is an effective way to assess the conveying behaviour of bulk particles (Cabrejos et al, 1994). The author suggested that the pick up velocity of a particle is proportional to the square root of particle diameter and particle density to the three-fourth power. He also noted that the pickup velocity is inversely proportional to the square root of the gas density. This implies that larger particles and heavier particles are difficult to move.

It has also been reported that smaller particles are not always more easily picked up (Hayden et

al, 2003). This work shows that for small particle diameters, the pickup velocity is not affected by changes in particle size (up to 20 microns) or the particle density; instead the particle pickup velocity is governed by the balance between lift forces and the attractive force, in the form of London-Van Der Waals forces, between the particle and wall.

Logic would dictate that particles of larger diameters (and therefore mass) are harder to move. However, from Hayden's work it can be seen that this is a rather simplistic view that seems to exclude other forces other than inertial forces. As such Hayden's work shows that there is a minimum pick up velocity for particles, which increases greatly for smaller particles where electrostatic forces have more effect on the overall movement of the particle than the inertial effects.

Particle size and particle shape both affect the overall turbulence of the flow field in a pipe (Ljus et al, 2002). Larger particles affect the turbulence more so than smaller particles. The paper also states that particles shape is an important factor in the effects on turbulence. From observation it was determined that spherical particles reduce turbulence close to the wall, whilst increasing turbulence in the centre of the pipe. Investigations into non-spherical particles in the same study show that non-spherical particles decrease turbulence across an entire pipe cross section.

Particulates in pneumatic conveying can be acted upon by the secondary flows generated by the bends in the pipes (Bilirgen et al 2001, Schallart et al 2000). In roped flow this normally occurs when particles in the particle rope lose momentum through collisions and then are able to be moved by the airflow. This explains the way that a rope slowly disperses (Schallart et al 2000) with a secondary flow.

Still considering the work of Schallart it can be seen by experimental results that different secondary flows disrupt the particles in different ways. A single bend producing the double vortex pattern leads to the particulate being spread around the outside either side of the pipe, whilst a large concentration of particulates stays in the centre of the flow. A double bend produces a strong single vortex that pushes the powder to the outside of the pipe and eventually spreads it around the wall like a food blender. Secondary flows do aid the disruption of the rope. However, it is the particle collisions in the rope core that lead to them losing momentum and being influence by the fluid phase.

2.4.4 The effects walls on pneumatic conveying systems

The walls of pipes in a pneumatic conveying system can affect a pneumatic conveying system in a number of ways. The different mechanisms involved generally influence the two components of the two-phase flow; namely the solid phase and the fluid phase.

Interaction between particles (solid phase) and the walls tends to vary from almost perfectly elastic collisions to entirely plastic collisions. In coal based pneumatic conveying, the walls of the pipes are often lined with basalt or similarly hard materials. The collision of particles and walls can often cause the degradation of particles.

The wall collision frequency has a direct effect on the pressure drop in pneumatic conveying as well as reducing the momentum of particles (Sommerfeld et al, 1999). Wall roughness greatly affects the frequency of wall collisions, as do non-spherical particles. When a particle strikes a wall it loses energy and bounces, the angle and velocity components of the bounced particle depend on a number of factors including the wall roughness and the physical properties of the particle and wall (Sommerfeld, 1998). Interaction between the air (fluid phase) and the wall tends to be a drag relationship.

2.4.5 Splitting devices and on-line monitoring

Fuel distribution is a key factor in allowing optimum combustion on large coal fired utility boilers, whether for NOx reduction, combustion efficiency or a NOx reduction strategy involving over fire air systems.

The particle roping phenomenon causes non-uniform distribution in situations where a gas/solid mixture needs to be split (Marcus, 1984). Any device designed to alter the split will need to take into account the particle rope, which has been identified to be responsible for unbalanced splitting at junctions in pneumatic conveying pipelines.

It is generally accepted, within the power generation industry, that front and opposed wall fired boilers implementing over fire air improvements require all burners to have a fuel flow within 10% absolute to achieve optimum results. This requirement comes from the need to take air off

the burners and to either re-direct or inject boosted air into the top of the furnace to stage the burn and reduce generation of thermal NOx.

The stoichiometric ratio of individual burners becomes very important when reducing secondary air to the burners, which for many older generation boilers comes from a common wind-box often with limitations on distribution and control.

Some plants with Selective catalytic reduction (SCR) for NOx control need to have optimum fuel balance across the boiler and even combustion balance in order to prolong the life of SCR catalysts. In SCR systems, ammonia vapour is used as the reducing agent and is injected into the flue gas stream, passing over a catalyst. NOx emission reductions over 80-90% are achieved. The optimum temperature is usually between 300°C and 400°C. This is normally the flue gas temperature at the economiser outlet.

Consequently, there has been a consistent need for technologies that allow even coal distribution to the burners, which then allows an easier task of distributing air evenly across the burners allowing better, controlled reduction of secondary air to the burners for over fire air staging of combustion.

The mal-distribution of PF to the burners is evident on many boilers with large differences in combustion properties across the boiler, or differences in burner flame characteristic. In more difficult applications, differences in fuel distribution can result in partially blocked pipes where long horizontal pipe runs exist and in extreme cases totally blocked pipes and extinguished burners.

The nature of power station design has seen many different pipework configurations utilising a pulverising mill to feed typically 4 to 8 burners, with each station often having a unique layout of PF pipework and geometries to transport the PF to the burners.

The poor distribution of PF comes from roping of PF, where PF twists and concentrates itself inside the pipe and then does not distribute itself evenly when presented with 2,3 or even 4 exits form the original PF pipe.

Historically, many power stations have moved to multiple pipes (4-8) exiting directly from the

classifier of the mill, although the resulting distribution often shows little improvement over the original design with splitting pipework from the mill. This is due to mal-distribution of PF when exiting the classifier to 4-8 pipes. Some plants have reverted back to using splits in the pipe from multiple pipes exiting the mill.

It is therefore imperative that novel methods are found that would allow the controlled distribution of PF at power station bifurcations, trifurcations and quadrafurcations. These methods, active or passive, need to accommodate vertical and horizontal splits and incur acceptable pressure losses.

In the United Kingdom, the Department of Trade and Industry (DTI) has launched seven individual studies, since 1990, into the use of splitting devices in an attempt to assess their potential and the level to which they are used in the power generation industry (DTI, 2001). This DTI report shows that there are many devices already in use for this purpose, which having varying degrees of success. Devices have been split into two main categories: Fixed-geometry and variable geometry devices.

2.4.6 Fixed geometry devices

Fixed geometry devices represent the simpler end of the market. They consist of a device put in place permanently and whose geometry is rarely changed. This suits most power stations or industrial processes.

The most commonly seen examples of this type of device are the "riffle packs" and "egg boxes", shown in figure 2.9. Riffle packs and egg-box type arrangements have been proven to give the ±5 % split performance required by many stations when applied in applications away from bends in the vertical. These designs simply splice up the cross sectional area and divide it left and right for a two way split. The riffle is often preceded with an "egg box" which is a chequer board of small ramps designed to split up the rope. This is because the riffle pack works better when the particulate passing through it are reasonably spread and this is what egg boxes are able to do. The most common riffle is the CERL developed by the Central Electricity Research Laboratories in the 1960s (Snowstill, 1968).

The effectiveness of the riffle pack is a function of its location with respect to bends / coal roping

phenomena and how tightly / close together the riffle packs are applied. In general, there is a limitation on the close packing of riffles based on the pressure drop. This is of special concern to plants that have limited Jim capacity or suffer from pipe blockages with long horizontal stretches of pipework and do not wish to add additional pressure drops to the pipework.

The other important factor is one of wear, with riffles often performing poorly in the latter half of their service, and in many cases making distribution worse with a localised hole, due to erosion on the front of the riffle, causing biasing of coal flow down a particular leg (Figure 2.9). Riffle plates or dividers are often made from Nickel hardened steel, as a plate type grid structure is required. Localised wear of riffles is exacerbated by concentrated PF or roping from a prior bend directly impacting the riffle plates. This can be a major factor in combustion performance.

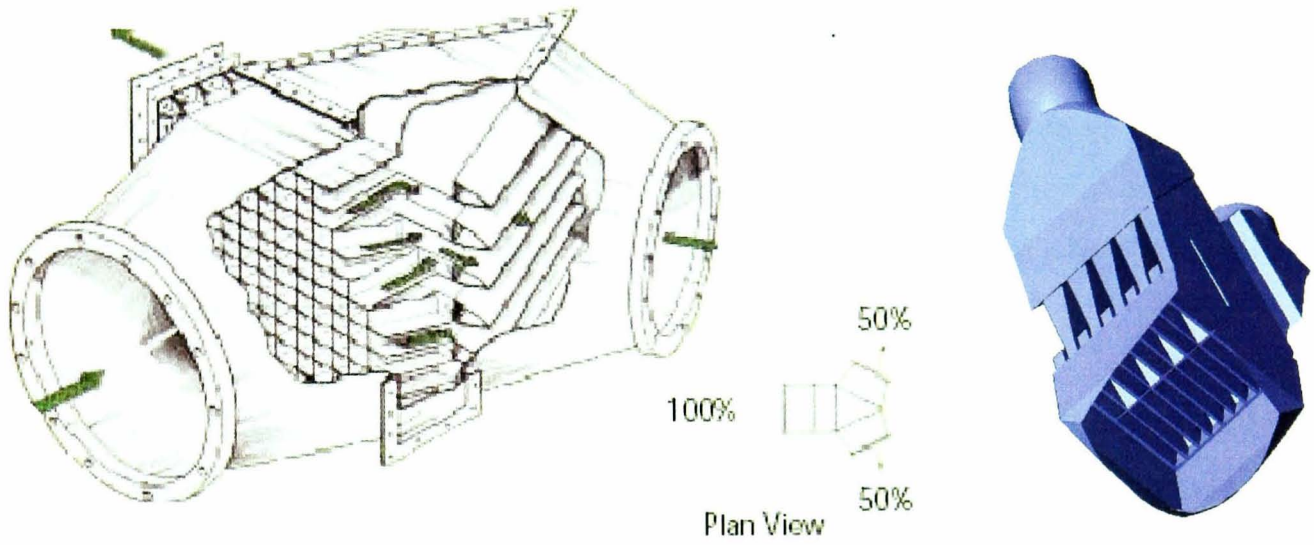

Figure 2.9 - CERL riffle and egg box bifurcator, insert shows rear view.

Normally riffles are applied for two-way splits in the vertical plane, and in many cases sit on top of each other to give one to four way splits. Riffles for three-way splits are also possible; again issues of abrasion wear and pressure drop are the main factors to be considered against the expected performance improvements. Hence, many stations do not have riffles, due to the issues listed above, or would like to remove them if similar performance can be achieved using a non-intelligent static solution that could give longer life, lower pressure drop and maintain split performance between scheduled maintenance.

Another common device employed is the "rope-breaker". The rope-breaker is the name given to any generic ramp or vortex generator. These devices work by deflecting the rope or breaking it. Whilst effective, they are not universal, poor logic can mean that rope breakers can be misplaced

in the pipe work.

Many companies and research groups have attempted to solve this problem and search for an illusive universal solution to the problem using a static device [Holmes et al 2000, Biligren et al 2001, Hilbert et al 1984, Macphail et al 1983)]. Quite often the devices are installed on a trial basis to see if the split is improved downstream.

Whilst static systems can prove effective, an intimate knowledge of rope dynamics in pipe systems is required. Amongst the devices tried are: ramps, vanes, swirlers, riffles and orifice plates, some devices are shown in figure 2.10. None of these devices have become an industry standard. Quite often misplacement or misalignment can lead to a low effectiveness of an otherwise excellent idea.

To describe the full range of static devices that have been tested or in use is far beyond the scope of this document. Instead a description of how most of these devices work seems preferable. Static devices fall into to two categories; particulate altering and flow altering. A small number of devices are designed to do both, whilst in many cases a device designed to do one, often ends up performing the other to a lesser extent.

Particulate altering devices work on the principle that moving the rope itself by deflection is the way of disrupting the particle rope. Usually it involves moving the particle rope to strike a splitting device (such as a trifurcator), this can incorporate gathering the rope to hit the splitting device. Another method is to attempt to spread the rope before a splitter. Essentially these methods tend to just include an obstruction to the flow, which induces mixing. The flow inducing devices are designed to induce fluid motion in the hope of disrupting the rope through fluid motion.

It had been considered that in the mass of the particle rope, the particles within the rope structure are not affected by fluid flows (Cook et al, 1979). This means that rope breaking devices designed to move a rope through secondary flows or alteration of the conveying fluid will have to look to moving the entire mass of the particle rope, not just the individual particles. This means that in order to disrupt the rope you have to be able to affect the entire mass of the rope.

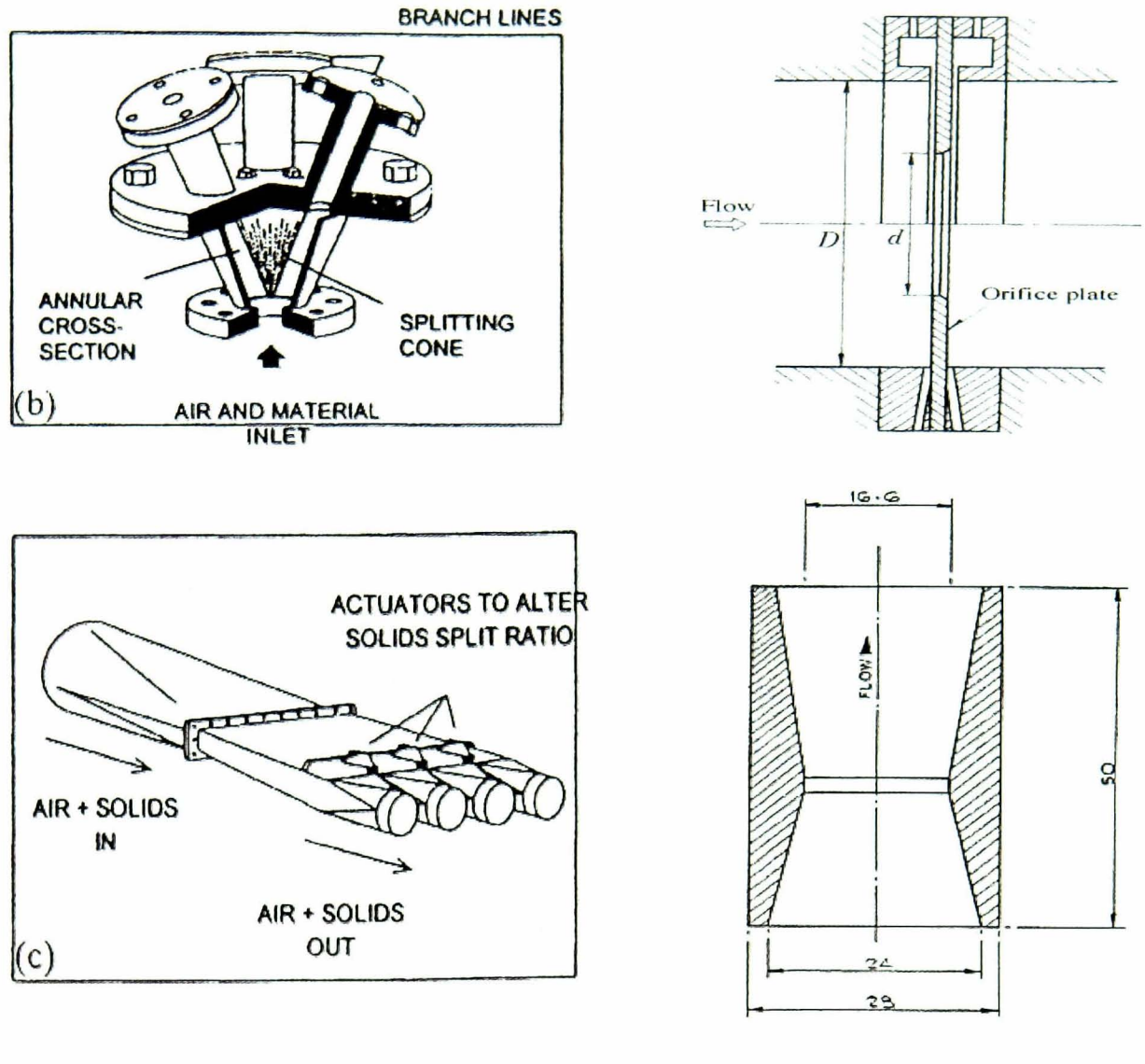

Figure 2.10 - A selection of other devices from the top left clockwise: a splitting cone, an orifice Plate, a venturi and automated splitting veins.

A serious device therefore has to change the momentum attained by the rope as it travels through the pipe network. These devices often have high blockage ratio and high-pressure drops across them. Fixed geometry devices suffer from a few general problems:

- The design is optimised for a single operating condition.
- Performance varies with wear,
- The distribution cannot be adjusted online.

2.4.7 Active systems

Active systems (or variable-geometry systems) are less common in power stations. An active system involves some mechanism being activated, dependent on some reading downstream of the

split. Some example mechanisms are moving ramps or plates, introducing backpressures to the pneumatic system (Holmes et al, 2000). These systems can be very crude or very complex, but the key to these devices is measurement. Accurate measurement of splits is needed for any active system to be effective. Such a system would be a feedback system to allow it to adjust itself based on the downstream split information.

Work on basic splitting devices (such as a simple moving plate) has been investigated by Levy. (Levy et al, 1998). This work requires an online value for the current splits in the pipe network so that devices can be altered.

Numerous methods of metering and controlling the two-phase mixture exist. Like many flow problems, a metering system for PF should be unobtrusive and robust. Methods ranging from laser sheet measurements, Laser Doppler Anemometry and Capacitance tomography have been employed. These techniques often run along side conventional methods such as Iso-kinetic sampling, rotor-probe sampling and simple mass collection. The following sections attempt a concise overview of the various techniques available.

2.5 Experimentation

2.5.1 Preface

Power station trials for new splitting devices are often not possible because of access, cost and risks. Test rigs were developed by numerous academic and industrial researchers to facilitate the transition from concept to product. This section details some of the facilities and gives an insight into the importance of scaling and experimental techniques appropriate for this work.

2.5.2 Dynamic similarity and scaling criteria

Laboratory experiments on PF conveying must be conducted on correctly scaled rigs. It is inconceivable to always construct test rigs at full scale, but a scale model has to be able to give useful results. This means preserving all the relevant dimensionless numbers, which in this case are Reynolds number (Re), Froude Number (Fr) and Stokes number (St).

The Reynolds Number (Re) is the ratio between the inertial and vicious forces in the conveying medium. Usually in the range concerning pneumatic conveying the inertial forces are dominant. As long as the Reynolds number is well into the turbulent regime it is not important to pay close attention to its value (Macphail et al, 1983):

$$\mathrm{Re}_d = \frac{\rho_f u D}{\mu}$$ **Equation 2.1**

The turbulence region is considered to be when $\mathrm{Re}_d > 2000$ (Massey, 1998)

The Froude Number (Fr) represents the ratio of the inertial forces to the gravitational forces. It is usually defined as:

$$Fr = \frac{u^2}{gD}$$ **Equation 2.2**

The Stokes Number (St) represents the ratio of the particles inertial forces to the drag forces acting on said particle. It can also be considered to be a ratio between the aerodynamic response time of the particle and the characteristic time of the fluid. It is defined as for a pipe:

$$St = \frac{\tau_p}{\tau_f} = \frac{\rho_p d^2 u}{18 \mu D}$$ **Equation 2.3**

For a given flow regime, a small Stokes number (<<1) implies that the inertial effects are small and that the particle will rapidly respond to changes in fluid motion. A large stokes number (>>1) indicates that the particle motion is independent of the carrier gas flow as they will not be able to respond to changes.

From these equations it can be seen that it is very hard to get a situation where all the dimensionless number matched to those in a real power station (Macphail et al, 1983). The most common way of scaling dense phase suspended flow is to use the average stokes number (the Stokes number of the average particle diameter) and the concentration of the particulates in air (i.e. the air to fuel ratio) (Crowe, 1998). Cook and Hurworth (Cook et al, 1979) suggest that the Froude number is dominant because it relates to gravity and settling of powder in pipe networks.

The type of particle used in an experimental rig should also be considered. The differing ratios between the particle diameters, the wall roughness and pipe diameter could prove important. It

has been argued that it is not necessary to scale particles and that once the rope has been formed the particles do not behave individually; instead they operate as a collective mass. By scaling an experimental rig by Stokes number, the relative effects of the fluid flow on the particle arc taken into account. A variety of different particles have been used in scaled test facilities, ranging from coal dust (Macphail et al, 1983) to glass beads (Giddings et al, 2004).

2.5.3 Measurement Techniques

Numerous methods of metering and controlling the two-phase mixture exist. Like many flow problems, a metering system for P.F. should be unobtrusive and robust. Methods ranging from laser sheet measurements, Laser Doppler Anemometry and Capacitance tomography have been employed. These techniques often run along side conventional methods such as Iso-kinetic sampling, rotor-probe sampling and simple mass collection. The following sections attempt a concise overview of the various techniques available.

Numerous laser techniques are employed in various experimental set ups. Three of particular interests are Particle Image Velocimetry (PIV), Laser Sheet Visualisation (LSV) and Laser Doppler Anemometry (LDA). Key to these experimental techniques is their non-intrusive nature. PIV works by introducing tracer particles into a flow field and tracking them by use of images taken with a camera. These images are then processed using various algorithms to calculate particle velocity. This process is used for pneumatic conveying at the University of Nottingham.

LSV can also be used to illuminate areas of high particle density; once again an area is illuminated with a laser sheet. An image of this sheet is then taken by a camera. The image is then analysed using software to threshold areas of high particle density. Laser Doppler Velocimetry (LDV) is used extensively by some researchers, particularly researchers at Lehigh University. (Yilmaz 1998). The work of this university is detailed below.

PIV (Dantec, 1997) is a measurement technique for obtaining instantaneous whole field velocities. In PIV the property actually measured is the distance travelled by particles in the flow within a known time interval. These particles are added to the flow and known as seeding.

The type of seeding particle is chosen to follow the flow, and in order to detect their movement, an area of the flow field is illuminated by a light sheet. The laser is pulsed to produce a

stroboscopic effect, essentially freezing the image of the particles in time for the duration of the pulse. The position is detected with a CCD-camera (CCD - charge coupled device) that is positioned at right angles to the light sheet and synchronised with the laser pulse to capture the image at the correct time. From a series of images taken close together, the course of a particle can be tracked. Figure 2.11 shows a schematic of the experimental set up of a PIV system.

The PIV systems used at the University of Nottingham consists of two Nd:YAG 150mJ pulsed laser is used to generate laser light sheet at 532 nm at 15 Hz pulse frequency. The use and maintenance of the lasers is detailed in their instruction manuals (Quantel, 1997). The camera used is a Kodak Megaplus 1M pixel CCD camera that is set up to grab the image. The set up usually consists of the lasers and camera system link to a Dantec processor. The Dantec processor runs a piece of software called Flowmap.

PIV has been used to investigate pneumatic conveying systems by several authors. For PIV to work correctly you have to be able to distinguish individual particles. In a particle rope, the particles are no longer distinguishable as individuals even with laser light. PIV only works at low load densities (Jakobsen, 1996) when the particles can be picked up as individuals rather than a dense cloud. When this occurs algorithms designed for tracking particles are unable to work, as the programme's logic is unable to distinguish particles.

In pneumatic conveying systems the particulate is often moved by the secondary flows as well as momentum from bends etc. (Schallert et al, 2000). PIV requires a plane within which the particles lie, if the majority of particles are moving through the plane rather than along it, the plane can be obscured, particularly in dense flows.

The development of digital photography has aided PIV techniques. It eliminates time consuming photographic development periods. (Grant, 1997) This allows many multi-image and multi-step procedures to be taken as well as allowing instant knowledge of whether the images are coming out well or there has been some error in the set up.

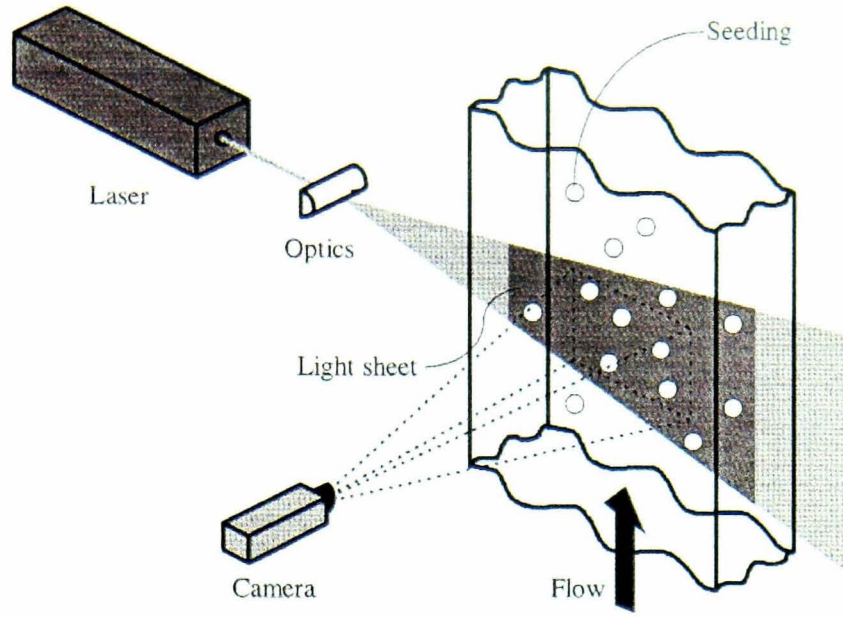

Figure 2.11- Schematic of a PIV system (Dantec, 1997)

Some researchers at the University of Nottingham (Giddings et al, 2004) used LSV to measure the splits in a pneumatic conveying system. The data from the laser sheets were captured by a camera and digitised into computer images. From this, image-enhancing software was used to conduct a pixel count. This would give an indication of the split and allow the splitting device to be moved to improve the split. The University of Nottingham team proposes to implement a feedback loop that allows automatic control of the plate via the data from the laser sheet images. (Giddings, 2003) High speed video cameras used in combination of LSV can be used to investigate the dynamics of the rope during operation.

The LDV measurement technique allows simultaneous measurements of particle and gas velocities by adding small tracer particles to the flow. This method employs the Doppler effect. Laser light is emitted from an optic into the flow through a clear barrier. The laser light is then reflected into a set of transducers. The data from their transducers then uses cross-correlation algorithms to calculate particle velocity. From the intensity of the reflection the transducer is able to measure the particle concentration across the cross section area of the pipe. The data gain from the experiments can be placed in graphical form and compared with other running conditions at the same point, or predicted results from a CFD package.

The work at Lehigh University involves using a reflective fibre-optic measurement system. (Yilmaz et al, 1997) This method allows LDV to be taken at any point with viewing port, by simply taking the probe there. The fibre optic probe has also been used in experiments to detect

the different splits caused by various pneumatic splitting points. The results then allow the implementation of orifice plate and other devices to alter the airflow and therefore the PF flow in a particular leg of the splitting device.(Schallert et al, 2000). Much of the work of Lehigh University utilises the LDV techniques and its application to new PF problems.

A relatively new process used in modem pneumatic conveying plants is electrostatic measurement. It is common, in solids pneumatic transport, for the conveyed solids to develop charge. (Cheng, 1996). The electrification is caused by (Coulthard et al, 1997):

- Frictional contact charging
- Charge Transfer from one object to another
- Charging of a conductor by inducement due to the presence of a nearby charge.

Electrostatic measurement devices therefore are able to measure the current due to:

- Charging due to particles striking the inner surface of the probe.
- Charging due to the inducement when charged particles pass within the vicinity of the probe but do not actually come into physical contact with it.

During operation of a test facility the current detected can be considered to be proportional to the concentration. Whilst not a value that can be used universally to simply calculate a solid load, it can be used to compare the split of the same material between several pipes. This means that electrostatic measurement is particularly useful in pneumatic conveying splits for comparing the relative flows. (Masuada, 1994)

One commercial available electrostatic measurement product, currently on the market, is the pfmaster from ABB. The Pfmaster has been tested by several studies (Coultard, 1997, Cheng, 1997). The Pfmaster is used in a variety of UK power stations for the purpose of flow balancing. Figure 2.12 shows a standard set up for the Pfmaster. Uses of devices similar to the Pfmaster devices could be utilised with active splitting devices and allow the automatic actuation of some device in the pipe to affect the split. Accuracies for this sort of device have been quoted to within 1-2% (DTI, 2001)

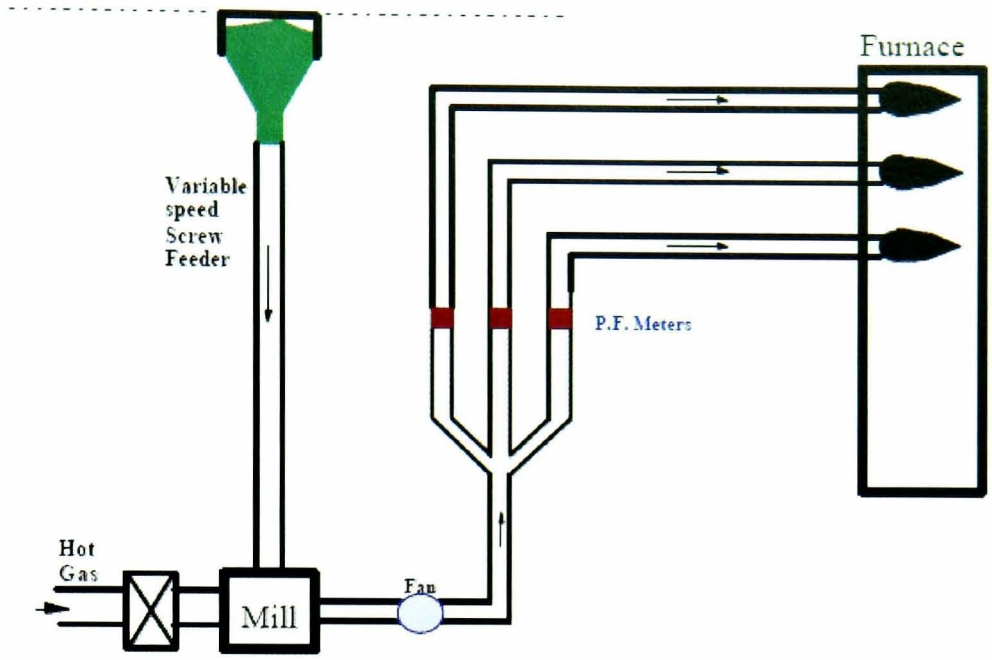

Figure 2.12 - Set up for a standard PFMaster metering set up.

The use of sound to measure the amount of particles in a pipeline has been used in the petrochemical industry for sometime (DTI, 2001). Passive acoustic sensors measure the sound generated by moving particles impacting on the pipe wall. A high frequency range is measured to attempt to eliminate any noise in the system (such as any mechanical noise etc.) An active acoustic system uses an ultrasonic signal and then measures the amount of absorption.

The Clampon device is a good example of a passive acoustic sensor (Clampon Pamphlet 2000) the device has a sense installed after a bend when the majority of the particulate is concentrated next to the wall in the form of a particle rope. From here it measures the amount of noise generated and compares it to calibrated information. This sort of device is said to be accurate to 7.5%.

The CSIRO device is a good 'example of an active acoustic system. The measurement technique is based on the ultrasonic transmission at 60kHz through the PF pipe. The set up of this system uses Doppler shift theory to calculate the velocity of the particles in the pipe. (Tallon, 1999)

A Range of extractive methods exists for pneumatic conveying systems. These represent intrusive techniques that physically sample the two-phase flow for their information. Procedures such as iso-kinetic sampling and rotor probe sampling are examples of extractive methods. These are common sampling techniques in modem power stations.

Rotor probing consists of taking a probe that rotates through the cross section of the pneumatic conveying pipe. It normally consists of two tubes with multiple holes that extract particles at certain points. The two tubes rotate at different radii so as to cover more area of the pipe. The probe is usually inserted after a split. The relative measurement of the powder collected allows a measure of the effectiveness of the split to be made. Automatic versions of the rotor probe system can exist (DTI, 2001). However, it is designed as a portable test rather than an online measurement device.

2.5.4 Experimental test facilities

MacPhail (MacPhail et al, 1984)) investigated the phenomena of particle roping and suggested possible solutions to the problem. An experimental rig was constructed to test hypothesis and device ideas. The experimental rig was constructed from metal piping with a clear glass pipe section including a bend. The cross section of the pipe was a 100mm and used pulverised coal dust as the particulate material. The work focused on scaling the rig according to running conditions in three large coal-fired power stations. This work highlights the importance of accurate scaling for meaningful experimental results. Without scaling, it is impossible to know whether the same phenomena would occur in a full-scale pneumatic conveying set up.

Giddings (Giddings et al, 2002) carried out work on the quarter scale rig at the University of Nottingham. This rig will form part of the work being conducted in the current research so all previous studies on it are very important. The rig is quarter scale and consists of steel pipework designed with clear Perspex sections that allow the use of laser sheet visualisation. The rig is adaptable to several different configuration.

The 1/4 scale rig has been successfully used for observing behaviour in two-phase flow (Giddings et al, 2004). This experimental study suggests that once the particle rope has been formed, the position is determined by the wall conditions imposed on the model due to the low air velocities in the boundary layer. This work suggests that in order to control the split, the position of the rope must be controlled by either moving the rope away from the wall or moving the wall-bound rope into a pre-determined position. The configuration and operation of this rig are dealt with in the methodology section of this thesis.

The work of the Energy Research Centre, at Lehigh University USA, is of great interest (Biligren,

et al 2000, Yilmaz et al, 1997, Akilli et al, 2001). The pipe loop at the University has a 0.154m bore like the rig at the University of Nottingham. It the system is closed loop and consists of two 6.1m horizontal pipes and a 304m riser fixed together in a vertical U bend. At the end of the U-bend is a cyclone for extracting the smallest particles. The rig has a range of 15m/s-30m/s. The measurements are taken from the fibre optic LDV procedure described in the measurement section. The Lehigh test facility operates with coal powder as opposed to a particle to model coal. The rig also doesn't seem to be scaled to power station conditions.

2.6 **Computational and numerical**

The main computational method that will be looked at in the course of the work will be Computational Fluid Dynamics (CFD). CFD is the analysis of systems involving fluid flow, heat transfer and associated phenomena such as chemical reactions by means of computer-based simulation. (Verstaag, 1991) The code used throughout this work is Fluent 6.x, from Fluent.Inc.

An important part of CFD usage is confidence in the results and many authors often carry out investigations into the most suitable model to use (Levy et al 1998) based on available computational power, time available and required accuracy.

Levy (Levy et al 2002) carried out investigations into the suitability of their respective codes with the use of validation experiments. Validation of a specific CFD model is vitally important. The set up and validation for the CFD models used in this thesis is presented in the methodology chapter along with a brief description of how CFD works. However, there are several CFD investigations made by various authors that of interest and these are described below.

Frank (Frank et al, 2002) details a full CFD simulation of the University of Nottingham's 1/4 scale rig. It presents a 3-dimensional Eularian-Lagrangian approach developed by Frank et al. Frank's work concerns itself with the effects of particle-wall collisions and focuses on their important in two phase flow. Frank's work uses an in house CFD code, which is reasonably advanced and runs on a cluster of PCs designed for solving this type of problem. This study shows that CFD can accurately predict velocities and particle densities. It also shows the relevance of applying CFD to the existing 1/4 scale rig.

Giddings (Giddings et al, 2002) details an investigation into the effects of altering the wall

conditions on a numerical model. This did not concentrate on modelling the wall roughness, but instead the co-efficient of reflection in the normal and tangential plane. These co-efficients range between 1 and 0 and represent the amount of momentum conserved in that direction in a collision. The author used the positions of concentration based on LSV results and compared them to CFD results with different combinations of the two co-efficients of reflection. Whilst the work does not lead to a perfect solution it highlights the importance of particle-wall conditions in CFD modelling.

Mason (Mason et al, 1998) carried out a range numerical and computational studies on pneumatic conveying pipelines. The focus of this work was to see the effects that bends had on the concentration of particles in bends. The CFD programme used was PHOENICS from CHAM Ltd. UK. The study shows that CFD programmes are able to successfully model both rope formation and dissipation in a computationally model pipe network. This is useful to this work as the concentration of this work will be the formation and dissipation of particle ropes.

Chapter 3

Experimental Methodology

3.1 Preface

This section describes the experimental methodology undertaken. All the experiments in this work were carried out on the University of Nottingham's quarter scale pneumatic conveying test facility described below.

This rig is able to model the conditions in coal-fired power stations. These allow actual scale models of possible devices to be tested accurately, their effects on particulate splits could be assessed and the results related to real power station conditions.

This chapter is divided into different sections. The first section is a description of the rig and its functions. The second section presents information about the particles chosen for the experiments. The third section describes the LabVIEW programme used in the experimental facility and how it operates. The fourth section will deal with dynamic similarity of the quarter scale rig. The section will end in a conclusion on the experimental methodology.

3.2 Quarter Scale Test Facility

3.2.1 Overview

The one-quarter-scale test facility was constructed in association with Greenbank Terotech to model the flow of coal in a pneumatic conveying system. The facility is constructed from steel pipe lined with basalt. Clear glass and Perspex sections have been included to allow observation of the conveyed material.

The facility is modular and can be arranged into a number of scenarios to allow both bifurcator and trifurcator cases to be considered in both horizontal and vertical. A schematic of the rig operation is shown in figure 3.1.

The facility has on -line split readings from weigh hoppers and adjustable velocity to accurately scale the rig to model the conditions in real life coal -fired power stations. The test facility runs on negative pressure so in the event of an air leak in the pipe work; air is drawn into the system preventing powder being released. The operation of the facility is carried out using a PC running software written in LabVIEW.

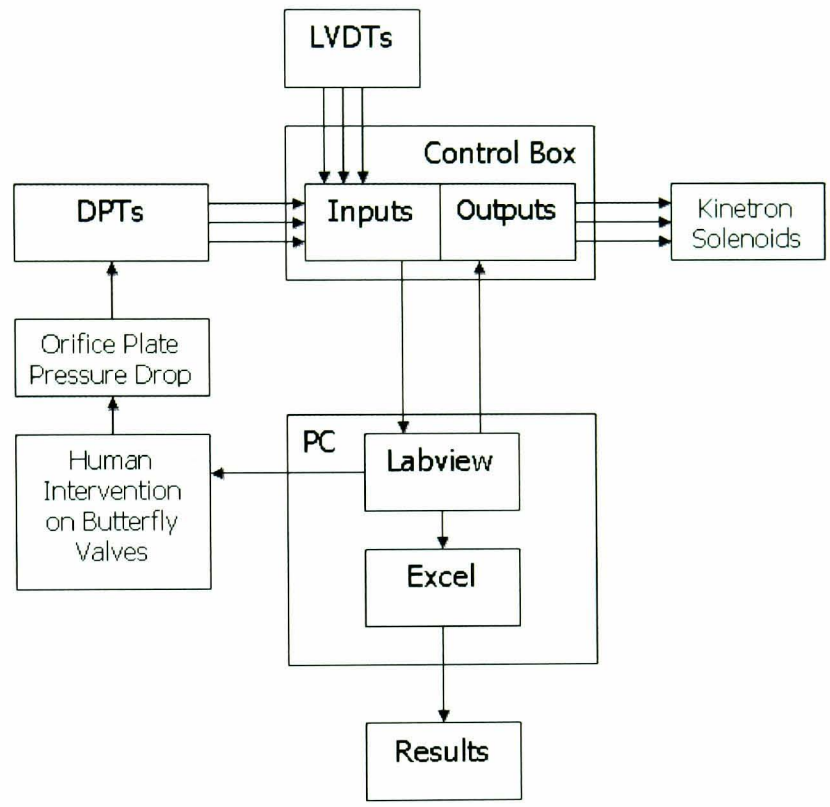

Figure 3.1 - Overview of quarter scale rig.

3.2.2 Description of the Test Facility

The main aspects of the test facility are shown in figure 3.2. The air for the rig enters the facility from inside the building; this limits temperature fluctuations between tests. It is drawn in through a meshed pipe opening, which extends for about a pipe diameter. From here the air follows the pipe network until it reaches the rotary feeder.

The powder starts in the main hopper, above the rotary feeder. This hopper can be filled from a port located at its top. A ball valve is positioned on the main hopper to act as a pressure release. The particulate is fed from the hopper through the rotary feeder.

Figure 3.3 shows the storage hopper clearly and figure 3.4 shows the schematic for the rotary

valve. The feed rate is set as a frequency of rotation on the feeder's control panel. The design of the rotary feeder has been selected to minimise the pulsing effect of the particulate flow from the hopper. The duel bucket arrangement provides a more continuous particle feed.

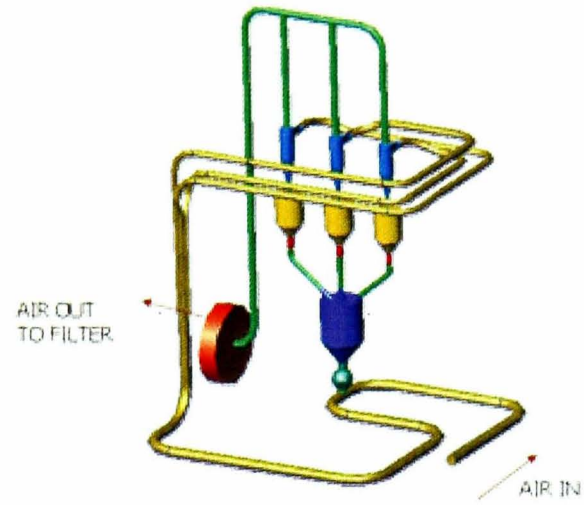

Figure 3.2 - Outline of the experimental facilities.

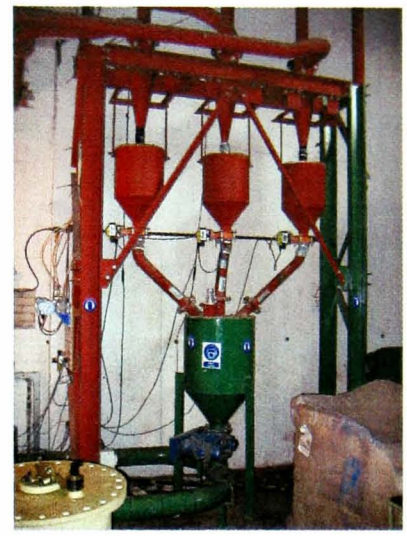

Figure 3.3 - Storage hopper and weigh hoppers

The driving fan is centrifugal in design; it is a Howden HD76K direct drive centrifugal fan. It is driven by an electric motor and regulated via an ABB controller. The maximum fan speed on installation was 25 m/s. However, due to wear over time, the maximum safe operating velocity of the rig is now reduced to around 18m/s.

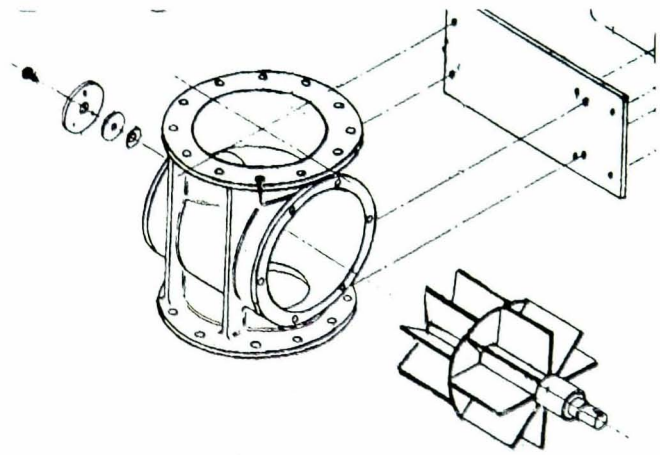

Figure 3.4 - Schematic of the rotary valve

The two -phase mixtures of air and particles continue through to the test section. The test section is the area of the bend where devices are installed in an attempt to improve the split. The test section is constructed from Perspex piping to allow viewing of the device in action.

After the test section the pipe network splits into smaller pipes, the splitter can be either a bifurcator or a trifurcator depending on the power station scenario that is being investigated. Either of the splitter types can be used in any of the pipework scenarios. A photo of the bifurcator is shown in figure 3.5 and a photo of the trifurcator is shown in figure 3.6. The bifurcator has a transparent area into which a riffle-box splitting device can be inserted.

Figure 3.5 - Bifurcator for the test facility

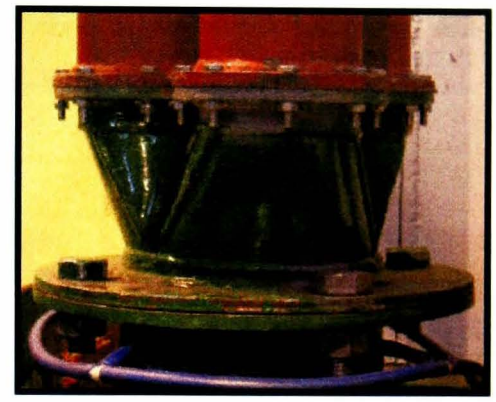

Figure 3.6 - Trifurcator for the test facility

The velocity in each of the pipes after the splitter is controlled by butterfly valves someway downstream of the split. The relative velocities have to be balanced before tests take place. The velocities can be read off from the Labview programme. Following the split, the smaller diameter pipes travel back outside and the flow is restricted by an orifice plate in each pipeline. The pressure drop across the orifice is fed back to the PC via a Rosemount Differential Pressure Transducer (DPT) and converted to a velocity.

The flow then continues to the cyclones. A cyclone at the end of each pipe separates the air from the particulates. The air outlet from the cyclone passes through a filter to remove the small particles before discharging into the atmosphere. The extraction unit has to be shaken between tests to remove clogged powder. The air is passed through a particle extraction unit and vented to atmosphere. The extraction unit draws the particles through the cyclone. The particles are removed by the extraction device leaving only air to escape to the atmosphere.

The separated particles from the cyclones empty into a weigh hopper. Each weigh hopper has a linear variable differential transducer (LVDT). These devices transfer a displacement of the transducer into a voltage that can be measured. The voltages from the LVDTs are sent to the PC where it is used by the Labview programme to calculate the mass flow rate and the mass collected. The levers holding the weigh hoppers are attached to a spring to return the hopper

position to zero after being emptied. During operation the readings from the LVDTs can be observed through the Labview interface.

The weigh hoppers are fitted with Kinetrol air valves on the bottom, which when opened allow the powder to flow back into the main hopper. These valves are controlled from the Labview programme. An electrical pulse sent from the programme can open or close the air valves instantly. The air valves can also be operated manually. When the rig is in operation, the valves remain closed so the particles can be weighed in the weigh hoppers.

3.2.3 Possible pipe configurations

The quarter scale rig can be arranged into a multitude of configurations. Two configurations were used in the course of this work. The first configuration, shown in figure 3.8, consists of a single 90° bend before the splitting device. The second configuration, shown in figure 3.9, consists of two 90° bends at right angles to each other before the splitting device.

3.3 Conveyed particles

Fillite particles are used in the test facility. These are silicate glass spheres; they are hard, inert and hollow. Fillite is primarily added into plastic, resins and rubbers to reduce the weight of objects constructed from these materials. The chemical composition of the hollow shell is approximately 65% Silica ($SI0_2$) and 35% Alumina (AI_20_3). The fillite hollow spheres are chosen for a number of reasons:

- No risk of explosion as with saw dust, flour and coal dust.
- The larger mean diameter allows better scaling according to Stokes number.
- Unlike some other powders, it is not an irritant on the skin or poisonous.

A Malvern Particle Size Distribution Analyser was used to characterise the fillite. This is important for the modelling of the rig in CFD. The used and unused fillite are shown in figure 3.10. The degradation of the particles over time is clear from figure 3.11. This shows that fresh powder will have a different Stokes number to that of used powder. The experiments are carried out with used powder, but only for a limited number of runs. This is done to try and maintain an average stokes number. The size analysis also shows the range of particles removed from the flow by the cyclone.

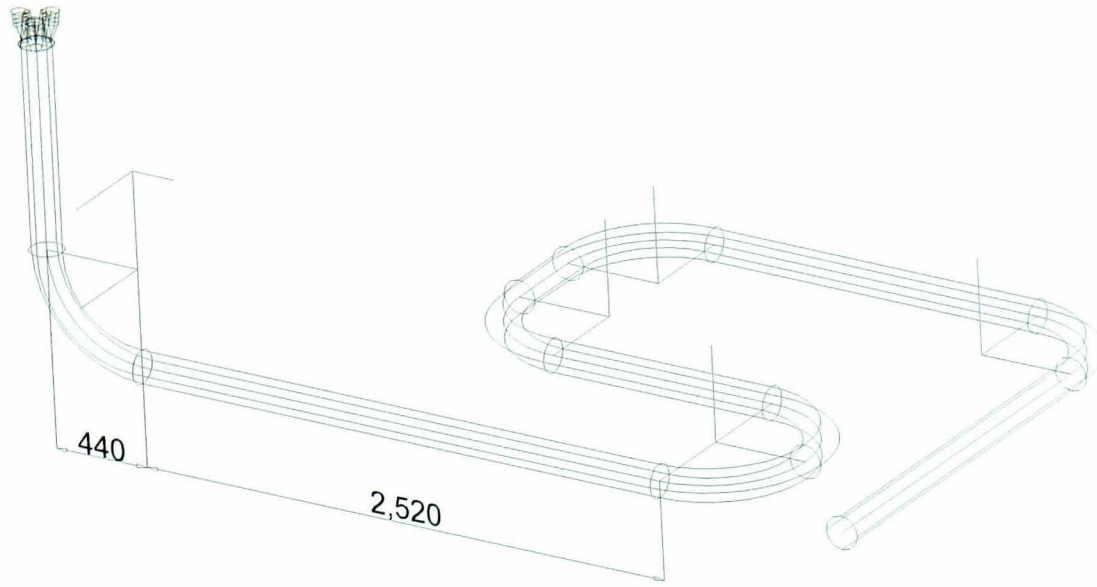

Figure 3.7 - Scenario 1

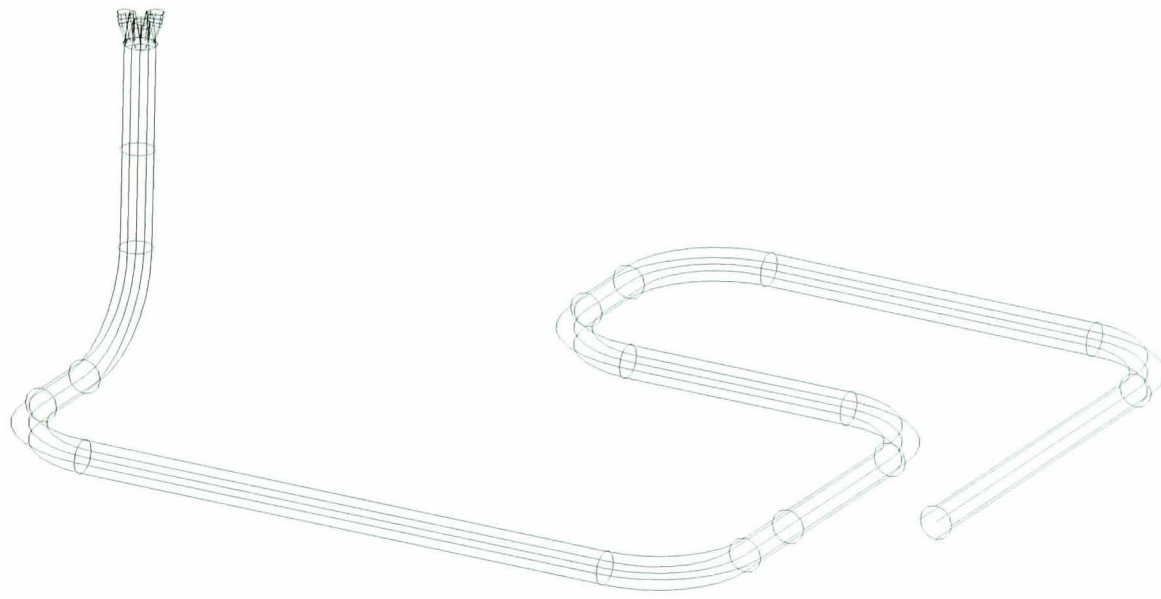

Figure 3.8 - Scenario 2

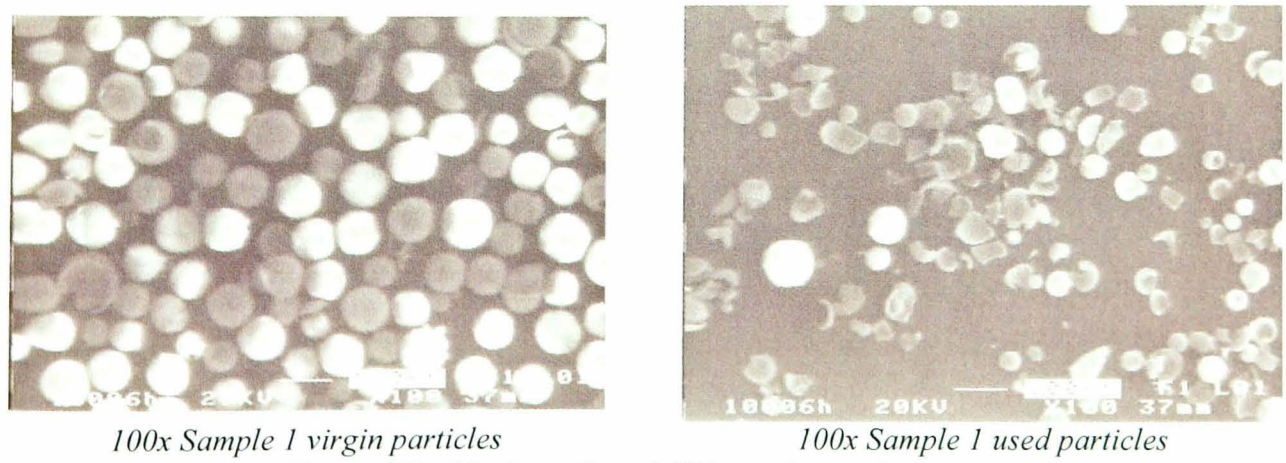

100x Sample 1 virgin particles *100x Sample 1 used particles*

Figure 3.9 - Virgin and used fillite under a microscope.

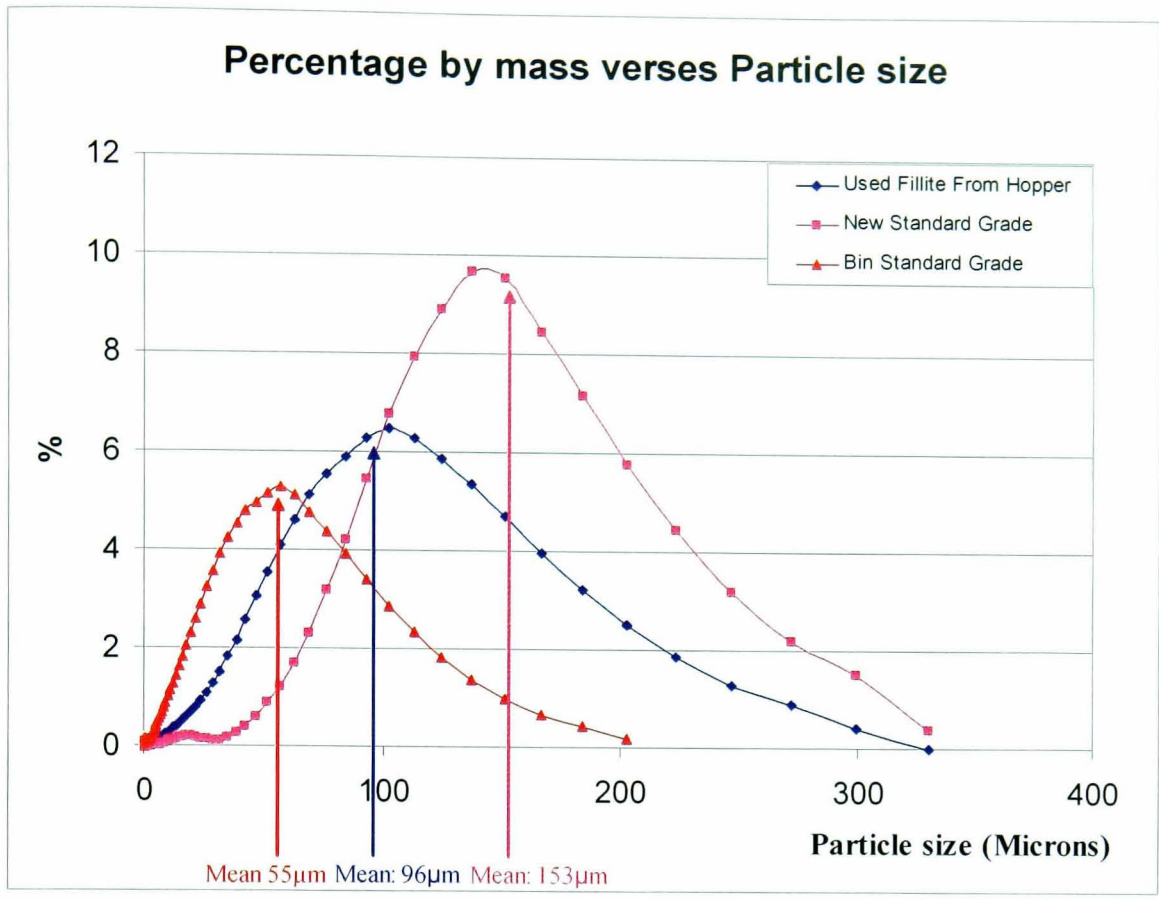

Figure 3.10 - Particle size distributions for fillite in the quarter scale rig.

The fillite tends to take about 20 test cycles or 5 minutes of continuous running to get the particles to the "used" standard. After that the particles can be used on about 30 test cycles before the mean diameter of the power begins to drop. The powder in the rig is changed every 50 test cycles. As the particulate degrade the mean particle diameter slowly drops, as shown in figure 3.11. The testing is only attempted whilst the particulate are on the plateau.

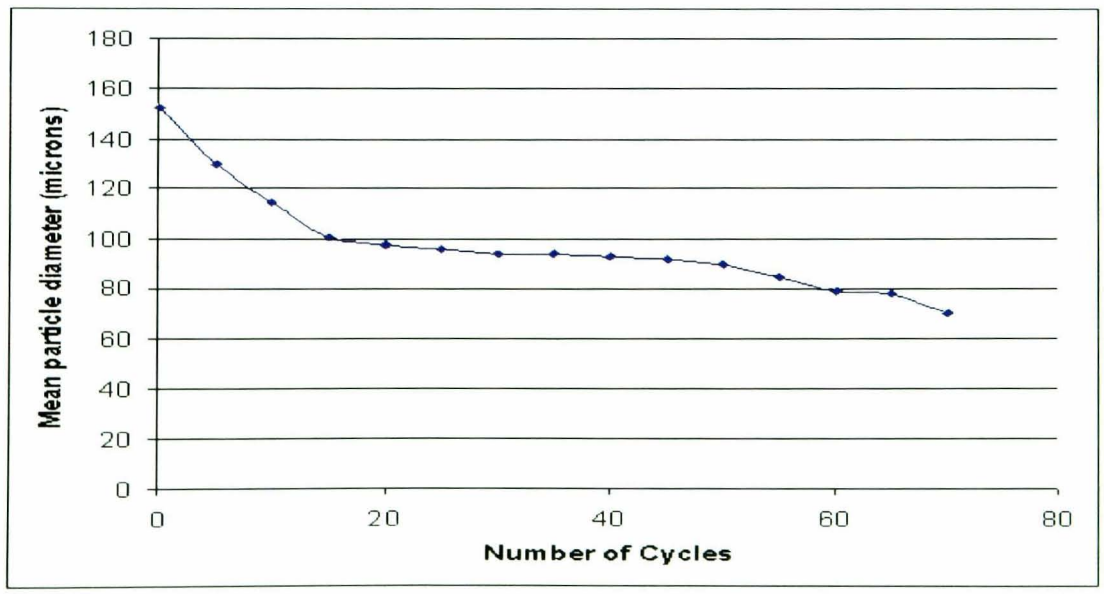

Figure 3.11 - The mean particle diameter degradation with the number of cycles.

The fresh particles are initially spherical and after being used for about 20 runs the particles begin to break up and become used, the loss of their spherical shape is shown in figure 3.12. Some of the particles are almost like eggshells or shards; this alters the characteristics of the powder going through the rig. This eggshell shape would have a higher drag co-efficient than a sphere. This would lead to an entirely different splitting characteristic in the same flow conditions.

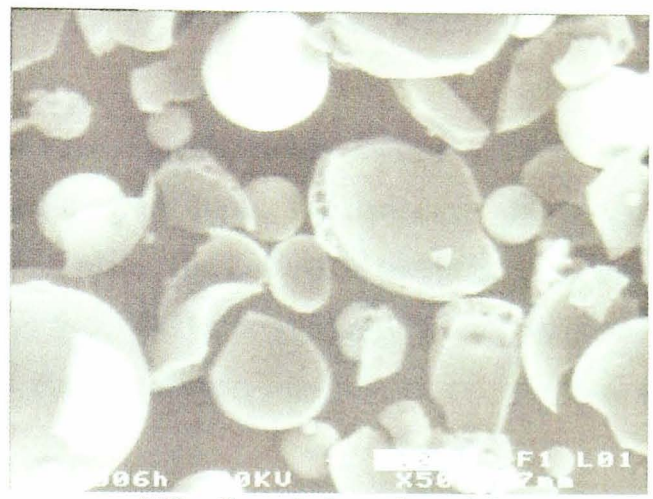

500x Sample 1 used particles
Figure 3.12 - Shell -like shards of the fillite.

3.4 Pressure Measurement

Pressure drop measurement in the pipe network is as important as the powder split information. It is important to have a comparison between the different splitting devices to be studied through pressure drop.

The additional pressure drop that a splitting device adds to a pipe network is one of the features that assesses whether a device can be installed into a power station. Many power stations have very tight levels of additional pressure drop they can allow; hence a device has to have as low a pressure drop as possible.

The quarter scale rig has a pressure drop measurement system installed into it. There are two rosettes of pressure tapings attached to the pipe network. Each rosette consists of 4 pressure tapings connected together by piping so as to measure an average pressure of the four tapings. The first rosette is after the bend where any device would begin. The second rosette is positioned just before the trifurcator. The distance between the centre points of the rosettes is 5 pipe diameters. These two rosettes allow the pressure drop across the test section to be measured. The pressure drop of a device is calculated by taking the pressure drop with the device in and

subtracting the pressure drop of just a straight 5 pipe diameter test section.

An electronic manometer is used to measure the pressure drop across 5 pipe diameter section. The average value for the duration of an experimental test is outputted and recorded for each test. There is a ±1 % error on the electronic manometer.

3.5 Labview programme

Labview is a graphical programming language, as opposed to a text-based language, used to create programs in a block diagram form. The language allows the construction of a virtual instrument with a virtual front plate. The LabVIEW programme for the rig is shown in figure 3.13 and the front plate is shown in 3.14. The programmer simply drags and drops blocks to represent the virtual instrument and then links them together with inputs from the Data and Acquisitions (DAQ) card.

The Labview construction program contains the following:

- Extensive library of functions
- Library for data acquisition
- Data presentation
- Data storage

The Labview programme controls and monitors a range of functions on the quarter scale rig. There are two programmes that are needed to operate the rig. The first programme monitors the various readings from the DAQ card, amongst its functions are:

- It monitors the signals from the LVTDs and converts the voltage into a mass based on previous calibration using weights. It both displays the raw voltage reading from the LVTD as a graph and stores the converted mass information in the output spreadsheet.
- It monitors the signals from the DPTs and converts them into velocities. It displays the velocities and also calculates the 6" pipe velocity from the 4" pipe velocities. It also stores the velocities in the output spreadsheet.
- The computer measures the time passed for the experiment. It both displays it and outputs it in the output spreadsheet.

The second Labview programme allows the control of the Kinetrol valves allowing the weigh

hoppers to be emptied remotely.

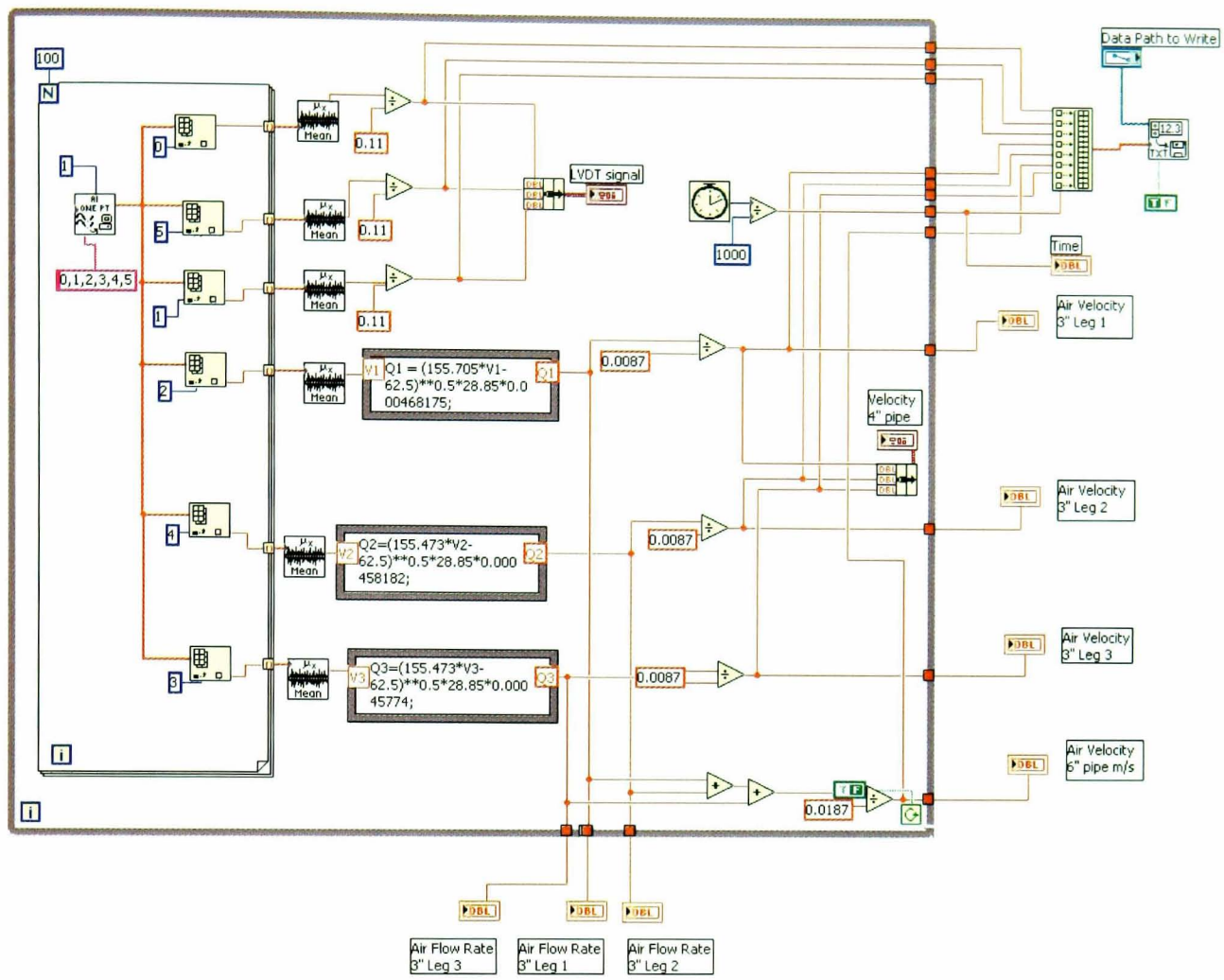

Figure 3.13 - Layout of the main LabVIEW programme.

The Labview programme interfaces with a control board, which takes the form of a PCI board in the PC. This connects to a DAQ control card into which all the inputs from the various transducers are fed and the outputs leave to the various devices. The acquisition card is positioned in its own box that is connected to the PC. The DAQ card takes voltages from the inputs to the card and reads them as signals in the LabVIEW programme.

The Labview programme is designed to take a hundred samples a second from the inputs and present an average voltage over that time. Mathematical controllers and expressions are then used to convert these raw voltages into the measurement they indicate.

3.6 Dynamic Similarity

3.6.1 Scaling of the quarter scale rig

Scaling and dynamic similarity are fundamentally important to any fluid dynamics problem. Correct scaling allows comparison between experimental models and full -scale processes. Dynamic similarity, in pneumatic conveying, is usually assessed based on dimensionless numbers, primarily Reynolds, Stokes and Froude, as well as the air to fuel ratio. Two approaches are suggested by the literature as to the correct way to scale a rig:

- Stokes number and concentration (Crowe, 1998)
- Froude number (Cook, 1979)

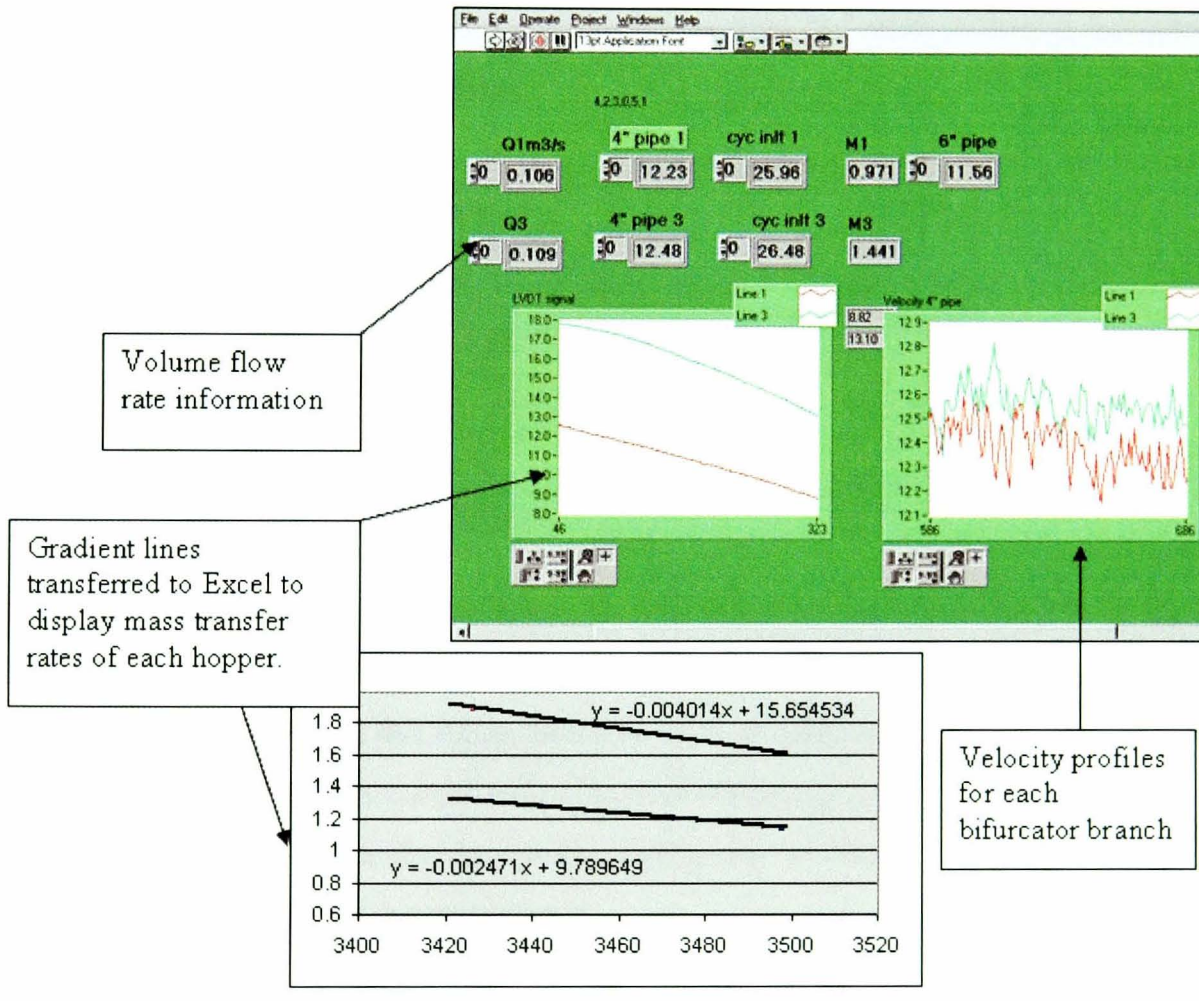

Figure 3.14 - Front plate and explanation of instruments.

The current experiments are related to rope disruption and particle movement. The requirements for a good scale model are for the correct modelling of the interactions between flow and particles. Hence using a scaling approach based on stokes number is appropriate.

The approach taken in this work is to scale according to Stokes number based on the average particle diameter and on the concentration of solid phase to air phase. The experimental running conditions have to be chosen so that the rig is dynamically similar to a power station. The average running conditions in three large coal-fired power stations are given by MacPhail (MacPhail, 1983), the figures are given below in Table 3.1.

Table 3.1 - MacPhail's findings (MacPhail, 1983)

	Drax	Matla	Lethabo
Stokes Number	6.9	4.32	4.7
Reynolds Number	6.34E+05	1.32E+06	6.66E+05
Froude Number	65.6	50.56	52.06
Air: Fuel Ratio	1.54	1.52	1.55

The experiments have been scaled using recent figures from Ratcliffe on Soar power plant. Table 3.2 shows the current running conditions.

Table 3.2 – Ratcliffe-on-Soar running conditions

Pipe Diameter (m)	0.66
Particle Density (kg/m^3)	1750
Average Particle Diameter (m)	6.00E –05
Dynamic Viscosity (kg/ms)	1.85E –05
Kinematic Viscosity (m^2/s)	1.57E –05
Gravity Constant (m/s^2)	9.81
Velocity (m/s)	22
Air -to -Fuel Ratio	1.5:1

The Stokes number is based on the average particle size, this was determined from the Malvern Analysis carried out on the fillite. The Stokes number calculated from the Ratcliffe conditions is 0.632. The Stokes number of the rig at 16m/s is 1.78. A table of the dimensionless number for both the test rig and Ratcliffe calculated on current operating procedures is given in Table 3.3. This is as dynamically similar the rig can be made given the limitations of the experimental rig and the material properties of the particulates.

For a given flow regime, a small Stokes number («1) implies that the inertial effects are small and that the particle will rapidly respond to changes in fluid motion. A large Stokes number (» 1) indicates that the particle motion is independent of the carrier gas flow as they will not be able to respond to changes.

Table 3.3 - Current dimensionless numbers for Ratcliffe and the test Facility.

	Ratcliffe on Soar	Test Facility
Stokes	0.632	1.78
Froude	13.48	0.648
Reynolds	113000	210000

The Stokes number for both the rig and the Ratcliffe conditions are close to unity (they lie equidistance on either side of unity). To get this Stokes number, the velocity for the experiments is 16m/s. The running conditions for the quarter scale rig when scaled to the conditions at Ratcliffe are shown in Table 3.4.

Table 3.4 - Running conditions of the test facility.

Pipe Diameter (m)	0.1524
Particle Density (kg/m^3)	800
Average Particle Diameter (m)	9.00E-05
Dynamic Viscosity (kg/ms)	1.85E-05
Kinematic Viscosity (m^2/s)	1.57E-05
Acceleration due to Gravity (m/s^2)	9.81
Velocity (m/s)	16
Maximum Air-to-Fuel Ratio	3:1

3.6.2 Limitations of the quarter scale rig

The quarter scale rig possesses a variety of limitations in scaling.

The experimental rig is unable to achieve more than 3:1 air to fuel ratio for more than a few seconds before running out of powder. Power stations normally run at air to fuel ratios of close to 1.5:1. It was initially decided to run at higher air to fuel ratios by continuously feeding powder into the system.

Several problems were discovered. Firstly the weigh hoppers connected to the cyclones could not hold sufficient powder to run at higher air to fuel ratios before blocking up all the way into the cyclone. Secondly even running with the weigh hoppers open into the storage hopper and additional powder being added to the hopper, the system cannot exceed approximately 2:1 before the rig cannot lift that amount of powder and the system chokes. The motive air due to weight of powder outweighing the force supplies causes this choking. Finally increasing the frequency of the rotary feed beyond 3:1 (Approximately 35Hz), the rotary valve does not have time to fully

empty or fill during the turn. This is due to the packing characteristics of the particulates. This leads to a pulsing effect meaning the supply is not constant between 2:1 and 3:1.

An another limitation is the particle sizing used in this rig is unfortunately dependent on what particles could be used in the laboratory environment. One of the key ways of making the Stokes number closer to the power station values would have been to use smaller particles. Unfortunately such particles would class as either explosives (such as floor or coal) or irritants. An additional the cyclones used for the extraction system in the rig means that smaller particles in the system would be automatically removed.

3.7 Conclusion to Experimental Methodology

The experimental methodology presented in this chapter details the quarter scale rig used for all the experimentation in this thesis. The chapter has shown that the quarter scale rig can be scaled appropriately to replicate dynamically similar conditions to that of a full scale power station. There are limitations to the experimental set up; the quarter scale rig only has limited configurations, the upper limit of the air: fuel ratio is fixed at 3: 1 whilst power stations tend to run at double that 1.5: 1 or higher and of course the degradation of the particles.

The focus of the experimentation is on whether a device improves the current split. So in the course of this work experiments will be set up for certain geometries and tests run as a control. A device will be rated if it offers improvement over the control conditions. Due to the dimensional similarity between the test rig and full scale power stations it could be assumed that installation in an actual power station would lead to improvement. This approach requires an in depth assessment of each device to see if the phenomena seen in the quarter scale rig would scale to that of a power station.

Chapter 4

Computational Fluid Dynamics Methodology

4.1 Preface

This section describes the computational models used in this thesis and the reasons for choosing these models. Computational Fluid Dynamics (CFD) is the analysis of systems involving fluid flow, heat transfer and associated phenomena such as particle tracking. The technique is very powerful and spans a wide range of industrial and research applications. The CFD is used primarily as a predictive tool as to rope formation and behaviour. Key to this work is the idea of installing a device in the area of the rope and then having the device disrupt the rope and produce a homogenous mixture. CFD, as shown through the validation in this chapter, is a useful tool in this process.

4.2 An introduction to CFD

The basis of CFD is the non-linear fluid flow equations developed by Navier and Stokes (Massey 1998). These equations are difficult to solve except by the numerical techniques in CFD and even then only though iterative processes. CFD programmes use the finite-volume process; this involves dividing the volume into discrete volume cells, this is known as discretisation.

Linear equations are solved to approximate fluid parameters at discrete points in the flow region. Finite-difference equations have been developed relating the changes in variables between cells according to the partial differential equations describing the transport of properties in the flow. These equations are formulated from the Navier-Stokes equations for continuity, momentum and upon the energy balance equation based on the first law of thermodynamics. Further equations are used to apply further complexities to the flow such as species transport, particle tracking and turbulence. The basis of these equations is introduced by Versteeg and Malalasekera (1995).

4.3 The structure of CFD

The basic steps of a CFD simulation are essentially the same irrespective of the code these include:

- Discretisation of the computational domain, termed pre-processing
- Carrying out the iterations based on the Navier-Stokes equations, termed solving.
- A suitable graphical or numerical representation of the data, termed post processing.

4.3.1 Pre-processing

The most important step of CFD is discretisation. The computational model is divided up into smaller domains to allow individual calculations to be carried out on each individual domain. In this work the domain is a volume and is divided into smaller connected blocks of volume. This method of discretisation is often referred to as grid generation and the discretised volume is known as a grid.

The quality of the grid plays a significant part in both the accuracy and stability of the computation. A poor grid can affect the physics of the flow simulated and the length of time required to solve (Versteeg and Malalasekera, 1995). Grid generation can be divided into a number of steps.

First the domain must be given a finite size, in the current work this means a finite volume of pipe must be considered. In theory the entire process with mills, pipe work and boiler could all be simulated. However, a reasonable sized grid must be constructed based on the availability of computational memory and computational run time.

In the current work the pipe work from mill exit to pipe splitter is often selected. It is sometimes necessary to limit the pipe work in cases of very long runs. A user will have to decide what features to keep and whether a simplification needs to be carried out. The computational domain is often constructed in a Computer Aided Design (CAD) package.

After the domain is created the domain is divided into the sub-domains; these sub-domains are referred to as cells. The collection of cells is often referred to as a Mesh. Most pre-processors can be used to adapt a structured body fitted mesh to the domain. The user has to specify the cell size

or spacing and then the programme will place the cells. A user can choose to refine certain areas, such as using a fine mesh in areas of fast moving flow or high-pressure gradient.

The next step to apply boundaries to the grid, boundary types can be changed in the solver. There are many different types of boundary; their usage is dependent on the type of model and the physics surrounding the flow to be modelled. The name and use of a boundary is dependent on particular code, certain boundaries can only be used for certain models and other boundaries can be considered unsuitable for certain models. The work carried out in this thesis makes use of only velocity inlets, pressure outlets and walls. These boundaries are considered suitable for this type of simulation.

Once the grid has been constructed and boundaries applied, a manual and computation check of the mesh is made. Factors looked for are the node point distribution, the smoothness and skewness of cells and whether there has been any unreal volume created. Due to the nature of the meshing algorithms, occasionally non-positive volumes are created, which will lead to solution problems later on.

4.3.2 Solver

The Solver is the part of the CFD code that works out the numerical computation. It essentially consists of all the equations and discretisation system to allow them to be broken down and solved iteratively. The most important equations in the solver are the Navier-Stokes equations.

The Navier-Stokes equations take account of the full three-dimensional, viscous nature of fluid motion and are equally valid in laminar and turbulent flow regimes. Starting from the principles of conservation of mass, momentum and energy, the Navier-Stokes equations can be derived by considering a small element of fluid. In order to derive the equation for the conservation of mass one must equate these fluxes to the rate of change of mass within the volume. In a similar way the conservation equations for momentum and energy are derived. (Versteeg 1995)

The Navier-Stokes equations can only be solved for a very limited range of flow problems. They can however be simplified to a manageable form by making appropriate assumptions about the flow conditions. By time-averaging the Navier-Stokes equations and ignoring instantaneous fluctuations a set of robust equations can be set up for a range of real life problems.

In combination with boundary conditions and fluid properties a CFD model then solves the algebraic equations iteratively to determine the value of each flow variable within each cell in the grid. As a result CFD can simulate the flow physics of complex problems, if correct models are chosen and correct values are chosen. It is possible through poor choice of model to get results that are incorrect. Part of the user's job is to determine whether the figures given out from the CFD solver fit the assumptions and hypothesis of the flow behaviour.

4.3.3 Postprocessor

Post processing is the part of the programme responsible for displaying the results of the iterations. The postprocessor is the part of the CFD code that is of most interest to the user. It is here that he is able to look at contours, graphs and plots of various fluid properties of the system. From these the user is able to determine the characteristics of the fluid flow.

Once again a user must be careful not to display data poorly, incorrect scaling and misjudged planes can show incorrect flow behaviour. Data can also be outputted so it can be put into spreadsheet programmes like EXCEL where the data can be more easily manipulated.

4.4 FLUENT

The CFD code used exclusively throughout this work is FLUENT 6.x from Fluent Inc. FLUENT is a general-purpose CFD package, commercially available for use in industry. FLUENT represents the Solver and Postprocessor of the CFD programme, the Pre-processor for FLUENT is called GAMBIT. In addition to these two programmes, CAD files are often used to model the initial domain for ease of construction.

4.4.1 Turbulence Modelling in Fluent

Turbulent flows are of great industrial importance; they are very complicated to model, as they are three dimensional and time-dependent. Whilst, it is now possible for powerful computers to carry out Direct Numerical Simulation (DNS) or Large Eddy Simulations (LES) for precise answers, for the majority of industrial answers, fast and effective solutions are desired. For this they turn to turbulent models that can be solved relatively quickly and to a reasonable degree of accuracy.

To solve the conservation equations for a turbulent flow, different turbulent models can be selected in FLUENT. For the steady and non-compressible turbulent flow, each variable at a point in the computational region is expressed as a sum of the time average term and fluctuating term. There are two turbulence models used by FLUENT that are suitable for this work. These are the k-ε models (and its derivatives) and the Reynolds Stress model.

The standard k- ε model uses empirical constants determined by matching experimental data for simple turbulent flows, it has been in use for over 20 years. It is first suggested by Launder and Spalding (Launder, 1974), the k- ε model consists of two differential equations, the dependent variables of which are the turbulence energy k and the dissipation rate of the turbulence energy ε.

The k- ε model is considered to be the simplest model that permits the prediction of both near-wall and free-shear-flow phenomena without adjustments to its constants. Also being simple means that it is relatively fast and uses fewer computer resources. This has made the k- ε model a favoured turbulence model for industrial work.

The k- ε model has limitations; it is isotropic and has difficulties where curvature and rotational effects are significant (Fisher, 1994). Both curvature and rotations of flow are present in pipe networks. Fluent Inc. (Fluent Users manual 2005) also states that the k- ε model is unable to predict transitional flows or the return to a laminar regime.

The k- ε model has two variants; these are the realisable k- ε model and the RNG k- ε model. The Fluent Users manual should be referred to for the details for these models and their uses.

In the Reynolds Stress Model (RSM) the individual Reynolds stresses, components of the conservation of momentum equation, are calculated by solving the transport equations. The transport equations are derived from the conservation equations. Full details of the RSM are given in the Fluent User guide (Fluent, 2005).

The RSM can provide a more accurate prediction of the flow field due to the calculations of individual Reynolds stresses. This model does require a lot of computational power, due to the large set of complex equations. Additionally, it has been found to be more difficult to obtain convergence for RSM than for other models.

For this work both the k- ε model and the RSM were used. The k- ε model was used mainly for case studies and for quick cases to test quick ideas were accuracy was not of great importance. The RSM was used on the final cases to look at flow behaviour where accuracy was of great importance. All the results presented in the thesis use the RSM.

4.4.2 Solid Phase Modelling

Correct modelling of the behaviour of the solid phase in a pneumatic conveying system is of great importance. There are two routes to solid phase modelling: Lagrangian and Eularian.

Lagrangian involves tracking a set of packages that represent the mass of the flow. These packages are assigned size and density and are affected by the flow appropriately. The mass is therefore split up into discrete elements; it is therefore referred to as discrete phase modelling. Lagrangian tracking tends to be good for relatively dilute flows.

Eularian tracking involves introducing the solid phase as another fluid that is given all the properties of that substance. The mass is therefore treated as a continuous phase; it is therefore referred to as continuous phase modelling. Eularian tracking tends to be good for relatively dense flows.

For the current work, Lagrangian tracking was used, as most of the cases run are comparably dilute. Whilst there is an issue with Lagrangian tracking not modelling particle-particle interactions, it was considered to be the most efficient model in terms time and computational power. It means that FLUENT will tend to overestimate the concentrations of the rope. This is due to particles not colliding and slowly spreading themselves out and particles co-existing in the same cell when normally they would collide and spread out. Similarly rope velocities will be overestimated due to the lack of plastic collisions between particles. This loss of momentum would use energy in the deformation of the particles and hence slow the velocity of the particles involved.

In FLUENT injections are set up to model the solid flow using the Lagrangian model. The type of injection can be tailored to represent a great due of different flow types. The injection conditions used for the purposes of this work tend to be injected as a surface (usually the velocity inlet). The

particles are injected at 2m/s less than the fluid velocity to represent the degree of difference between the air speed and the particle speed. This is commonly known as the slip velocity. (Schallart, 2000). The size distribution of the particles injected is arranged as a Rosin Rammler distribution based on Malvern-size analysis of actual particles (whether they are coal or fillite)

4.4.3 Solution algorithms

Solution algorithms are a tool to dictate to the method in which the iterations are carried out. FLUENT uses a control-volume-based technique to convert the governing equations to algebraic equations that can be solved numerically.

By default FLUENT stores discrete values for fluid properties at the cell centres, when face values of a cell are required the value is interpolated from the cell centre. This is accomplished by using an upwind scheme. Upwinding is the process of deriving the face value of a cell from quantities "upwind" of the cell, relative to the direction of the flow velocity.

FLUENT presents several upwind schemes; the two used in the work of this thesis are the First Order Upwind Scheme and the Second Order Upwind Scheme. First Order Upwind works by assuming that the cell centre value of any field variable is a cell average; hence the cell centre value will be the same as the face value. The Second Order Upwind works by using Taylor series to apply a gradient throughout the cell, based on the surrounding cells. Hence, the face value of a cell will be calculated based on the two cells that form the face.

The Second Order Upwind solutions tend to be more computationally intense and more accurate than First Order Upwind solutions. Almost all cases used in this thesis use Second Order Upwind, with only a few very complicated ones using First Order Upwind for initial values and then changing to Second Order.

4.5 CFD Operational Procedure

4.5.1 Preface

The most important part of running any CFD case is how individual cases are set up and the procedure used in their construction. The following section details various procedures carried out in an attempt to get a more accurate CFD model.

4.5.2 Grid Independence

In many studies, it can be shown that local flow characteristics are not independent of grid size and design. Normally the grid is continually refined and has the solution rerun in the solver until the difference in solution between the old and the new mesh is with in 99% (i.e. there is no discernable change in the result from refining the mesh).

This is called checking for grid independence. Usually only a single field variable is used in the comparison, such as pressure or velocity profile. The details of the grid independence test undertaken for the two scenarios is detailed in Appendix A.

4.5.3 Boundary Conditions

The boundary conditions used in the work used in thesis are detailed in Appendix B. The appendix details the choices of boundary condition and the reason for choice.

One of the major problems with FLUENT is the inability to generate a correct profile for air coming along a pipe. When using FLUENT it is usual to reduce the length of a pipe network and concentrate on modelling the area of importance. In small runs the velocity profile of the air at the velocity inlet can be modelled as plug flow, as the air comes from the mill, which tends to not allow the development of the velocity profile. However, if the profile is from a long pipeline the velocity profile will have developed a more classical profile. This profile can be described by applying a 1/7th power law of the velocity. Using an Excel file and describing the co-ordinates as polar co-ordinates it is possible to impose this power law profile to the pipe and replicate the effects of long pipelines before the start of the case. An excel macro was set up to generate the profile based on the node co-ordinates outputted by fluent to describe the velocity inlet.

4.5.4 Convergence criteria

FLUENT, and most CFD programmes, solve the complex equations involved via iterations. There are several ways of telling if iteration has solved. The way preferred by the author is to look at the averaged residuals of the various field variables. The way suggested by the Fluent manual is to allow the residuals to descend to a certain pre-determined level. The residual is the difference between the new value and the value of the last iteration of that field variable. This author often uses the method of allowing the residuals to plateau so that the size of the residual becomes approximately constant. On the residual graphs plotted by FLUENT this behaviour appears as a plateau.

When introducing coupled discrete phase calculations a simple plateau doesn't occur, instead a "saw-tooth" pattern with peaks coinciding with the discrete phase model calculations appears. When using the discrete phase model, convergence is assumed by this author to be when each "saw tooth" descends to the same point.

Normally if the case is showing no indication of settling out a residual of $1x10^{-6}$ is considered sufficiently converged.

4.5.5 Solution procedure

The CFD solution is usually obtained as follows; firstly a solid domain is constructed in AutoCAD and exported as an ACIS solid. The solid is then imported into GAMBIT where a body fitted mesh is applied and the boundary types are set up. The mesh is now exported into FLUENT, where the boundary conditions and models are applied to the mesh.

The mesh is also smoothed and check for negative volumes or cells of extreme skewness. The case is then run, first with just the fluid flow and then using the converged solution the case is run again, this time with Lagrangian particle tracking. The discrete phase is coupled with the fluid flow so discrete phase iterations are carried out approximately every 30 fluid flow iterations.

Once the case has been solved, grid independence checks are carried out, this can usually be laborious and often a completed case without particle injections is used to confirm grid independence.

4.6 Validation of CFD

When using CFD, it is important that the solution gained through computation relates to real life situations within a certain margin of error. Computer simulations have to relate to real situations, otherwise the point of carrying out the computation is a bit pointless.

To validate the choice of models and schemes used in the CFD simulations done for this thesis a test case was run on the quarter scale rig and then a computational model of the same flow scenario and conditions. Once run, it will be possible to see what correlation in rope position and splits are obtained between the experimental and the computational simulation. This test will show whether the CFD programme FLUENT can model, within acceptable limits.

4.6.1 Validation scenario

The scenario used for the validation case consists of a 6" pipe going through two 90° bends from the horizontal to the vertical and the vertical riser of 5 pipe diameters before encountering a trifurcator. Figure 4.1 shows a schematic of the pipe layout. The double bend configuration will lead to a secondary flow pattern of a single clockwise vortex.

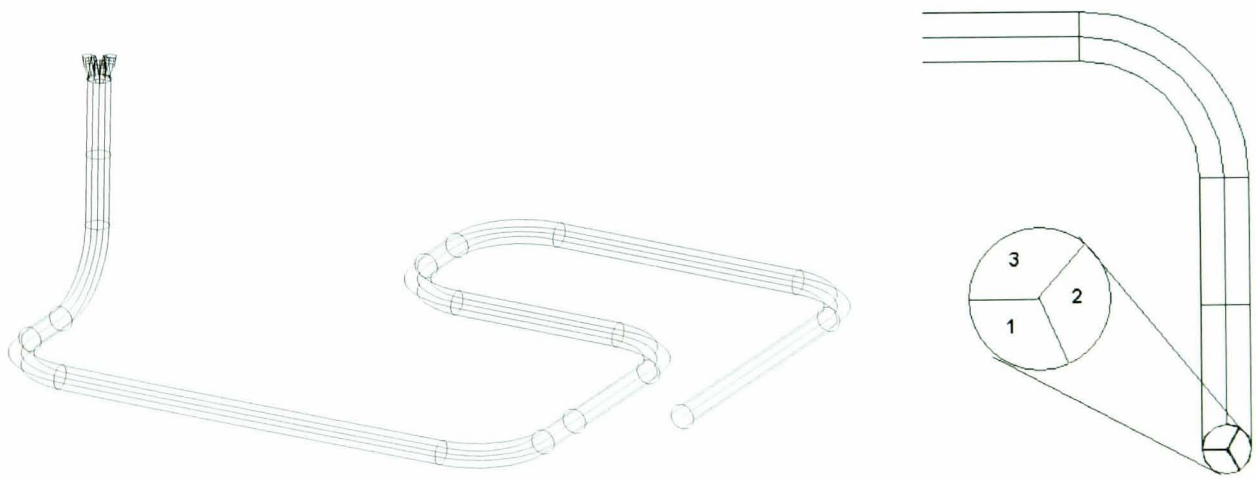

Figure 4.1- Layout of the validation scenario showing the labelling of the outlets.

4.6.2 Experimental Set up

For the validation a series of cases were run experimentally on the quarter scale rig. The running conditions are shown below in table 4.1.

Table 4.1- Running conditions for validation case

Pipe Diameter (m)	0.1524
Particle Density (kg/m^3)	800
Average Particle Diameter (m)	9.00E-05
Dynamic Viscosity (kg/ms)	1.85E-05
Kinematic Viscosity (m^2/s)	1.57E-05
Acceleration due to Gravity (m/s^2)	9.81
Velocity (m/s)	16
Maximum Air-to-Fuel Ratio	3:1

4.6.3 Experimental Results

The experiment was carried out for a range of Air to Fuel Ratios. The splits data is shown in table 4.2 and figure 4.2. The position of the rope as seen from the front of the rig is shown in figure 4.3. It shows a spiralling rope that goes around the outside of the pipe, clockwise, eventually exiting at outlet 3.

4.6.4 CFD Set up

The domain was constructed in AutoCAD and then exported into Gambit. After an initial mesh was constructed and run with on the gas phase, grid independence was undertaken. A mesh of 500,000 tetrahedral cells was generated and the results were considered to be grid independent.

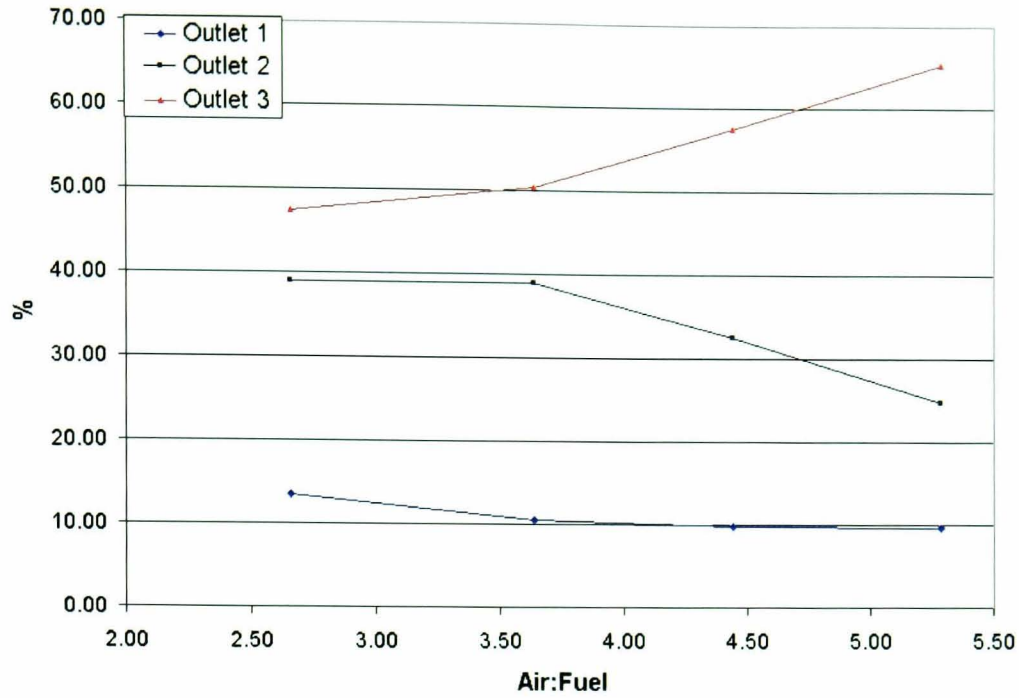

Figure 4.2 - Splits of the various experiments.

Table 4.2 - Experimental Results from validation experiment.

Air: Fuel Ratio	Mass Flow (kg/s)	Split 1 (%)	Split 2 (%)	Split 3 (%)	Actual A: F	Max/min
3:1	0.139	13.60	38.99	47.41	2.66	3.48677
4:1	0.102	10.59	38.92	50.49	3.63	4.76852
5:1	0.083	9.88	32.53	57.59	4.44	5.82927
6:1	0.0697	9.76	24.82	65.42	5.28	6.70588

Figure 4.3: Photograph of the spinning rope.

The data for the CFD set up was based on an Air to Fuel ratio of 3:1. The particle size distribution was based on Malvern Size Analysis of used particles so as to replicate the particle conditions in the rig. The rest of the conditions were replicated from the test conditions for the experiment.

4.6.5 CFD Results

First the air phase only of both models was compared using pressure drop measurements from the experimental rig. The rig gave a value of 81pascals for the 5 pipe diameter piece of straight. The CFD computation calculated 82.1pascals. The second set was to compare the solid phase. From the CFD cases a set of splits data was produced. This can be seen in table 4.3 the data is compared with the nearest experimental case.

Table 4.3 - Comparison of experimental and computational results.

	Outlet 1 Split (%)	Outlet 2 Split (%)	Outlet 3 Split (%)	AFR	Max/Min
RSM	10.9	11.5	77.6	3	7.1
Experimental	13.60	38.99	47.41	2.66	3.48

4.6.6 Discussion of validation results

From the simple validation of checking the pressure drop in the vertical rise monitored for pressure difference we see a similar result. From looking at table 4.3 the immediate consideration is that they are entirely different and do not show the correct behaviour, but a few considerations need to be made.

Firstly the FLUENT code contains no way of adequately modelling particle-particle interactions whilst using Lagrangian particle tracking. In the experimental results the particle rope is dominated by particle-particle interactions forcing particles to spread away from the rope core as the rope moves up the vertical riser. Hence the rope is naturally more spread out due to these collisions in the experimental. Without extensive alteration to the CFD code it is not possible to replicate these collisions. If you compare the CFD result split with the experimental data for 6:1 Air to fuel ratio you see that there is a greater degree of agreement. At lower air to fuel ratios there is less particle-particle interaction, similar to the CFD results where there is no Particle-particle interaction modelled.

The CFD also assumes that the particles are spherical and whilst lots of the particles are spherical, lots of the particles will break into egg-shaped particles. FLUENT does contain the ability to alter the shape factor of the particles. The shape factor is value between 1 and 0 with 1 = spherical and 0 = a disk. The rig is designed to remove broken particles and whilst the assumption is that only spherical particles remain it cannot be avoided that there will be larger fillite fragments.

Despite the three described flaws with the CFD model described above, the RSM does predict correctly: the position of the rope core and the spinning rope. CFD is useful for predicting the position of the rope core, as it is usually this area that is of interest with regards to a device that improves the splitting.

4.6.7 Conclusion of validation test

The validation test shows that CFD can be used to predict the location of a rope core. Whilst the accuracy of the split information is lacking, this is due to a failing in the CFD code. From the validation test it can be seen that CFD can be used as a predictive tool for looking at rope formation and dispersion, both important to the outcome of this project. This author finds the CFD valid for its purpose.

Chapter 5

Conceptual Design and Development

5.1 Preface

Before a design can be installed it has to be developed. A key part of this work is the development of a marketable device usable in coal-fired power stations. The development of a product follows a particular route. The design process consists of various steps. The first step is to identify a need. From the literature review it can be seen that there is a definite need for a device that can be installed in coal-fired power stations to improve the bulk solid split. From this one ideas for the product can be generated.

The design process goes through several steps, (Figure 5.1) the first step is investigation, and this has been carried out through the literature review. The need has been identified. The next couple of steps are covered in this chapter. Firstly is the product design specification, this lays out a broad set of parameters for the designed product. Then there is the generation of ideas.

This chapter concerns itself with the generation of ideas and some preliminary testing utilising CFD to investigate the possibility of the designs. A lot of the conceptual and developmental work was conducted computationally and only viable ideas moved onto the testing phase. By the end of this chapter a set of viable ideas will be identified, explored and created as test sale devices to be used in the quarter scale rig.

The chapter is divided into different sections dealing with the conceptual design process; first it details the process itself in identifying a problem and then moves to the generating and then selection of solutions to this problem. The solutions will be eliminated based on computational simulation of the problem. The outcome of this chapter is to produce several devices to be tested experimentally.

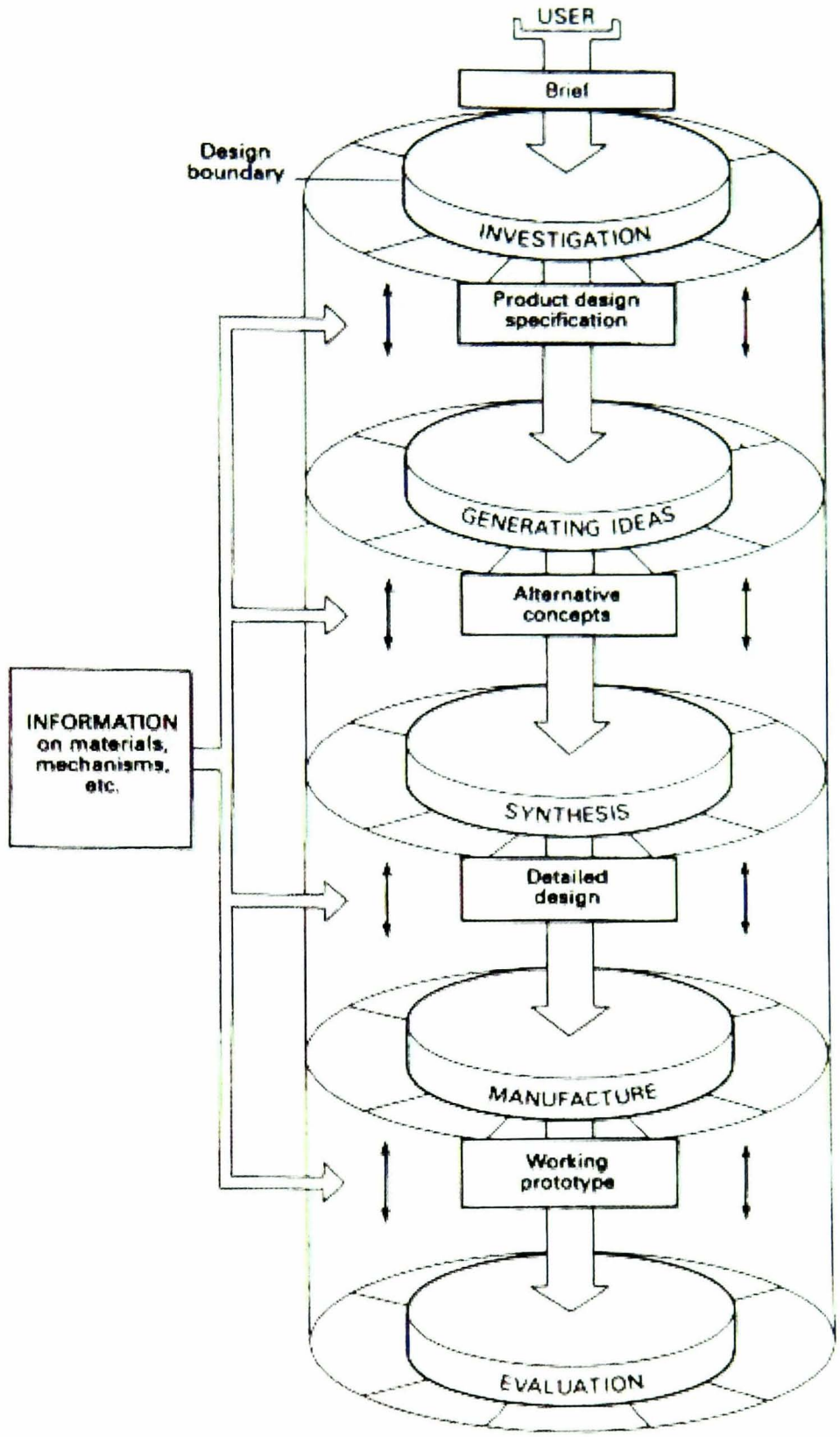

Figure 5.1- Design Process

5.2 Design Process

5.2.1 Design Brief

Initially the concept was to design a splitting device that was universal to all pipe networks, upstream conditions and splitter designs. This would mean that the device would have to work in both a horizontal and vertical configurations. Such a device even in a design brief is ambitious. So instead it was decided to focus on vertical configurations where outlets from the splitting device are located equidistant from the centre of the splitting device. So put simply: *Design a device that provides an equal bulk powder split in vertical configuration in a coal fired power station.*

5.2.2 Wants and Needs

The approach to assembling a design specification for a device is to assemble a list of wants and needs for a product. This approach allows identification of the most important features a product requires. The wants and needs chart is displayed in Table 5.1.

5.2.3 Product design specification

From the "Wants and Needs" table a Product design specification can be constructed, bringing in more specific requirements for the device:

- The device must be able to be retrofitted into existing pipe networks.
- Should attempt to provide an even split regardless of splitter type.
- The device should be ideally passive.
- Able to withstand flows of up to 25m/s.
- Should not have a pressure drop greater than 400Pa and ideally below 200Pa .
- The device should act to disrupt or displace the particle rope, which is responsible for most poor splits.
- The device must be able to be manufactured for a reasonable price.
- The device must have a maximum blockage ratio of 30%
- The device cannot spark on particle impact.
- Low maintenance and long product lifetime
- The device must comply with all British Standards
- Must fit within a reasonable envelope for installation.
- Operate in the vertical position for vertical splits.

Table 5.1 – Table of wants and needs for device specification

Need/Want	Weighting	Requirement
		Geometry
N	-	Must allow retrofitting into existing pipe network.
W	H	Contain the device within 2 pipe diameter.
W	M	Achieve an equal split regardless of splitter geometry.
W	M	Maximum blockage of the device is to 30%
		Kinematics
W	L	Device is to be passive
		Forces
N	-	Be able to withstand turbulent flow at 2Sm/s
W	L	Mass should not exceed 400kg
N	-	Device should withstand a 'back flash' of up to 200psi.
N	-	Pressure-drop across the device no more than 400pa.
		Energy
W	L	Device should consume less that 4kW
N	-	Can only use up to 5 bar pressure dirty air and 1 bar clean air
		Materials
W	M	Resistant to corrosion
W	H	Resistant to temperatures up to 100°C
N	-	Device must not spark on particle impact.
W	M	Achieve a life of S years
		Safety and Ergonomics
N	-	Device must comply with British Standards
W	L	Control over the device should be computational.
		Maintenance
W	M	Minimum 4 years between refitting.
W	M	Zero maintenance
		Cost
W	H	Must not require the purchase of expensive tools to manufacture.
W	H	Must be affordable to manufacture

5.2.4 Looking at the Problem and Brainstorming ideas

When attempting to generate a new device or idea one method often employed by the author is brainstorming. With reference to the design specification a range of ideas were generated.

5.2.5 Discussing brainstorming

From the brainstorming many ideas were generated. Many of which had to be developed beyond their initial idea. Some ideas could be discounted immediately during brainstorming due to the design specification. Any design that was easily eroded or would promote too much pressure drop could be discounted.

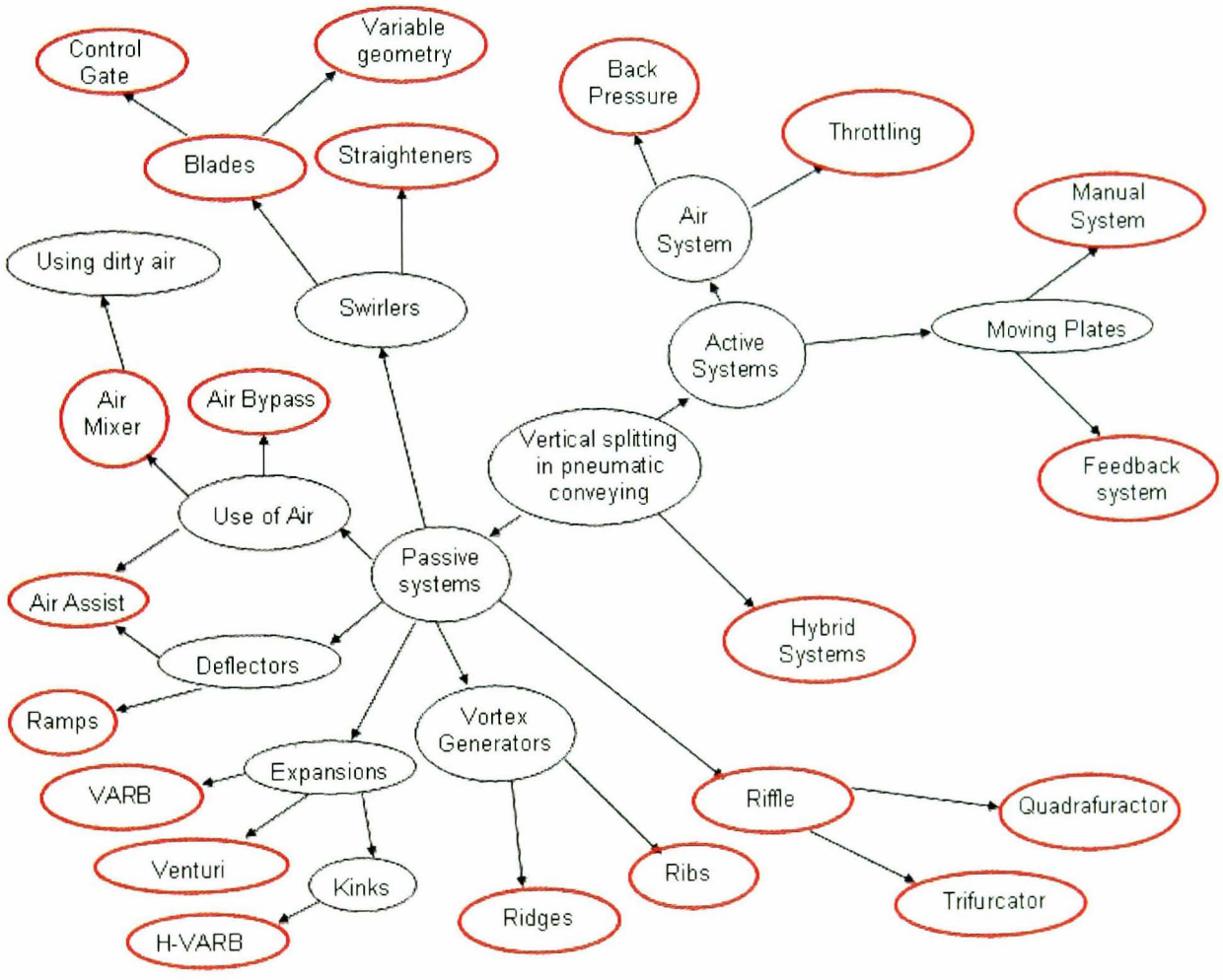

Figure 5.2 - Brainstorm for product development

Key to disrupting the particle rope is moving the particles. The particles have to either be moved physically (by deflection) or by inducing flow phenomena to move the particles. When considering a flow inducing device, the concept of stokes number being a response time of the'

particle divided by the response time of the fluid. The aim of a device would be to either reduce the response time of the particle or increase the response time of the fluid. Several areas initial ideas are considered below.

An active system would represent the most modern approach to the problem. The technology is in place to create a feedback system that would alter the split based on downstream readings from a measurement device. Two simple ideas that could be implemented at the University of Nottingham test facility are that of moving plates and back pressure. Several authors in the literature review (Levy et al 2001, Holmes et al 2000) detail the use of an active system.

The idea of using expansions and contractions to move PF is one used by many authors. Expansions slow the air speed velocity and therefore lower the response time of the particles, making it more likely to be acting upon by secondary flows. Venturi like contractions have been used to gather the particles (Levy et al 2001), by forcing the particles together through a contraction the hope is that you can move the rope. Expansions and contractions do promote higher-pressure drops.

The use of added air or recycled air at strategic points to disrupt the coal is one that has been considered. Essentially the air would work to disrupt the particle rope. The adding of clean air into the system could risk an explosion in the pipe network. With this in mind other ideas could work on moving air from one part of the pipe network to another.

Vortex generators are small inserts designed to promote turbulence and small vortexes. Previous undergraduate projects at the University of Nottingham have focused on using vortex generators to disrupt the particle rope. However, the change in the response time of the fluid due to a single row of vortex generators would be minor and have limited time to take effect on the particle. Hence, the only practical way of implementing the vortex generators is with multiple rows of vortex generators. This leads to a so called "pineapple skin" on the pipe wall.

Ramps work on the principle of altering the direction of the particulate. Ramps work in a similar way to a venturi, creating a physical obstacle that the particle rope has to overcome. The problem with a simple ramp is the creation of blockage. To create a ramp with a long enough rise to alter the direction of the particles often will create a large blockage. An advanced type of ramp is the riffle box, which consists of a set of ramps that divide the powder between the different legs of a

splitting device.

Deflectors are similar to ramps in that they provide an obstruction to the flow. The idea is that they act like guide vanes and force the two phase mixture in the desired direction. As they are less substantial than a ramp they are more susceptible to erosion.

5.3 Initial Ideas

5.3.1 Preface

After Brainstorming several ideas had to be developed into possible devices. Below are detailed 9 possible devices. Each of these device ideas will be assessed and several discarded. The cost of constructing all the ideas presented below would be prohibitive so only the most promising devices can be carried forwards.

To differentiate the best devices CFD will be performed on them to see how promising they are and how they compare with each other.

5.3.2 Elimination of initial ideas

The number of initial ideas needs to be reduced to a manageable amount, not all ideas can be tested. As well as preliminary tests into many of these ideas carried out on the rig, simple CFD was under taken utilising the k-ε model for quick CFD simulation. From the data gathered from these tests elimination as to what device was put into full experimental testing was decided.

Both the Offset and the Expansion both performed well in simple computer simulation. They were easy to manufacture for the Perspex rig utilising simple pipe cutting and vacuum forming techniques. These devices were considered for further experimental testing.

The moving plate was designed as an active device to work on a simple bifurcation arrangement of the rig. The view was to manufacture a device that would operate multiple transversing blades in front of the trifurcator. However, the cost of upgrading the Labview controller to operate multiple stepper motors for the actuation was too great. Also the lack of an accurate measurement device that was online for the purpose of feedback adjustment was not realised at

the time for this scale of rig. This work was continued on the bifurcator and a paper written for on the subject is presented in Appendix C.

The idea of introducing air injection was dismissed early on despite promising CFD results. Firstly power stations are generally unhappy at injection of air into their systems due to the change of air:fuel ratio locally to the point of a explosive mix. Secondly the air supply used for the system was unreliable at best in the laboratory and consistency of supply could not be guaranteed.

A three-way riffle works on the idea inspired by the CERL riffle produced by the Central Electricity Generating Board. The complexity of such a construction for our configuration of trifurcator would have been very difficult to manufacture affordably for this project. In addition, the preliminary CFD carried out on such a design highlighted a particularly high-pressure drop. The high-pressure drop ruled the device out entirely.

The sponsors of the project inspired the deflecting blades design, however after an initial experimentation it was shown that the blades would have to be significantly large and intruding into the flow to be of any significant improvement. The idea was suggested under the false assumption that a spinning flow is more defused than a non-spinning flow. There is no real evidence to support this.

The ribs concept was seen as favourable, however the concerns about erosion in full-scale applications and consistent construction techniques for the ribs at experimental scale meant that they design was not continued for the full scale experimental investigation.

The control gate was not viewed as usable with a rope flow. However, if the rope was dispersed the control gates could be used to alter the flow. Hence the control gate was taken forwards to used in conjunction with a dispersing device like the offset and expansion to "trim" the flow.

5.3.3 The Offset

Description

The OFFSET consists of a pipe section cut at angles and then twisted to produce a kink.

This design prevents a large variation in cross sectional area and hence reduces the pressure drop of the device as compared to a simple ramp in the pipe.

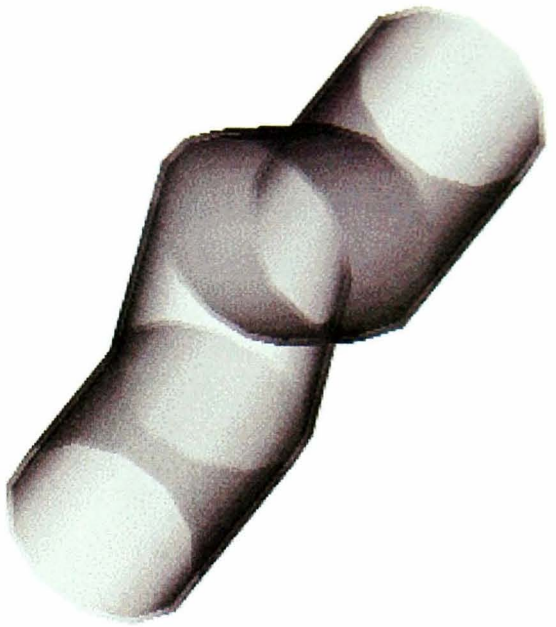

Figure 5.3 – Isometric view of the offset

Method of operation

The OFFSET is designed to deflect the particles off of the wall into the centre of the stream to aid dispersion.

The recirculation created after the OFFSET prevents the particle rope from reattachment with the wall for some distance after the offset itself.

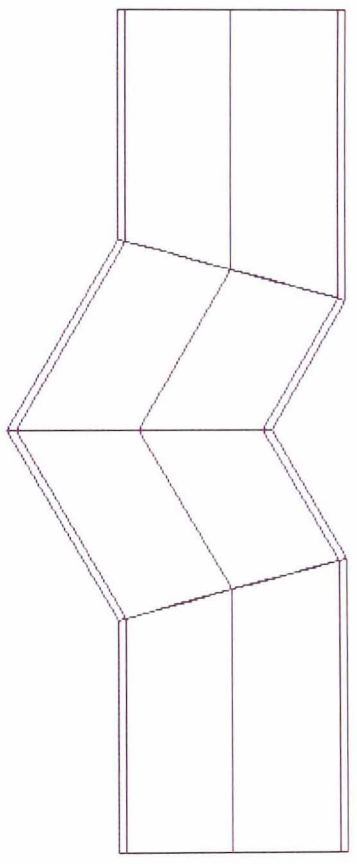

Figure 5.4 – Profile of the offset

Pros

- Low pressure drop
- Easy manufacture
- Low cost

Cons

- Position of the rope needs to be known.
- Offset might cause problems for design envelope.

Other Notes

- Would require investigation into optimum angle for the offset.

5.3.4 Expansion

Description

The EXPANSION consists of a simple expansion in the pipe.

Entering the EXPANSION the slope outwards is gentle, whilst at exit the contraction is more extreme.

Figure 5.5 – Isometric view of the expansion

Method of operation

The EXPANSION is designed to slow temporarily the two phase flow allowing more time for mixing.

The extreme contraction on exit of the EXPANSION is designed to provide some level of deflection for the particulate away from the wall of the pipe.

Pros

- Simple to manufacture
- Low cost
- Low pressure drop
- Universal for rope position

Cons

- Expansion might cause design envelope problems.

Other Notes

- Would require investigation into optimum angle for the expansion

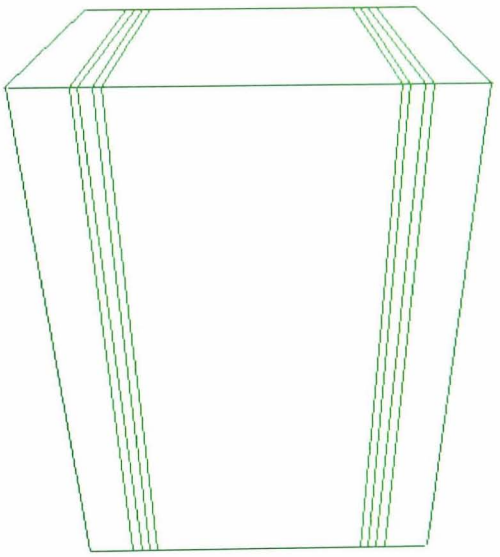

Figure 5.6 – Profile view of the expansion

5.3.5 Moving plate.

Description

The MOVING PLATE is the only initial idea to involve an active system.

The device consists of a single angled plate designed to be traversed across the pipe by a stepper motor.

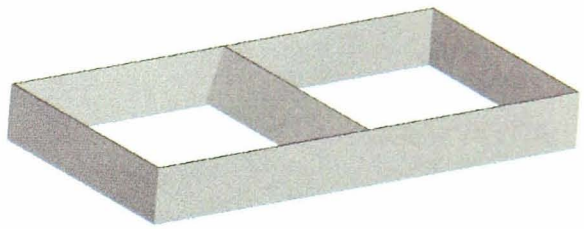

Figure 5.7 – Isometric view of the plate

Method of operation

Using Laser Sheet Visualisation (LSV) the relative particle loadings of the outlets of a splitter will be assessed and in response an angled blade will be moved to disrupt the particle rope.

The blade continues to move until the split improves.

Pros

- An active system is the only way to deal with constantly changing flow conditions.

Cons

- An active system requires downstream measurement.
- An active system requires a level of control.

Other Notes

- Will utilise additional experimental procedure to examine.

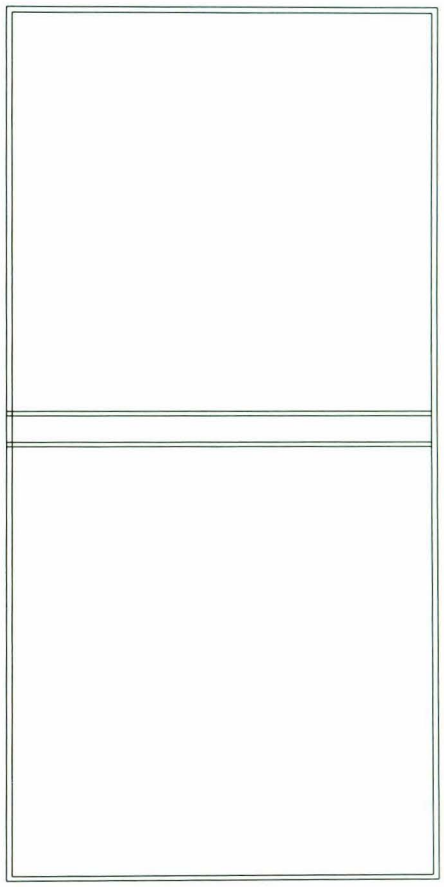

Figure 5.8 – Plan view of the plate

5.3.6 Air Ring

Description

The AIR RING consists of several air injectors positioned in a rig.

Method of operation

Using an external air supply, air injectors would be positioned to inject a quantity of air into the system in an attempt to disrupt the particle rope.

Whilst to alter the path of heavier particles would require a high pressure probably not available in a power station.

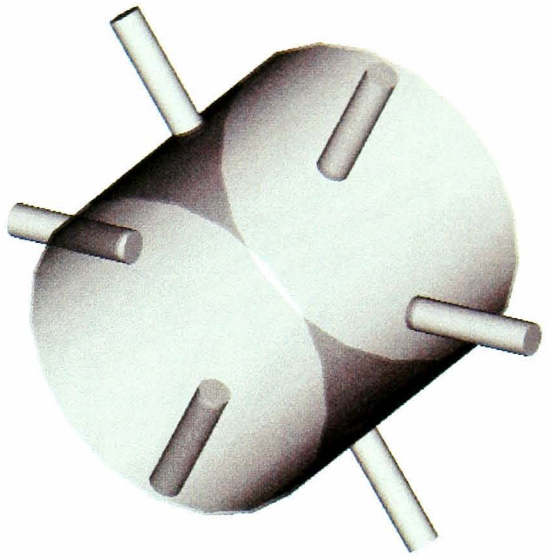

Figure 5.9 – Isometric view of the air ring

Pros

- No obstruction in the pipe

Cons

- Means injecting air into the fuel:air mixture and altering the overall ratio.
- Experimental scale version will require constant supply from a pressurised line.

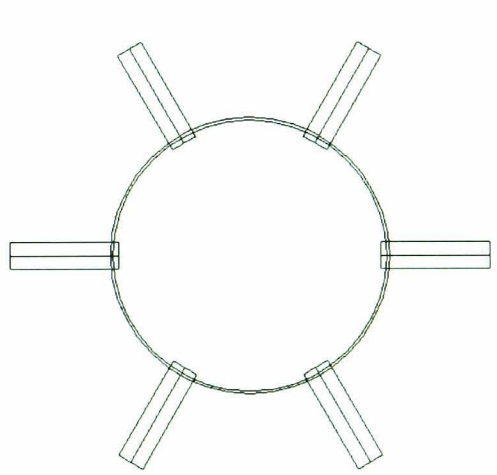

Figure 5.10 – Plan view of the air ring

Other Notes

- Coal-fired power stations do not like injecting additional air into their pipes.
- Coal-fired power stations tend to have two external pressure lines. A clean one at 1 bar and a dirt one at 5 bar

5.3.7 Three way Riffle

Description

The THREE WAY RIFFLE essentially transforms the pipe into three splitting equally both powder and air.

The device is based on a common CERL bifurcator Riffle.

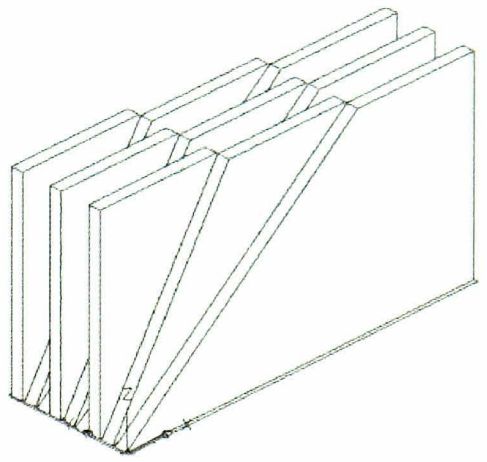

Figure 5.11 – Schematic of a three way riffle

Method of operation

The THREE WAY RIFFLE divides the pipe up using a number of ramps dividing equally the cross section of the pipe between the three outlets.

The idea is that the rope, regardless of where it strikes the riffle will be divided equally between the three outlets.

Pros

- Tried and tested method of powder splitting, work well with a bifurcator.
- Simple device, no moving parts.

Cons

- High Pressure drop
- Highly susceptible to erosion.
- Very complex design.

Other Notes

- Not universal for every three way split.

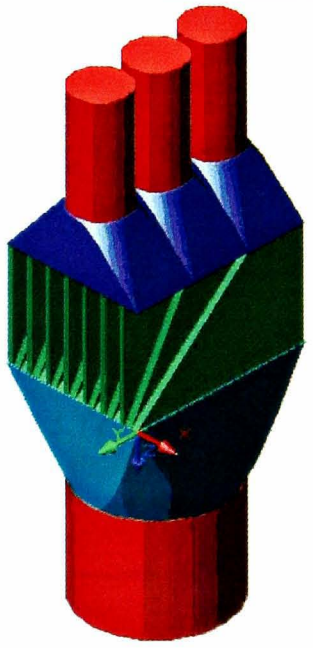

Figure 5.12 – Isometric view of a three way riffle

5.3.8 Deflecting Blades

Description

The BLADES consist of a row of movable blades that can induce spin to the rope.

The spinning rope will then spread out and become more defuse.

Method of operation

The BLADES are positioned to act as deflectors and to impart to the particle rope a degree of spin.

It has been considered that a spinning rope will diffuse more than a non-spinning rope.

Pros

- Simple device
- Easily adjusted dependent on flow
- Possibly adapted for an active system.

Cons

- Susceptible to erosion
- Based on assumption that a spinning round creates dispersion.
- Significant blockage ratio.

Other Notes

- Based on communication with sponsor.

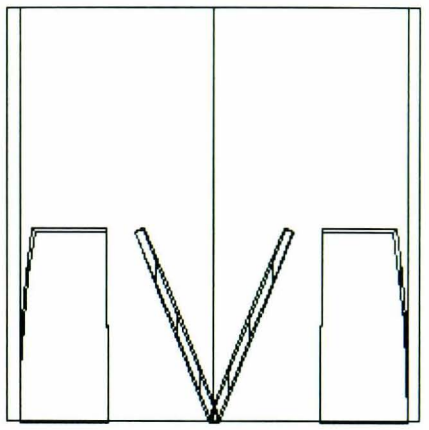

Figure 5.13 – Side view of the deflecting blades

Figure 5.14 – Isometric view of the deflecting blades

5.3.9 ribs

Description

The RIBS are chisel shaped inserts into the pipe.

They are arranged as an almost skin layer. The design of the arrangement will be something to optimise.

Figure 5.15 – Isometric view of the ribs device

Method of operation

The RIBS act like ramps lifting the particles into the centre of the pipe.

The RIBS design also disrupts the secondary flows making them less uniform.

Pros

- Simple and easy to fit.
- Universal

Cons

- Susceptible to erosion.
- Possible high pressure drop.
- Have to be applied over a long distance.

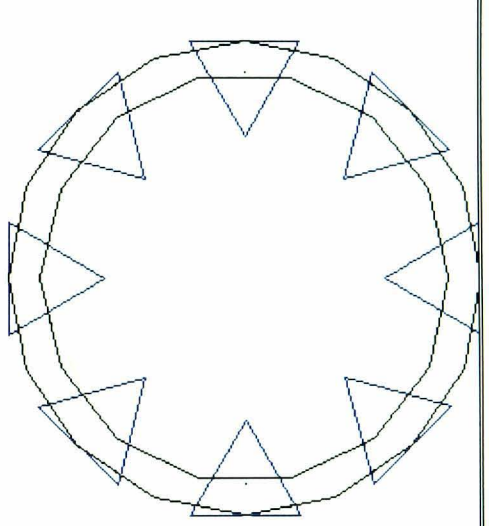

Figure 5.16 – Plan view of the ribs device

Other Notes

- A range of different ribs were considered.
- RIBS essentially work on the ideas vortex generators.

5.3.10 Control Gate

Description

The GATE is designed to work in a similar to the BLADES.

They consist of three blades arranged in a Mercedes sign shape. This control gate is design trifurcator.

Method of operation

The control gate is designed to provide fine tuning to existing devices. The gates are positioned to shift the particulate heading down one outlet to another.

It is designed to work with another device and not on its own.

Pros

- Obvious in its usage.
- Can be adapted into an active system.

Cons

- Susceptible to erosion.
- Limited movement of gates

Other Notes

- Design as an additional device to another solution. Is designed for fine tuning.

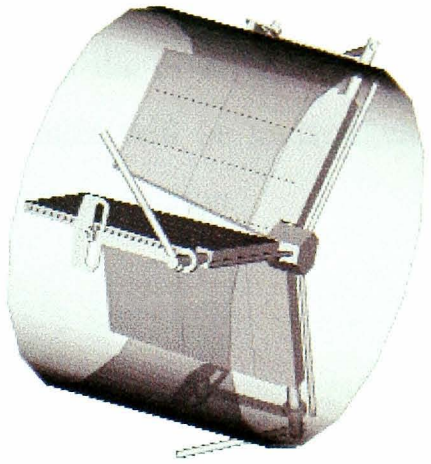

Figure 5.17 – Isometric view of the control gates

Figure 5.18 – Plan view of the control gates

5.4 Development of Ideas

From the initial geometry of both the Offset and the Expansion it can be seen that there is the possibility for altering the angle, and therefore height, of the offset and altering the relative heights and width of the Expansion. These changes will be undertaken in a parametric study in the CFD results section and the experimental section.

5.5 Conclusion to the conceptual design stage

From the conceptual design the focus has been on end product. Realistic constraints on the design of the device have been made so that whatever is produced from the thesis is a product that can meet the needs of real PF-fired power stations to help them in PF powder balancing.

The design process produced three possible ideas to be tested, two passive systems and one active system. The Expansion and the Offset devices both act differently, the expansion attempts to affect the flow conditions and therefore the particles, whilst the offset attempts to be a low pressure ramp. The control gate was viewed to be used as a split trimmer to help provide additional accuracy.

The next step in the process is to look at modelling of the proposed devices with a view to optimising them and testing their effectiveness.

Chapter 6

Computational Fluid Dynamics Investigation

6.1 Preface

Following the conceptual design stage, three ideas were identified for progression and testing. Whilst all the initial ideas were investigated with CFD, it is not possible to detail all the cases of initial CFD. This section describes the further investigation into the two passive systems chosen; the Offset and the Expansion. The focus of these investigations was to identify geometrical arrangements that could improve the effectiveness of the device and identify the geometries that needed to be verified experimentally.

This chapter builds on the CFD set up in the CFD methodology chapter, but in addition it employs stochastic tracking which allows several individual paths of particles to be plotted and give a better representation of the split over a period of time. Both devices will be compared to a blank geometry without the device in the position of the device.

The investigation into the Offset was carried out with a non-spinning/double vortices roped flow, which is generated by a single 90° bend scenario as described previously. The investigation into the Expansion was carried out with a spinning rope, which is generated with a double 90° bend scenario as described previously.

The criteria for a good device is one that provides an even split across the 3 outlets of the trifurcator. The two ways of determining this are:

1.) The distance that the rope core is moved into the centre of the pipe, indicated by a value around of 0.5 for the normalised distance from the outside bend.
2.) The maximum/minimum value which is the highest percentage split of the three outlets divided by the lowest.

Appendix A and B both detail the boundary conditions and grid independence tests undertaken for the work in this thesis.

6.2 The Offset

6.2.1 Preliminary investigation

The offset consists of a single piece of pipe cut at several places and rotated to create a "kink" in the pipe. The Offset consists of several important areas, the actual offset and the deflecting face. These are shown in figure 6.1. As stated previously, the geometry used for the offset utilised single bend geometry, as the offset would work best when the location of the rope is known. Figure 6.2 shows the geometry used for the CFD study into the offset.

From the initial concept of the offset, the crescent shaped ramp will capture most of the particle material and move it into the centre of the pipe system. From here it will more easily disperse and split with greater ease.

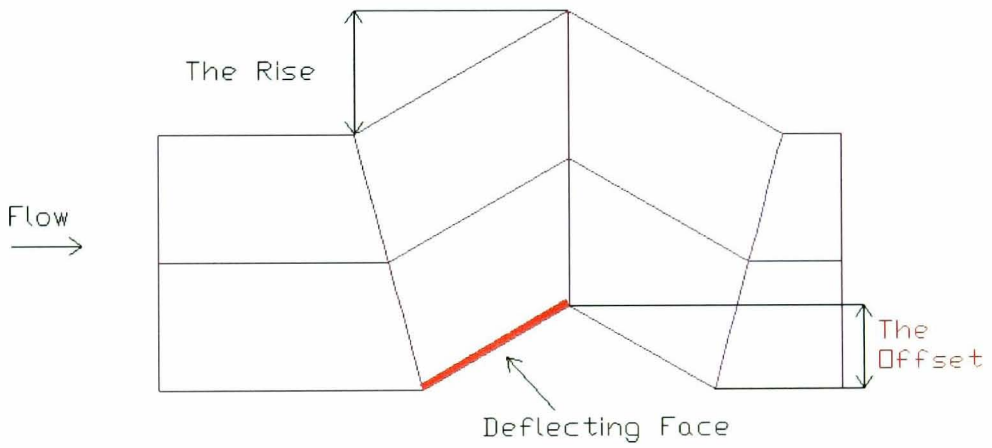

Figure 6.1 – Offset profile showing the deflecting face and offset.

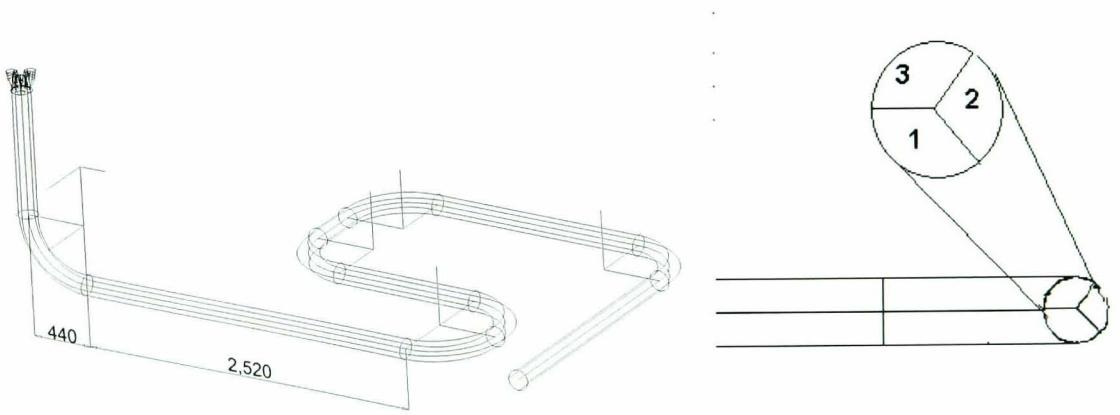

Figure 6.2 – Geometry used in the Offset device CFD

As predicted the Offset deflects particles from one side of the pipe to the other. Being able to

design a device that moved the particles away from the boundary layer at the walls into the centre of the pipe would allow the particles to be more evenly distributed. The CFD predicts that the Offset device will hurl the particles to the other side of the pipe. CFD has the tendency to overestimate particle motion, as it does not take into account particle-particle interactions. Figure 6.3 shows the flow in the Offset compared to a blank section. The particle rope begins against the wall and is spread by the Offset shape.

From Lagrangian particle tracking, based on fillite particles in the ¼ scale rig, the graphs in figure 6.4 show the difference the Offset device makes to the split when positioned 2 pipe diameters upstream from the split. At 2 pipe diameters the difference is very pronounced, the large peak seen in the graph for the straight section is greatly reduced.

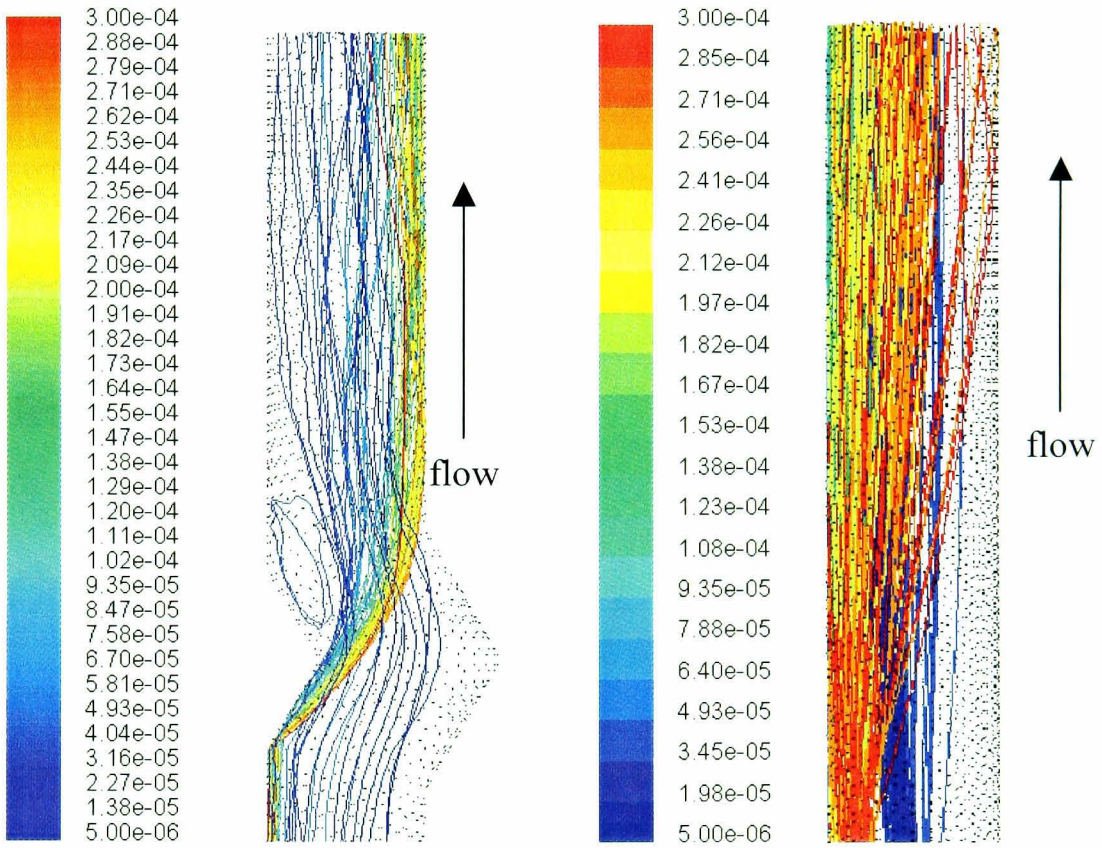

Figure 6.3 – Particle tracking comparison between the Offset device and a blank pipe in the single bend geometry. The flow is against gravity in this diagram.

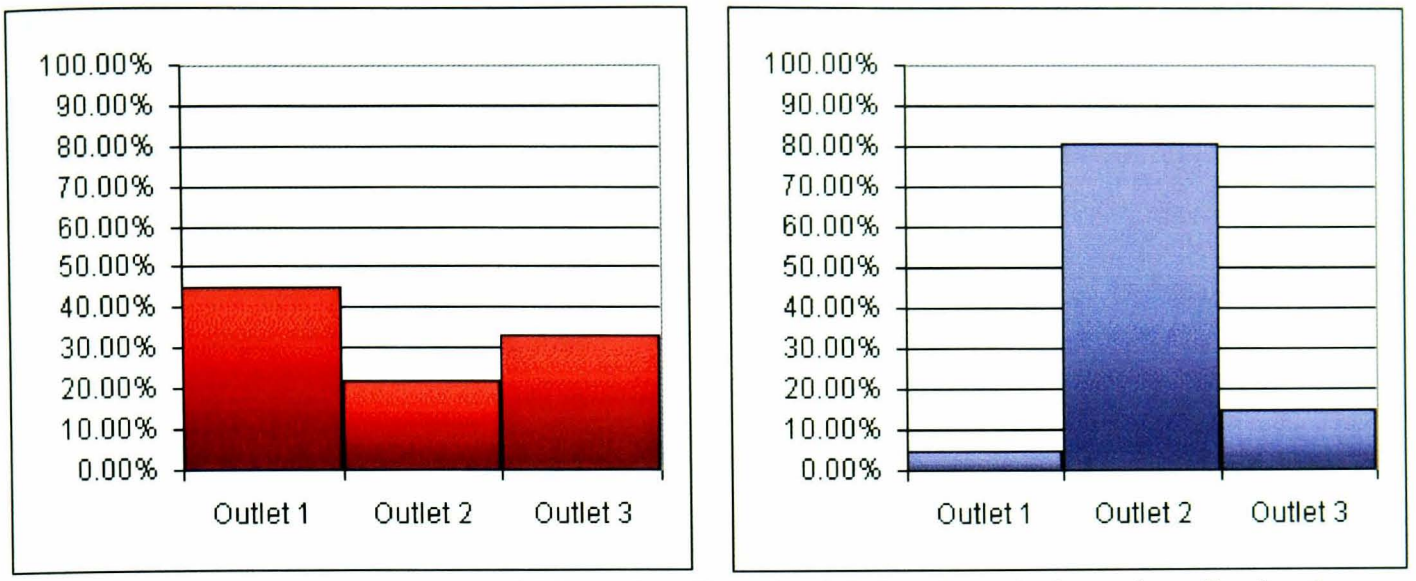

Figure 6.4 – Split data from the CFD on the offset, the right hand graph shows the split after the installation of the Offset device, the left hand is before.

The simulated pressure drop at the conditions of the rig was 80pa above that of a blank section. This low value can be attributed in part to the shape of the offset. The offset is designed to keep an almost constant cross section so there is little pressure loss from expansion or contraction.

When looking at the velocity vectors of the Offset it can be seen that directly after the offset itself there is a re-circulation that helps keep the particle rope from returning to the back wall. This can be seen in figure 6.5.

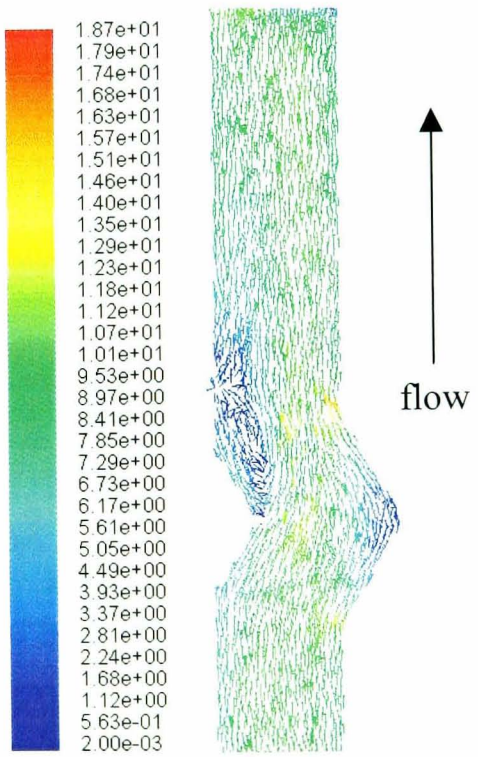

Figure 6.5 – The re-circulation is indicated by the blue arrows in the above plot

6.2.2 Parametric Studies

There are two major variables that affect the construction and placement of the Offset if the overall length of the device is to be maintained:

- The distance the Offset is positioned from the splitter box.
- The angle of the deflecting face.

The placement of the Offset was investigated looking at a parametric study. The study involved three cases with the Offset positioned 0,1,2,3 pipe diameters from the splitter box to see what effect this had on the particle tracking. The geometry used for this parametric study was a straight pipe with no bend preceding it. The object was to see what affect it had on particle size and the airflow through the pipe. Figures 6.6 and 6.7 shows the cross-section of two of the cases. In both these cases the flow is left to right and gravity acts right to left.

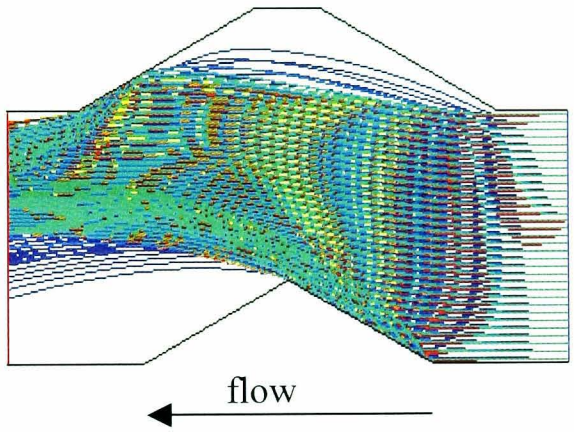

Figure 6.6 - Offset position 0 pipe diameters from the trifurcator

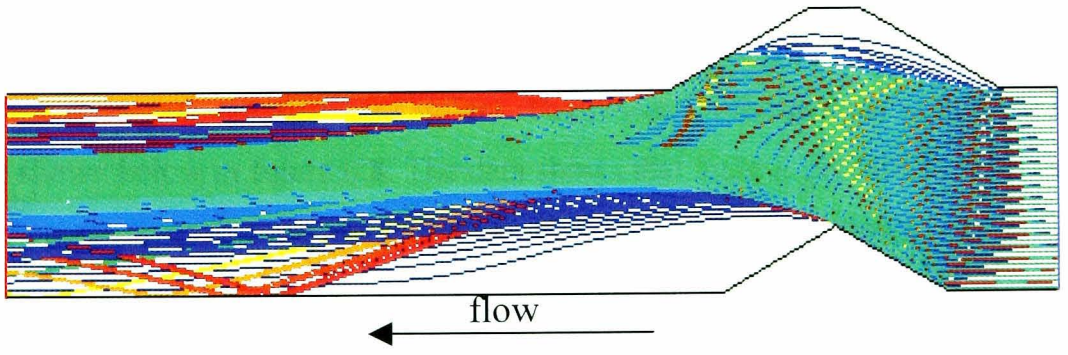

Figure 6.7 – Offset position 3 pipe diameters from the trifurcator.

From figures 6.6 and 6.7 it can be seen how the Offset works by gathering the particle streams into a single position at the centre of the pipe. The particles do not return to the outside of the

bend for at least 2 pipe diameters. The table 6.1 shows the normalised distance from the outside wall (the wall with the deflecting face on) the highest particle density point reaches for this study. The best position would be for the point of highest particle density would be have a normalized distance from the outside bend of 0.5 which would be the centre of any splitter box. The highest particle density point in this simulation is assumed to coincide with the core of the particle rope.

Table 6.1 – Results of the parametric study in position of the offset from the splitter

Pipe Diameter	Normalised distance of the rope core from the outside bend
0	0.75
1	0.61
2	0.55
3	0.52

The angle of the deflecting face is another variable. The "standard" Offset is a 30° angle so a range of angles from 50 to 20 in 10 degree increments were modelled and processed with a 2 pipe diameter distance between the Offset and the splitter to see what distance from the wall they would give. The results are shown in Table 6.2.

Table 6.2 – Results of the parametric study in the angle of the offset

Angle (°)	Normalised distance of the rope core from the outside bend
20	0.40
30	0.55
40	0.57
50	0.58

From the results it shows that there is a variation of the distance from the wall to the angle of the Offset. However 30-50°, are all very similar. The results of the powder split from the particle tracking are shown below in figure 6.8. The data shows that there is perhaps an optimum shape of Offset at the operating conditions at a particular distance from the splitting device.

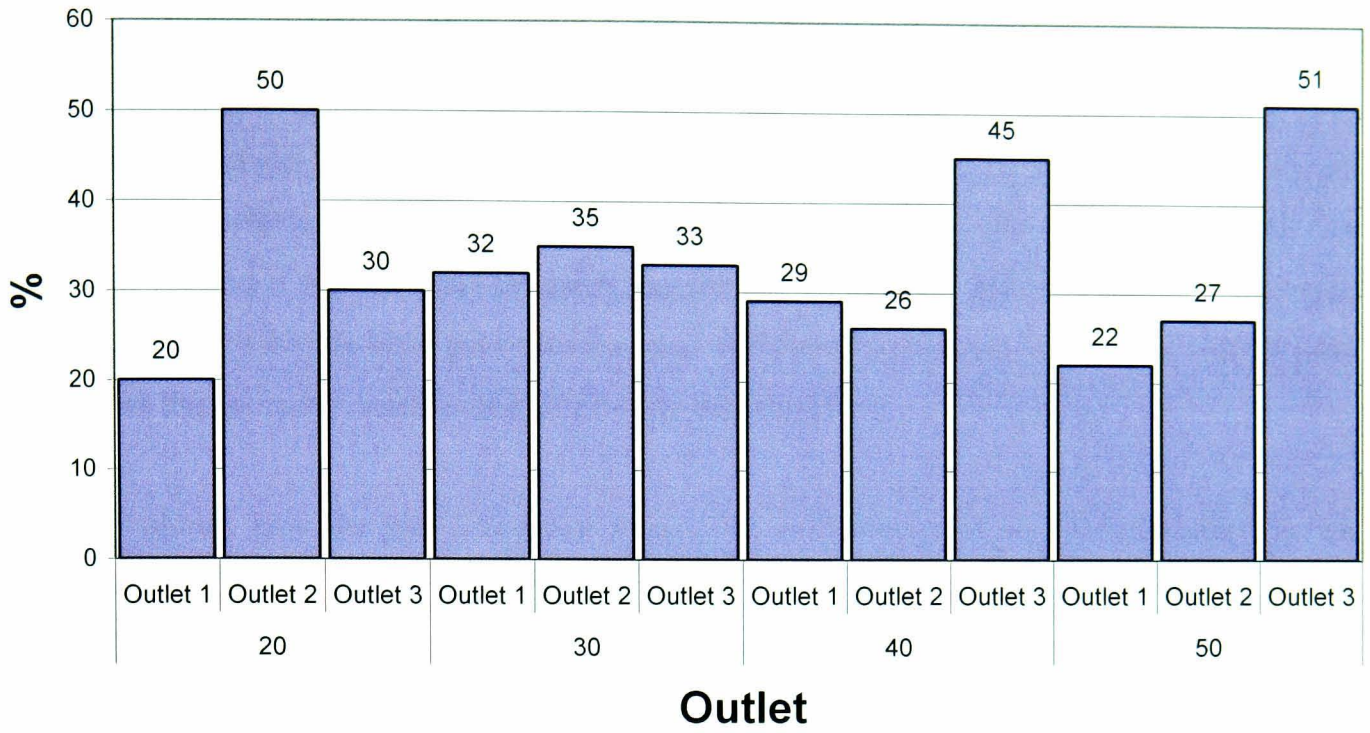

Figure 6.8 – The CFD results for the various Offset designs.

6.2.3 Offset Conclusion

From the CFD investigation into the Offset it can be seen that the Offset can alter the split favourably. In addition there are two major variables that can be altered to change the effectiveness of the device. These are the distance from the splitting box and the angle of the deflecting face. The CFD indicates that there is an optimum distance and angle for a certain set of conditions. However, the shortcomings in the CFD code, including the lack of particle-particle interactions means that this behaviour must be investigated experimentally.

6.3 The Expansion

6.3.1 Preliminary Investigation

The Expansion demonstrates a two-fold effect on the particle rope in CFD. Firstly the expansion acts a deflecting ramp, moving the particulates into the centre of the pipe. The secondary effect is to slow the flow of particles and air allowing them to spread more as they spin around the expansion.

The Expansion is designed to be universal, it doesn't require any knowledge of where the rope will enter the device, and this is ideal for any spinning rope situation. The spinning rope, coupled with the expansion spread the rope far more than a non-spinning rope. Figure 6.9 shows the general design of the Expansion with the two parameters that can be changed if the overall: Maximum Diameter and Expansion Height. As stated previously, the geometry used for the expansion utilised a double bend geometry, as the expansion was able to work in a universal position and that a double bend generates the most difficult rope to break, a spinning rope. Figure 6.10 shows the geometry used for the CFD study into the offset.

The CFD shows how the particles move around the expansion and are then deflected by the contracting wall of the expansion. Figure 6.11 shows a comparison between a blank pipe and a sample Offset device. The CFD predicts that the Expansion device will deflect the particles into the centre of the pipe. CFD has the tendency to overestimate particle motion, as it does not take into account particle-particle interactions.

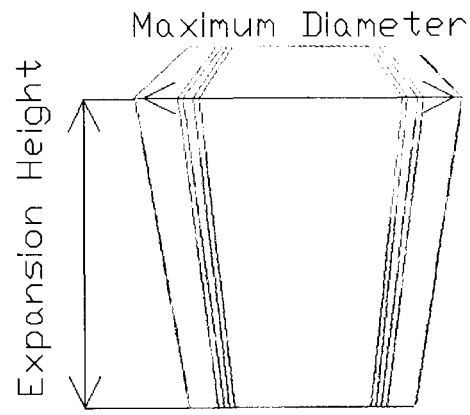

Figure 6.9 – General design of the Expansion

From initial investigations into the Expansion in CFD it was shown that computationally the Expansion had an effect, however a single shape had to be conceived upon to carry forward to experimental testing, the time required to construct a mould for a clear Perspex offset was not inconsiderable and so a standard shape had to be decided upon through CFD.

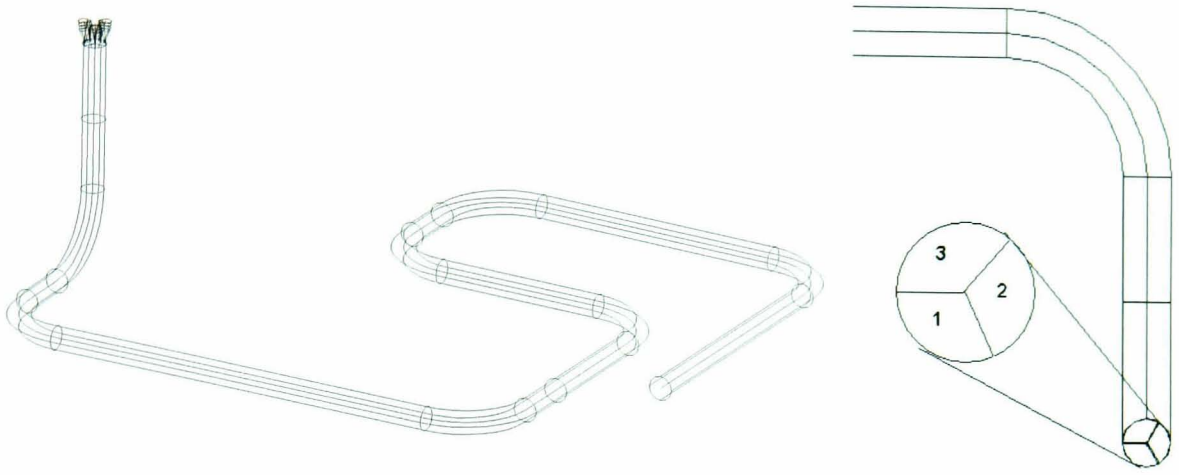

Figure 6.10 – Rig layout used for the experimental testing of the Expansion with the three outlets labelled.

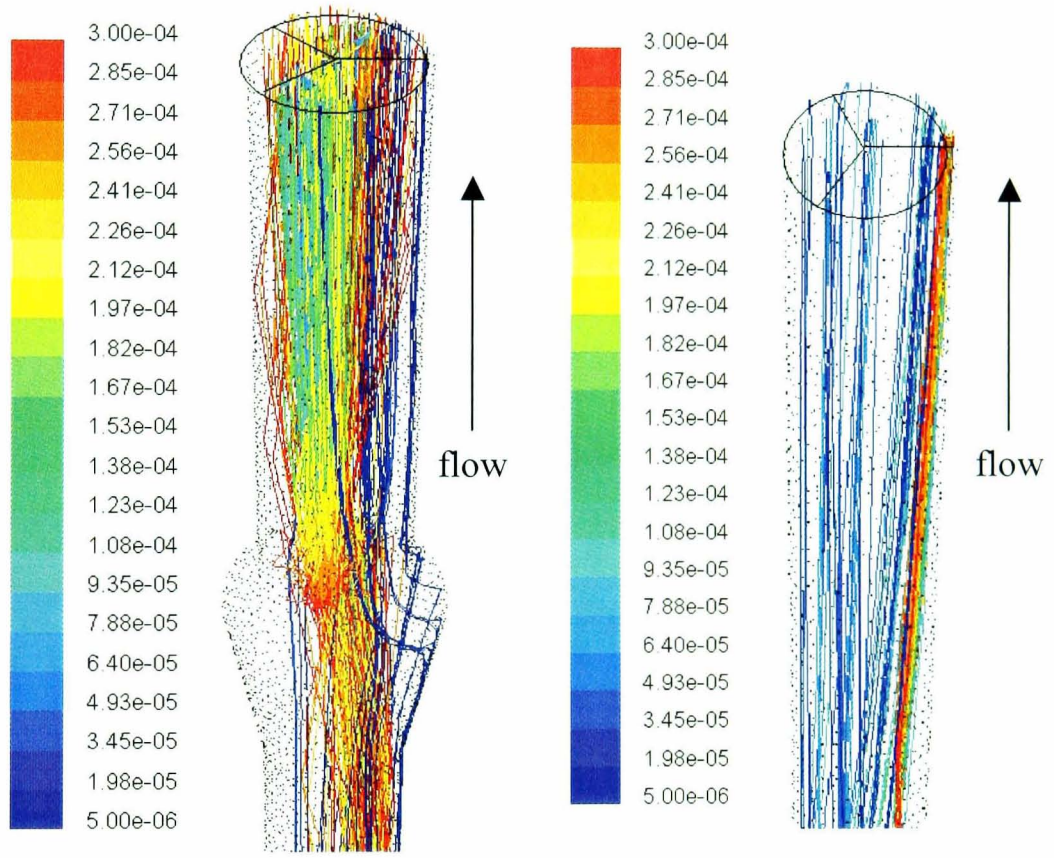

Figure 6.11 – Comparison between a sample offset and a blank pipe, particles coloured by particle size.

6.3.2 Parametric study.

Two dimensions were established to describe the Expansion, it was diameter of the point of largest area of the expansion and height where the largest area occurred. These were presented as dimensionless numbers. Due to constraints in the rig, all the devices would be 1.5 pipe diameters in length so they could be easily swapped into the rig. Table 6.3 shows below the devices tested

computationally, with their dimensionless numbers and a maximum over minimum split value. The close the Maximum/minimum is to unity, the better the split. The table is divided into 3 sections: a constant largest diameter; a constant standard height for the expansion based on the best result from the first set of tests and a section showing the results of a blank section. Based on the results a design with an expansion diameter of 1.3 and an expansion height of 0.8 was chosen for manufacture.

The pressure drops for the expansions were low, the pressure drop for the chosen design was 60pa in addition to the normal pressure drop in the pipe. Like the Offset, this is an acceptable level for most devices for installation in the power station.

Table 6.3 – Results of the parametric study in the dimensions of the expansion

Maximum Diameter	Expansion Point	Maximum/Minimum
Constant maximum diameter		
1.5	0.25	1.781
1.5	0.5	1.865
1.5	0.75	1.753
1.5	0.8	1.735
Constant expansion height		
1.5	0.8	1.735
1.4	0.8	1.733
1.3	0.8	1.682
1.2	0.8	1.817
1.1	0.8	2.011
Blank Section		
Blank Section		1.912

6.3.3 Aggressive Venturi

Following the parametric study it was decided to test if adding a small venturi to the Expansion before or after would improve the split. The results of the test using the optimised Expansion are shown in table 6.4 below. Figure 6.12 and 6.13 show the geometries of the venturi post expansion and venture pre-expansion respectively. As you can see they seemed to make the split worse. However, it was deemed relatively easy to construct the small venturi and test it to see if particle-particle interactions improved the results of these aggressive venturi additions.

Table 6.4 – Results of parametric study investigating the aggressive venturi

Expansion Style	Maximum/Minimum
Venturi Pre-Expansion	1.789
Venturi Post-Expansion	1.882
Standard	1.682

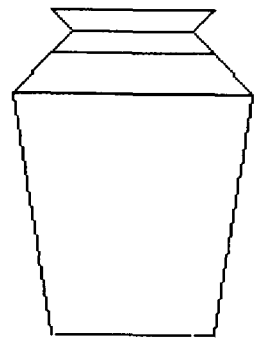

Figure 6.12 Venturi Post-Expansion

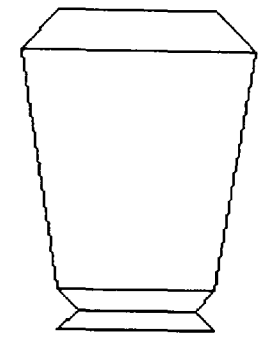

Figure 6.13 Venturi Pre-Expansion

6.3.4 Expansion Conclusion

The Expansion has been seen to be successful in improving the powder balance in the CFD model. It is believed that the degree of improvement in powder balance will be greater in full-scale testing and on the experimental rig due to particle-particle interactions which are not modelled by the CFD.

Two parameters to describe the Expansion were identified and from parametric study an optimum device was designed to be manufactured and tested in the experimental rig. In addition, a small venturi will be included before and after to test the theory that expanding either the contraction or expansion sections of the device would not benefit the design.

6.4 Discussion of CFD results

From this section on CFD results it is possible to identify areas of interest for further investigation via experimentation. It has identified that according to CFD there is a pronounced change in the effectiveness of the Offset device dependent on both its placement from the split and the angle of the Offset. This is because the offset acts as a ramp and the ramp diverts the particles away from their initial position. The slight return to outside wall of the bend is because there is a re-circulation caused after the offset. The formation of this area of re-circulation is a key area of interest for experimental analysis of offset in addition to experimentation into a changing angle of Offset.

For the expansion it showed that there is little improvement or change in the powder balance for changing the dimensions of the expansion. Due to the expense of manufacturing the Expansion

shape, identifying the best choice through parametric analysis will prevent wastage in additional shapes being made. The investigation also showed that the aggressive venturi shape provided no benefit, however the sponsor of the project insisted that they had seen better results when the same shape was installed in front of other expansions so the idea will have to be investigated experimentally.

6.5 Conclusion of CFD results

This section has compared the results computationally of the Offset device and Expansion device in their designated scenarios to a blank section. The results indicate that there will be a significant improvement in the powder balance through incorporating these devices into a pneumatic conveying pipeline.

In addition the CFD results have been used to essentially prototype the best shape for the Expansion device. The use of CFD to test scenarios relatively quickly in comparison to experimental without the labour cost and wastage is one of the key advantages of CFD being used in conjunction with experimental work.

A key point from the CFD result section is the deficiency in current CFD code to perform particle-particle interactions in the fuel:air ratios present in pneumatic conveying in power stations. Further improvements in this area would work towards making CFD more accurate and more representative in the field of pneumatic conveying.

Chapter 7

Experimentation: Passive Systems

7.1 Preface

This chapter focuses on the results and discussion of the passive devices tested in the course of this work. After investigating the chosen ideas, of the Offset and Expansion, using CFD, scaled experimentation is the next step in testing the various ideas. Though the quarter scale rig is modular, it is not infinitely flexible and only a limited number of scenarios can be recreated with the rig. There are two common vertical splitting scenarios:

- A standard rope - A single bend before the split, thus giving standard secondary flows. The standard, single bend, secondary flow pattern is shown in figure 7.1.
- A spinning rope - A combination of bends before the riser produces a single vortex in the secondary flows and in turn produces a spinning rope. An example of this vortex is shown in figure 7.2.

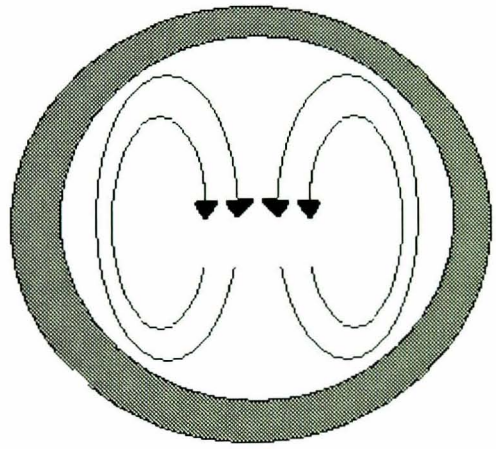

Figure 7.1 - Standard Secondary Flows present in a single 90° bend scenario

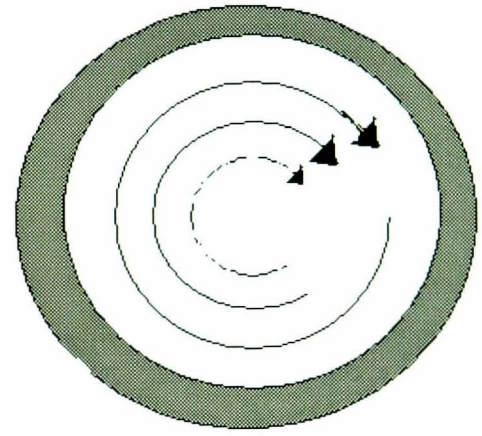

Figure 7.2 - Single vortex secondary flows present in the double 90° bend scenario

In the quarter scale rig both scenarios are possible. Scenario one (figure 7.3) is created by having a long horizontal run followed by single 90° bend rising into the vertical. Scenario two (figure 7.4) is created by having a long horizontal run followed by two perpendicular 90° bends rising into the vertical. Both scenarios terminate in a trifurcator. Both scenarios have different problems and obviously different solutions. The various device ideas brought forward from the initial ideas chapter will be tested in both scenarios.

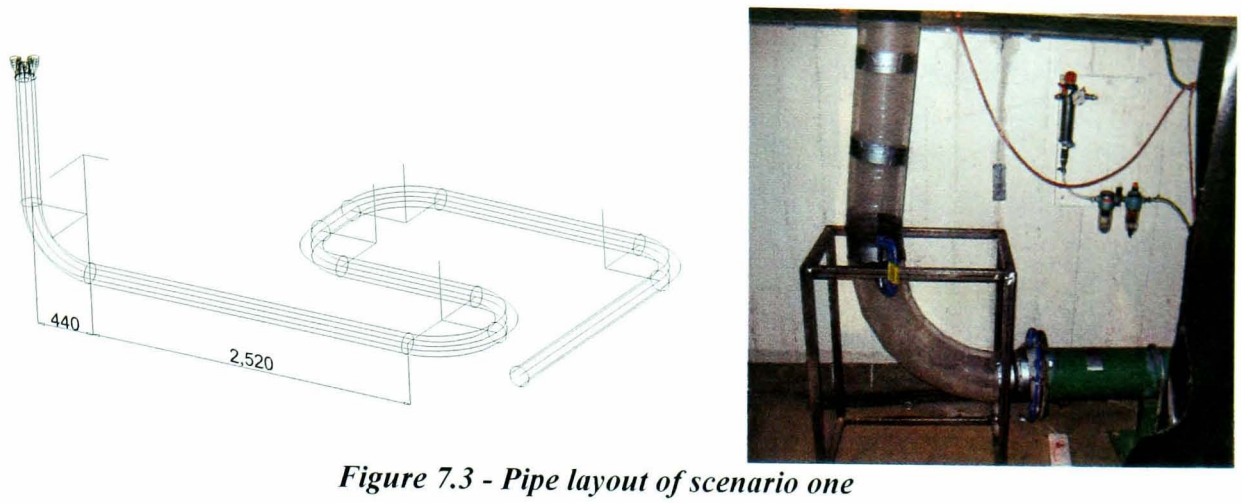

Figure 7.3 - Pipe layout of scenario one

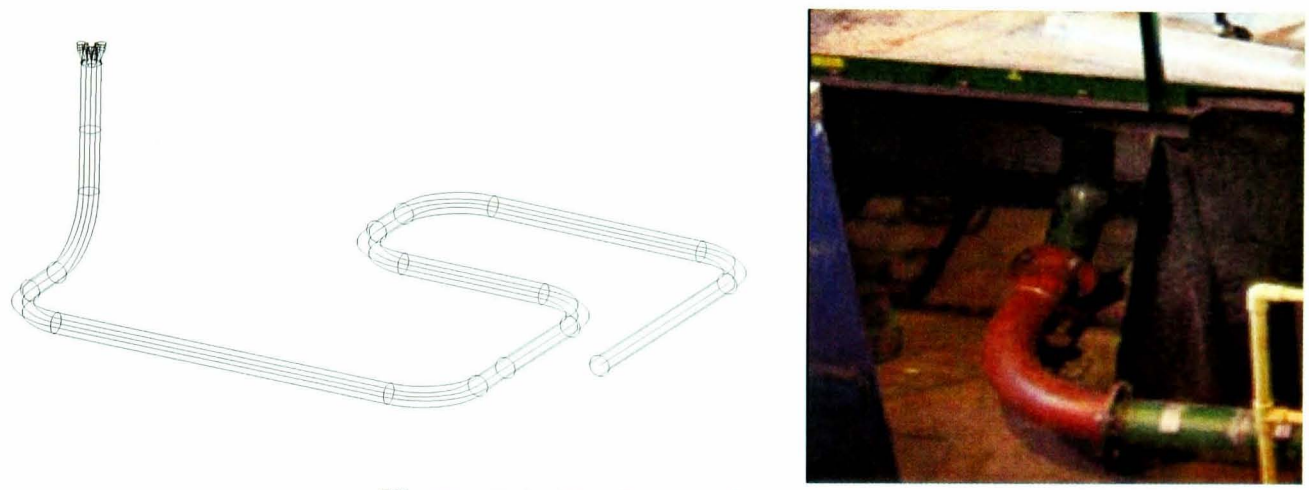

Figure *7.4 - Pipe layout of scenario two*

The chapter is split into the several sections. Firstly, it will deal with data interpretation, which includes error analysis. Then the control experiments and their results will be detailed. These experiments represent the benchmark for improvement. Then the results of the experimental tests carried out on the various devices will be detailed. Finally the chapter will end with a conclusion summing up the experimental test findings.

7.2 Data Interpretation

7.2.1 Preface

Interpretation of the data from the rig is vital for the experimental procedure. Whilst the raw data from the rig can be useful to a certain extent, processing of the data is very important in determining split information. In addition to processing information, the data has to be presented in an informative way so that patterns and behaviour of certain devices can be identified.

7.2.2 Processing data.

The Lab VIEW programme outputs its readings as a text file. This text file can be imported into excel to create a spreadsheet. Each line of the spreadsheet represents the outputted data sampled for that particular time. The Lab VIEW programme outputs a processed value based on an average of a 100 readings twice a second. It outputs a value for the current mass in each of the weigh hoppers, a velocity for each of the 4" outlets, a velocity for the 6" pipe and the time at which the sample was taken.

For the time of the experiment these values can be extracted and put into a different table. From this table an average velocity can be calculated as can the total mass collected and the mass flow rates. The mass flows are calculated by plotting a graph of the mass reading verses time for the experimental period and then the gradient of the graph is mass/time and hence the mass flow rate. This is done for each of the weigh hoppers.

7.2.3 Uncertainty and Calibration

The computer controlled nature of the experiment means that timing and human error in measuring values has been reduced to acceptable levels, $\leq 10\%$. The base uncertainty and possible non-linearity in the measurement transducers still needs to be considered and accounted for. Four devices represent the majority of the error in the rig are: The LVDTs, the DPTs, the Rotary Feed and the Fan.

An LVDT is an inductive displacement sensing device that produces an AC output voltage proportional to the mechanical displacement of a small iron core. They are simple and rugged, have completely step-less resolution. The voltage is produced by the movement of the iron core through a coil producing a change in the magnetic field; this will then induce a current in the wire. Figure 7.5 shows a schematic of their construction.

Despite purported accuracy of the devices, there are many loses associated with the LVDT. A good example is the hinge mechanism on the weigh hoppers, where loses and friction can effect the displacement of the transducer. Calibration had to be undertaken to determine what displacement equated to what voltage induced. This was done by placing weights on the weigh hopper and seeing how the voltage changed as the hopper was loaded and then unloaded.

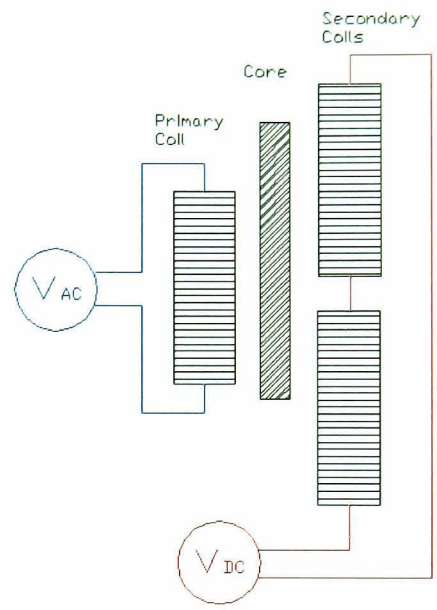

Figure 7.5 - Schematic of an LVDT

Three different starting points were considered for calibration, firstly with using 0 kg as the zero point, then using 2.5 kg as the zero point and finally using 4.75 kg as the zero point. These were all performed on a single LVTD to examine non-linear behaviour. From figures 7.6 - 7.8 it can be seen that there is a certain amount of hysterias and the non-linearity.

The LVDTs will only be used for measuring with increasing mass and only over a range of about 0kg to 4kg. The loading line is more linear than the unloading line. A series of tests were carried out to investigate each of the LDVTs for a range over 4kgs just loading mass onto it.

Figure 7.6 and table 7.1 shows the tests on the loading of individual LVDTs. The gradient shows that over the range of 4kg that the gradient indicates approximately 0.11 volts per kilogram. The value of the gradient for each L VDT test is used in the LAB view programme so as to give an easy conversion of voltage to mass.

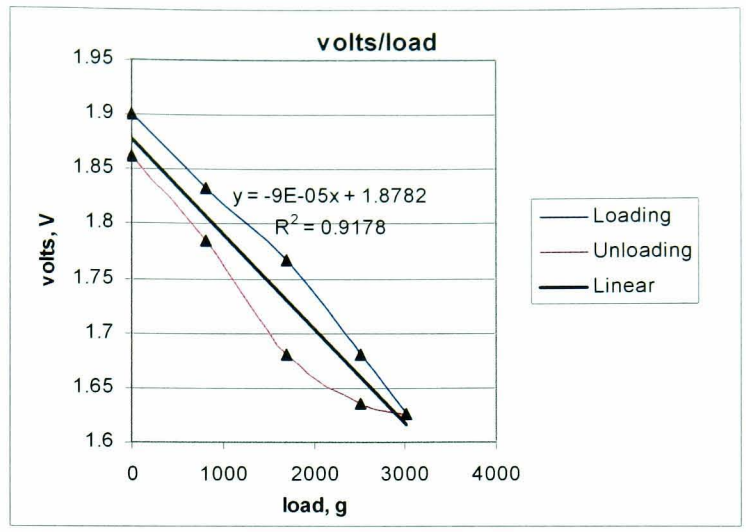

Figure 7.6: Loading/Unloading of LVDT between 0kg and 3kg

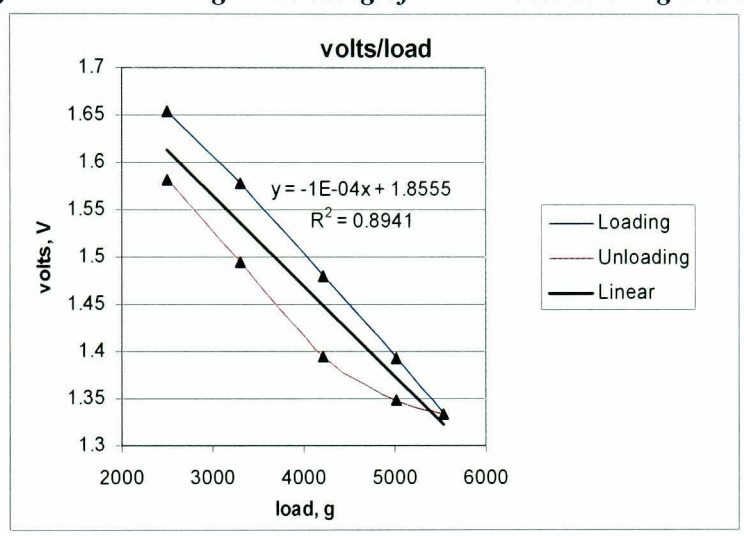

Figure 7.7: Loading/Unloading of LVDT between 2.5kg and 5.5kg

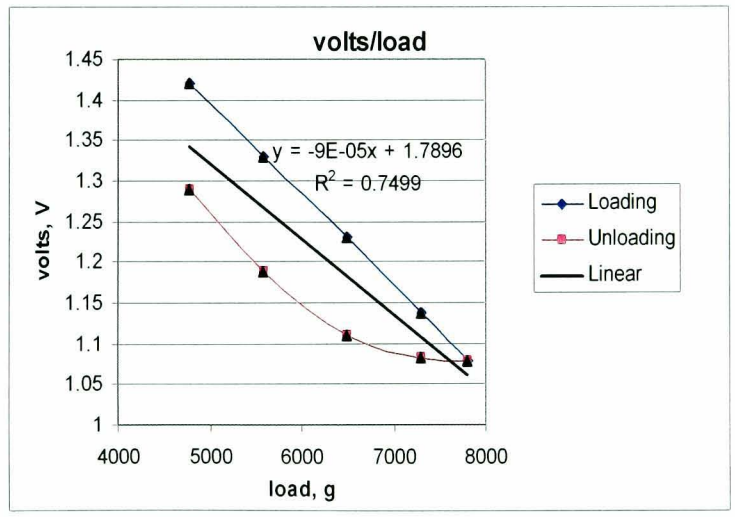

Figure 7.8 - Loading/Unloading of LVDT between 4.75kg and 7.75kg

Table 7.1 - LVTD voltage calibration data

Mass (kg)	Outlet 1 (V)	Outlet 2 (V)	Outlet 3 (V)
0	0.967	1.603	2.02
0.5	0.919	1.548	1.987
1	0.865	1.492	1.936
1.5	0.813	1.437	1.878
2	0.754	1.377	1.82
2.777	0.676	1.29	1.734
3.569	0.578	1.196	1.649
4.357	0.497	1.098	1.545

The non-linearities occur mainly whilst unloading and hence the weigh hoppers will be fully emptied between runs to avoid any non-linearities. A small degree of error will exist, even from the assumption of a linear relationship between the voltage and the mass. These were calculated using the regression tool in Excel. The errors are presented below in table 7.2 along with the individual gradients for each LVDT.

Table 7.2 - Error Analysis Summary for LVDTs

	Gradient	Standard Error	Percentage Error
LVDT 1	-0.11	±0.0011	1.01%
LVDT 2	-0.12	±0.0008	0.69%
LVDT 3	-0.11	±0.0025	2.26%

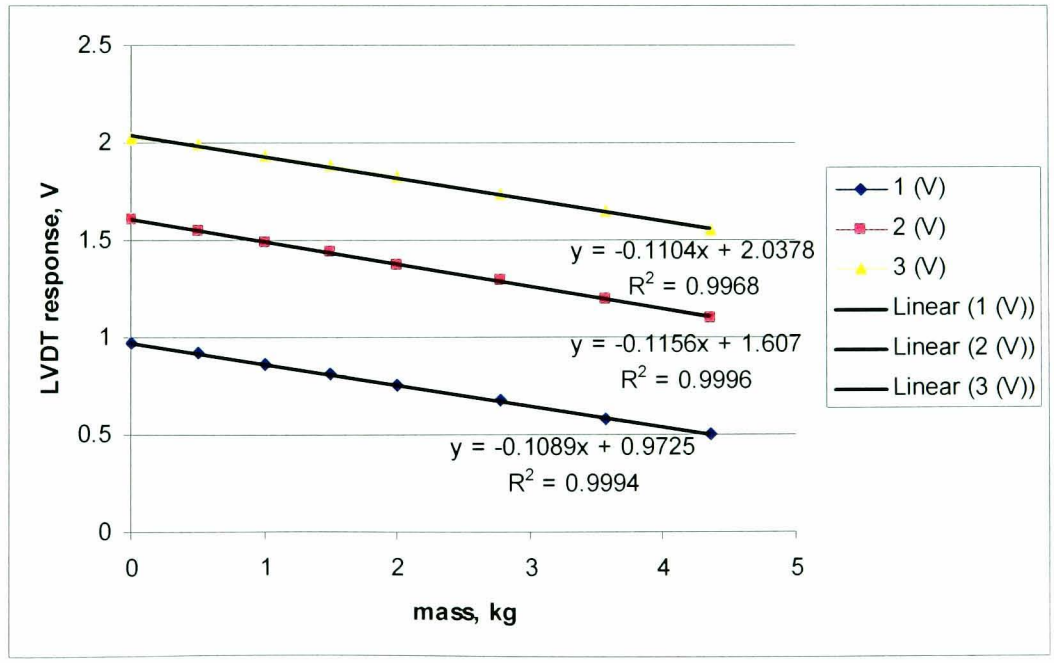

Figure 7.9 - Loading of the individual LVTDs

The differential pressure transducers (DPT) are used on the rig to measure the velocity of the air. The DPT contains a diaphragm to contact the fluids and protect the measuring set up isolated from the measured fluids, most of which may be corrosive. Due to the existence of this

diaphragm, most pressure transducers can be used as pressure differential transducers, as long as the second (lower) fluid is introduced into the other side of the diaphragm. When measuring the pressure the DPTs are measuring the pressure difference between the measured pressure and the pressure of atmosphere gauge pressure

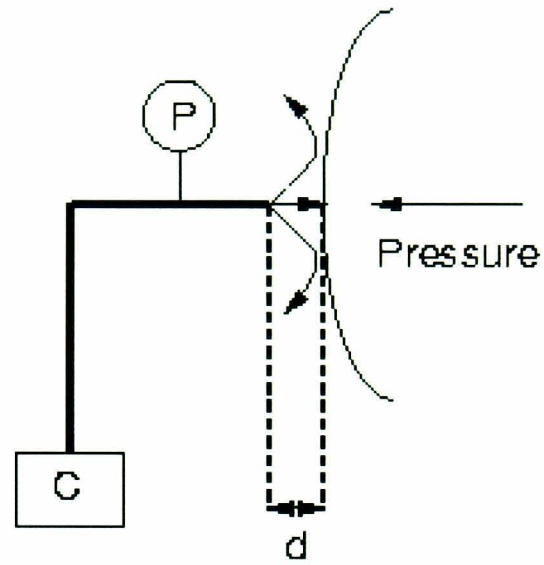

Figure 7.10 - Schematic of how the pressure transducer works.

This gauge works on a capacitance, the diaphragm is moved by the pressure which in turn affects a di-electric substance in a capacitor which is then calibrated to give a voltage that equates to a pressure drop. Figure 7.10 shows the schematic for the pressure transducer; d represents the di-electric, P the reference pressure and C the computer.

The DPTs are positioned so they measure the differential pressure across an orifice plate to function as an Orifice based flowmeter as per BS EN 1042. With the use of theory this allows the calculation of the velocity in the LABview programme for each leg of the rig. According to the manufacturers details of the DPTs they possess accuracy for the calibrated span of ±0.85% taking into account accuracy for vibration, temperature affects and static Pressure effects (Rosemount August *2004).* Under ideal running conditions this falls to ±0.075%. When considering both the LVDTs and DPTs it also needs to be considered that the Data and Acquisition (DAQ) board, used to receive the voltages from these transducers, is only accurate to ±μ1V.

The rotary feed operates using a ball valve to feed powder into the rig. The rate for the rotary feed is set in a frequency of rotations of the ball valve. However the amount of powder moved is not constant and an error in the feed can lead to an error in the AFR. Experimentation was undertake to investigate the appropriate setting on the rotary feed to get desired AFR. Table 7.3 shows the

calculated AFR for a set frequency of the rotary feeder. The Fan normally runs at a constant velocity, however, the throughput velocity is altered by a number of factors:

- Particle loading
- Number of Kinetrol valves closed.
- How clogged the extraction bags are in the extraction unit.
- Environmental factors.

Table 7.3 - Frequencies for the Rotary Feed to produce a specific AFR

Rotary Feed Frequency (Hz)	AFR
35.5	3:1
26.7	4:1
21.3	5:1
17.8	6:1

The air speed velocity therefore fluctuates during operation and can vary quite substantially. This can cause an error in the set AFR. Both the above problems are solved by collecting the data from the weigh hoppers and the DPTs about velocity and mass collected after the experiment. The DPTs, which report the velocities in the three branch pipes, transmit their readings of velocity twice a second. When the data is process an average of the 120 velocities read during the experiment is used to determine an average velocity.

7.3 Experimental Errors

Experimental study will always have a level of uncertainty in the results outputted. All measurement techniques have a certain degree of error present in them. In a process as complex as the rig there are many sources for error. The outputted values of the rig that are recorded twice a second are:

- The air speed velocity in the 6" pipe
- The air speed in each of the 4" pipes.
- The mass collected in each weigh hopper.
- The time at each reading.

From these values you can calculate:

- The AFR
- The mass flow rate in each of the outlet legs.
- The particulate split information.

7.3.1 Error in the AFR

The AFR is used to compare results of different scenarios. Whilst the AFR varies due to fluctuations, the values can be calculated from the outputs of the rig. However, these outputs themselves contain composite errors.

The mass of particulate collected can be calculated from the total mass of fuel collected in the weigh hoppers. This value is gained from the calibrated voltages from the LVTDs. This data is fed via a DAQ card with an uncertainty of ±μ1V. This uncertainty would equate to ±1e-6Kg or a thousandth of a gram. This error is so small it can be ignored. In addition, the error from the calculation of the gradient as presented in Table 7.2.

Another error in the mass of particulate collected that cannot be calculated constantly is the amount of mass removed from the system by the extraction units. Whilst it could be feasible to weigh the extracted dust, it was found to vary based on the age of the powder, also not all powder outputted into the bin and was still caught in the extraction bags.

An estimation of the percentage of the powder based on observation will be that no more than 1 % of the powder is extracted per test. A composite error in the mass collected can be estimated as ±5%.

7.3.2 A composite error in the mass

The air speed in the three 4" pipes is controlled by the DPTs. The manufacturer's error for the voltages is ±0.85%. The DPTs also fed their voltages through the DAQ which has an uncertainty of ±μ1V This will equate to less than 1/500th of a metre per second and hence can be ignored.

The velocity for each test is an average of 120 readings, two readings every second. The individual error in each experiment will depend on the standard deviation of the individual experiment. But due to the high number of readings it will be small. An average experimental run yielded an error of 2%. This gives a composite error of approximately 3%

The calculation of the AFR is a quotient. The calculation is the mass of air, calculated from the velocity divided by the total mass. The uncertainty in the total particulate mass is ±5% and the

uncertainty in the air mass is ±3%. The relative error in a quotient is calculated from:

$$\frac{\partial R}{R} = \left|\frac{\partial a}{a}\right| + \left|\frac{\partial b}{b}\right| \qquad \textbf{Equation 7.1}$$

Essentially this is a simple addition of errors and thus the estimated error in the AFR is ±8%.

7.3.2 Error in mass flow rate

The mass flow rate is calculated from the gradients of the graphs, the value of the LVTD has a maximum uncertainty of ±2.4%. The time based on the computer clock has an uncertainty so small it not of any consequence to the calculation. This means that the uncertainty in the mass flow is ±2.4%.

7.4 Control Experiment

Both scenarios require a control experiment to compare the results of the various devices. It is from these experiments that the improvement in split will be assessed. Both control experiments utilise a trifurcator and then a 5 pipe diameter rise from the bend to the splitting face of the trifurcator. Both control experiments use "used" powder and run at the conditions shown in table 7.4.

Table 7.4 - Operational conditions for control experiments

Pipe Diameter (m)	0.1524
Particle Density (kg/m^3)	800
Average Particle Diameter (m)	9.00E-05
Dynamic Viscosity (kg/ms)	1.85E-05
Kinematic Viscosity (mol/s)	1.57E-05
Acceleration due to Gravity (m/s^2)	9.81
Velocity (m/s)	16
Maximum AFR	3:1

7.4.1 Scenario 1

As described above this scenario consists of a single 90° bend with a radius/diameter ratio of 1.7. There is then a vertical riser that extends for 5 pipe diameters. At the end of the riser there is the splitting face of a trifurcator. This face looks like a Mercedes symbol. The three outlets are labelled Outlet 1, Outlet 2 and Outlet 3. A layout of where the outlets lie is shown in figure 7.8.

Table 7.5 – Split by mass flow rate through the geometry of scenario 1

AFR	Mass Flow (kg/ms^{-1})	Split 1 (%)	Split 2 (%)	Split 3 (%)	Actual AFR	Max/min
3:1	0.1066	24.30	53.28	22.42	3.23	2.38
4:1	0.0918	26.58	47.93	25.49	3.83	1.88
5:1	0.0712	11.80	49.86	38.34	5.01	4.23
6:1	0.0656	16.16	45.27	38.57	5.66	2.80

Table 7.5 shows the results of the split by mass flow rate of the particulate, whilst figure 7.12 shows the relationship between the splits. The individual splits move towards an equal split (33%/33%/33%) as the AFR decreases except at 3:1 nominal AFR where it deviates slightly. Theory would suggest that as the AFR decreases that inter-particle collisions in the rope would increase due to the increased amount of particulate. This would cause the rope to be more dispersed and hence provide a better split.

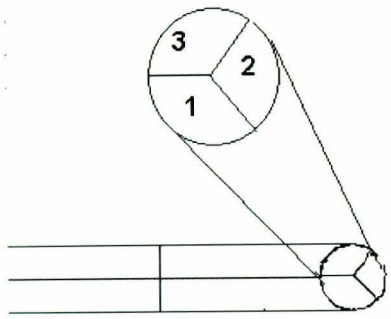

Figure 7.11 – Position of the outlets for scenario 1

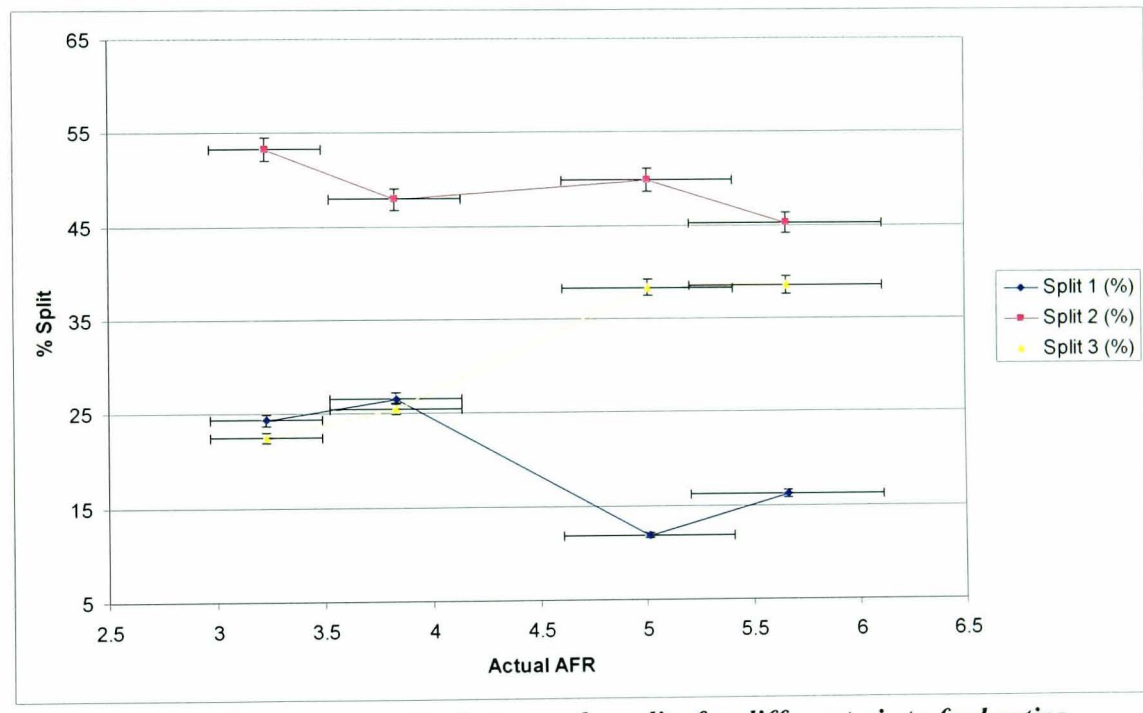

Figure 7.12 – Relationship between the splits for different air to fuel ratios.

7.4.2 Scenario 2

As described above this scenario consists of two 90° bends with a radius/diameter ratio of 1.7 positioned perpendicular to each over to transfer a horizontal run into a vertical riser. There is then a vertical riser that extends for 5 pipe diameters. At the end of the riser there is the splitting face of a trifurcator. The three outlets are labelled Outlet 1, Outlet 2 and Outlet 3. A layout of where the outlets lie is shown in figure 7.10. Table 7.6 shows the results of the split by mass flow rate of the particulate, whilst figure 7.14 shows the relationship between the splits.

Table 7.6 – Split by mass flow rate through the geometry of scenario 2

AFR	Mass Flow (kg/ms^{-1})	Split 1 (%)	Split 2 (%)	Split 3 (%)	Actual AFR	Max/min
3:1	0.139	13.60	38.99	47.41	2.66	3.49
4:1	0.102	10.59	38.92	50.49	3.63	4.77
5:1	0.083	9.88	32.53	57.59	4.44	5.83
6:1	0.0697	9.76	24.82	65.42	5.28	6.71

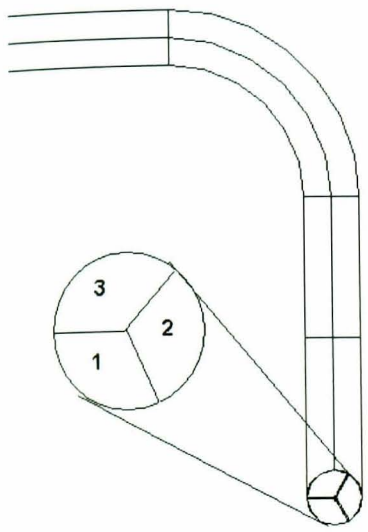

Figure 7.13 – Position of the outlets for scenario 1

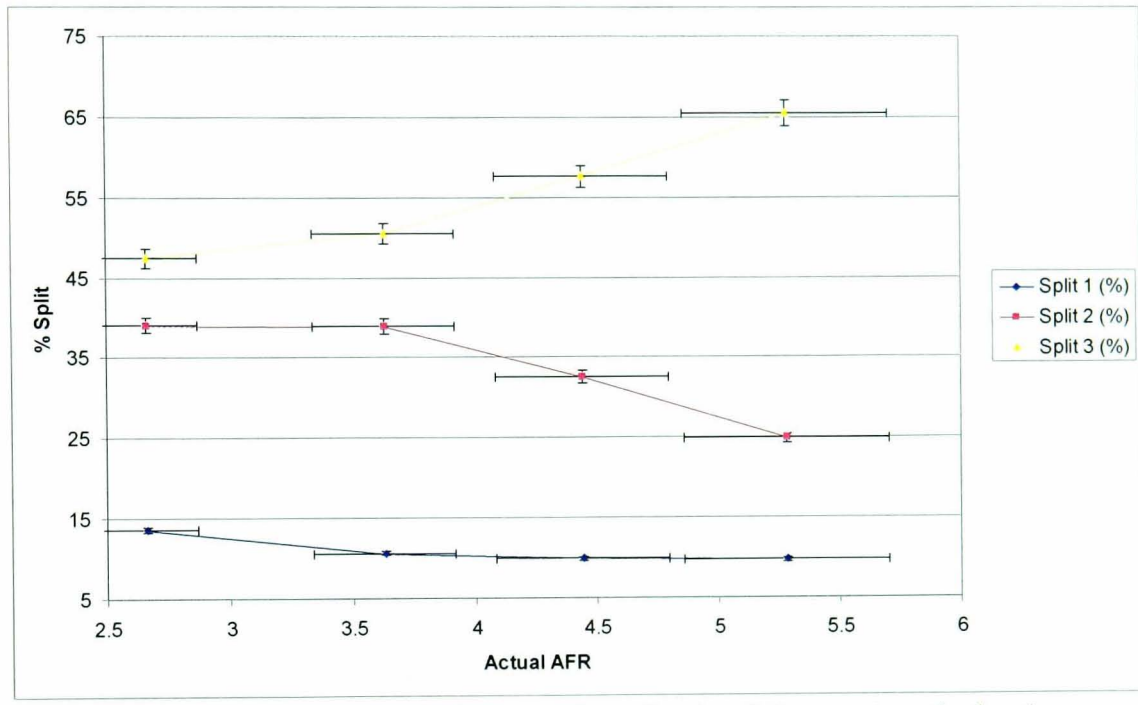

Figure 7.14 – Relationship between the splits for different air to fuel ratios.

7.4.3 Description of experimental results

The experimental results section is divided into the results for scenario one and the results for scenario two. Both sets of experiments were carried out with the conditions stated for scenario one and scenario two.

When presenting each set of results they will include the splits based on the mass collected and the splits based on the mass flow rate in each outlet pipe as well as the corresponding calculated overall mass flow rate and the air to fuel ratio. The industry standard used to measure the split is "The max/min ratio", this will be presented for each split. A max/min of 1.0 represents a perfect split, regardless of the number of outlets. If the minimum value is the same as the maximum value then all the outlets must be the same. Power industry normally given tolerance is about 5% on a split.

As well as numerical data a graph showing the change in the splits between the three outlets and

how it varies with AFR will also be presented. These graphs are useful to see how the rope position, indicated by the split, moves dependent on the air to fuel ratio.

7.5 Results for Scenario 1

7.5.1 Preface

For scenario one, a single 90° bend, the objective is to move the rope away from the wall. From the work of Giddings et al (2002), it is theorised that moving the bulk of the powder into the centre of the vertical riser, away from the wall, will aid the dispersion of the particulate. The nature of the secondary flows in the riser show that dispersion increases with distance from the bend. This means that any device installed needs to be installed as close to the bend as possible.

7.5.2 The Offset Device.

The offset consists of an angled "kink" in a pipe that appears on both sides of the pipe. This means that the cross sectional area does not change as much as a Venturi. From the initial ideas the Offset was seen as the most favourable 90° bend. A photograph of the offset can be seen in figure 7.15

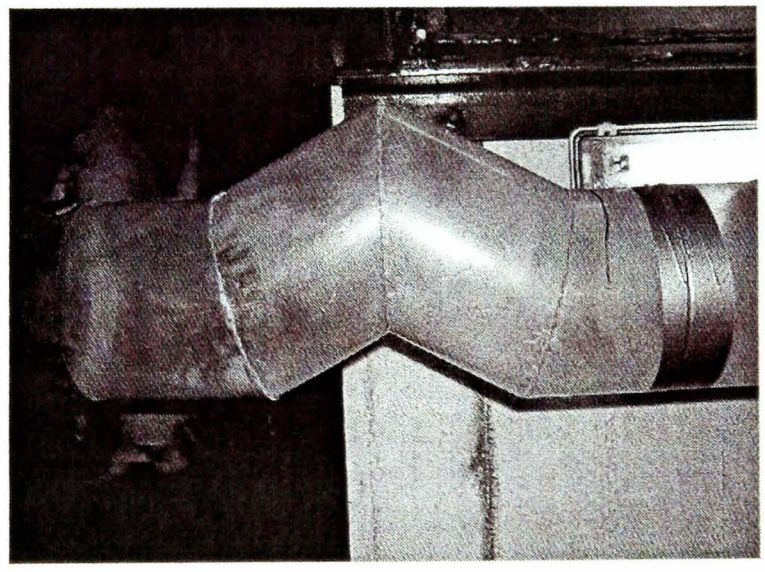

Figure 7.15: The Offset device

The offset is designed to operate by altering the direction of the momentum of the "Rope Core", The author of this work considers the Rope Core to be area of the rope that constitutes the

majority of the heavy particles. This area of the rope consists of particles whose Stokes number is »1. Changes in the airflow direction will not affect these particles. The Offset is designed to deflect the particle rope with the

deflecting face into the centre of the pipe and then allow the height between the deflecting face and the trifurcator outlets disrupt the rope further. A schematic shown in figure 7.16 shows the different parts of the Offset.

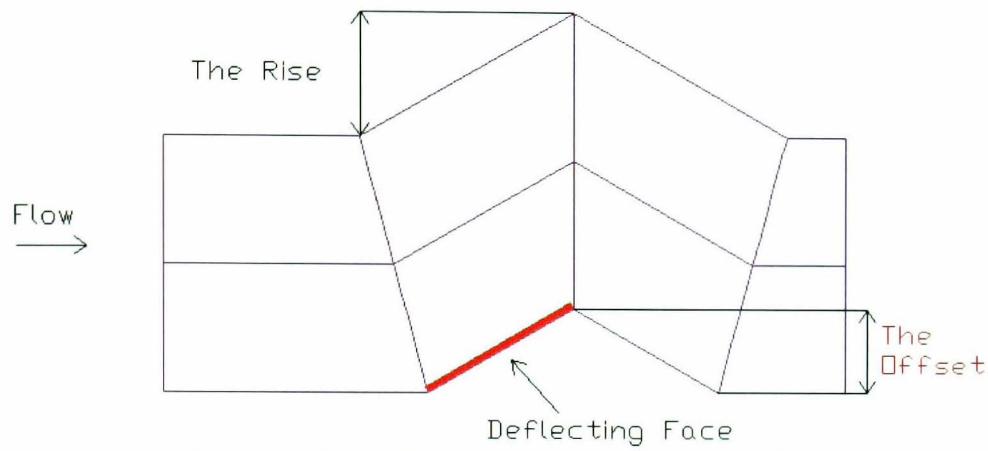

Figure 7.16 – Different parts of the offset device

A diagram in figure 7.17 shows the geometry involving the Offset and its distance from the trifurcator. The offset is positioned as close to the pipe bend as possible with the current construction of Offset. The photograph in figure 7.18 shows the overall positioning of the Offset. The same range and test conditions were undertaken for this experiment as for the control tests. This involved 4 different AFR operating at a nominal 16m/s.

Different angles for the offset were tried to examine the effect it would have on the particle splits. The same offset height was maintained for the alternative offsets. Offsets for 20, 30, 40 and 50 degrees were constructed and tested to see what improvement they could make. The results for the 30 degree offset are shown in figure 7.19.

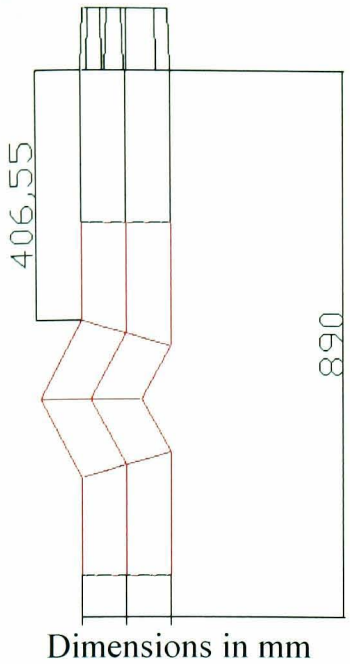

Figure 7.17 – Offset in situ

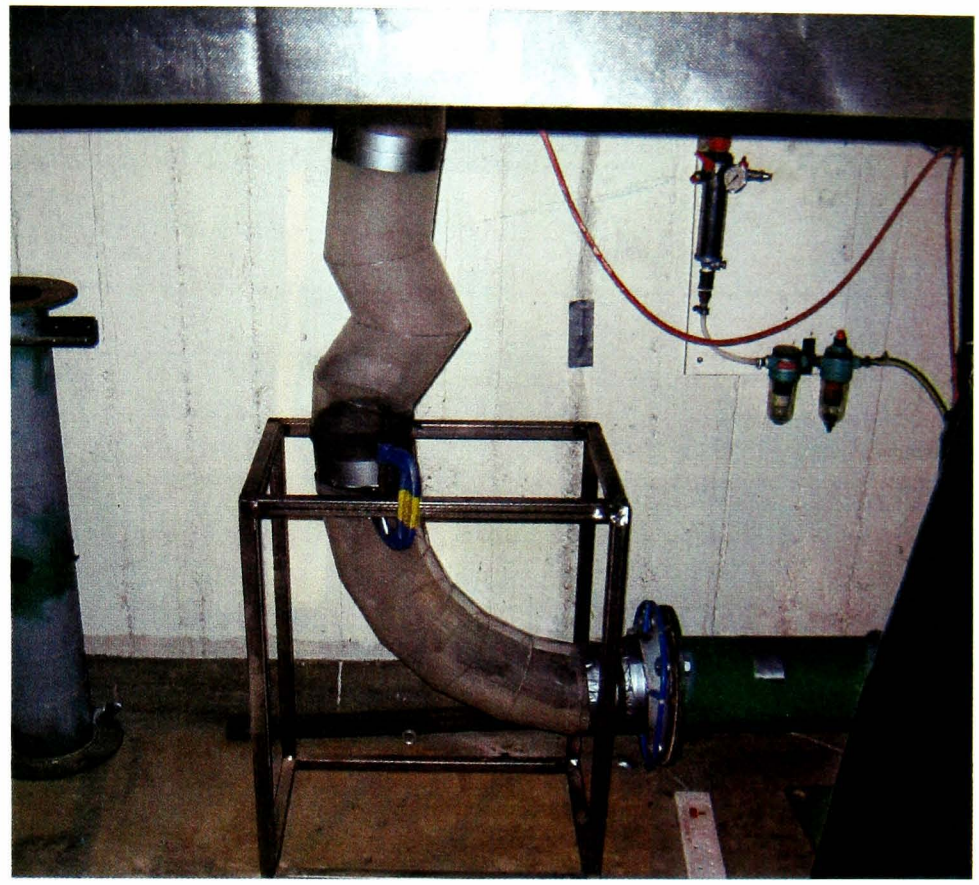

Figure 7.18 – Overall positioning of the Offset device

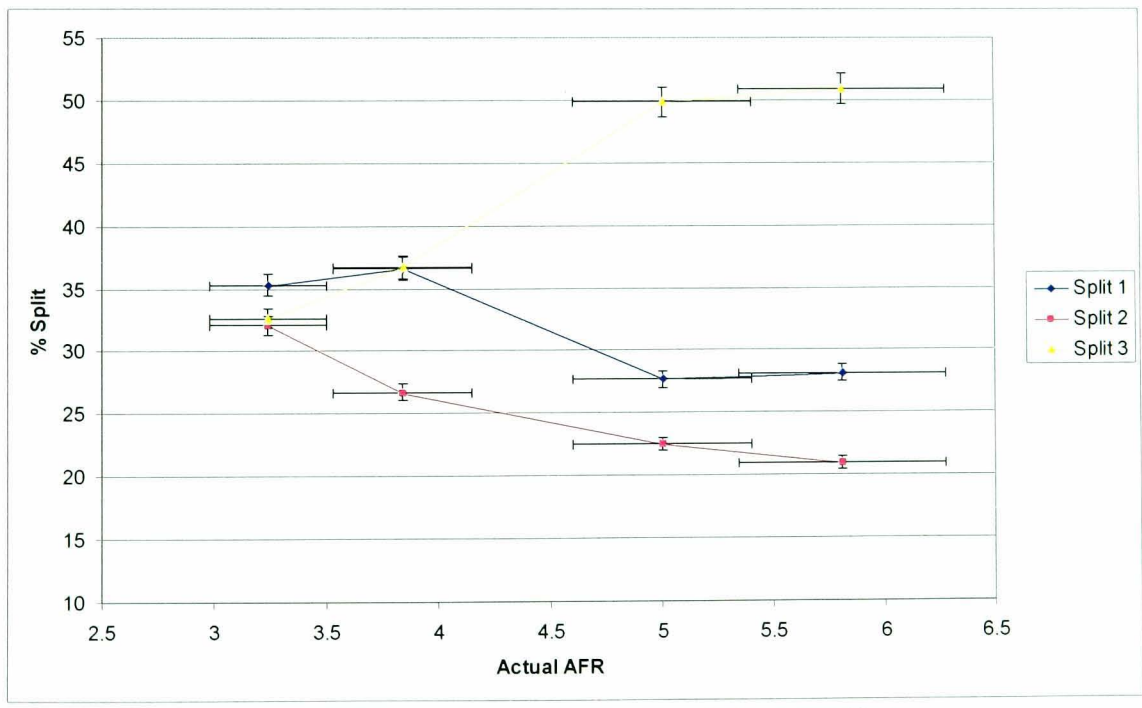

Figure 7.19 – The results for the 30 degree offset.

7.5.3 Alternative 1 (20°) Offset Device

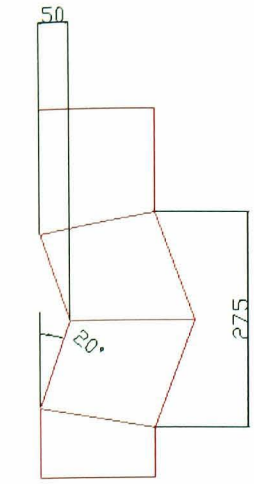

Dimensions in mm

Figure 7.20 – Offset 20° dimensions

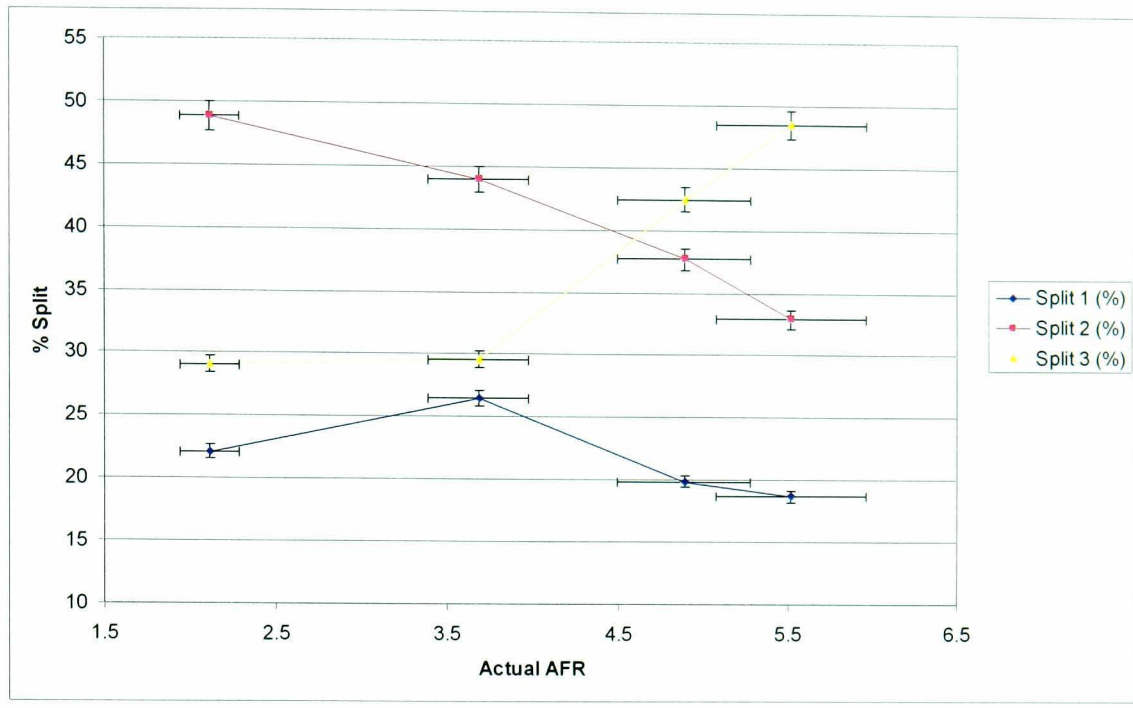

Figure 7.21 –Results for the 20° Offset device

7.5.4 Alternative 2 (40°) Offset Device

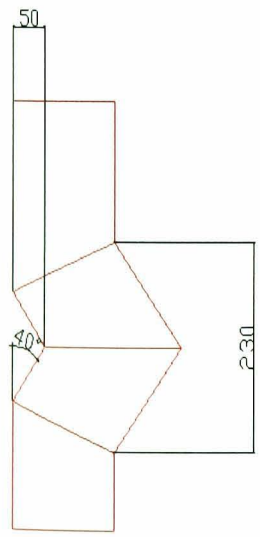

Dimensions in mm

Figure 7.22 – Offset 40° dimensions

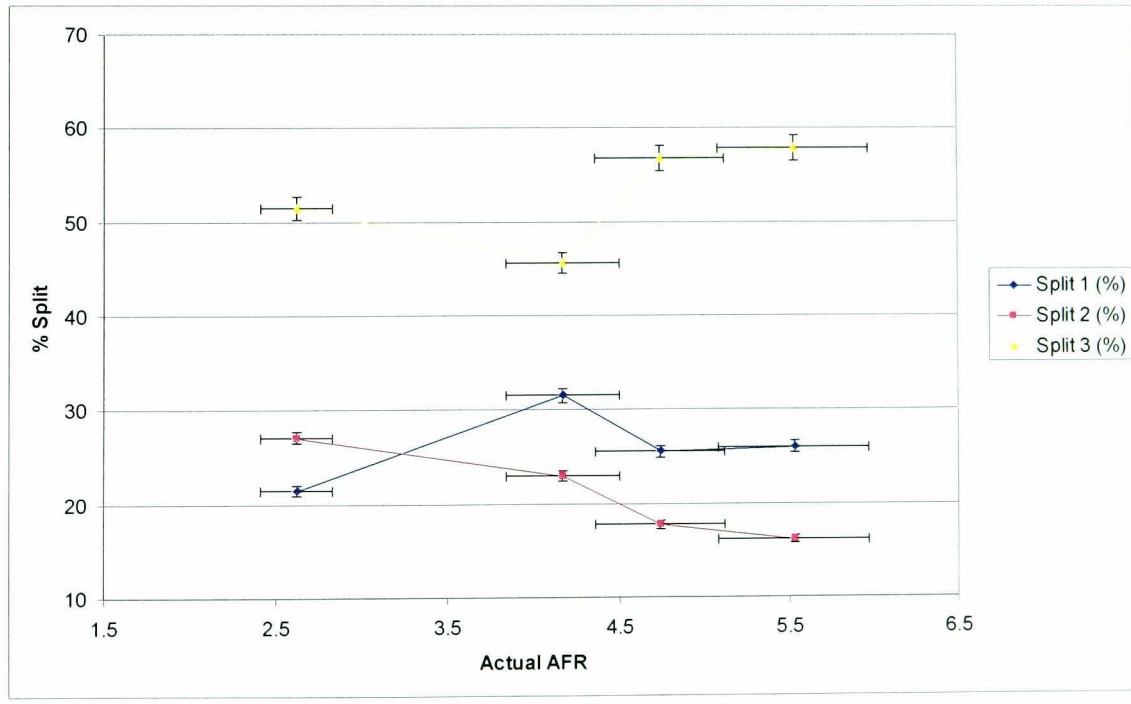

Figure 7.23 – Over Results for the 40° Offset device

7.5.5 Alternative 3 (50°) Offset Device

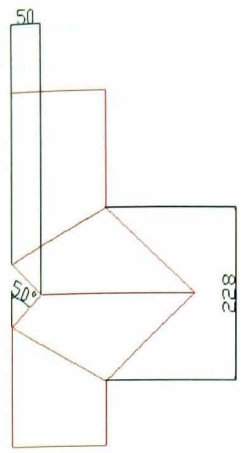

Dimensions in mm

Figure 7.24 – Offset 50° dimensions

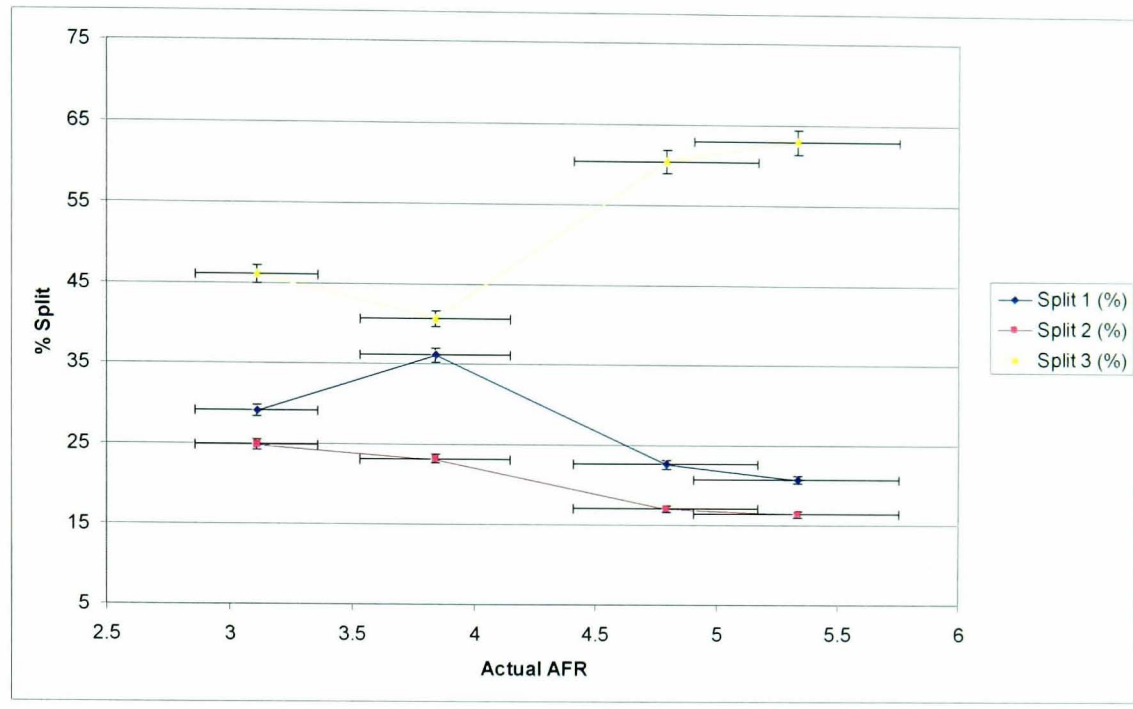

Figure 7.25 – Results for the 50° Offset device

7.5.6 Expansion in scenario 1

The expansion was designed as a universal device to function regardless of the angle at which the, but was designed to work with a spinning rope. It was not expected to be a large improvement. The design of the Expansion is described in the section on the scenario two experiments.

7.5.7 Comparison

The maximum over minimum ratio is a good indication of split when comparing different devices. A maximum over minimum value of 1.0 indicates a perfect split. The maximum over minimum values for all the devices and air to AFR are presented in a graph in figure 7.28 for comparison.

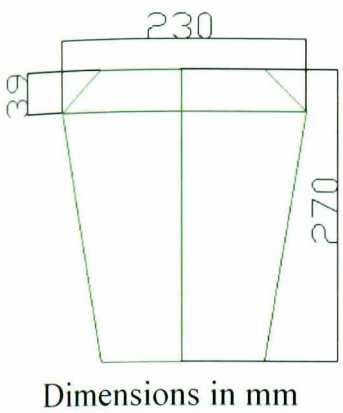

Dimensions in mm

Figure 7.26 – Dimensions of the expansion

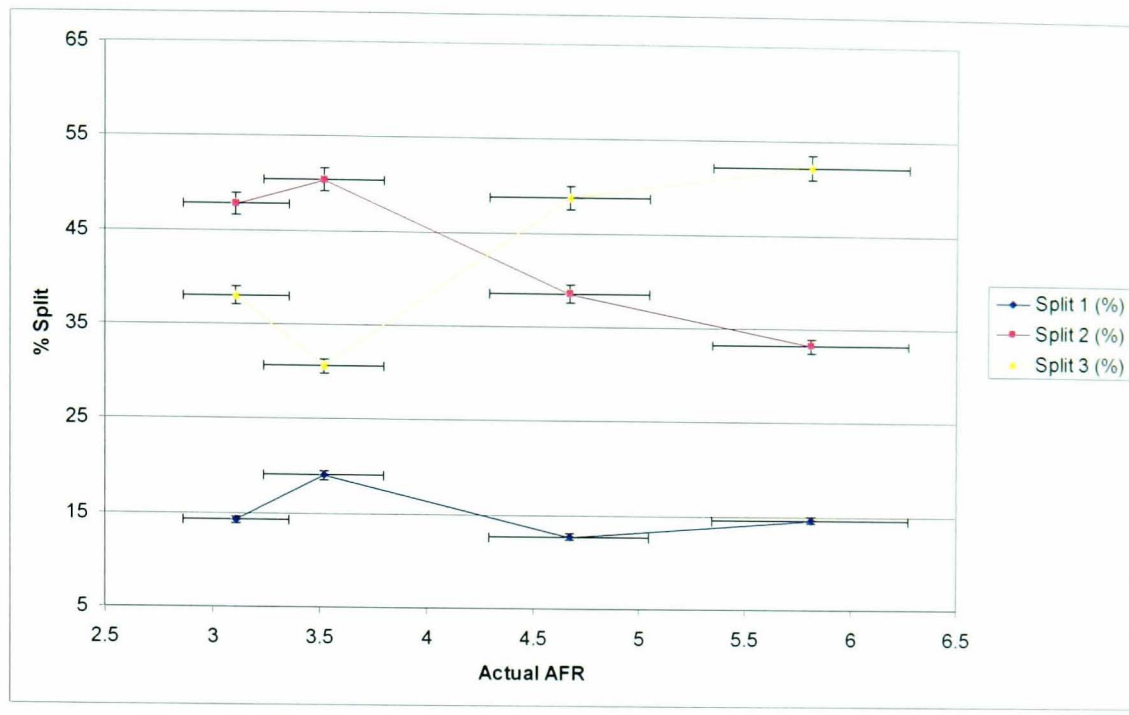

Figure 7.27 – Results for the Expansion for the single bend scenario

From this graph it can be seen that the most effective device is a 30 degrees in dimension. However, the splits are by no means perfect. The addition of a "fine tuning" device or a semi active system will improve the level of control.

In addition to splits data, the data collected from the pressure tapping to indication which device has the lowest pressure drop. Taking the pressure drop across 5 pipe diameters the various devices were compared at the same running conditions. These were a 3:1 AFR, 16m/s.

The pressure drop was an average value taken from readings measured over a minute of constant use. These results are displayed in table 7.12. From the pressure drops, it can be seen that the Expansion is the lowest followed by the Offset with pressure drop increasing as the angle of the Offset increases.

7.6 Discussion of Experimental for Scenario One

7.6.1 Preface

From the experimental results conducted for scenario one, it is obvious that out of the two type of devices employed in this scenario the Offset device is superior to the Expansion. The Expansion is designed for spinning ropes and was not expected to improve the powder balance. The offset has several interesting features that have to be examined in more depth.

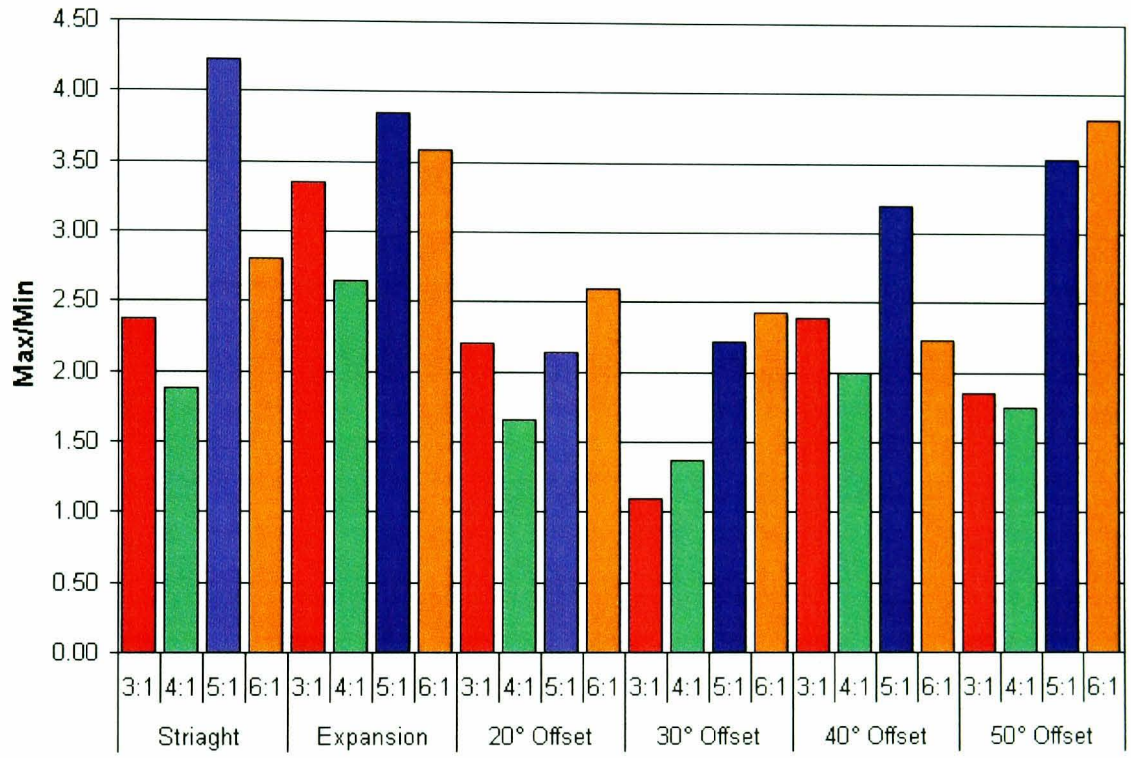

Figure 7.28 – Comparison of results for scenario 1

7.6.2 Assessment of Performance

From the results of the tests the Offset improves the split over the control scenario; the split improves as the AFR drops and the mass of particulate increases, similarly to the control scenario. This behaviour is shown for all Offsets, figure 7.29 shows the AFR plotted against max/min values for the different types of Offset.

All the Offsets follow the same approximate pattern, a pattern matched by the straight section. As the AFR decreases (i.e. the amount of particulate increases) the split is much improved. This bodes well for a translation to power plant scale as power stations regularly run at AFR approaching 1.5:1 - 1.2:1. From the graph it appears that the 30° Offset works the best and that

for the geometry of scenario one there is an optimum angle of the deflecting surface. This optimum lies around the 30° geometry.

Table 7.7 - Pressure Drops for the devices tested in scenario 1

Device	Total Pressure Drop	Device Pressure Drop
Straight	81 Pa	-
Expansion	150 Pa	69 Pa
20 ° Offset	186 Pa	105 Pa
30 ° Offset	196 Pa	115 Pa
40° Offset	200 Pa	122 Pa
50° Offset	216 Pa	138 Pa

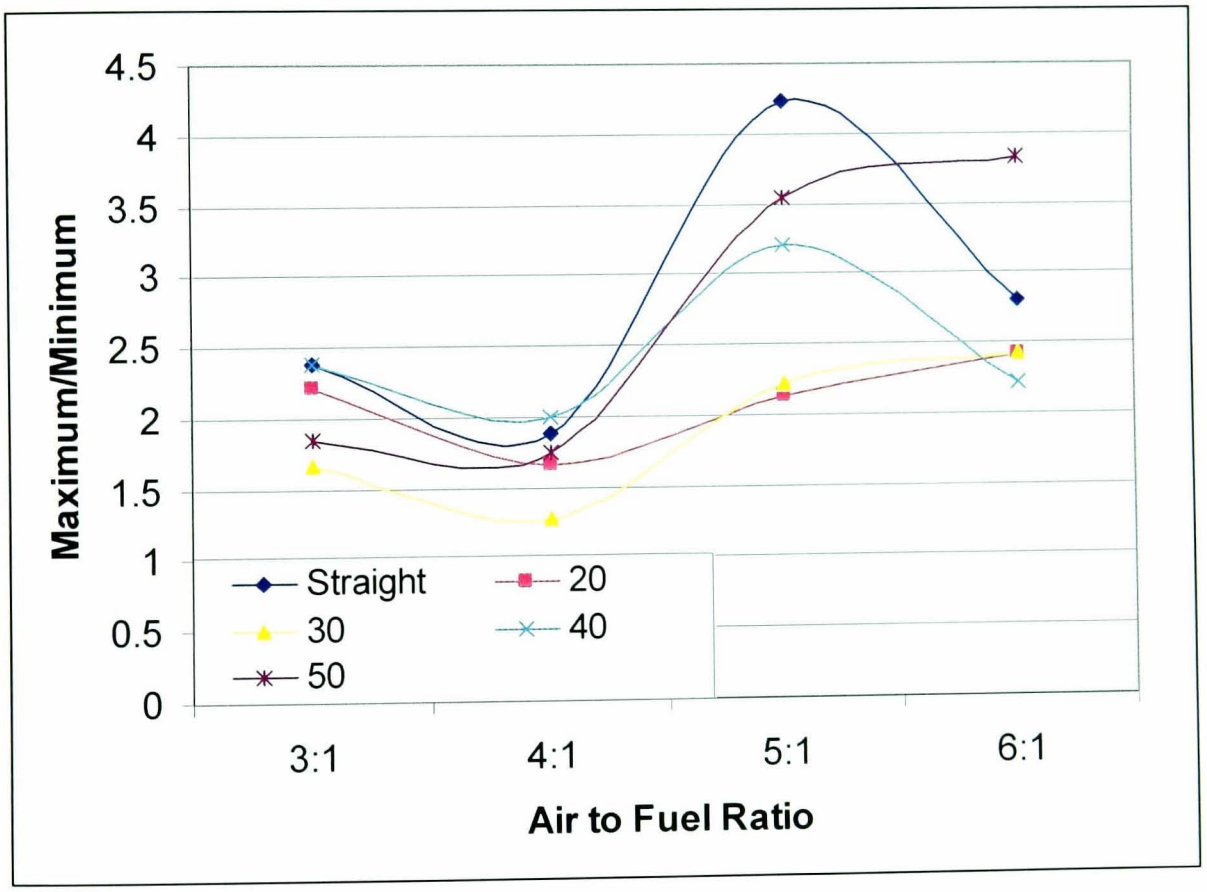

Figure 7.29 – Comparison of different Offsets at different AFR

7.6.3 Rope deflection

The Offset seems to perform exactly as designed, moving the powder away from the wall. The CFD done on the Offset predicted that the particles being flung to the far side of the pipe. However, the photographs taken of the Offset in operation show the deflecting surface moving the particles into the centre of the flow. A sample photograph can be seen in figure 7.30. In comparison the CFD overestimates the degree of this deflection, the CFD prediction is shown in figure 7.31.

The deflection is caused by altering the direction of momentum of the rope core from vertical to an angled path. This extreme momentum change allows the rope to move into the centre of the pipe and hopefully disperse.

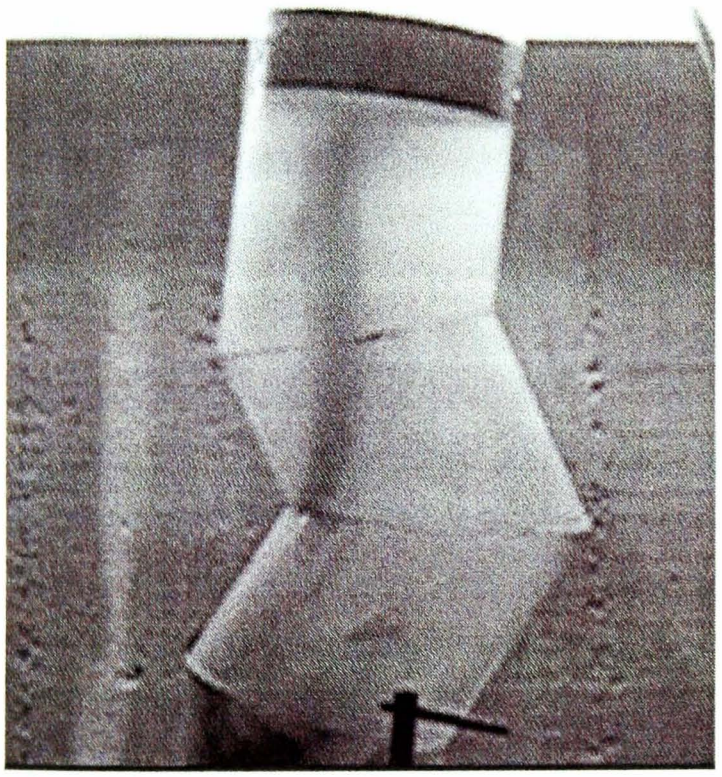

Figure 7.30 - Separation of the particle rope from the pipe wall.

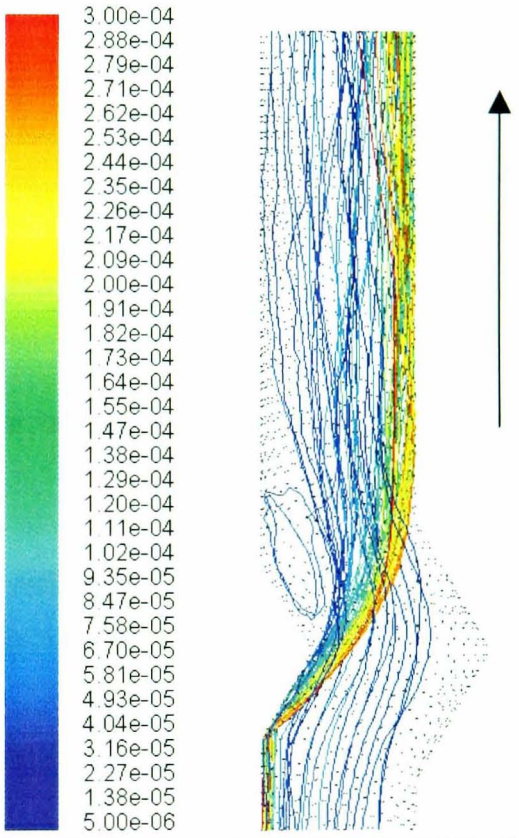

Figure 7.31 – Separation shown in CFD, flow in arrow direction

7.6.4 Boundary Layer Separation

In addition to deflecting the particles, deflecting surface also creates an adverse pressure gradient that causes boundary layer separation over the Offset. This has the effect of creating an area of re-circulation following the offset. This boundary layer separation prevents the majority of

smaller particles, of Stokes number 1 or less, from reattaching to the wall immediately after the Offset. The re-circulation can clearly be seen through observation of the particulate material. It is also predicted in CFD as shown in figure 7.32

The boundary layer is the layer of fluid next to a wall surface. This area of fluid tends to travel slower than the mainstream velocity with the particles travelling theoretically zero at the wall surface. A profile of a velocity profile can be seen in figure 7.33.

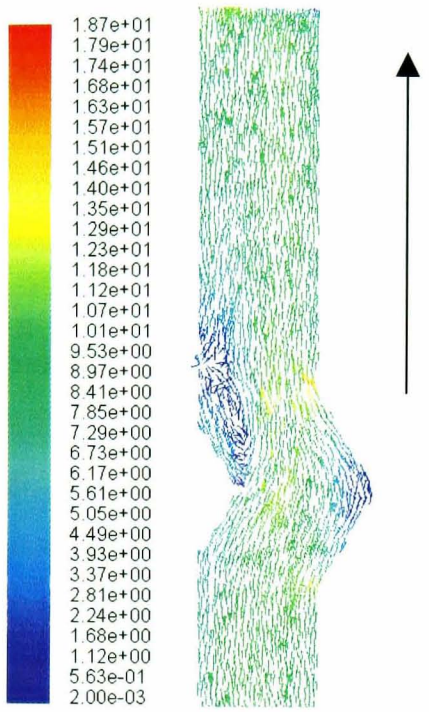

Figure 7.32 – CFD representation of the re-circulation, flow in arrow direction

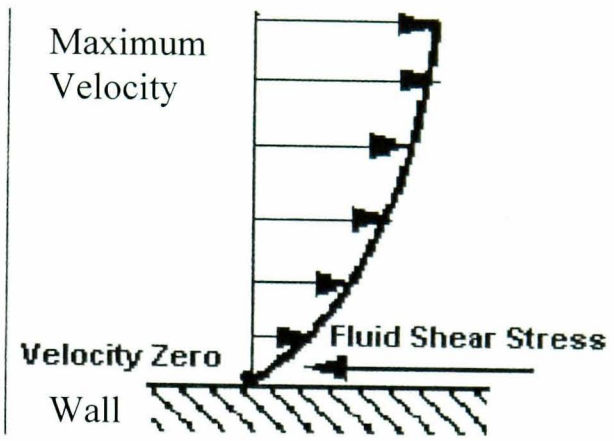

Figure 7.33 - Profile of a typical velocity profile

Flow development in the boundary layer depends on the pressure distribution along the wall. If the pressure gradient is favourable then the boundary layer remains well attached to the wall. With an adverse pressure gradient, the pressure starts to rise in the direction of the flow and the boundary layer tends to separate from the body surface. This mechanism is shown in figure 7.34

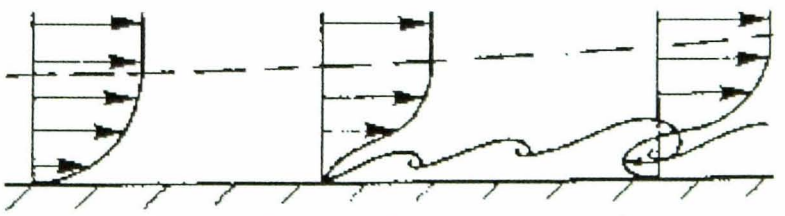

Figure 7.34 – Boundary layer separation

As the velocity in the boundary layer drops towards the wall, the kinetic energy of fluid particles

inside the boundary layer appears to be less than that at the outer edge of the boundary layer. This means that while the pressure rise in the outer flow may be quite significant, the fluid particles inside the boundary layer may not be able to get over it. Even a small increase of pressure may cause the fluid particles near the wall to stop and then turn back to form a re-circulating flow region characteristic of separated flows. This increase in pressure is seen after the offset.

The boundary layer separation that occurs in the offset is similar to the boundary layer separation that occurs after airfoils at large angles of attack.

7.6.5 Optimisation of the Offset

It is possible that through extended optimisation to design "the Offset" so that the re-attachment of the boundary layer could coincide with an area considered optimal for powder balancing.

The shape of the Offset has been designed so that the actual cross sectional area is not drastically reduced. This is done to prevent pressure drop from constriction. The offset does create a pressure drop. This pressure drop increases as the angle of the offset increases. This pressure drop is associated with the drastic change in direction of the mass of air striking the offset. The offset achieves a relatively low pressure drop as indicated in the comparison section.

To optimise the Offset, first the areas for optimisation have to be identified and then what effect changes to these areas will have. The two features that can be altered in Offset are the; the angle of the offset and the height of the offset.

The current experimental work involves changing the angle and keeping the offset height the same. Altering the angle and keeping the offset height constant leads to the device becoming longer in length. A successful device will have to fit within 2 pipe diameters, in the 1/4 scale rig this equates to 304.8mm.

7.6.6 Conclusion

Whilst not a perfect split for all scenarios, the Offset presents an improvement over the straight

scenario. The position of the Offset in the pipe is always as close to the bend as possible. The reason for this is that a vertical rise of pipe aids the dispersion of powder and improved the split (Giddings, 2000).

Despite the almost perfect Max/Min for an AFR of 3: 1 using the 30° Offset, it should be possible to further engineer the ability to fine tune the Offset so it is possible to improve the split further for a range of AFR. The introduction of a device like the Control Gate could yield this improvement.

7.7 Results from Scenario 2

7.7.1 Preface

Scenario two consists of two 90° bends perpendicular to each other. In this scenario the rope is spinning and as such the heavier particulate material is next to the wall. A device has to not only try to lift the rope away from the wall and disrupt it in scenario 1, but also to cope with an unknown rope position as the position of the rope can alter drastically based on the air speed.

7.7.2 The Expansion

From the section on initial ideas, the most favourable device for use with a double 90° bend was the Expansion. The expansion design is based on observations from other expansion style devices used for other purposes, particularly particle sizing, and it was noticed to provide a good level of mixing.

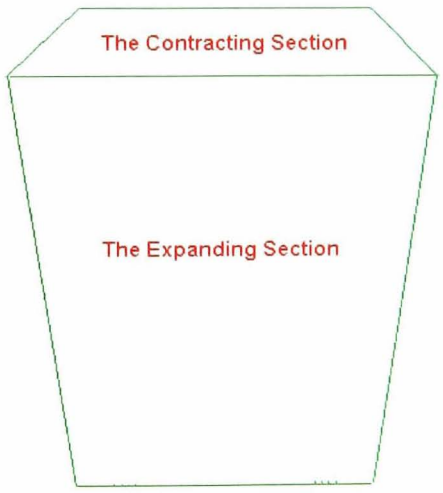

Figure 7.35 – Expansion layout

The structure of the Expansion is shown in figure 7.35. The Expansion consists of an expanding

section and a contracting section. The angles are chosen based on the previously described particle-sizing device.

From the results it can be seen in figure 7.37, the Expansion provides a significant improvement on a straight section. However, it is believed that the split can be improved further by either adding a Venturi before or after the expansion to prolong the period of expansion. It is predicted that this will create significant additional pressure drop.

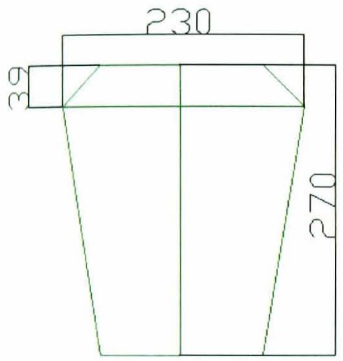

Dimensions in mm

Figure 7.36 – Dimensions of the expansion

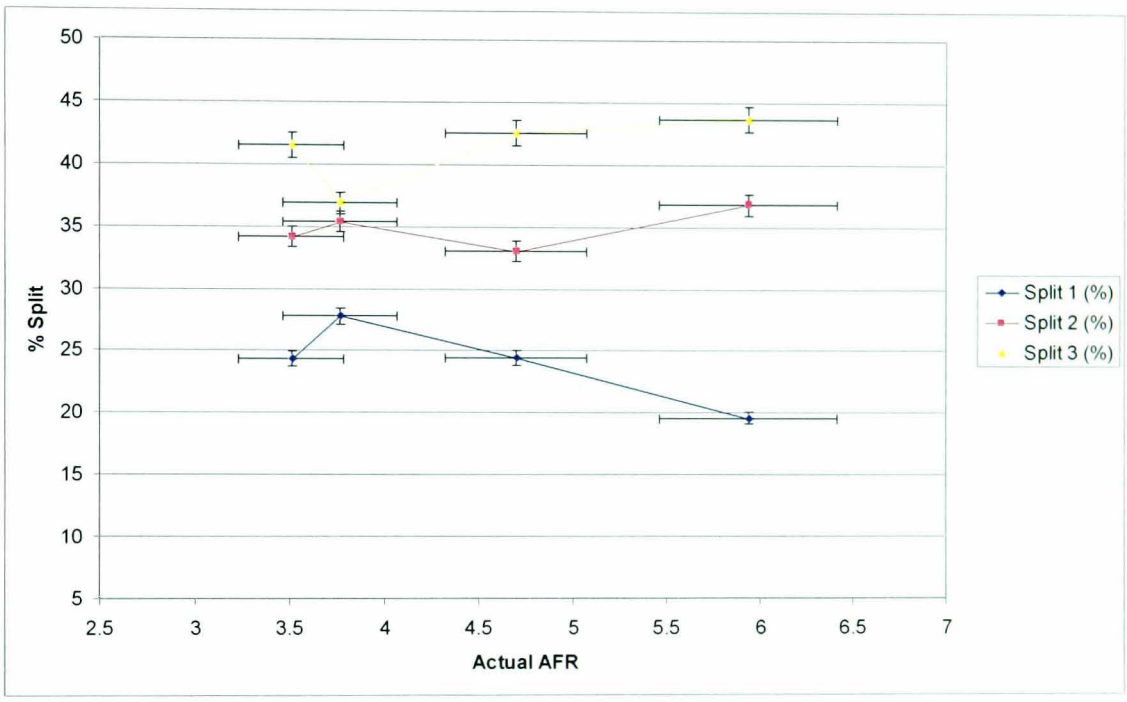

Figure 7.37 - Results for the Expansion in the double bend scenario

7.7.3 Venturi Expansion

This device is essentially the Expansion with a very short Venturi upstream of it. The Venturi provided an area reduction to approximately 75%. The idea behind this device is that the initial Venturi will concentrate the particulate and then the Expansion will disperse it. This device unfortunately had exceptionally high pressure drop, so much so that the rig's fan struggled to maintain the air velocity. The split data was also a significant reduction in comparison to just the Expansion. The layout of the device is shown in figure 7.38. The Results for this device are shown graphically in figure 7.39.

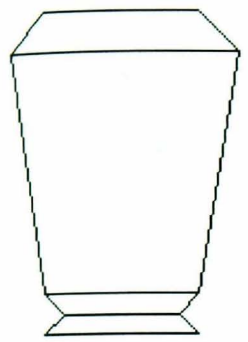

Diagram to Scale

Figure 7.38 – Dimensions of the venturi expansion

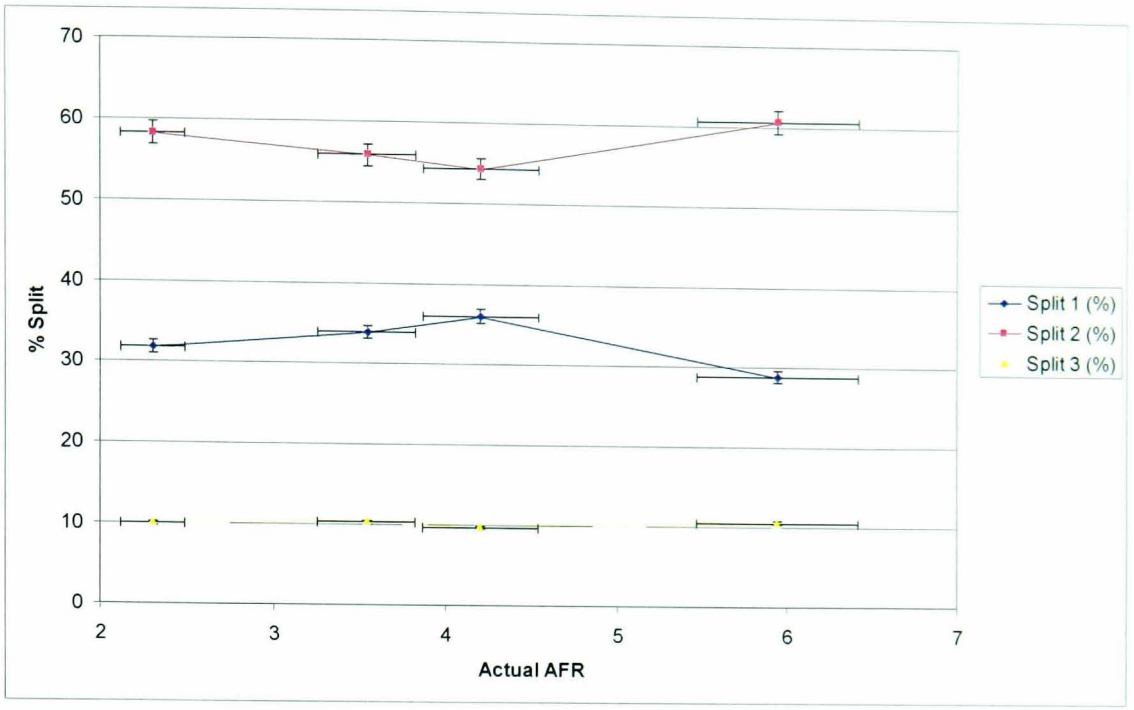

Figure 7.39 - Results for the venturi expansion in the double bend scenario

7.7.4 Expansion Venturi

This device is similar to the last device, employing both an Expansion followed by a Venturi. This device extends the expansion area and hopefully improves the amount of deflection the particles have leaving the Expansion. The addition of the Venturi not only increased the pressure drop, but did not create an improvement in the split. The layout of the device is shown in figure 7.40. The Results for this device are shown graphically in figure 7.41.

7.7.5 The Rotating offset

The Offset was designed for single bend geometries; it works on knowing where the rope is positioned in the pipe. When this is known the deflecting surface is orientated so the rope will strike it. Hence in a spinning rope scenario, if it could predict the position of the rope accurately, with CFD for example, the Offset could be positioned to deflect the rope. The 30 degrees Offset was used for these tests.

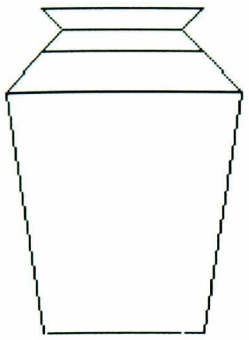

Diagram to Scale

Figure 7.40 – Dimensions of the expansion venturi

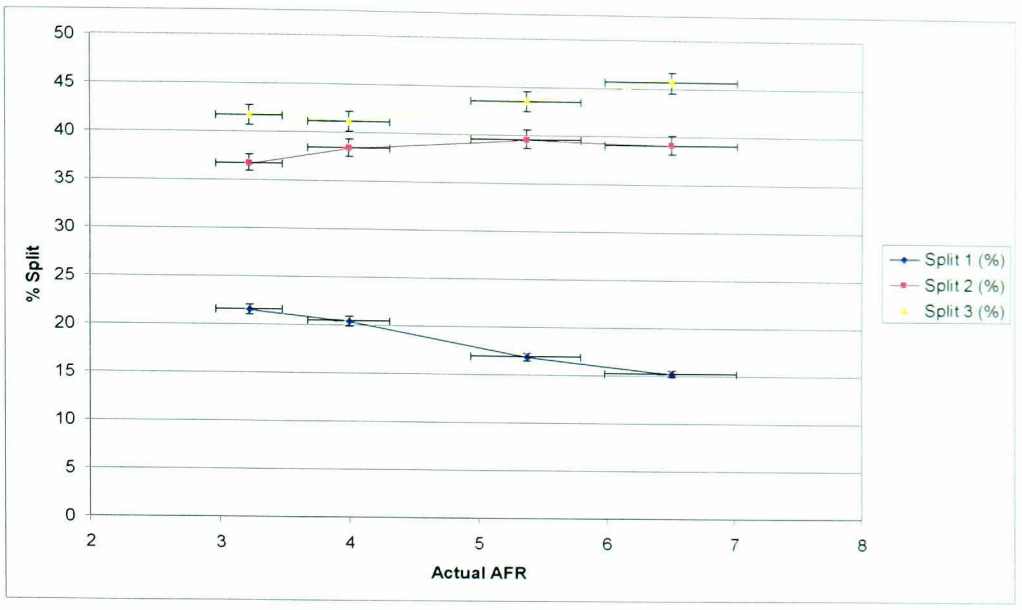

Figure 7.41 - Results for the expansion venturi in the double bend scenario

The pipe was assigned degrees, with 0°/360° indicated by figure 7.43. This positions the deflecting offset in the opposite position to that chosen for the single bend scenario. From observation it is estimated that the rope was positioned at approximately 30 degrees clockwise around the pipe at the conditions stated for scenario 2. The Offset was run using the same conditions as previous tests, but was rotated in 30 degrees steps clockwise around the pipe.

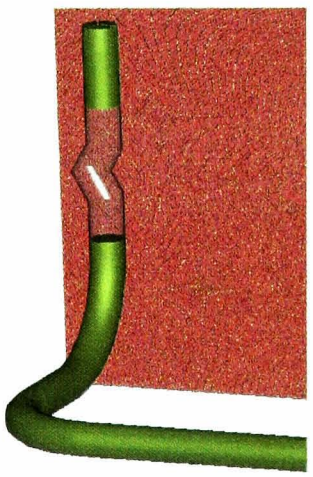

Figure 7.42 – Starting position of the deflecting Offset

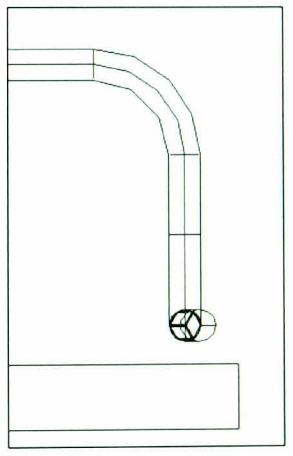

Figure 7.43 — Offset initial position

7.7.6 0° position Offset.

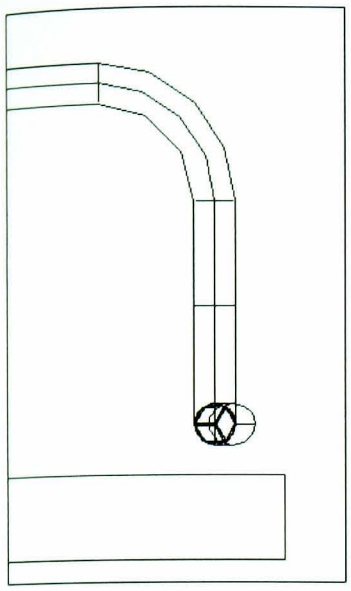

Figure 7.44 – Position 0° Offset

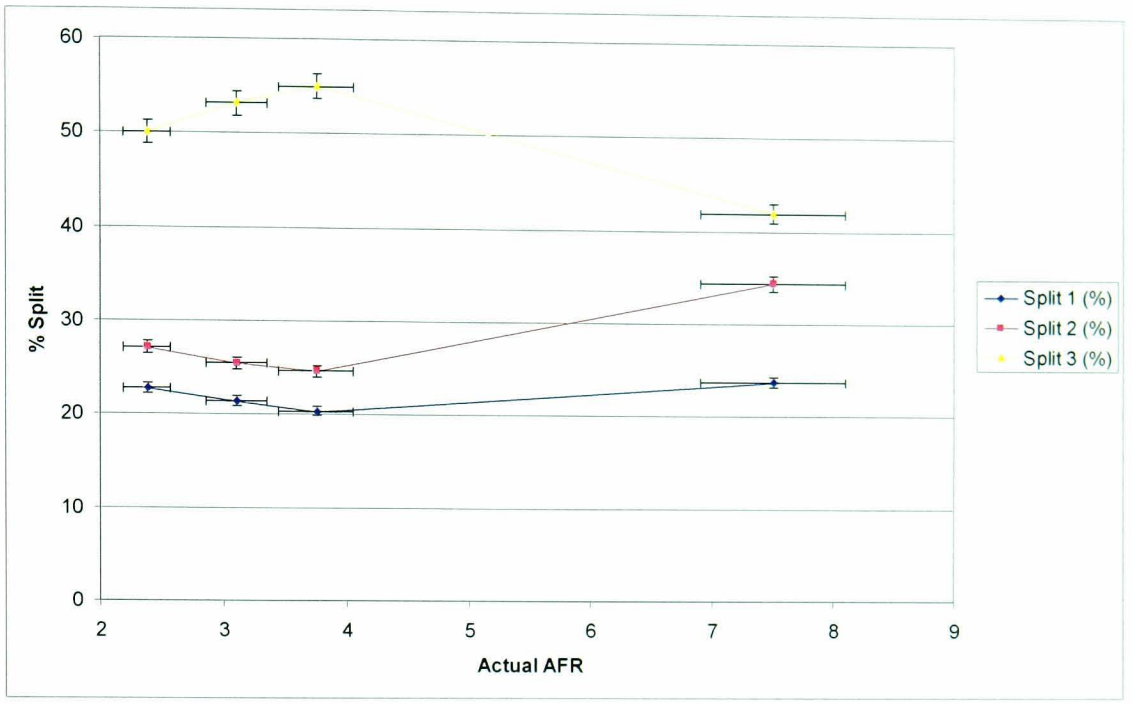

Figure 7.45 - Results for the Position 0° Offset in the double bend scenario

7.7.7 30° position Offset

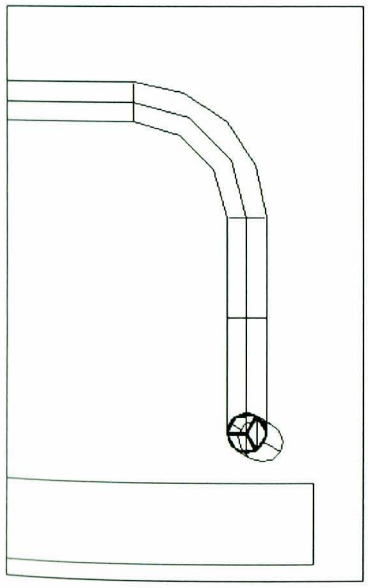

Figure 7.46 – Position 30° Offset

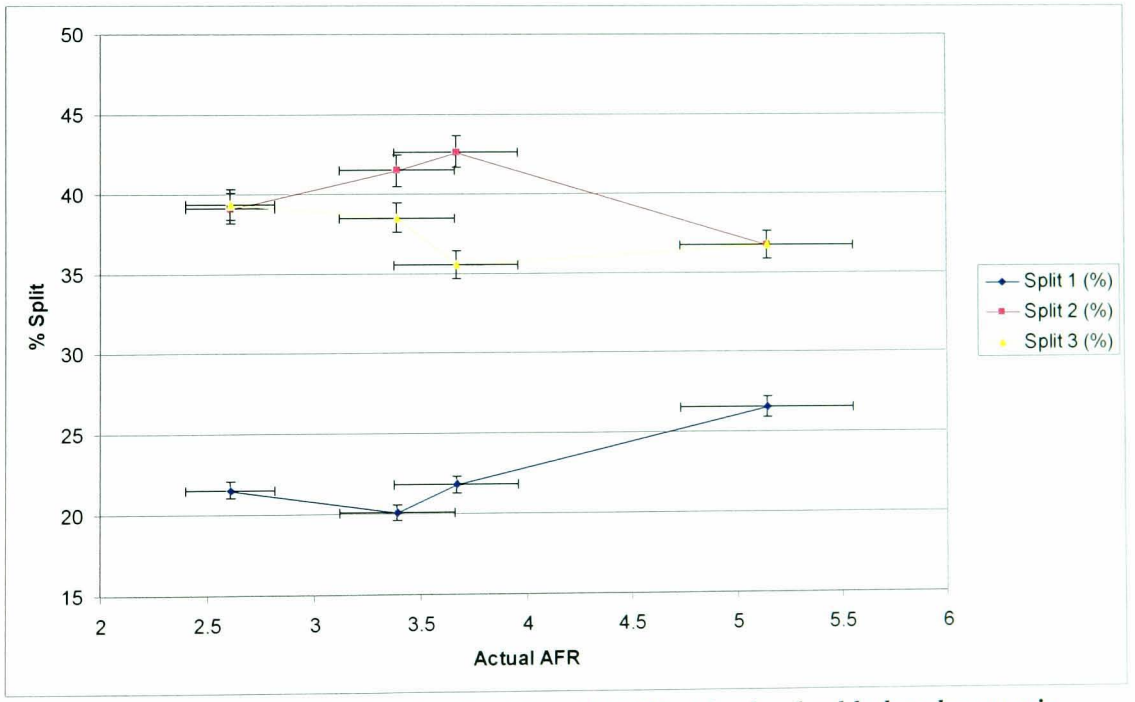

Figure 7.47 - Results for the Position 30° Offset in the double bend scenario

7.7.8 60° position Offset

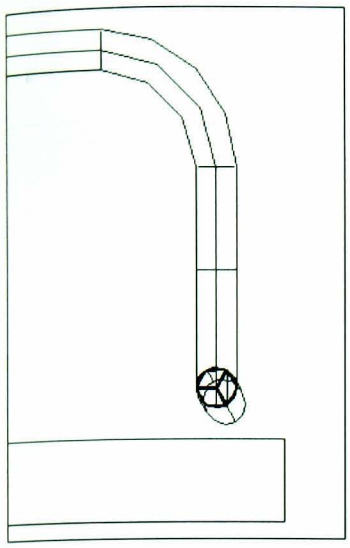

Figure 7.48 – Position 60° Offset

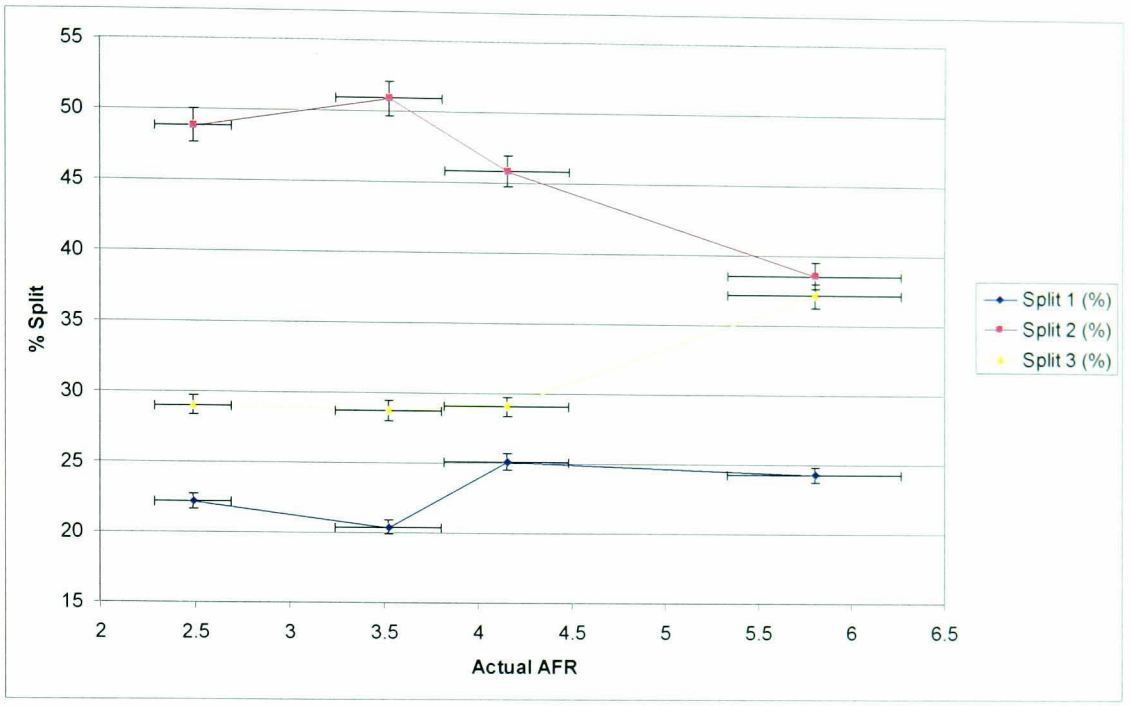

Figure 7.49 - Results for the Position 60° Offset in the double bend scenario

7.7.9 90° position Offset

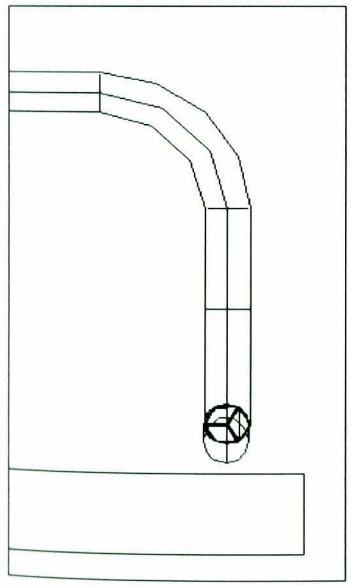

Figure 7.50 – Position 90° Offset

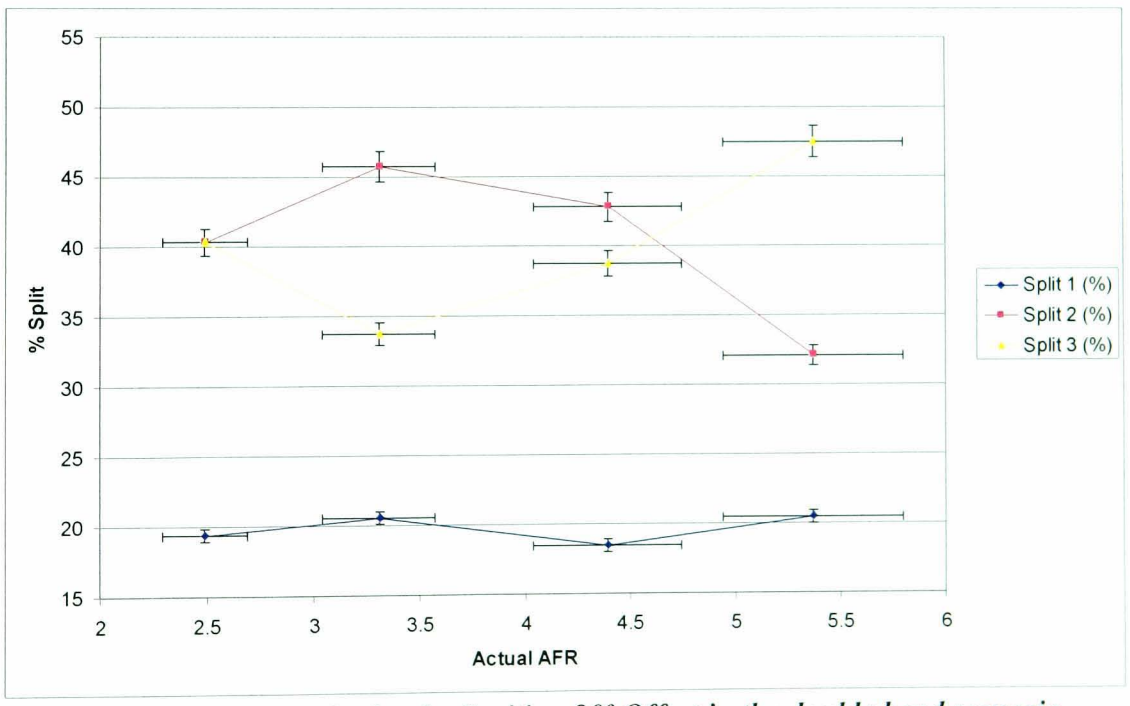

Figure 7.51 - Results for the Position 90° Offset in the double bend scenario

7.7.10 120° position Offset

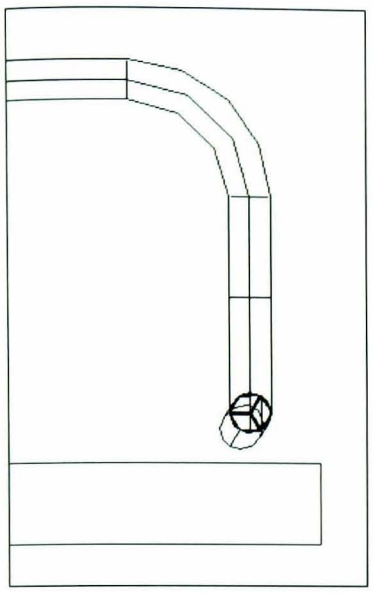

Figure 7.52 – Position 120° Offset

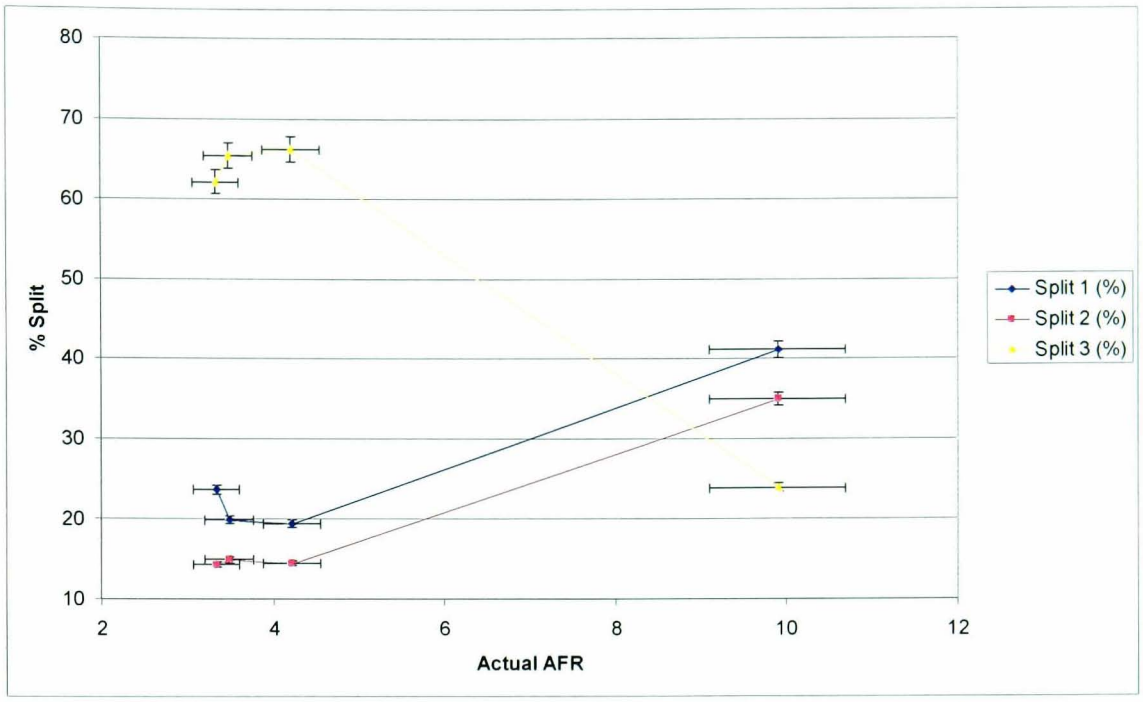

Figure 7.53 - Results for the Position 120° Offset in the double bend scenario

7.7.11 150° position Offset

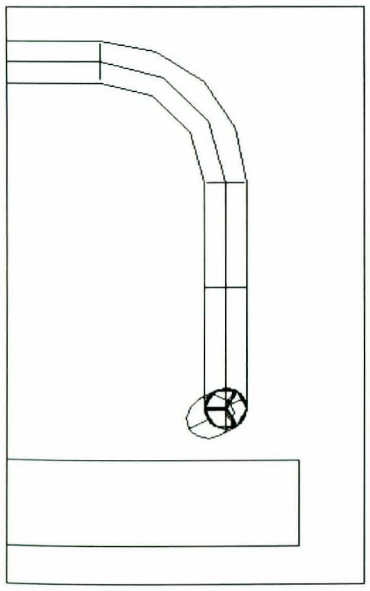

Figure 7.54 – Position 150° Offset

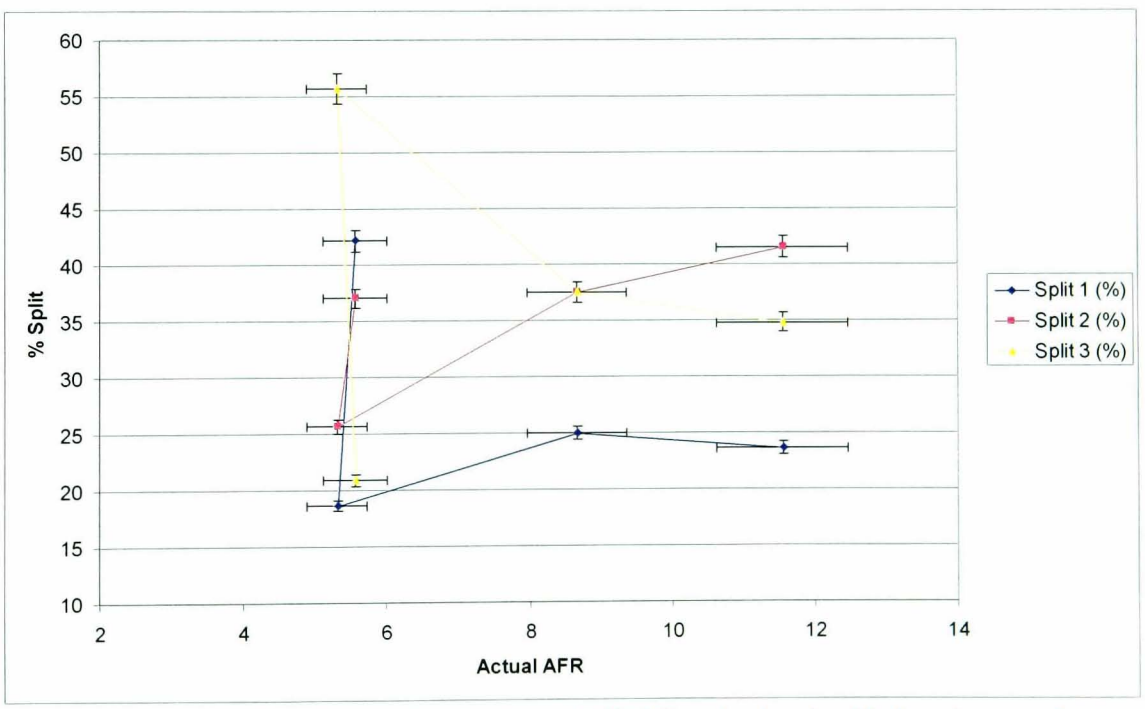

Figure 7.55 - Results for the Position 150° Offset in the double bend scenario

7.7.12 180° position Offset

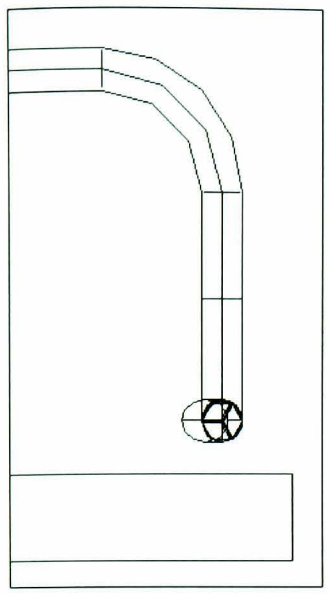

Figure 7.56 – Position 180° Offset

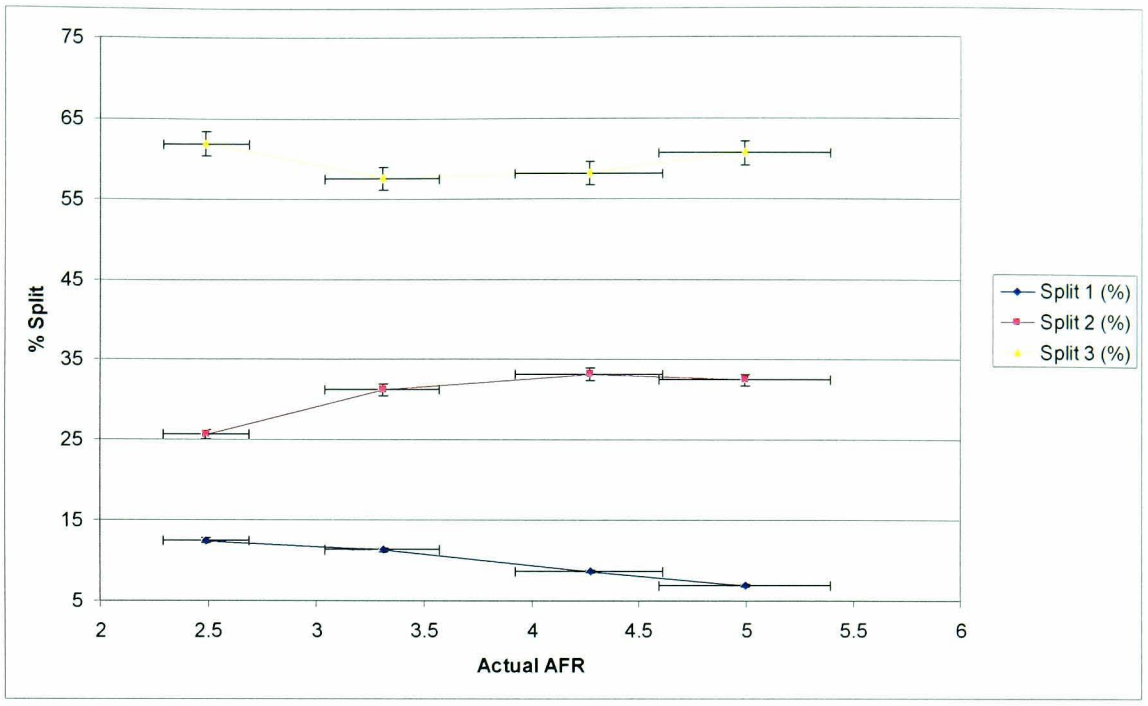

Figure 7.57 - Results for the Position 180° Offset in the double bend scenario

7.7.13 210° position Offset

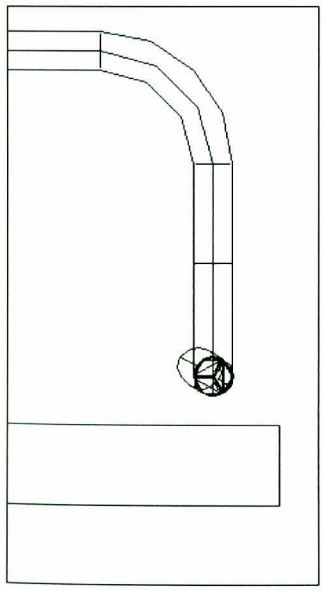

Figure 7.58 – Position 210° Offset

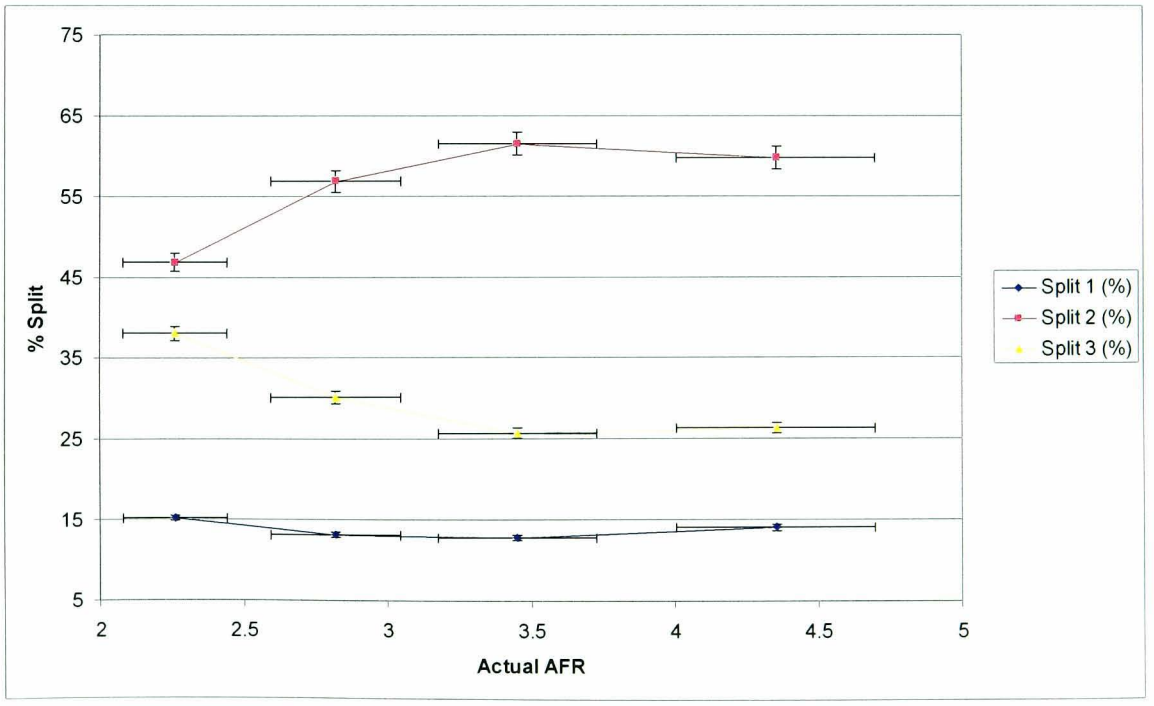

Figure 7.59 - Results for the Position 210° Offset in the double bend scenario

7.7.14 240° position Offset

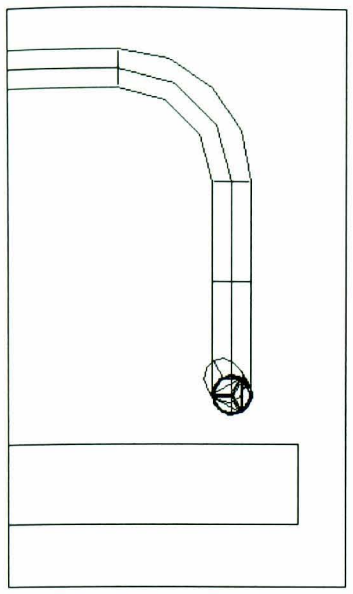

Figure 7.60 – Position 240° Offset

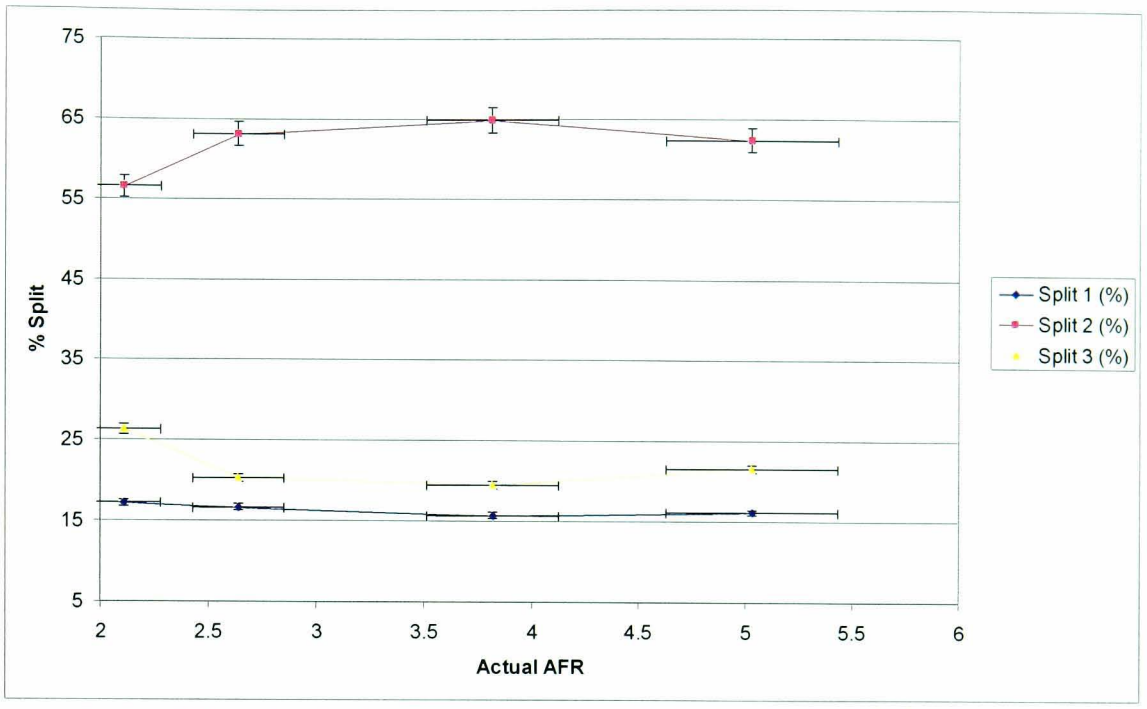

Figure 7.61 - Results for the Position 240° Offset in the double bend scenario

7.8.15 270° position Offset

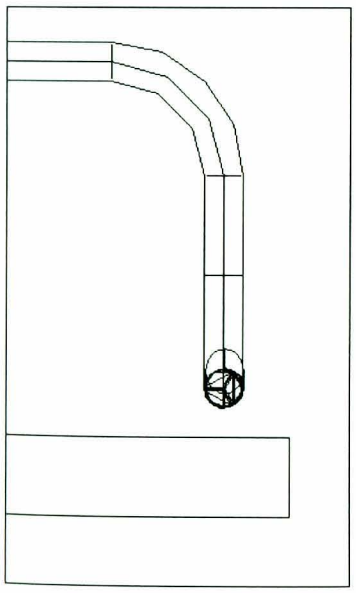

Figure 7.62 – Position 270° Offset

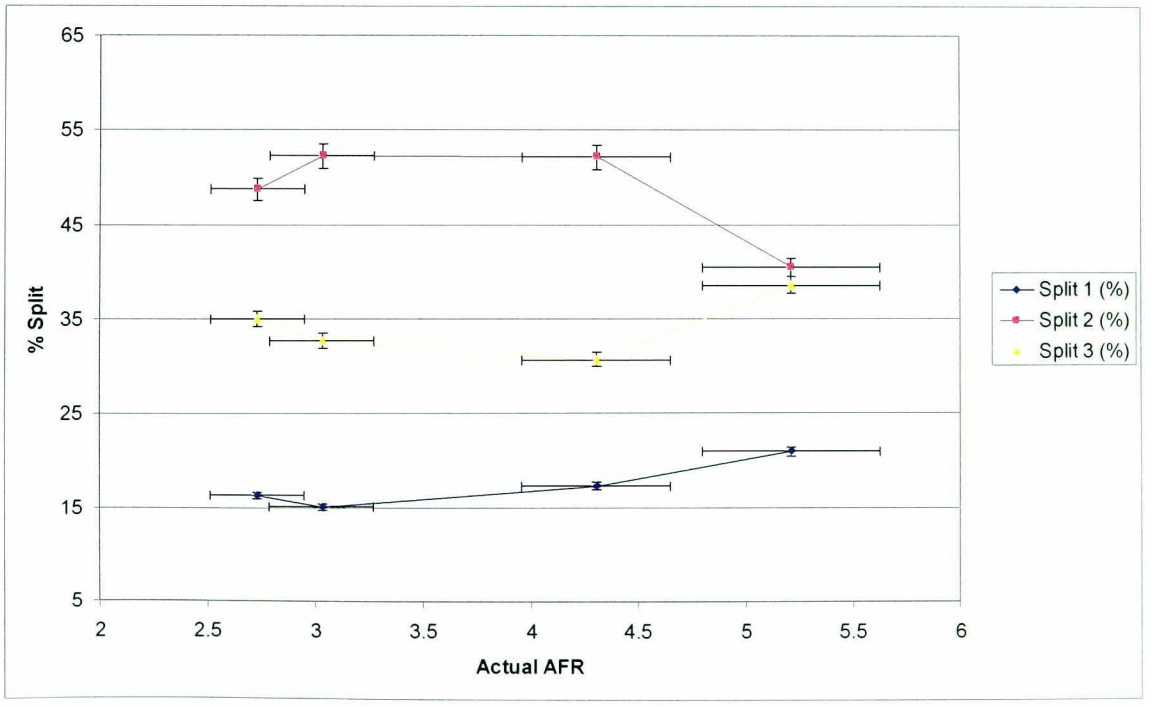

Figure 7.63 - Results for the Position 270° Offset in the double bend scenario

7.7.16 300° position Offset

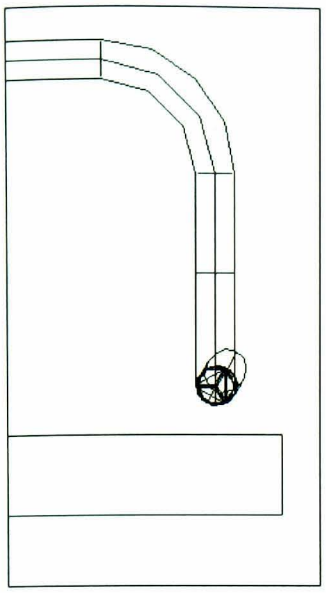

Figure 7.64 – Position 300° Offset

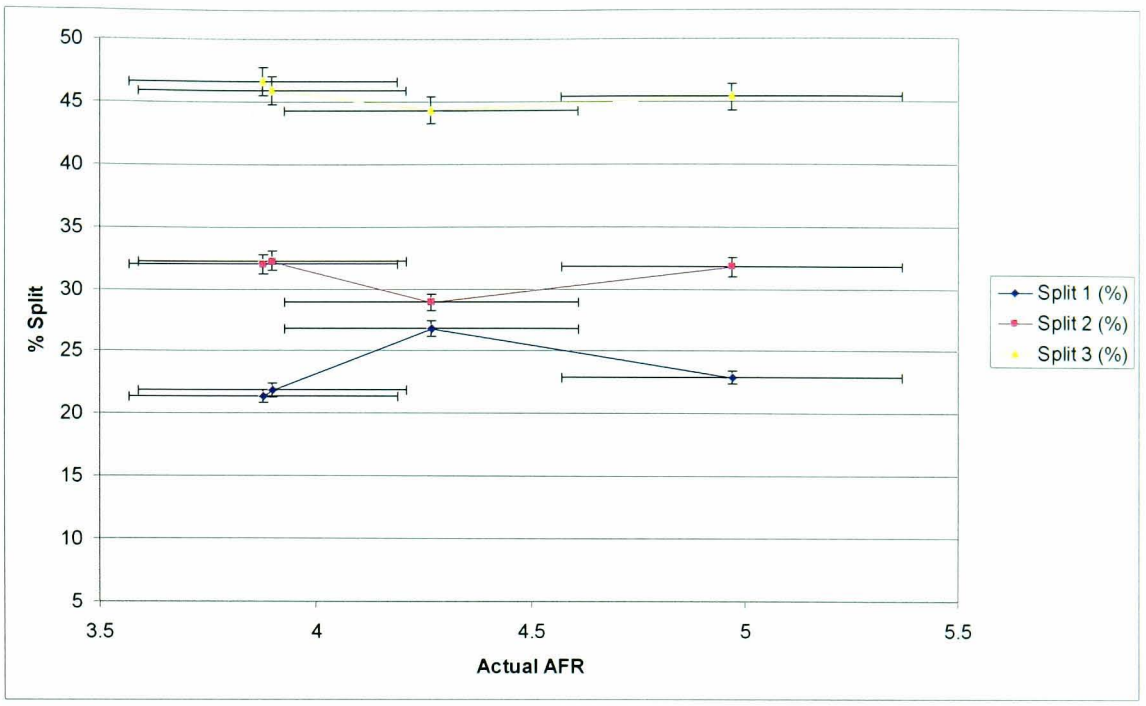

Figure 7.65 - Results for the Position 300° Offset in the double bend scenario

7.7.17 330° position Offset

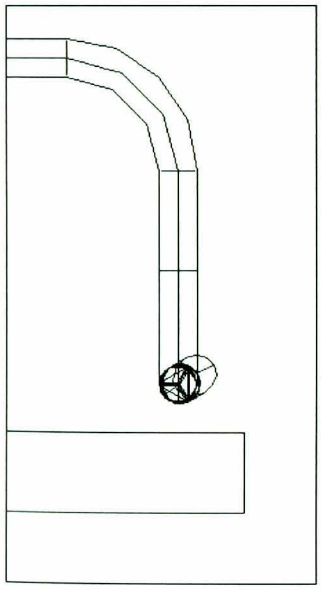

Figure 7.66 – Position 330° Offset

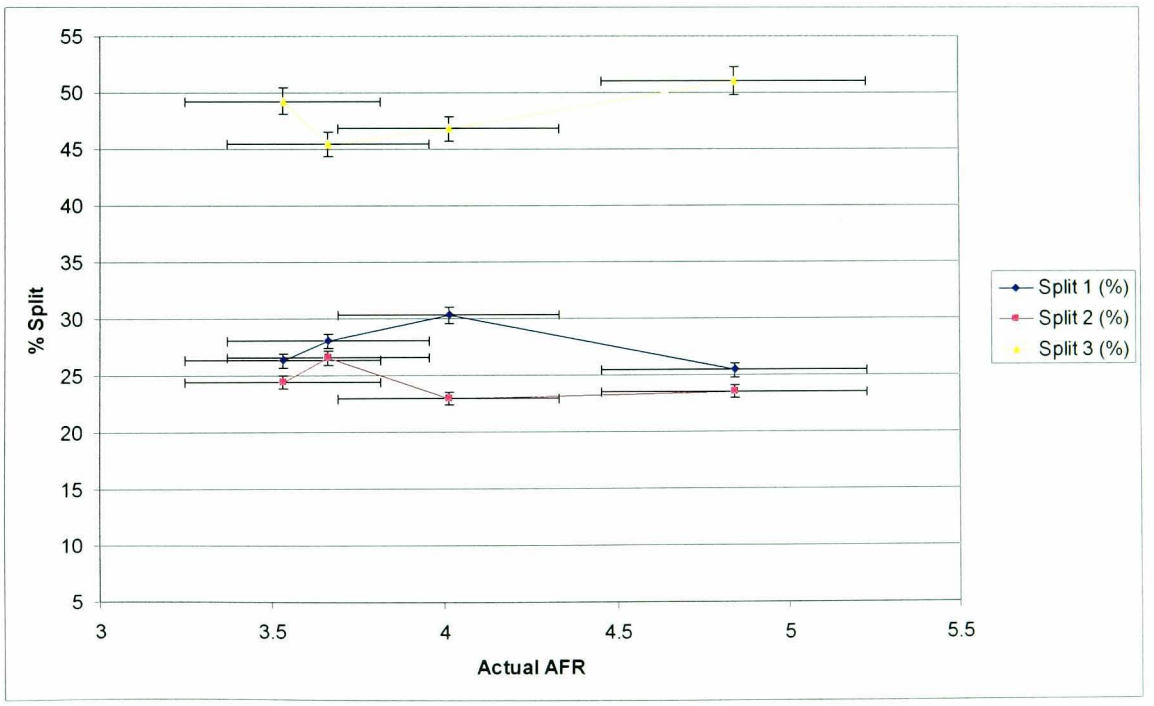

Figure 7.67 - Results for the Position 330° Offset in the double bend scenario

7.7.18 Rotating Offset Summary

Presented below is the summary of Max/min values for the rotating Offset. These are shown in table 7.28 and are shown graphically in figure 7.68. From these results it can clearly be seen that the orientation of the Offset affects the split significantly and that the position of the rope has to be known or calculated for the Offset to be installed effectively.

Table 7.8 – Summary of rotating Offset results

A:F	0	30	60	90	120	150	180	210	240	270	300	330
3:1	2.19	1.83	2.20	2.08	4.35	2.02	4.94	3.08	3.28	3.00	2.18	2.02
4:1	2.48	2.07	2.50	2.23	4.39	2.98	5.09	4.34	3.79	3.48	2.10	1.71
5:1	2.70	1.95	1.82	2.32	4.58	1.50	6.70	4.79	4.13	3.03	1.65	2.04
6:1	1.76	1.39	1.59	2.32	1.72	1.76	8.74	4.26	3.86	1.94	1.98	2.17

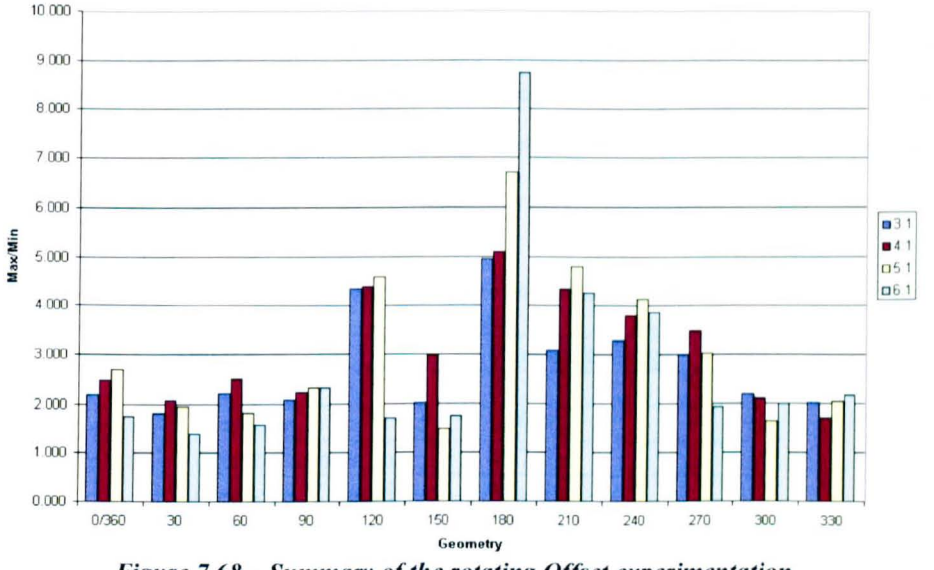

Figure 7.68 – Summary of the rotating Offset experimentation

7.7.19 Comparison

The maximum over minimum ratio is a good indication of split when comparing different devices. A maximum over minimum value of 1.0 indicates a perfect split. The maximum over minimum values for all the devices and air to fuel ratios are presented in figure 7.69 for comparison.

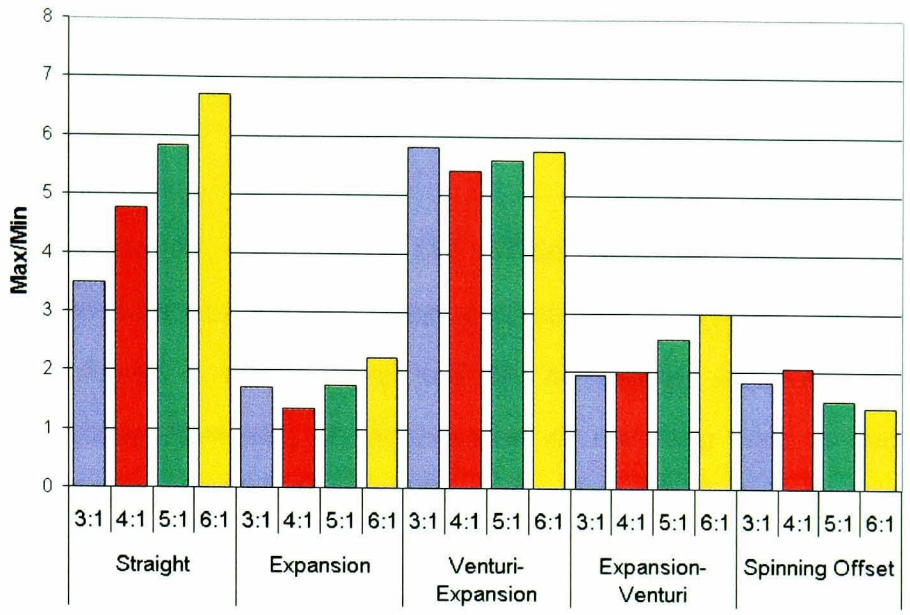

Figure 7.69 – Summary of double bend experiments

In addition to splits data, the data collected from the pressure tappings can be used as an indication of which device has the lowest pressure drop. Taking the pressure drop across 5 pipe diameters the various devices were compared at the same running conditions. These were a 3:1 AFR, 16m/s. The pressure drop was an average value taken from readings measured over a minute of constant use.

Table 7.9 - Pressure Drops for the devices tested in scenario 2

Device	**Pressure Drop**
Straight	82 Pa
Expansion	149 Pa
Venturi-Expansion	457 Pa
Expansion-Venturi	354 Pa
Spinning Offset	202 Pa

The pressure drop measurements are shown in table 7.29. These results show that the expansion provides the lowest pressure drop for a device. Both the Venturi-Expansion and the Expansion Venturi do not improve the results for the Expansion and increase substantially the pressure drop.

7.8 Discussion of Experimentation of Scenario Two

7.8.1 Preface

The results for scenario two are interesting, mainly as both the expansion and the spinning Offset provide marked improvements over the straight. The attempts at improving the Expansion, by extending either the contraction surface or expansion surface, provided to be ineffective and

merely increased the pressure drop of the device markedly.

7.8.2 The Rotating Offset

The experiments undertaken on rotating the Offset with the double bend scenario were undertaken to examine if the deflecting surface needs to strike the rope core. In the experiments it can be seen that the device is not universal and that its position alters drastically the degree of improvement it provides. However, if the position of the rope core is know through either empirical data or calculation it would be possible to fit such a device.

7.8.3 Assessment of the Expansion Devices

The Expansion demonstrates that it works with a spinning rope, providing an improvement over the straight in all AFR. This comparison is shown more clearly in the graph in figure 7.70 The Expansion provides significant improvement over the straight section for experimental tests involving a spinning rope.

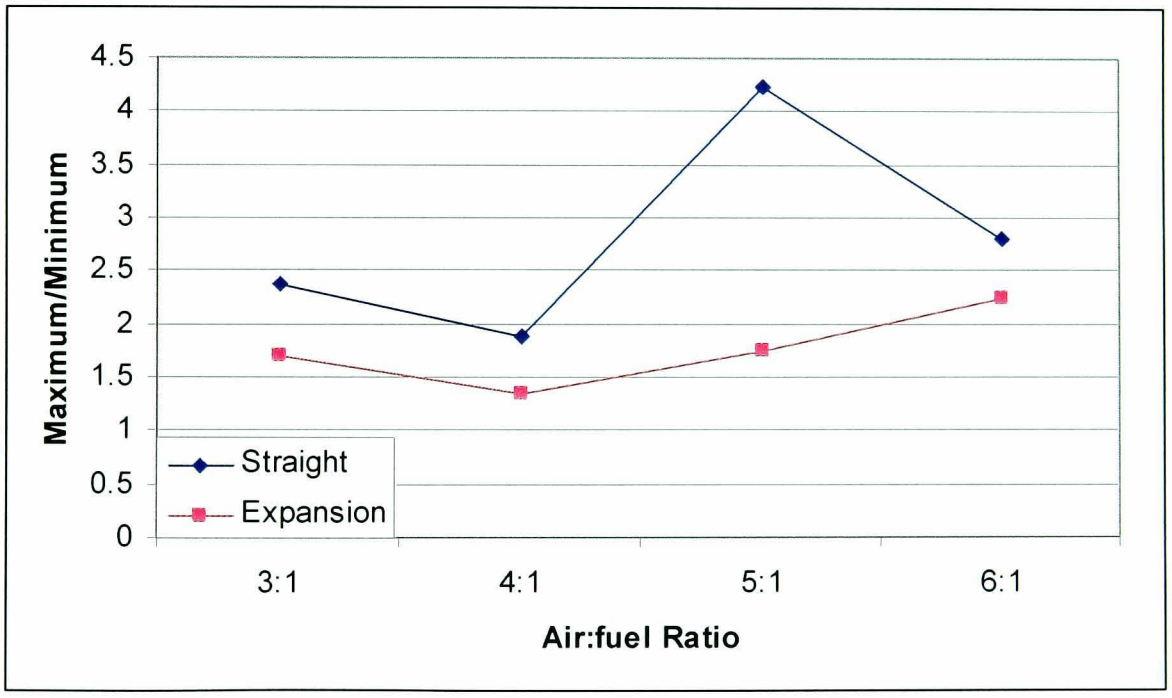

Figure 7.70 – Comparison between the Expansion Device and the Straight test section

7.8.4 Mechanisms for the Expansion

The Expansion seems to function by a combination of two mechanics. The first mechanic is that the expansion area slows down the spinning rope in the vertical axis.

The reduction in the vertical axis of spin means that the angle of rotation is widened. The tangential motion is caused by the secondary flows generated in the double bend. It is this mechanism that seems to spread the rope core out across a wider area.

The expansion causes a drop in the axial momentum of the air (and hence velocity) due to the continuity equation.

$$P_1A_1C_1 = P_2A_2C_2 \qquad \textbf{Equation 7.2}$$

By altering the cross-sectional are of the pipe the other values have to alter accordingly, the density of the air doesn't change and hence as the area of the pipe expands the mainstream velocity in the pipe must drop.

The contraction area then pulls this material back into the centre causing additional mixing by striking the upper surface of the Expansion device. This simple deflection acts like a ramp, similar to the Offset. The combination of the two mechanisms, the slowing of the particles combined with the deflection of the particles, helps to deliver a relatively dispersed rope.

7.8.5 Optimisation of the Expansion

The optimisation of the Expansion can work in several ways. There is the various angles of the Expansion and the lengths of the both the expansion and contraction areas. In the current work a small Venturi-like contraction was used to extend both the expansion and contraction area. Neither proved to be very effective, both increasing the pressure drop across the test section and failing to improve the powder balance. The comparison between the three Expansion-based devices is shown graphically in figure 7.71

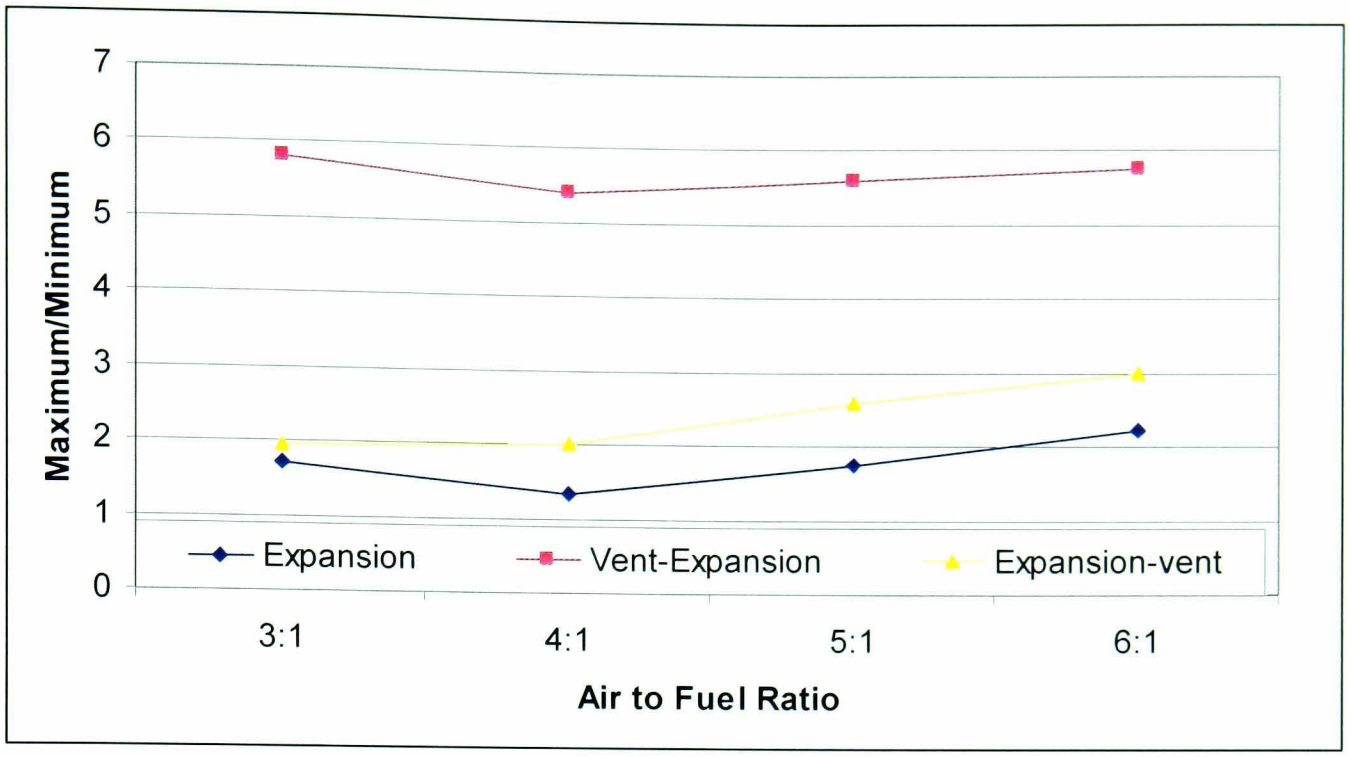

Figure 7.71 – Comparison of the different Offsets at different AFR

So adding a Venturi-like contraction to the Expansion has proved not to be a good method of optimisation for the Expansion. Other possible optimisation methods would require an alteration of the angles involved. This is an area for future research and development.

7.8.6 Conclusions

The powder balance is greatly improved by the Expansion. It is not perfect or at an acceptable level, but it does provide a massive improvement over the straight section for a spinning rope. It should be possible to further engineer the ability to fine tune the Expansion so it is possible to improve the split further for a range of AFR. The introduction of a device like the Control Gate could yield this improvement.

7.9 Control Gate

7.9.1 Preface

From the experimentation detailed for scenario 1 and scenario 2, it is possible to deduce that a method of "fine tuning" needs to take place. There are two options available; either optimise the exist device or implement another feature that will allow alteration of the splits.

Whilst the first option has already been partially undertaken, the second option refers to the implementation of the Control Gate concept. This device is designed for just this problem, fine tuning a split.

7.9.2 Description of the Control Gate

The control gate consists of three blades arranged in a Y-shape so as to match the outlets of a trifurcator. This arrangement is shown in figure 7.72. The blades are numbered 1 to 3 as shown in figure 7.73. When a blade is moved into the area of the outlet it will attempt to move powder from that outlet to the other outlet touching the blade. For example moving blade 1 clockwise so it occupies an area of Outlet (Leg) 2 then powder from outlet 2 will be diverted to outlet 1. The blades are limited to a rotation of approximately 15° either side of their neutral position. The blades are 2/3 of a pipe diameter long and designed in such a way that they can all move to the end of their travels without interfering with each other.

7.9.3 Experimentation

To test the effectiveness of such a device an experiment was set up to see if the Control Gate could realistically move particles from one outlet to another. The control gate used in these experiments was fitted with three blades approximately a pipe diameter. For the purposes of this experiment the blades extend out from just in from the splitting faces of the trifurcator.

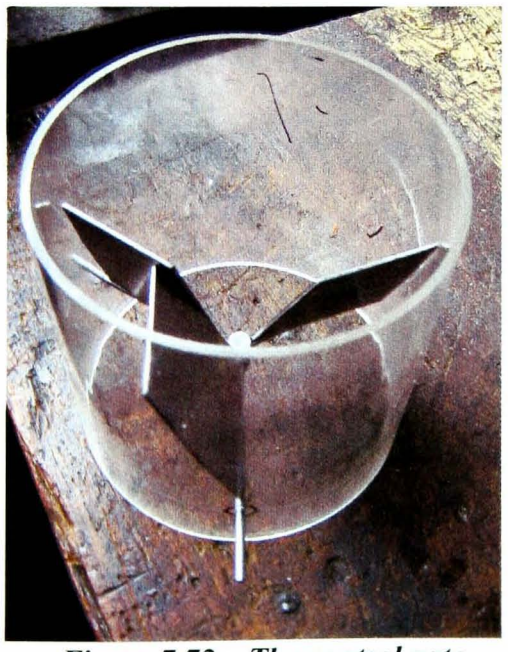

Figure 7.72 – The control gate

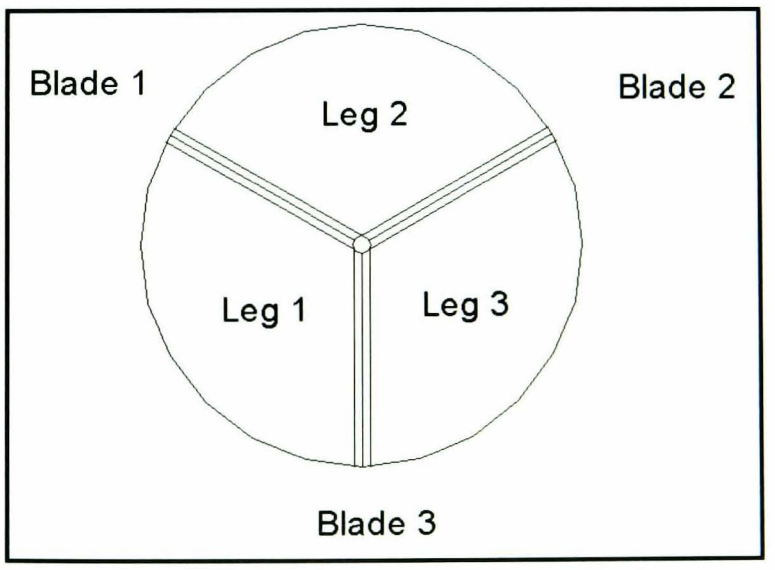

Figure 7.73 – Schematic of the control gate

The tests are run at 16m/s at a nominal AFR of 3:1. The purpose of the experiments was to demonstrate that after a device (in this case a 30 degrees Offset) it is possible with the mixed to flow to fine turn the individual values at the outputs by adjusting these flaps. A double bend scenario as described in the control experiments is used for these tests.

It should be noted that the initial "control" is different from the Offset results for scenario 2 as the Control gate blades essentially lower the point at which the split takes place. The results for the Control Gate tests are presented below in graphical form alongside a pictorial reference referring to blade position.

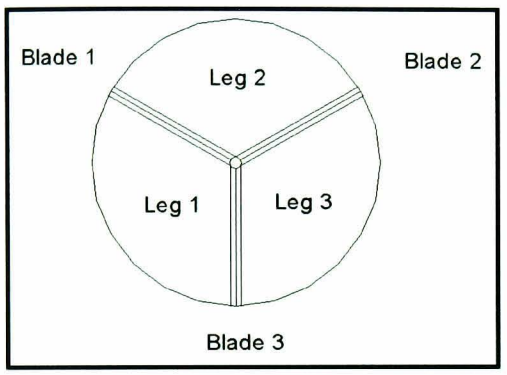

Figure 7.74 – Neutral Position

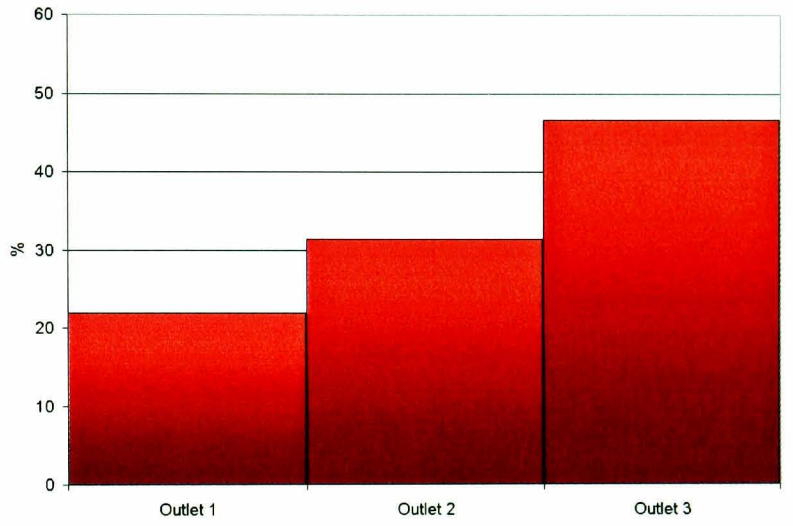

Figure 7.75 – Neutral position splits

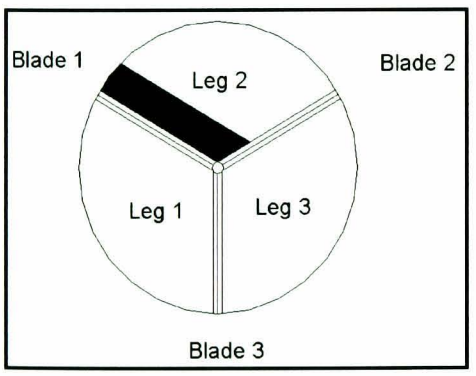

Figure 7.76 – Blade 1+ position

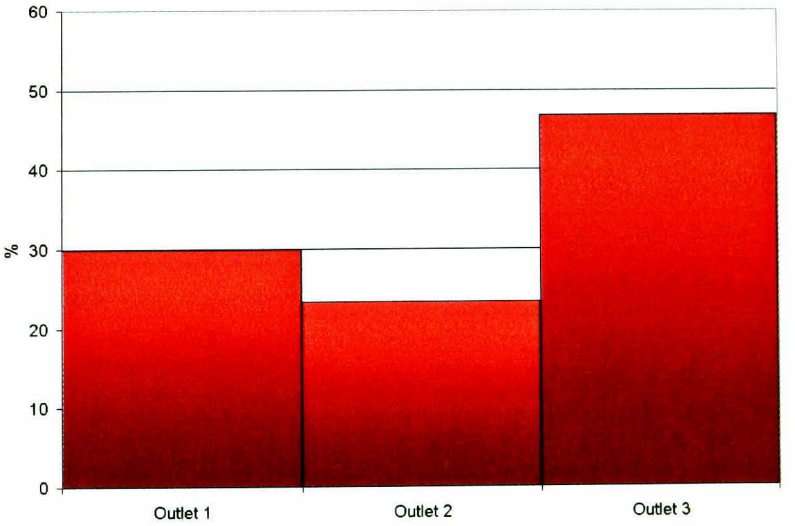

Figure 7.77 – Blade 1+ position splits

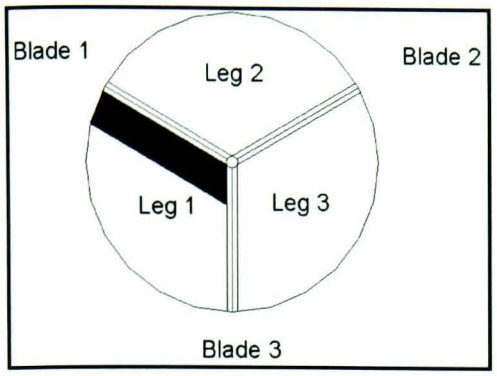

Figure 7.78 – Blade 1- position

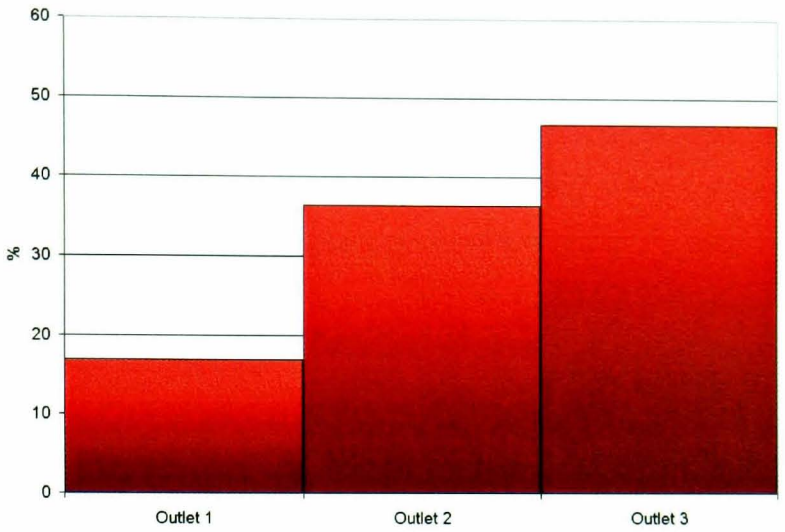

Figure 7.79 – Blade 1- position splits

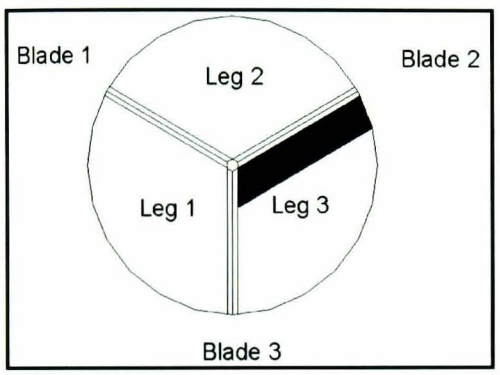

Figure 7.80 – Blade 2+ position

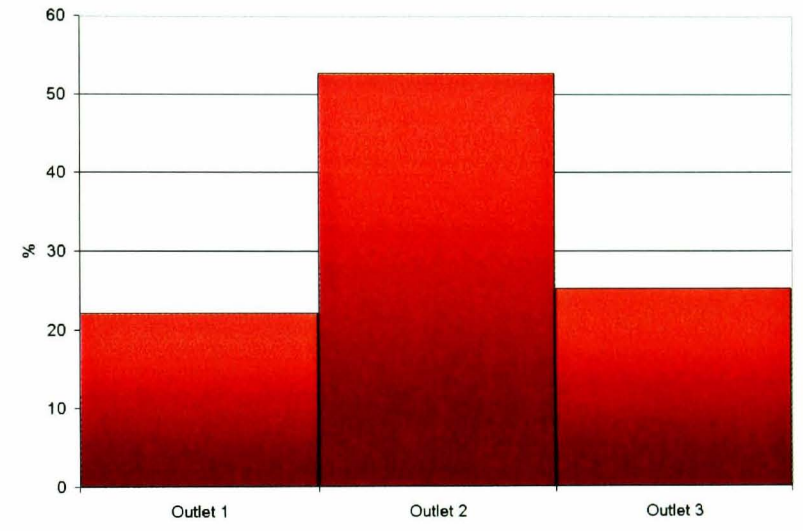

Figure 7.81 – Blade 2+ position splits

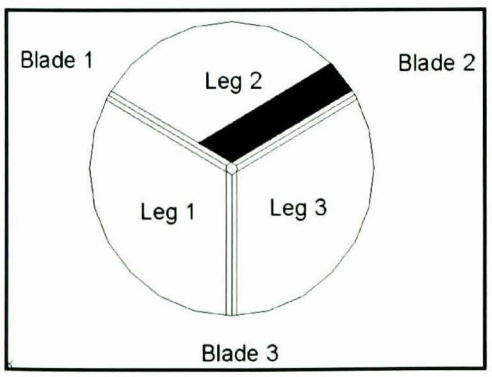

Figure 7.82 – Blade 2- position

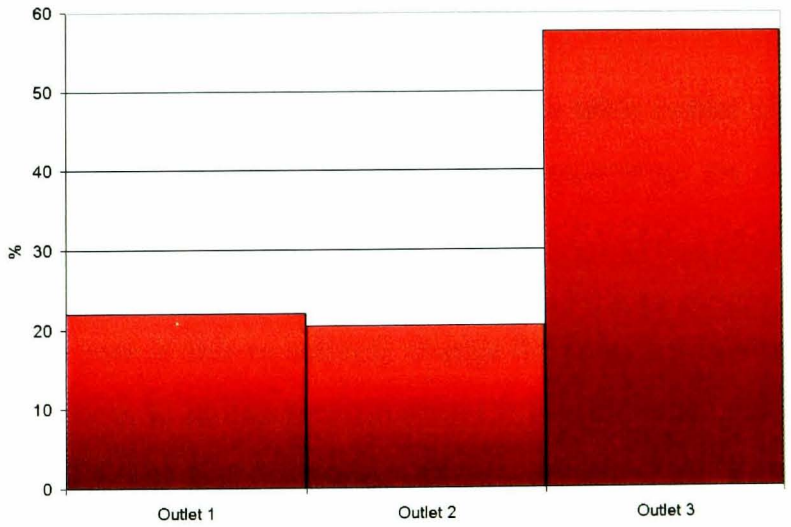

Figure 7.83 – Blade 2- position splits

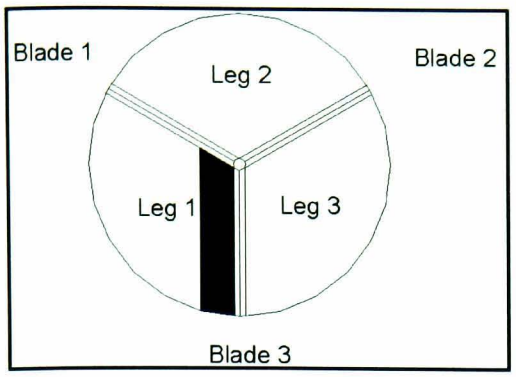

Figure 7.84 – Blade 3+ position

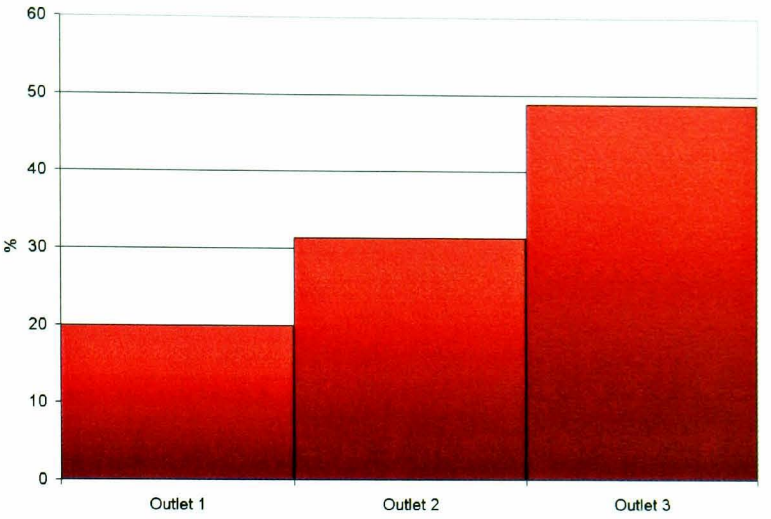

Figure 7.85 – Blade 3+ position splits

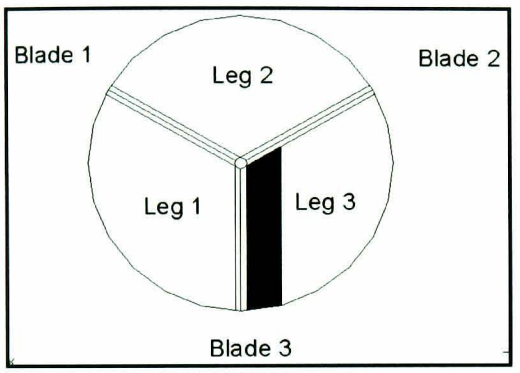

Figure 7.86 – Blade 3- position

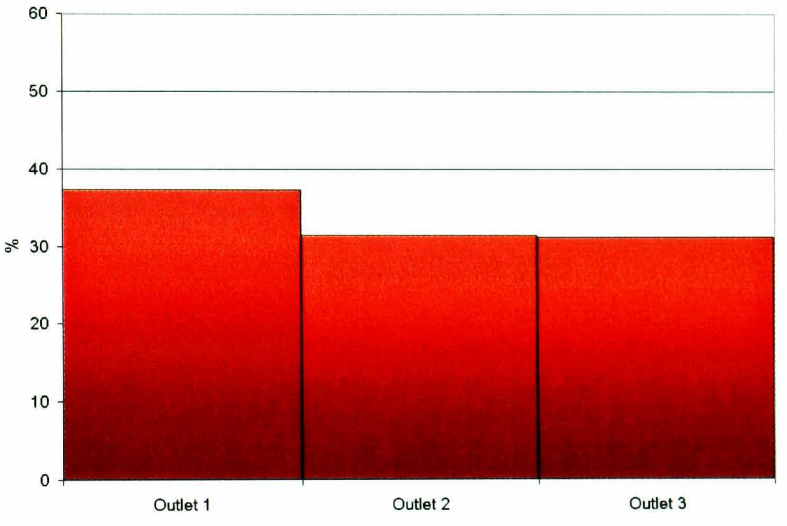

Figure 7.87 – Blade 3- position splits

7.9.4 Summary of Experiment

A summary of the experiments is included below in table 7.30. The key to the table is that x/y/z refers to blades 1/2/3, the + symbol represents a clockwise turn, the – represents an anti-clockwise turn and 0 represents a static position.

From the data it can be seen that the control gate is able to actively change the splits data through the movement of the three blades. With access to online measurements it would be possible to fine tune the splits to give a max/min ratio of 1.0 or approximately 1.0.

In an actual power station the running conditions constantly alter based on loading, power requirements and fuel type. Hence a position ideal for one set of running conditions would not be ideal for another set of running conditions, whilst it might only be a slight change it needs a level

of feedback, especially if there is online monitoring. This is dealt with in Appendix C a paper on the use of the active system.

Table 7.30 – Summary of Control Gate experiments

	Outlet 1	Outlet 2	Outlet 3
0/0/0	21.94%	31.42%	46.64%
+/0/0	29.93%	23.31%	46.76%
-/0/0	16.90%	36.40%	46.70%
0/+/0	22.07%	52.63%	25.30%
0/-/0	22%	20.42%	57.58%
0/0/+	19.91%	31.31%	48.78%
0/0/-	37.38%	31.40%	31.22%

7.9.5 Discussion

The results for the control gate are promising; they show that with the application of three little deflecting blades it is possible to alter the powder balance. Whilst on its own a wall bound rope would not be able to be deflected by the Control Gate, however a device like the Offset or the Expansion that deflect the particle rope off the wall allows the gate to do its job.

The device works by shifting particles heading down one outlet and forcing them to move down another. The movement of the blades essentially increases the area of the outlet and hence the percentage of particles that enter that outlet.

Appendix C details work undertaken on the moving plate device for a bifurcator scenario is similar to the control gate and demonstrates how a feedback system could be integrated into a similar method and create an active system of outlet balancing.

7.10 Conclusions

The experiments carried out in this chapter investigate the suitability of several devices designed for the purpose of improving the fuel splits at pneumatic conveying junctions. Three solid devices are tested and identified as possible future products for the power generating industry. These devices are designed for specific scenarios. These three devices are the Offset, the Expansion and the Control Gate.

The Offset has been designed for use in single bend geometries, but can operate in any geometry if the position of the rope can be estimated or calculated so that it strikes the deflecting face. This makes the device very useful. The device still has a degree of optimisation to be undertaken on the device and to see how it operates at different distances from the splitting device. Under the conditions it was set it performed well delivering Max/Min approaching The Expansion has been designed for use with a spinning particle rope. Spinning ropes occur when the bends preceding the vertical rise are positioned perpendicular to each other. The Expansion is designed to perform the same mechanisms on a rope regardless of where it enters the device. In this sense it is universal. The device still needs a level of optimisation. Under the conditions it was set it worked well to improve the powder balance for the spinning rope scenarios.

The Control Gate was designed to be able to fine tune the splits given by devices such as the Expansion and the Offset. The device works by simply deflecting particles with movable ramps. These movable ramps essentially alter the area of the splitter outlets and therefore alter the amount of powder passing through that outlet. The Control Gate experiments proved that this was the case and that in some experiments up to 20% of the powder from one outlet could be moved.

In conclusion the chapter has tested three devices generated in the conceptual development section and proved that under scalable experimental conditions these devices could prove useful in a power station pneumatic conveying network.

Chapter 8

Development and Deployment

8.1 Preface

The work described in this thesis is directly linked with industrial work. The result of the research and design that took place as part of this work has lead to development of several products that were deployed by the sponsor of this work GAIM LTD (Greenbank, Advanced, Instrumentation and Measurement), a division of Greenbank group UK.

The devices developed are the H-VARB (developed from the Offset), S-VARB (developed from the Expansion) and Control Gate. These were able to be installed into a variety of different stations with different problems for powder balancing.

These case studies were worked on with GAIM (Greenbank Advanced Instrumentation and Measurement), a division of Greenbank group. This section contains cases on the following power stations; Ratcliffe on Soar, Didcot, Nanticoke and West Burton

These examples of industrial employment are important to this thesis as they detail the success of the third aim of this thesis to design and have manufactured a product that could be installed full scale in coal-fired power stations, this chapter is the realisation of that aim. Whilst full geometry and details of splits cannot be given for commercial reasons these cases give a feel of the success enjoyed by the device.

8.2 Ratcliffe on Soar

8.2.1 Description of Ratcliffe on Soar Power Station

Ratcliffe is a 2,000MW coal-fired power station built on a 700 acre site south west of Nottingham. The station was commissioned in 1967 as part of the CEGB and came under E.ON UK's ownership at privatisation in 1990. Ratcliffe recently generated its 400,000th GW, believed to be a record in terms of output for any power station. However, Ratcliffe has many problems; it is not a very efficient power station and is having difficulties improving its emissions to fall in line with current government emissions targets. The key to reducing NO_X and improving efficiency is improving distribution using some sort of flow balancing.

8.2.2 Description of problem

The burner bank at Ratcliffe is fed from several mills; these mills tend to have two outlet pipes that travel most of the distance to the burner before splitting just before the burner wall into three pipes which each fed a burner. This construction method means that the network has a lower pressure drop than six separate pipes running to the burner wall. The original pipe layout had the pipes going into the horizontal and then splitting. It was decided to reroute the pipes and bring the split into the vertical, figure 8.1 and figure 8.2 show this change. The work was to concentrate primarily on two vertical geometries altered in this way.

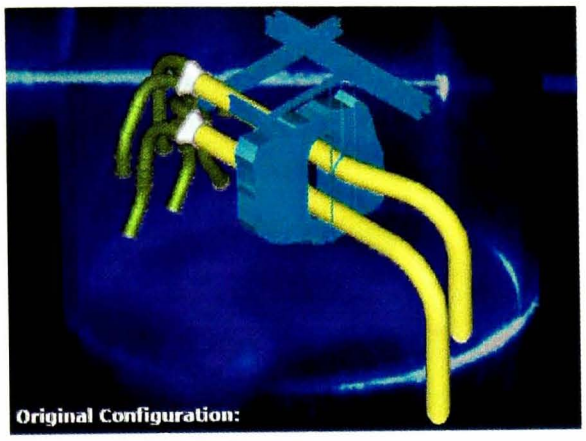

Figure 8.1 – Original Configuration at Ratcliffe power station

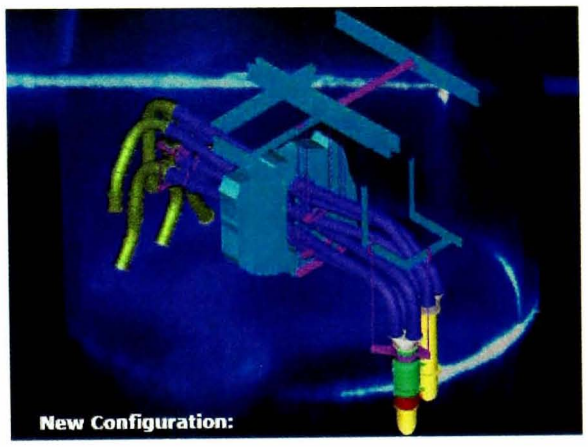

Figure 8.2 – New configuration implemented at Ratcliffe power station

Experience amongst station engineers has shown that a long vertical riser tends to improve the powder balance. After initial investigation into the splits, based on rotor-probe sampling, the split was still not within the power station operator desired tolerance. Whilst substantial improvements had been made by moving the split into the vertical, the operator not only wanted to improve the existing split, but to have a measure of control over them.

The splits before the installation of any device are given below in table 9.1. The split is presented over all six outlets from both trifurcator runs. The desired value would be 16.6% for each outlet.

8.2.3 Solutions

A number of possible solutions were considered. Any solution would need to take account of less favourable flows, improve the present flow, not increase pressure drop substantially and would allow a degree of control. A degree of control was desired as while the current design worked on the current operating conditions, a change in coal type or inlet velocity could

substantially shift the pulverised fuel split. Several CFD cases were run on the pipeline to locate the position of the rope in the vertical riser. After the long vertical riser the rope was relatively dispersed and the secondary flow patterns were relatively weak compared to the mainstream velocity.

Table 8.1 - Pre-device splits at Ratcliffe power station

	Trifurcator 1			Trifurcator 2		
Outlet	A	B	C	D	E	F
Split pre device	14.75%	20.82%	14.74%	18.33%	19.65%	13.01%
Deviation from Desired	-1.85%	+4.16%	-1.86%	+1.73%	+2.99%	-3.65%

The design of the control deice would be limited, as the operator did not require an online system. What was required was a system that could occasionally be checked and then altered at the burner face. Several devices were tested in CFD to see if they improved the split, figure 8.3 shows a graph summarising the various devices tested in CFD.

One idea suggested was a set of movable deflecting blades that would create spin of the particles. It was believed that spin would improve the particle mixing. From experimentation in the quarter scale rig and CFD conducted at the University of Nottingham, it was discovered that inducing spin only made the particle rope more concentrated and less likely to split.

The concept of having moving blades developed into positioning blades close to the trifurcator split to deflect the power from outlet to another. This is the basis of the control gate device, a CAD depiction of one is shown in Figure 8.4. Figure 8.5 shows black and white photographs of the actual control gate blades.

In addition to the installation of a control gate, a low-pressure drop device had to be considered to aid the split. The S-VARB was considered to be sufficient and ideal for a variable rope position in the vertical plane. The new layout was constructed with the trifurcator, followed by a control gate, followed by a VARB. Table 8.2 shows the splits from the power station following the installation.

8.2.4 Current Situation

The current situation is that the vertical installation is still installed and working very well. However, the cost of re-routing the pipes was too expensive. So a design was needed to work with the original horizontal pipe work.

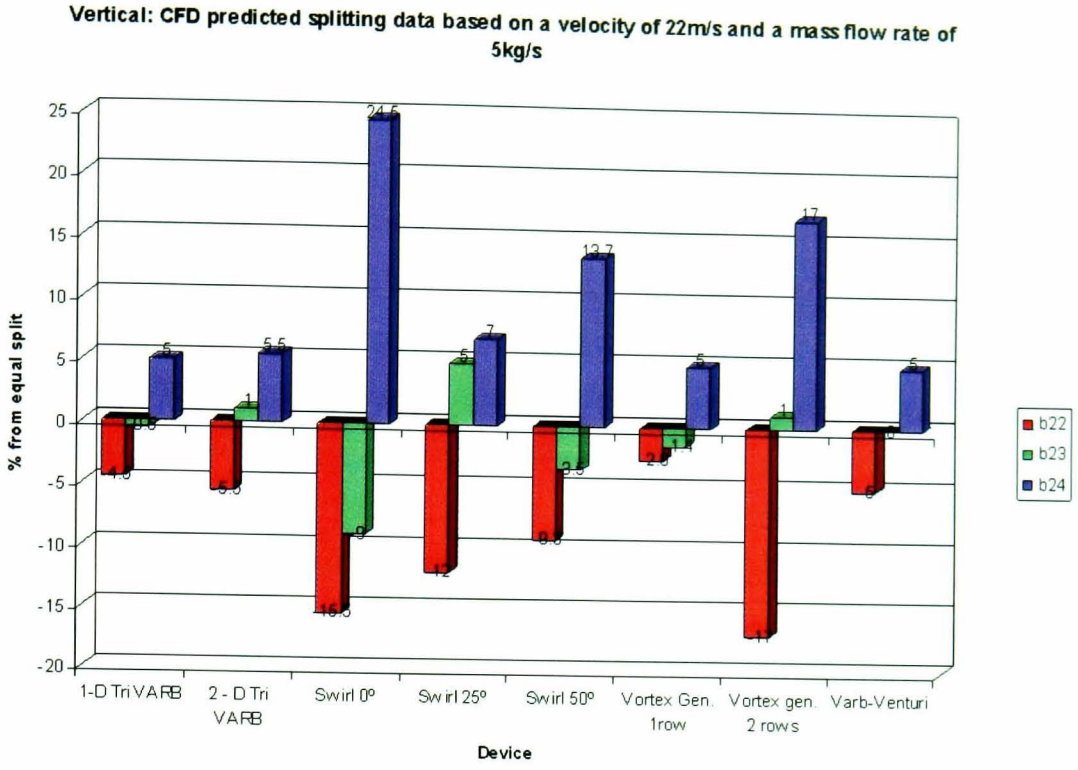

Figure 8.3 – CFD predicted data for devices to be installed at Ratcliffe

Figure 8.4 – CAD depiction of the control gate

Figure 8.5 – Actual control gate blades

Table 8.2 - Post device installation at Ratcliffe power station

	Trifurcator 1			Trifurcator 2		
Outlet	A	B	C	D	E	F
Split post device	15.97%	14.99%	16.31%	17.76%	18.79%	15.16%
Deviation from Desired	-0.69%	-1.67%	-0.35%	+1.1%	+2.13%	-1.5%

8.3 Didcot Power Station

8.3.1 Problem

Didcot power station in Didcot Oxfordshire is a sister station to Ratcliffe power station and possesses the same pipework. A study was undertaken for Didcot power station to investigate implementing the H-VARB device supplied by Greenbank Terotech. The layout of the pipe work is the same as at Ratcliffe on soar before the split was taken back into the vertical shown in figure 8.1. The study was computationally based and used CFD software.

Four pipe routes were investigated, based on measured data for Didcot mills E and G. Two routes from each mill were investigated. These were; G Mill A side, G Mill B side, E Mill A side and E Mill B Side. Three of the pipe routes were similar, G Mill B side, E Mill A side and E Mill B Side, whilst G Mill A side had a different layout.

8.3.2 Approach

The measured data obtained for Didcot Mills E and G, both A and B Sides was checked for precision using CFD of the four pipe routes. The specified running conditions and particle size information were used for these simulations. From the CFD it was possible to see where the high particle concentrations were and positions for the H-VARB can be recommended to disrupt these concentrations. Split trends are consistent between CFD and Measured data. These are shown in table 8.3.

Table 8.3 – This table shows the measured and CFD predicted splits.

E-Mill	**A-Side**			**B-Side**		
	E4	**E5**	**E6**	**E7**	**E8**	**E9**
Measured Split	24.5	49.5	26.0	32.9	44.1	23.0
CFD Split	5.5	70.8	23.6	21.9	40.6	37.5
G-Mill	**A-Side**			**B-Side**		
	G1	**G2**	**G3**	**G10**	**G11**	**G12**
Measured Split	50.7	29.8	19.5	23.5	45.2	31.3
CFD Split	39.9	35.1	25.0	17.8	59.1	21.1

8.3.3 Solution

The recommendations are to install a standard 30° incline H-VARB, with 216mm offset. This would then be followed by a control gate for fine tuning of the split; the control gate

would be fitted with flat blades. The H-VARB devices would be positioned with the deflecting face positioned in front of the outlet with the highest concentration of particles.

The installation of the H-VARB device took place in February 2006 and the improvements to the split gave the new splits to with in ±3%. This has lead to the installation and future installations at Didcot and the sister stations at Ratcliffe and Ferrybridge.

8.3.4 Current situation

The installation at Didcot is still ongoing at the time of writing. However, the installation at Ferrybridge is complete. Ferrybridge is again a exact copy of both Ratcliffe and Didcot. The installation at Ferrybridge has no flow meters to measure the coal balance. There is however data showing that the lost on ignition carbon in ash has been reduced by 6% from 12% to 6% for the units that the H-VARBs were installed on. This represents an improvement in both combustion and efficiency. The reduced carbon in ash means that the ash is more saleable to cement manufactures and the station requires less coal to generate the same amount of electricity delivering a double benefit. Following the successes at Ferrybridge and Didcot, Ratcliffe power station and looking to install four boiler sets of the device in 2007.

8.4 Nanticoke Power Station, Ontario

8.4.1 Description of Nanticoke

Ontario Power Generation's coal-fired thermal generating station in Nanticoke, Ontario is the largest of its kind in North America. Eight 500-MW generators produce a total of 4,000 MW of power at this 30-year-old generating station. The station has serious NO_X, SO_X and efficiency problems for sometime and are looking for any method to improve efficiency and reduce both NO_X, and SO_X.

8.4.2 Description of Problem

Nanticoke possesses a vertical splitter in the form of a quadrafurcator. Upstream of the quadrafurcator there is a small vertical riser preceded by a horizontal to vertical 90° bend. This leads to a strong rope forming in the bend due to the centripetal and inertial effects. This rope goes up the riser and then enters the quadrafurcator. The quadrafurcator consists of a 4-way junction in the vertical with a splitting pyramid dividing them. Figure 8.6 shows the outlay of the outlets.

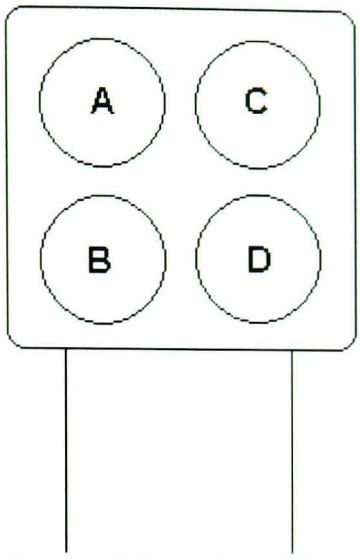

Figure 8.6 – Layout of the outlets of the quadrafurcator

Table 8.4- Showing splits in existing Ontario configuration.

	A	B	C	D	Max/min
Split	28%	19%	29%	24%	1.53

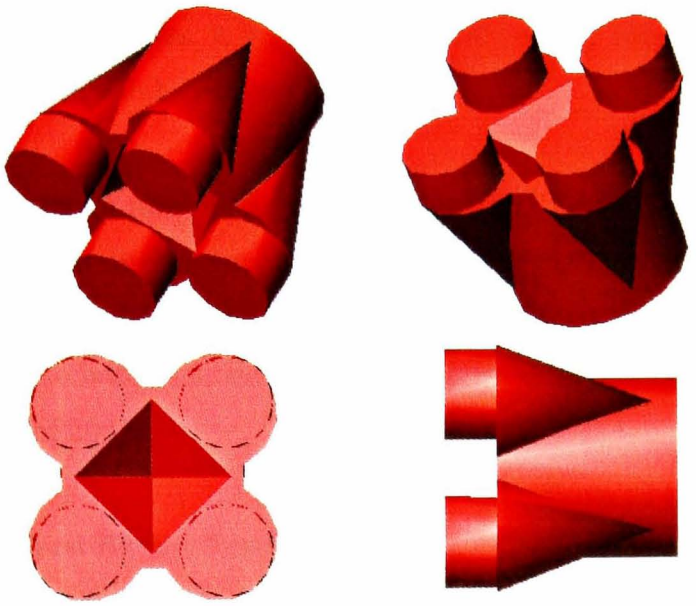

Figure 8.7 – Quadrafurcator showing splitting pyramid

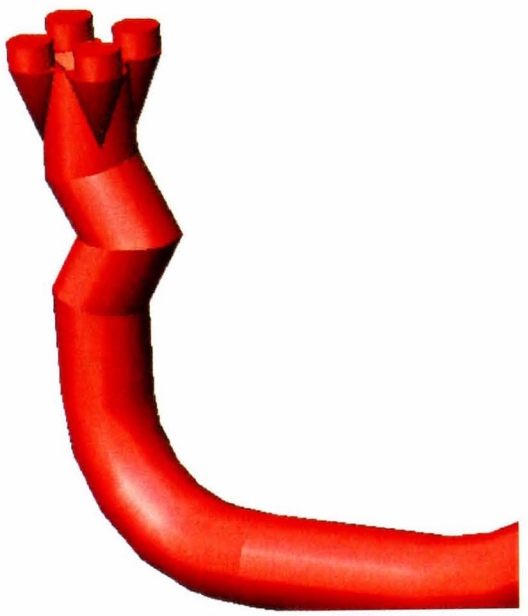

Figure 8.8 – Geometry of Nanticoke scenario

Such a splitting device assumes either a perfectly homogenous mixture or that the particle rope to strike the centre of the splitting pyramid as shown in Figure 9.7. With such a tight bend and dense rope this is unlikely to happen. The current solution to the problem is the installation of a shallow Venturi straight after the bend in the vertical riser. The current splits are shown in Table 8.3.

8.4.3 Solution

The proposed solution to the problem was to install a H-VARB device in the vertical riser in

the geometry and to install a control gate in front of the splitting pyramid. The geometry of the H-VARB solution is shown in Figure 9.8. The proposed solution has been tested in a similar trifurcator situation and has lead to a maximum over minimum ratio of 1.1 without control gates.

8.4.4 Current Situation

As of June 2006 a trial installation for the device was installed and trials have taken place. The installation utilises the H-VARB^{TM} device, a control gate, a special Quadrafurcator designed by Greenbank Terotech and a set of the PfMaster sensors supplied to OPG by Greenbank Energy in the USA.

Currently, the best distribution for side 1 is 11% RMS deviation and for side 2 is 10% RMS deviation. The guarantee asks for 12.5% RMS deviation. In terms of deviation from the a desired balanced split of +/-2% across all 8 burners. All that is required now is fine tuning of the control gates. It has been suggested by the station that if the trials are successful that a boiler set will be ordered early 2007.

The station have said openly that they not only see an improvement in efficiency from the improved distribution, but that the improved distribution will lead to better flame stability at low loads and prevent the need for co-firing the station with natural gas at these low loads. It has also been said that following completion of the trails a full boiler set will be ordered at the start of 2007.

8.5 West Burton Power Station

8.5.1 Description of West Burton

West Burton is a 2,000MW coal-fired power station that stands on a 410 acre site in north Nottinghamshire, nine miles north-east of Retford. The station runs 24 hours a day. The station has a tangentially fired boiler and the pipe network is designed to reduce the level of wear in the pipes and bends.

8.5.2 Description of Problem.

West Burton is an unusual vertical splitting case, in that the vertical split takes place in the direction of gravity. West Burton is a comer fired burner, this means that the burners all face

inwards from a comer; this is shown in figure 8.9. This is the T-fired configuration. This leads to better combustion of products and efficiency of the boiler.

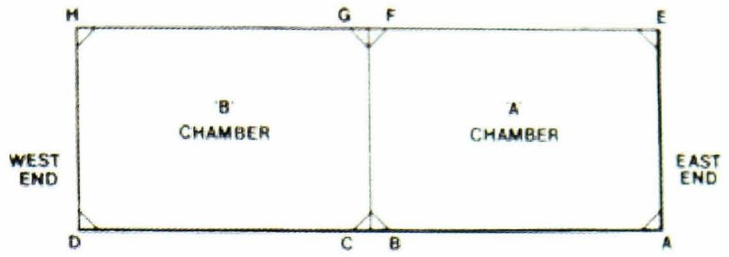

Figure 8.9 – The T-Fired boiler configuration

However, this configuration does lead to a very complicated pipe network as shown in figure 8.10. This leads to an unfortunate choice of split, which involves a bifurcation with riffle after a 90° bend. In addition there is very little room for modification.

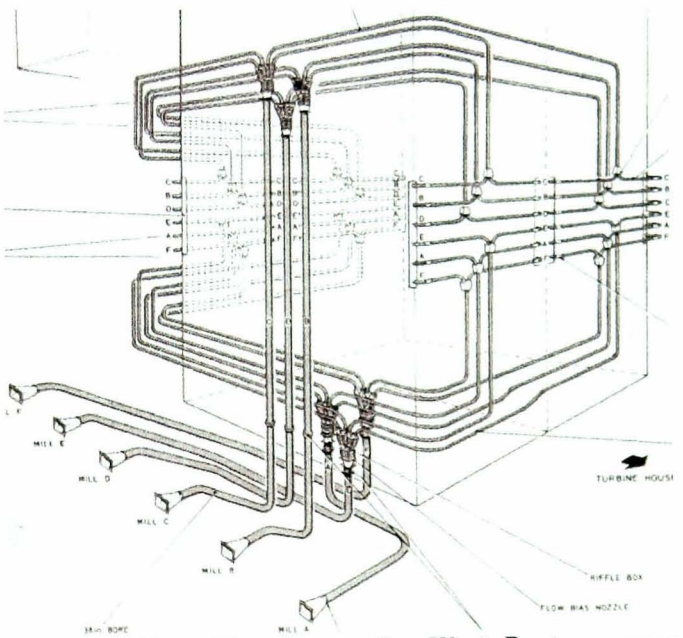

Figure 8.10 – Pipe layout for West Burton power station

The work was undertaken to investigate the phenomena where a riffle box located in the West Burton power station was not splitting equally. A sample bend is shown in figure 8.11.

Normally riffle boxes give a split between a perfect 50:50 split and a 45:55 split, which is often referred to as a classic riffle box split. The Rotor Probe tests carried out are shown in Table 8.5. This shows that the imbalance is greater than expected splits.

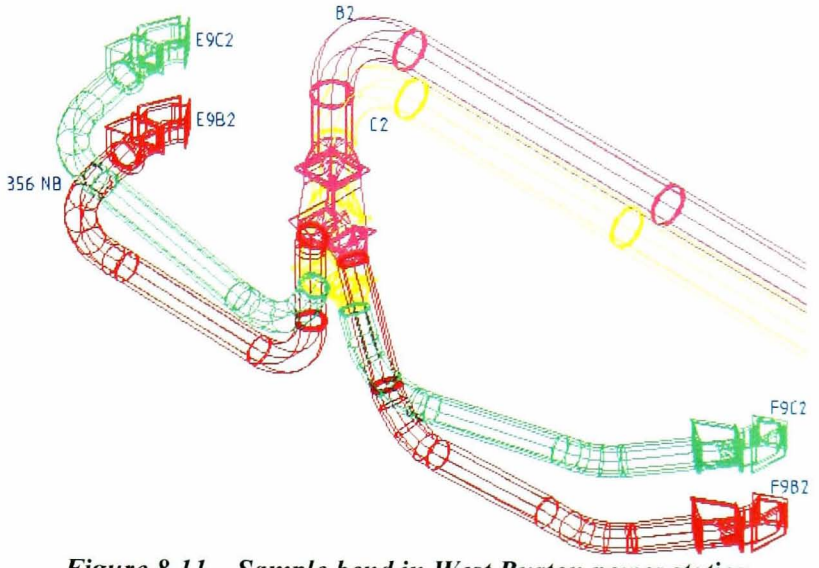

Figure 8.11 – Sample bend in West Burton power station

Table 8.5 – Rotor probe tests carried out at West Burton power station

Actual tertiary splits								
Burner	H	G	H	G	F	E	F	E
Test 1 / Test 2 high	28.53%	71.47%	0.00%	0.00%	28.26%	71.74%	0.00%	0.00%
Test 3 / Test 4 med	49.26%	50.74%	42.64%	57.36%	34.30%	65.70%	32.42%	67.58%
Test 5 / 6 Low	51.53%	48.47%	29.57%	70.43%	29.27%	70.73%	40.02%	59.98%
Burner	D	C	D	C	B	A	B	A
Test 1 / Test 2 high	40.37%	59.63%	42.92%	57.08%	42.79%	57.21%	38.97%	61.03%
Test 3 / Test 4 med	34.18%	65.82%	48.32%	51.68%	51.68%	48.32%	41.57%	58.43%
Test 5 / 6 Low	45.57%	54.43%	43.76%	56.24%	57.98%	42.02%	46.32%	53.68%

8.5.3 CFD Approach

A CFD study was undertaken to investigate the cause of the imbalance and consider alternatives to the current configuration. The investigation through computation fluid dynamics focused on one particular branch of the pipe network, that part that related to burners E and F. After refinement of the grid the pipe run was split into three sections, these sections of the pipe network were linked together through solution matching.

The three sections were considered: The quadrafurcator, the pipe run and the bifurcator. The focus was on the splitting in the final bifurcator so the quadrafurcator was ignored and solutions only dealt with horizontal pipe run and the bifurcator. The CFD data gave a prediction within 1 % of the actual data collected from the power station for one of the operating conditions. The tight bend means that there is no homogeneity in the particle

stream. Whilst the standard riffle will usually work with ropes, the distance between rope formation and the riffle is very short.

The difference in splits between different operating conditions will be due to different rope positions entering the final bend. A change of a few mms in the pipeline can move the rope area from over one or two riffles to maybe 3 or 4 altering the split at the bifurcator. Figure 8.12 shows the rope entering just a few riffles before the split.

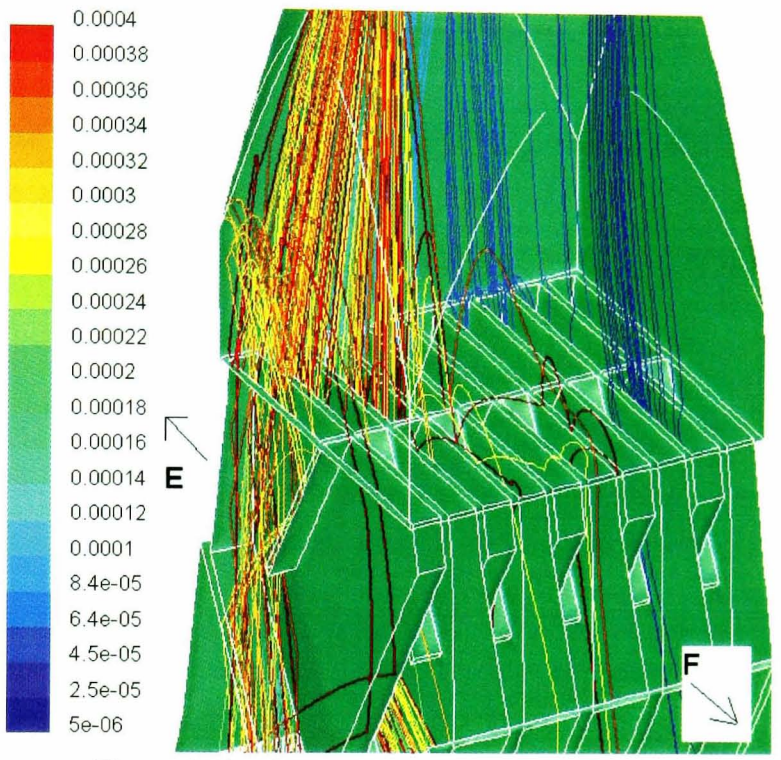

Figure 8.12 – CFD of the internals of a rifflebox

8.5.4 Solution

Several solutions to the situation were modelled. These were solutions that have been used in other cases and situations in the past, not all of them would have been suitable for the pipe configuration or construction envelope. These included expansions, Venturi and offsets.

The success of these solutions varied and was not always what was expected. The range of solutions modelled is detailed in the report. The worse split achieved was 9%:91 %, this was for the bifurcator rotated 90°. Whilst the best split achieved was 47%:53%. This was from simply installing an expansion just before the riffle.

So in conclusion it was discovered that the poor split is caused by the stratification of the powder in the bend. The lack of any distance between the last bend and the splitting box is the major cause of this. A trial installation is planned for early 2007.

8.6 Conclusion.

The use of these examples of industrial deployment has highlighted the contributions that PhD work light this makes towards the progress of industry. These deployments have allowed intimate knowledge of current practices, process tolerances and the needs and wants of power station operators and the range of forces acting on them when choosing a device. In addition the installation of these products are a result of this research show that the device is not only a success in the test conditions but also in full-scale industry.

In conclusion, these case studies demonstrate the positive contribution made to the industry through this thesis and demonstrates the achievement of one of the aims of this thesis, the production of a commercially viable product for the coal-fired power station industry.

Missing pages are unavailable

Chapter 9

Conclusions

9.1 Preface

An extensive investigation into pneumatic conveying and powder balance has been undertaken in this work. The work was multi-facetted, looking at product design, experimental testing, computational testing and industrial case studies. All this work combined has produced four viable products for the solution of powder balance in pneumatic conveying pipelines.

This chapter details the conclusions that can be drawn from the work and how they translate into both useful knowledge for the power generation industry and into viable products.

9.2 Aims completed

The aims of this thesis, as laid out in chapter One: Introduction, have been successfully completed. These aims were decided upon to not only develop devices and products, but also procedures and techniques that could be applied to future investigation.

The first aim of this work was to create a validated computation fluid dynamics (CFD) model a pneumatic conveying pipeline. This validated model could then be applied, with adaptation, to industrial scale scenarios and used in industrial case studies. This was achieved two viable models were selected from the turbulence modelling available and validation from both the quarter scale rig and industrial case studies was achieved.

The achievement in CFD modelling has been an understanding of the requirements for meshing domains and being able to quickly and effectively setup and run cases based on their required level of accuracy. The case studies chapter demonstrates how some of these models have already been ,pplied with success to industrial scenarios.

Another aim of the work was to develop several devices to attempt to solve the problem of powder imbalance at splitter boxes in pneumatic conveying networks. Four devices: The Offset; The Expansion; The Control Gate and the Active system have been developed for a range of different scenarios. It has been demonstrated that through development it is possible to tailor

these solutions to various real problems. The case studies section demonstrates how some of these devices have already been applied with success to industrial scenarios.

9.3 Devices

9.3.1 Preface

The main achievement in the eyes of the author is the successful development of several devices to suit certain scenarios. This provides a toolbox of possible configurations for a range of scenarios.

9.3.2 The Offset Device

The Offset device, whilst developed for a single bend and the standard secondary flow patterns, is remarkably adaptable. From the experimentation with the Offset installed into a double bend - spinning rope scenario (scenario two) it can be seen to provide an adequate level of particle dispersion. When combined with a device like the Control Gate, the Offset device can be installed into almost any scenario. However, to do so would require either accurate computation or numerical modelling or empirical knowledge of rope position (e.g. based on erosion patterns, mass imbalance).

The use of CFD in combination with empirical data will allow successful placement of the Offset device in an industrial scenario and allow it to be positioned so as to provide a reasonable split for a range of conditions.

9.3.3 The Expansion Device

The Expansion device has been developed for spinning ropes. Spinning ropes tend to be providing much worst powder balances in the quarter scale test facility than nonspinning ropes. The Expansion device was able to improve the powder balance significantly over a straight test section.

The Expansion represents a universal device for spinning ropes that when used in combination with the Control gate. It is only important to try to locate the device as far from the split as possible to allow the vertical riser to take full effect on the powder and naturally disperse it.

9.3.4 The Control Gate Device

The Control Gate device was developed as a fine tuning device to placed in addition to the other devices. Though initial tests with in on its own proved in effective, once the rope core had been disputed and powder was spread across the cross section of the pipe the Control Gate worked well to balance the powder at the splitter box.

9.4 Future Work

9.4.1 Preface

The work presented in this thesis whilst extensive is not inclusive of all possible optimisation and investigation avenues. This thesis represents a stepping-stone to further areas of research. The author will explore some of these, others by other members of the research group in future projects.

9.4.2 Optimisation of Devices.

Whilst some optimisation was undertaken in the course of this thesis on the various devices, it was not extensive, mainly due to the cost per unit of producing scale models of devices for testing and the time that production took.

A series of parametric studies into angles for the Expansion device and a more extensive investigation into angles and heights of the Offset device are needed to truly optimise the device. Optimisation will involve parametric studies carried out on CFD in an attempt to reduce the number of experimental models that need to be manufactured.

9.4.3 Testing of relegated designs.

In the course of this work several ideas were developed and then discarded so as to focus on a small number of devices. With development these devices might prove to be as effective or more effective as the devices described in this work.

9.4.4 Horizontal Testing

In pneumatic conveying pipeline networks not all splitting boxes are positioned in the vertical

direction of flow. The horizontal split is technically more difficult to achieve, as the biasing effect of the gravity will attempt to skew the split. Whilst horizontal splits are rare in power stations, they are usually the most troublesome.

The quarter scale rig can be configured into a horizontal set up and the existing devices could represent the basis for horizontal mixing devices. This alternative would represent a lengthy project in itself, but it would prove whether the devices discussed in this work are completely universal.

9.5 Conclusion

The work undertaken in this thesis was to example powder balancing in vertical splitter boxes. This has been successfully undertaken and has led the development of several devices for use in the power generation industry and several computational and numerical techniques and tools that can aid their installation. The thesis has been successful in all its aims and in its overall objective.

From the above sections it can be seen that there is extensive work that can be carried on from this thesis. Whilst some of this possible future works are extensive they would add valuable knowledge and devices to the field of pneumatic conveying.

Chapter 10

References

Laser Sheet visualization of 'PF' Roping: Particulate concentration and size analysis in pipeline cross-section.
10th International Symposium on Flow Visualization. Kyoto, Japan. 2002.

Gas-solid flow behaviour in a horizontal pipe after a 90° vertical-to-horizontal elbow.
Akilli, Levy, Sahin.
Powder Technology 116 (2001) 43-52

Mixing and dispersion of particle ropes in lean phase pneumatic conveying
Biligren, Levy.
Powder Technology 119 (2001) 134-152

Brilliant W Quantel Brilliat Q-Switched Nd:YAG Laser.
Brilliant, Instruction Manual.
Issue 1# 1999.

PF Settlement in the 660mm Bore Main Mill Outlet P.F. Pipes at Drax Power Station.
CEGB. Report.

British Science Museum Website: http://www.sciencemuseum.org.uk/
Checked September 2006

Carbon Trust Website http://carbontrust.com
Checked September 2006

Cabrejos PhD thesis, No Title
School of Engineering, University of Pittsburgh (1994).

A study of Electrostatic Pulverised Fuel Metering. PhD Thesis.
Cheng.
University of Teesside. 1996

Clampon Phamphlet, 2002

Pulversied Fuel Flow Distribution and deposition in a Glass Model and Comparisons with Full Size Plant at Drax Power Station.
Cook and Hurworth.
CEGB internal report 1979.

Recent research on Pulverised fuel settlement in Power Stations Pipelines, and the Significance of Roping.
Cook, Hurworth.
5th Int. Conference on The Pneumatic Transport of Solids in Pipes 1980.

Online Pulverised Fuel Monitoring at the Methil Power Station.
Coulthard, Cheng, Kane, Osbourne, Keech.
IEE Power Engineering Vol 11 No. 1. 1997

Multiphase Flows with droplets and particles.
Crowe, M. Sommerfeld, Y. Tsuji.
CRC Press LLC. 1998.

FlowMAP users Guide.
Dantec 1999

Dinglers Polytech. Journal. 407 (1847)

Drax Power Station Website: http://www.draxpower.com/
Checked September 2006

Renewable energy to take off in Europe? 2004 – overview and scenario for the future
European Commission memo
Directorate General for Energy and Transport (2004)

The Energy Challenge: A Report,
Dti (2006)

Potential Cost and Efficiency Savings Through Improved Multiphase Application in UK Fossil-Fired Power Generation.
DTI, Cleaner Coal Technology. Project Summary 268. 2001

Pulverised Fuel Flow Measurement and Control Methods for Utility Boilers.
Cleaner Coal Technology Programme.
Technology Status Report 014. Dti. 2001

Characterisation of the cross sectional particle concentration distribution in horizontal dilute flow conveying – a review.
Fokeer, Kingman, Lowndes, Reynolds.
Chemical Engineering and Processing. 2003

A Numerical Study of the Gas Particle Flow in Pipework and Flow Splitting Devices of Coal-Fired Power Plant.
Frank, Schneider, Pachler, Bernert. 10th Workshop on Two Phase Flow Predictions 2002

A ¼ scale test facility for PF transport in power station pipelines.
Giddings, Aroussi, Pickering, Mozaffari.
Fuel 83 (2004) 2195-2204

Bulk effect of particles in a one-quarter-scale rig of a coal fired power station coal delivery circuit.
Giddings, Aroussi, Azzopardi, Pickering.
CFD2003, Vancouver, Canada 2003

Investigation into the operation of a cement works precalciner vessel
Giddings PhD Thesis.
University of Nottingham. 2000

"A Vision for Clean Fossil Power Generation": Recommendations for a UK carbon abatement Programme for fossil fuel generation. 2004.
Government White Paper.

Particle Image Velocimetry: a Review.
Grant.
Proc Instn Mechanical Engineers Vol 211 Part C. 1997

Effect of particle characteristics on particle pickup velocity,
Hayden, Park, Curtis.
Powder Technology, Volume 131, Issue 1, 3 March 2003, 7-14

Splitting of Pneumatic Conveying Pipelines.
Hilbert.
Bulk Solids Handling 1984, 4(1), 189-192.

Techniques for control of splitting ratios of particulate materials at bifurcations in pneumatic conveying pipelines.
Holmes, Bradley, Selves, Farnish, Bridle, Reed.
Proc. Instn Mechanical Engineers. Vol 214 Part A. 2000.

Particle Image Velocimetry: Simultaneous two-phase flow measurements.
Jakobsen, Easson, Greated, Glass.
Measurement Science Technology 7 (1996) 1270-1280.

Balancing of Coal Flow to burners in pulverised coal boilers.
Levy, Yilmaz , Bilirgen, Wang, Sui.
26th International Technical conference on Coal utilization And Fuel systems, Clearwater, Florida, 2001

Prediction of pneumatic conveying flow phenimena using commercial CFD Software.
Levy, Bilirgen, Yilmaz.
Powder Technology 95 (1998) 37-41

Freight Pipelines : Current status and anticipated use.
ACSE Journal of Transportation Journal Vol. 124, no. 4 pp 300-310
Liu, Jul/Aug

Turbulence Modification by Particles in a Horizontal Pipe Flow.
Ljus, Johansson Almstedt.
Int. journal of Multiphase Flow 28 (2002) 1075-1090.

The use of particle image velocimetry to study roping in pneumatic conveyance.
MacCluskey, Easson, Greated. Glass.
Partition Systems Characteristic Journal 6 (1989) 129-132 D.R.

Assessment of the Efefectiveness of various P.F. Rope Destructor Devices on the Renthew P.F. Splitter Facility.
Macphail, Ballentyne, King.
Babcock Confidential Report. 1983

Minimum energy pneumatic conveying 1.
Marcus.
Dilute phase, Journal of Pipelines 4 (1984) 113-121

Measurements of Powder Flow Rates in Gas Solid flows based on static Electrification of Coal.
Mascada, Advanced Powder Technology 1994

A simulation system for pneumatic conveying systems.
Mason, Marjanovic, Levy
Powder Technology 95 (1998) 7-14

The effect of a bend on the particle cross-section concentration and segregation in pneumatic conveying systems
Mason, Levy.
Powder Technology 98 (1998) 95-103

Fluid Dynamics Sixth Edition 1998.
Massey

Technology status review of PF flow measurement and control methods for utility boilers.
Report No. COAL R201 DTI/Pub URN 00/1445
Miller, Baimbridge and Eyre, PowerGen plc (2000)

Overview: Pneumatic transport of Solids.
Powder Technology 88 (1996) 309-321
Molerus

Pacific Pneumatics Website: http://www.pacpneu.com/page14.html
Checked September 2006

Material Properties and flow modes in pneumatic conveying.
Pan.
Powder Technology 104 (1999) 157-163

Effect of a combnation of two elbows on particle roping in pneumatic conveying.
Schallart, Levy.
Powder Technology 107 (2000) 226-233

Further Development of the CERL Pulverised Fuel Riffle.
Snowstill
CERL Laboratory Report RD/L/R 1513, Job VC 058. 1968.

Fundamentals of coal combustion for clean and efficient use.
Coal Science and Technology 20 Elsevier
Smoot (Editor)

Modelling and Numerical Calculation of Turbulent Gas-Solid Flows with a Eular-Lagrangian Approach.
Sommerfeld.
KONA No.16 (1998)

Experimental analysis and modelling of particle-wall collisions
Sommerfeld and Huber
Int Jrl Multiphase Flow 25 1457-1489

Our Energy Future - Creating a Low Carbon Economy
Energy White Paper, UK Government (2003)

Kyoto Protocol,

UNFCCC, 1997.

An Introduction to Computational Fluid Dynamics: The Finite Volume Method.
Versteeg, Malalasekra.
Pretience Hall 2002

Formation and Dispersion of Ropes in Pneumatic Conveying.
Yilmaz, Levy.
Powder Technology 114 (2001) 168-185

Roping phenomena in pulverized coal conveying lines.
Yilmaz, E. Levy.
Powder Technology 95 (1998) 43-48

Roping Phenomena in lean phase pneumatic conveying, PhD Dissertation.
Yilmaz
Lehigh University, Bethlehem, PA 1997.

World Coal Insitution website: http://www.worldcoal.org
Checked September 2006

Appendix A

Grid Independence Study.

Grid Independence is a key factor in CFD. Grid Independence is vital to a CFD cases, in computational modelling the fineness of a grid can lead to different results. The idea of a Grid Independence is to continuously refine the fineness of the model and run the intended case focusing on physical results that can be observed. Usually only a single field variable is used in the comparison, such as pressure or velocity profile.

Normally the grid is continually refined and has the solution rerun in the solver until the difference in solution between the old and the new mesh is with in 99% (i.e. there is no discernable change in the result from refining the mesh). The value used in this thesis is the velocity profile over the outlet of the pipe. Other factors can be used, the author of this thesis

The procedure is as follows:

1.) Choose a course mesh regime for the selected mesh.

2.) Run the case with all the correct factors until completion.

3.) When the case is complete take a line across one of the outlets of the mesh.

4.) Take the velocity values across that line and plot them against their co-ordinates.

5.) Refine the mesh spacing of the mesh. If a particularly course mesh, halving the spacing size is a good step. If the mesh is quite fine perhaps reducing the mesh spacing by a single digit is sometimes enough

6.) Run the case again. Take a line and retrieve a list of velocities at co-ordinates.

7.) Compare the values at the co-ordinates. Repeat until the average difference between velocity results is within 99%.

After this procedure is completed the result is said to be Grid Independent. One problem with the procedure is that one has to weigh the computational power available to solve the process and the problems with having cells so small that you are attempting direct simulation. CFD is a modelling method, various corollaries used in the basis of CFD break down if direct simulation methods are used with standard CFD codes such as the RSM and k-ε methods. These are detailed in "An Introduction to Computational Fluid Dynamics: The Finite Volume Method" by H.K. Versteegand W. Malalasekra. These are both references in the references section.

Appendix B

Settings for CFD simulation

The settings used for all the CFD simulation in this work are presented below. This section does not go into the theory behind the models or the application. This is adequately covered in the FLUENT users guide and in "**An Introduction to Computational Fluid Dynamics: The Finite Volume Method" by H.K. Versteegand W. Malalasekra. These are both references in the references section.**

This section exists mainly as a reference for future users of FLUENT to replicate the results of the thesis if so desired. For all the cases in the thesis are

These are the standard co-efficients of the Reynolds Stress Model in Fluent.

CMu	= 0.09
C1 – Epsilion	= 1.44
C2 – Epsilion	= 1.92
Cs	= 0.22
C1-PS	= 1.8
C2-PS	= 0.6
C1' - PS	= 0.5
C2' - PS	= 0.3
TKE Prandtl Number	= 1
TDR Prandtl Number	= 1.3

The cases utilised the Standard Wall functions and the Wall Boundary Conditions from the k-Equation. The turbulence specification method used is hydraulic diameter and turbulence intensity factor. The calculation for the Turbulence Intensity factor is shown in Equation A.1, RE is the Reynolds number of the flow. The calculation for the hydraulic diameter is shown in Equation A.2.

$$(0.16 * RE^{0.125}) * 100\% \qquad \textbf{Equation A.1}$$

4 * Perimeter / Diameter **Equation A.2**

Appendix C –

Moving Plate Paper

THE VISUALISATION AND CONTROL OF PULVERISED COAL CONVEYING.

D. Giddings*, A. Aroussi*, E. Mozaffari*, S. Pickering*, J. Roberts*, P. Rogers*
*** School of Mechanical, Materials, Manufacturing Engineering and Management**
University of Nottingham, Nottingham, NG7 2RD.

Keywords: *Pulverised Fuel, Feedback, Image processing, Control.*

ABSTRACT

A one-quarter-scale rig of coal fired power station pipe work, with optical access in steel pipes, has been constructed at The University of Nottingham. Flow visualisation of the dispersed powder shows concentrated regions of particles in cross sections. This uneven dispersion determines the division of powder at junctions in the pipe-work, which causes reduced control of furnace operation.

Using image analysis techniques – established and developed - the concentration of the particles can be quantitatively assessed. This can then offer a means of controlling the dispersion by use of simple deflection devices within the junction.

Previous work in the field by Huber and Sommerfeld [1] viewed the cross section of glass pipes in circuit of diameter 80 mm. Velocities up to 30m/s and solid loading up to 2 kg of spherical glass beads (mean diameter 42μm) per kg of air were achieved. Video images using continuous wave laser illumination were analysed and calibrated to give mass flow of powder per unit area. Yilmaz and Levy [2] used discrete point visualisation using a fibre optic probe in a 154 mm-diameter pipe circuit using pulverised coal with typical size distribution used in power stations. Both papers indicated the importance of the formation of 'ropes' due to pipe bends.

In the Nottingham based rig, air velocities up to 18 m/s can be achieved with solids loading up to 170 g/s. The powder used in the rig was cenospheres (hollow glassy spheres) having mean density of 700 kg/m^3, which allowed dynamic similarity between rig and power station to be reasonably well achieved.

In this work the powder, post-splitter, was inspected using visualization and the bulk splitting of the mass was measured in weigh hoppers. Inspection of the images captured by CCD camera shows arrested particles since the pulse duration is in the order of 5 ns. By appropriate choice of a threshold level, the data gained from the images gave a comparable measure of the bulk mass split to the weigh hopper measurements.

After four horizontal bends and one vertical bend in the circuit, the wall bound nature of the dispersion was clearly seen and spiralling motion described by other researchers was observed [3]. The dispersion was analysed in a two-way splitter with glass walls. In addition, a simple deflection device in the two-way splitter was found to be capable of altering the distribution of powder in the downstream pipes. This paper describes attempts to achieve split control using feedback to the deflection device from the optical information after processing by customised image processing software.

1 INTRODUCTION

This paper describes the ongoing work at The University of Nottingham investigating pulverised fuel conveying in the power generation industry. Pneumatic transport of pulverised fuel is being studied at The University of Nottingham using a purpose-built test rig. Hollow 'glassy' spheres of the same order of size as pulverised fuel are circulated in relatively lean air suspension in a pipe system that is one-quarter scale of the typical power station. Two and three-way splitters are included to simulate splitting at the station. Viewing sections have been developed that allow laser anemometry to be performed before and after the splitter. Of specific interest is the formation of the particle 'rope' as the stream of air and particles travels through bends and the subsequent effect of the 'rope' on bulk distribution of the transported solid. Laser sheets illuminate the particles such that in sufficiently lean conditions, individual particles can be identified and analysed to produce information about size, distribution, and velocity.

The current work describes development of a simple device with feedback control the distribution of powder to pipes downstream of a two-way junction (bifurcator) in the pipework. The feedback loop employs laser sheet images on the cross section of each downstream leg. The images can be processed to give an indication of the mass split and that information provides a signal to control the movement of a single inclined plate at the base of the bifurcator across the cross-section. The plate deflects the concentrated section of the stream of particles rising into the bifurcator and can be moved to such a position that the mass split becomes equal. This paper details the bulk mass split for different positions of the splitting plate and the development of signal from the laser sheet images.

2 PREVIOUS WORK

Transmission of pulverised solids in air is standard procedure in chemical engineering plants. Several modes of transport have been identified that are distinguished by the air to solid mass ratio and the transport velocity as described in the early paper by Zenz [4]. The 'phase diagram' showing pressure drop for varying gas velocity and air to solid rate ratio was established. Distinctly different characteristics are observed as the air to solid ratio is decreased; in horizontal conveying the solid phase is prone to settling on the pipe wall so that saltation can occur and in vertical pipes slugs of solid agglomeration form. Power stations use pneumatic transport to deliver pulverised coal to the furnace between 1.8 and 3 kg/s air to kg/s solid and air velocity in the order of 25m/sec. The phase diagram indicates that this is dilute phase flow, away from the region of saltation. The suspension is sufficiently dense to prevent explosion and lean to allow analysis using optical techniques.

Since coal is conveyed from ground level mills to several positions on furnaces at some height above, bends in pipe-work are inevitable, and thus the established 'roping' effect occurs. The effect of a single vertical pipe bend was analysed using CFD by Levy and Mason [5]. They showed that two counter-rotating vortices form, which promote remixing of the particles after they have been thrown by centrifugal action to the outer pipe wall. Schallert and Levy [3] report that in a test rig, the effect of two bends on the rope is that following the second bend a stationary spiral is formed. They measured the spiral on the rig and predicted it by CFD.

Yilmaz and Levy [2] demonstrated the use of the time of flight method of particle velocity and concentration measurement. Velocity was determined from two closely streamwise positioned fibre optic probes using continuous wave laser light and the concentration was determined by the obscuration of laser light over small distance by comparison with calibration data. The data obtained usefully shows the overall pattern of the rope.

Huber and Sommerfeld [6] performed tests in a test rig having 80mm pipe bore using glass beads having mean size by number distribution of 40μm. Laser light sheet from a continuous wave laser was used to get video images of the two-phase flow in cross sections. Each frame of the CCD camera was 0.04 s duration. Images were processed to show particle concentration.

3 METHODOLOGY

A test rig, constructed by Greenbank Terotech Ltd, has been commissioned at The University of Nottingham. It is purpose-built to simulate the transport of coal laden air in the power station. The rig is further described by Giddings et al [7]. For these experiments the bifurcator is fitted as the splitter and the line 2 is not operational. Weigh hoppers, with displacement measured by LVDTs, for line 1 and line 3 are used to measure the powder delivery rate to the two legs of the bifurcator. The output signals are measured via a 6024E National Instruments card with Labview processing. Measurements are also taken of the airflow in the two lines from orifice plates downstream of the cyclone powder separators. The flow rate of air in the experiments described here was 16 m/s in the 6" inlet pipe and the powder flow rate was 80 g/s giving an approximate solid to air ratio of 0.2. Following the bifurcator the pipe diameter is nominally 4" diameter. A schematic of the entire pipe-work of the test rig and a photograph of the experimental test section are illustrated in Fig 1.

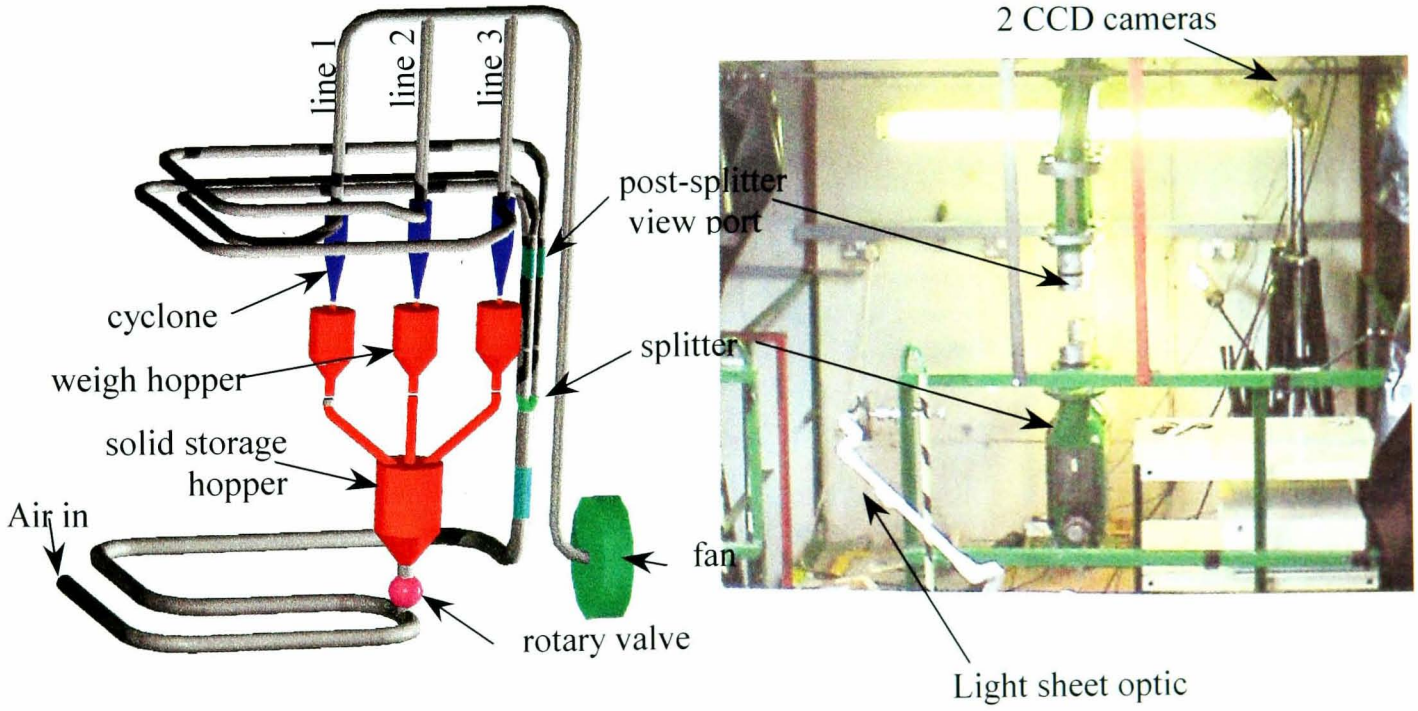

Fig. 1 – ¼ scale Rig at the University of Nottingham and camera setup.

A Nd:YAG 150mJ pulsed laser is used to generate laser light sheet at 532 nm at 15 Hz pulse frequency. The light sheet is placed so it crosses both post-splitter view ports and illuminates both cross-sections when powder is flowing. The light sheet is horizontal and positioned such that it passes through both pipes with equal intensiy. For each downstream pipe, a Kodak Megaplus 1M pixel CCD camera is set up to view the illuminated section at an angle of approximately 45° to the horizontal. Both cameras have equal aperture setting and equal viewing area, thus giving equal exposure to the illuminated cross section of powder.

The cameras are connected to a Dantec Dual processor which contains the image capturing hardware. The images captured by the Dantec system are then processed using custom software produced in-house at the University of Nottingham to clarify the distribution of powder in the pipe and to provide a numerical indication of the relative density of powder in each pipe for comparison. Each image is an 8 bit grey scale bitmap, with 0 to 255 intensity value for each pixel. In the software routines the whole image is inspected pixel by pixel, histogram equalisation is performed to highlight areas that are not visible due to low intensity, and the intensity levels divided in to ten ranges, which are coloured blue (cold) through to red and white (hot) to indicate relative levels of particle concentration in the image. This gives us pictures positioning the particulate. To assess the split, from the raw pixel data all the pixels with an intensity value above a 100 were summed together and taken as a value of the split.

In the bifurcator splitting box is a single plate attached to an assembly that allows it to be moved across the path of the flow. The plate can therefore be placed at a range of positions in the splitting box. The moving assembly is attached to a stepper motor which is computer driven.

The bifurcator design is based on a established power station bifurcator, intended to be used with internal devices to control the rope. The devices are not included in this work. Instead, a non-standard control technique is presented. At the base of the bifurcator is a throat section, which reduces the pipe bore to nominal 5". This directs the rising stream of particles that rise in a spiral on the wall of the vertical pipe below toward the pipe centre line. The plate is inserted immediately above this, to one side in the position that the rope is known, from previous experiments, to reside during operation. In the experiment, weigh hopper readings and photographic images were taken whilst the plate was translated across the bifurcator.

4 RESULTS

Results are listed in the form of analysed light sheet photographs and weigh hopper reading from the same test period. Fig. 2 shows the actual split results from the weigh hoppers.

Dimensionless Position	% split by mass	
	Line 1	Line 3
0.28	51	49
0.26	58	42
0.23	58	42
0.20	55	45
0.18	55	45
0.15	52	48
0.12	50	50
0.10	50	50
0.07	50	50

Fig. 2 – Readings from the weigh hoppers

With the naked eye you cannot see a measurable difference between the images. Fig. 3 shows a bad split (on the left) and a good split (on the right). From observation of the images, quantification is not possible, hence further image processing was required to produce some numerical value. With the selection of pixel threshold, an investigation was carried out, but the value of a 100 was chosen as Fig. 4 shows that there are a large number of pixels below a hundred that are not illuminated. After choosing the threshold a count of the number of pixels was taken from the image from each leg. These were added together as the total number of pixels and percentages were taken from them for a measure of the amount of powder in each leg. The results for this are shown in Fig. 5.

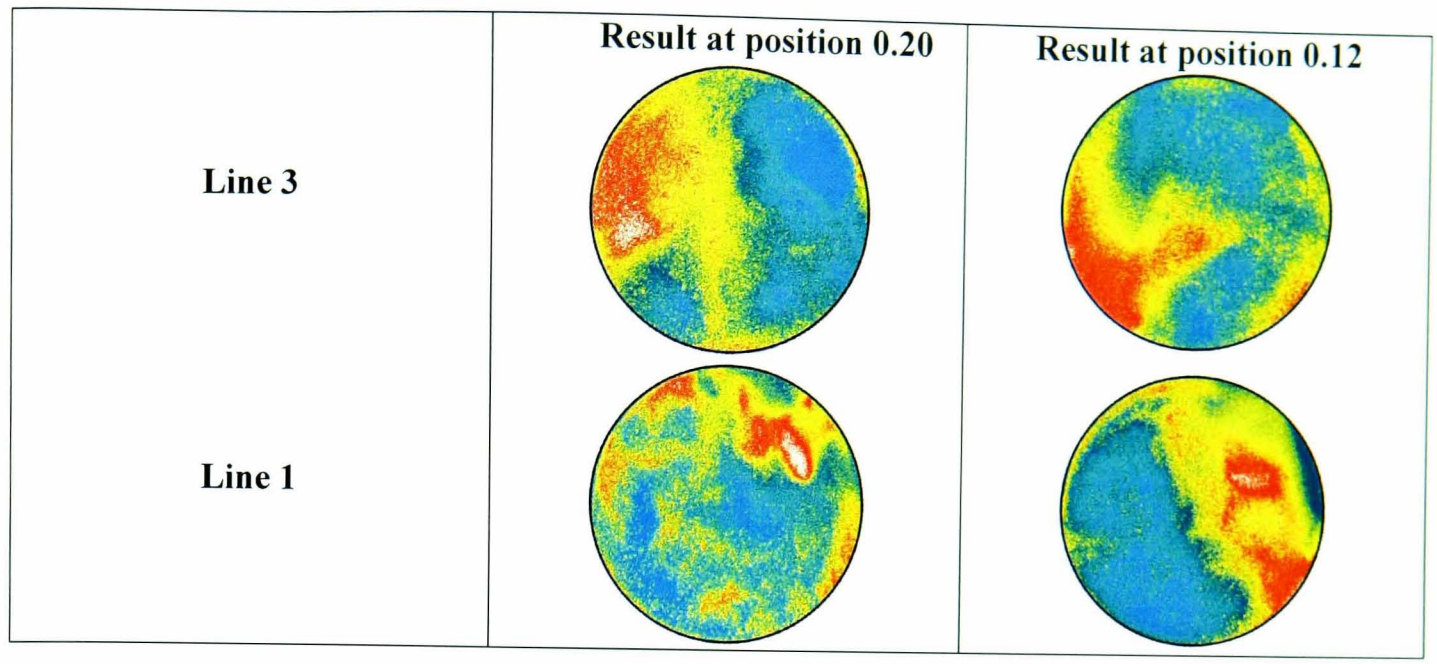

Fig. 3 – Pixel intensity in a histogram chart of ten levels images.

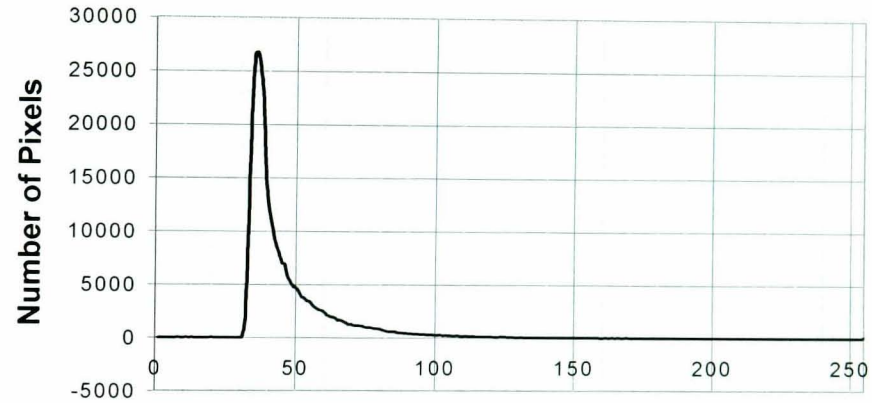

Fig. 4– Pixel intensity verse number of Pixels.

Dimensionless Position	% split by pixel	
	Line 1	Line 3
0.28	55	45
0.26	53	47
0.23	67	33
0.20	65	35
0.18	52	48
0.15	61	39
0.12	50	50
0.10	-	-
0.07	49	51

Fig. 5– Numerical value given by for the splits by the laser sheet visualisation

The comparison between the numerical values given by the light sheet and the values given by the weigh hoppers are compared in Fig 6.

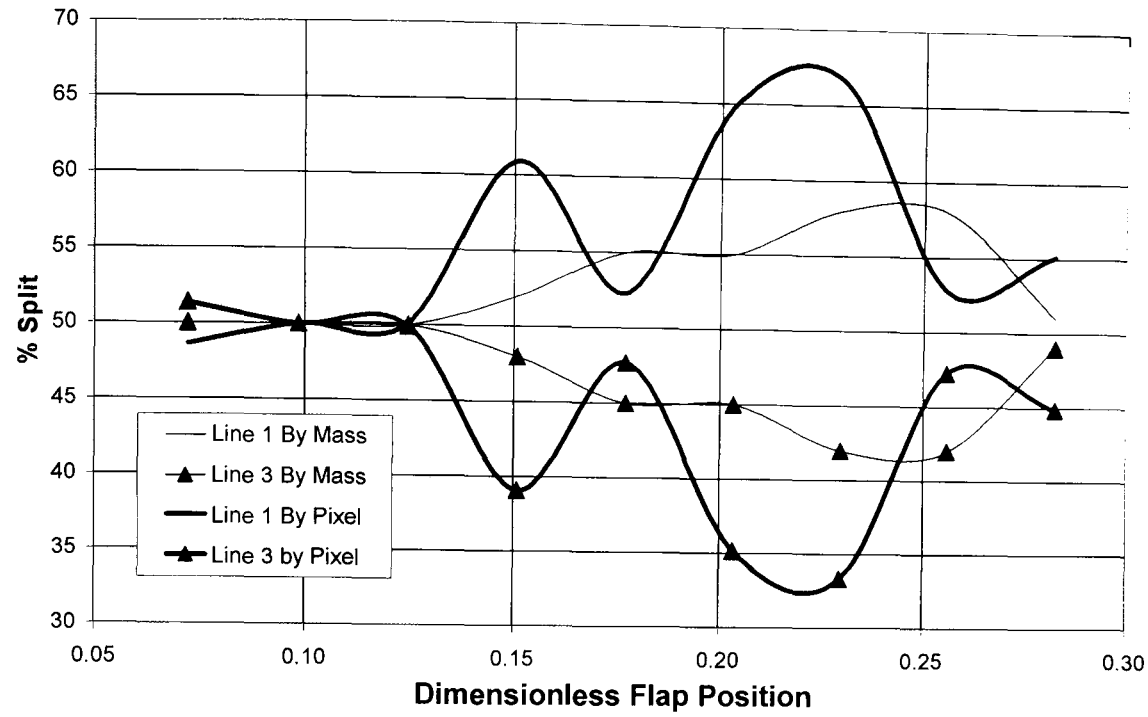

Fig. 6 – Actual (by mass) and predicted (by pixel) values of split ratio obtained at various plate positions

5 DISCUSSION

From the results it can be seen that the position of the plate across the bifurcator does affect the bulk mass splitting (fig 2). There are two areas where a 50-50 split appears from the plate position. As images that looked at the rope formation in the pipe before the bifurcator were not taken as part of these experiments, the reasons for this observation are uncertain. Future work will investigate this phenomenon.

In these results, when an 8% difference is referred to it is only demonstrating a difference 4% of the mass flow rate between the two bifurcator legs. Thus the measuring technique must be sensitive to this reasonably small difference.

The results of visualization did not show a clear distinction, as expected from the above point. The required sensitivity was produced by the numerical analysis of the intensity of the pixels in each image.

From the image processing data in fig. 5 it can be seen that whilst the image data does not follow the bulk mass split precisely, it does indicate the correct bias of the split. The comparison between the split by weigh hopper and the split by pixel number is clearly presented in fig. 6.

The results contained within show the potential for real life application (i.e. in the power station industry). Implementation as feedback control device would require coupling the image processing system to the motor. Further work and investigation is intended into the level of threshold to select before pixel counting or averaging the results over a number of taken images.

6 CONCLUSION

This paper presented an experimental procedure by which laser sheet visualisation is used to capture images of the powder in the bifurcator legs, post-splitter. These images were processed to give a measure of the amount of material going down each leg from the histogram

distribution of pixels intensity values. The histogram showed that there is a great number of pixels with intensity values below the visible level. After eliminating these, the remaining pixels provided the numerical measure of power density in the light sheet. The numerical results were compared with measurements taken from weigh hoppers attached to the individual legs of the bifurcator. Reasonable agreement was observed.

The tests ran show that it would be possible to use the numerical value from the laser sheet visualisation to produce a control signal to drive the motorised plate. In this way feedback can be produced to control the split. Further work is intended on the image processing to produce a more precise prediction of the split.

7 REFERENCES

1. Huber, N and Sommerfeld, M. 1994. Characterisation of the cross-sectional particle concentration distribution in pneumatic conveying systems. Powder Technology 79, 191-210.
2. Yilmaz, A and Levy, K. 1998. Roping phenomena in pulverised coal conveying lines. Powder Technology 95, 43-48.
3. Schallert, R, and Levy, E. Effect of a combination of two elbows on particle roping in pneumatic conveying. Powder Technology 107, 226-233.
4. Zenz, F.A., 1948, Two Phase Fluid-Solid Flow, Industrial and Engineering Chemistry, Vol 41, No. 12, pp 2801-2806
5. Levy, A. and Mason, D.J. 1998. The effect of a bend on the particle cross-section concentration and segregation in pneumatic conveying systems. Powder Technology, 98, pp 95-103
6. Huber, N. and Sommerfeld, M. 1994. Characterisation of the cross-sectional particle concentration distribution in pneumatic conveying systems. Powder Technol' 79 pp191-210
7. Aroussi, A, Giddings, D, Mozaffari, E, Pickering, S.J. The use of laser techniques in characterising the two-phase air-solid flow in power plant pipework. Ninth International Conference of European Association for Laser Anemometry, University of Limerick, Ireland, Sept 2001

Appendix D

Tables of results for experimentation

1.0 Scenario 1

Table 1 – Split by mass flow rate through the geometry of 30° Offset

AFR	Mass Flow (kg/ms^{-1})	Split 1 (%)	Split 2 (%)	Split 3 (%)	Actual AFR	Max/min
3:1	0.1082	35.30	32.07	32.62	3.24	1.10
4:1	0.0921	36.59	26.71	36.70	3.84	1.37
5:1	0.0712	27.67	22.47	49.86	5.00	2.22
6:1	0.0615	28.13	20.98	50.89	5.81	2.42

Table 2 – Split by mass flow rate through the geometry of 20° Offset

AFR	Mass Flow (kg/ms^{-1})	Split 1 (%)	Split 2 (%)	Split 3 (%)	Actual AFR	Max/min
3:1	0.1651	22.11	48.82	29.07	2.11	2.21
4:1	0.0967	26.47	43.95	29.58	3.68	1.66
5:1	0.073	19.86	37.67	42.47	4.89	2.14
6:1	0.0648	18.67	32.87	48.46	5.52	2.60

Table 3 – Split by mass flow rate through the geometry of 40° Offset

AFR	Mass Flow (kg/ms^{-1})	Split 1 (%)	Split 2 (%)	Split 3 (%)	Actual AFR	Max/min
3:1	0.134	21.49	27.09	51.42	2.62	2.39
4:1	0.086	31.51	22.91	45.58	4.17	1.99
5:1	0.0756	25.53	17.72	56.75	4.74	3.20
6:1	0.065	26.00	16.15	57.85	5.53	2.22

Table 4 – Split by mass flow rate through the geometry of 50° Offset

AFR	Mass Flow (kg/ms^{-1})	Split 1 (%)	Split 2 (%)	Split 3 (%)	Actual AFR	Max/min
3:1	0.1133	29.13	24.89	45.98	3.11	1.85
4:1	0.0927	36.14	23.19	40.67	3.84	1.75
5:1	0.0744	22.58	17.07	60.35	4.79	3.54
6:1	0.067	20.75	16.42	62.84	5.33	3.83

Table 4 – Split by mass flow rate through the geometry of Expansion

AFR	Mass Flow (kg/ms^{-1})	Split 1 (%)	Split 2 (%)	Split 3 (%)	Actual AFR	Max/min
3:1	0.1145	14.24	47.77	37.99	3.11	3.36
4:1	0.1016	19.00	50.39	30.61	3.52	2.65
5:1	0.0773	12.68	38.55	48.77	4.67	3.85
6:1	0.0624	14.58	33.17	52.24	5.81	3.58

2.0 Scenario 2

Table 5 - Results for Expansion in double bend scenario

AFR	Mass Flow (kg/ms^{-1})	Split 1 (%)	Split 2 (%)	Split 3 (%)	Actual AFR	Max min
3:1	0.1036	24.32	34.17	41.51	3.51	1.71
4:1	0.0933	27.76	35.37	36.87	3.77	1.34
5:1	0.0766	24.41	33.03	42.56	4.70	1.74
6:1	0.0598	19.57	36.79	43.65	5.94	2.23

Table 6 – Results for the Venturi Expansion in double bend scenario

AFR	Mass Flow (kg/ms^{-1})	Split 1 (%)	Split 2 (%)	Split 3 (%)	Actual AFR	Max/min
3:1	0.1301	31.82	58.19	9.99	2.30	5.82
4:1	0.0844	33.89	55.81	10.31	3.54	5.41
5:1	0.0711	36.01	54.29	9.70	4.20	5.59
6:1	0.0503	28.83	60.64	10.54	5.94	5.75

Table 7 - Results for Expansion Venturi in double bend scenario

AFR	Mass Flow (kg/ms^{-1})	Split 1 (%)	Split 2 (%)	Split 3 (%)	Actual AFR	Max/min
3:1	0.0928	21.55	36.75	41.70	3.22	1.94
4:1	0.0749	20.43	38.45	41.12	3.99	2.01
5:1	0.0556	16.91	39.57	43.53	5.37	2.57
6:1	0.046	15.22	39.13	45.65	6.50	3.00

Table 8 - Results for Position 0° Offset in double bend scenario

AFR	Mass Flow (kg/ms^{-1})	Split 1 (%)	Split 2 (%)	Split 3 (%)	Actual AFR	Max/min
3:1	0.1495	22.81	27.16	50.03	2.38	2.19
4:1	0.1148	21.43	25.44	53.14	3.1	2.48
5:1	0.0949	20.34	24.66	55.01	3.75	2.70
6:1	0.04749	23.77	34.32	41.90	7.5	1.76

Table 9 - Results for Position 30° Offset in double bend scenario

AFR	Mass Flow (kg/ms^{-1})	Split 1 (%)	Split 2 (%)	Split 3 (%)	Actual AFR	Max/min
3:1	0.1342	21.54	39.12	39.34	2.61	1.83
4:1	0.1042	20.06	41.46	38.48	3.39	2.07
5:1	0.0971	21.83	42.64	35.53	3.67	1.95
6:1	0.0694	26.51	36.74	36.74	5.14	1.39

Table 7.10 - Results for Position 60° Offset in double bend scenario

AFR	Mass Flow (kg/ms^{-1})	Split 1 (%)	Split 2 (%)	Split 3 (%)	Actual AFR	Max/min
3:1	0.1412	22.17	48.80	29.04	2.49	2.20
4:1	0.1006	20.38	50.89	28.73	3.52	2.50
5:1	0.086	25.12	45.81	29.07	4.15	1.82
6:1	0.0622	24.28	38.59	37.14	5.80	1.59

Table 11 - Results for Position 90° Offset in double bend scenario

AFR	Mass Flow (kg/ms^{-1})	Split 1 (%)	Split 2 (%)	Split 3 (%)	Actual AFR	Max min
3:1	0.1421	19.35	40.32	40.32	2.49	2.08
4:1	0.1076	20.54	45.72	33.74	3.31	2.23
5:1	0.0818	18.46	42.79	38.75	4.39	2.32
6:1	0.067	20.45	32.09	47.46	5.37	2.32

Table 12 - Results for Position 120° Offset in double bend scenario

AFR	Mass Flow (kg/ms^{-1})	Split 1 (%)	Split 2 (%)	Split 3 (%)	Actual AFR	Max min
3:1	0.1129	23.65	14.26	62.09	3.34	4.35
4:1	0.1096	19.80	14.87	65.33	3.49	4.39
5:1	0.0899	19.35	14.46	66.18	4.22	4.58
6:1	0.0372	41.13	34.95	23.92	9.90	1.72

Table 13 - Results for Position 150° Offset in double bend scenario

AFR	Mass Flow (kg/ms^{-1})	Split 1 (%)	Split 2 (%)	Split 3 (%)	Actual AFR	Max/min
3:1	0.0627	42.11	37.00	20.89	5.57	2.02
4:1	0.067	18.66	25.67	55.67	5.31	2.98
5:1	0.0416	25.00	37.50	37.50	8.67	1.50
6:1	0.0313	23.64	41.53	34.82	11.55	1.76

Table 14- Results for Position 180° Offset in double bend scenario

AFR	Mass Flow (kg/ms^{-1})	Split 1 (%)	Split 2 (%)	Split 3 (%)	Actual AFR	Max/min
3:1	0.14135	12.52	25.61	61.87	2.49	4.94
4:1	0.108	11.30	31.20	57.50	3.31	5.09
5:1	0.0841	8.68	33.17	58.15	4.27	6.70
6:1	0.0721	6.93	32.45	60.61	4.99	8.74

Table 15 - Results for Position 210° Offset in double bend scenario

AFR	Mass Flow (kg/ms^{-1})	Split 1 (%)	Split 2 (%)	Split 3 (%)	Actual AFR	Max/min
3:1	0.1515	15.18	46.80	38.02	2.26	3.08
4:1	0.1238	13.09	56.79	30.13	2.82	4.34
5:1	0.1022	12.82	61.45	25.73	3.45	4.79
6:1	0.0814	14.00	59.71	26.29	4.35	4.26

Table 16 - Results for Position 240° Offset in double bend scenario

AFR	Mass Flow (kg/ms^{-1})	Split 1 (%)	Split 2 (%)	Split 3 (%)	Actual AFR	Max/min
3:1	0.165	17.21	56.48	26.30	2.11	3.28
4:1	0.1341	16.63	63.09	20.28	2.64	3.79
5:1	0.0943	15.69	64.79	19.51	3.82	4.13
6:1	0.0719	16.13	62.31	21.56	5.03	3.86

Table 17 - Results for Position 270° Offset in double bend scenario

AFR	Mass Flow (kg/ms^{-1})	Split 1 (%)	Split 2 (%)	Split 3 (%)	Actual AFR	Max/min
3:1	0.1285	16.26	48.72	35.02	2.73	3.00
4:1	0.1171	15.03	52.26	32.71	3.03	3.48
5:1	0.0825	17.21	52.12	30.67	4.30	3.03
6:1	0.0684	20.91	40.50	38.60	5.21	1.94

Table 18 - Results for Position 300° Offset in double bend scenario

AFR	Mass Flow (kg/ms^{-1})	Split 1 (%)	Split 2 (%)	Split 3 (%)	Actual AFR	Max min
3:1	0.0888	21.40	31.98	46.62	3.88	2.18
4:1	0.0884	21.83	32.24	45.93	3.90	2.10
5:1	0.081	26.79	28.89	44.32	4.27	1.65
6:1	0.0699	22.89	31.76	45.35	4.97	1.98

Table 19 - Results for Position 330° Offset in double bend scenario

AFR	Mass Flow (kg/ms^{-1})	Split 1 (%)	Split 2 (%)	Split 3 (%)	Actual AFR	Max/min
3:1	0.0983	26.35	24.42	49.24	3.53	2.02
4:1	0.096	28.02	26.56	45.42	3.66	1.71
5:1	0.0881	30.31	22.93	46.77	4.01	2.04
6:1	0.0735	25.44	23.54	51.02	4.84	2.17